

DEVELOPMENT OF FLUORESCENT WHOLE-CELL BACTERIAL
BIOREPORTERS FOR DETECTION OF INORGANIC ARSENIC AND
CADMIUM

A THESIS SUBMITTED TO
THE GRADUATE SCHOOL OF NATURAL AND APPLIED SCIENCES
OF
MIDDLE EAST TECHNICAL UNIVERSITY

BY

EVİRİM ELÇİN

IN PARTIAL FULFILLMENT OF THE REQUIREMENTS
FOR
THE DEGREE OF DOCTOR OF PHILOSOPHY
IN
BIOTECHNOLOGY

SEPTEMBER 2019

Approval of the thesis:

**DEVELOPMENT OF FLUORESCENT WHOLE-CELL BACTERIAL
BIOREPORTERS FOR DETECTION OF INORGANIC ARSENIC AND
CADMIUM**

submitted by **EVİRİM ELÇİN** in partial fulfillment of the requirements for the degree
of **Doctor of Philosophy in Biotechnology Department, Middle East Technical
University** by,

Prof. Dr. Halil Kalıpçılar
Dean, Graduate School of **Natural and Applied Sciences**

Assoc. Prof. Dr. Can Özen
Head of Department, **Biotechnology**

Prof. Dr. Hüseyin Avni Öktem
Supervisor, **Biotechnology, METU**

Prof. Dr. Ayşe Meral Yücel
Co-Supervisor, **Biotechnology, METU**

Examining Committee Members:

Prof. Dr. Füsün İnci Eyidoğan
Educational Sciences, Başkent University

Prof. Dr. Hüseyin Avni Öktem
Biotechnology, METU

Prof. Dr. Ayşe Elif Erson Bensan
Biotechnology, METU

Prof. Dr. Ayşen Tezcaner
Engineering Sciences, METU

Assist. Prof. Dr. Oya Akça
Molecular Biology and Genetics, Harran University

Date: 02.09.2019

I hereby declare that all information in this document has been obtained and presented in accordance with academic rules and ethical conduct. I also declare that, as required by these rules and conduct, I have fully cited and referenced all material and results that are not original to this work.

Name, Surname: Evrim Elçin

Signature:

ABSTRACT

DEVELOPMENT OF FLUORESCENT WHOLE-CELL BACTERIAL BIOREPORTERS FOR DETECTION OF INORGANIC ARSENIC AND CADMIUM

Elçin, Evrim

Doctor of Philosophy, Biotechnology

Supervisor: Prof. Dr. Hüseyin Avni Öktem

Co-Supervisor: Prof. Dr. Ayşe Meral Yücel

September 2019, 188 pages

Environmental heavy metal contamination in many regions of the world is a serious problem of ecological health. Fast and constant monitoring of their levels is significant for both preventing their accumulation and taking an immediate action for removal. As an alternative approach to standard laboratory techniques, various biosensor systems for detection of heavy metals have been proposed. Bacterial biosensors hold great promise for in-field detection of heavy metals.

In this study, two different whole cell *Escherichia coli* bioreporter strains were developed for detection of inorganic arsenic and cadmium. In their presence, reporter gene expression increases which is detected as fluorescent signal later interpreted as a measure of available metal level in sample. Following cloning studies, arsenic and cadmium bacterial bioreporter strains were characterized for their metal specificity and detection limits by using different media and induction plans. In liquid assays, arsenic bioreporter could detect arsenite and arsenate at 10 µg/L after 2 hours, and cadmium bioreporter could detect cadmium of 2 µg/L after 1.5 hours of induction. Additionally, the arsenic bioreporter could estimate the bioavailable arsenic level in contaminated groundwater sample.

To be integrated into a portable device, immobilization of arsenic bacterial bioreporter was investigated using agar and alginate biopolymers. Entrapment parameters of polymer concentration and cell density were evaluated. Immobilized cells were characterized for their metal specificity and detection limits by using different media. Agar and alginate immobilized bioreporter systems could detect arsenite and arsenate of 25 µg/L and 150 µg/L within 5 hours and 2 hours, respectively.

The results demonstrated that these bacterial arsenic and cadmium bioreporter strains are applicable in determining the environmentally safe concentrations of these two most abundant heavy metals.

Keywords: Heavy Metal Pollution, Arsenic, Cadmium, Bacterial Bioreporter, Green Fluorescent Protein, Cell Immobilization

ÖZ

İNORGANİK ARSENİK VE KADMIYUM TAYİNİ İÇİN FLORESAN TAM HÜCRE BAKTERİYEL BİYORAPORTÖRLERİN GELİŞTİRİLMESİ

Elçin, Evrim
Doktora, Biyoteknoloji
Tez Danışmanı: Prof. Dr. Hüseyin Avni Öktem
Ortak Tez Danışmanı: Prof. Dr. Ayşe Meral Yücel

Eylül 2019, 188 sayfa

Çevresel ağır metal kirliliği dünyanın birçok yerinde ciddi ekolojik sorun oluşturmaktadır. Ağır metal seviyelerinin hızlı ve sıkça izlenmesi hem birikmelerine engel olmak hem de ayrıştırılmaları için derhal önlem almak açısından önemlidir. Standart laboratuvar tekniklerine alternatif olarak, ağır metal saptamak için çeşitli biyosensör sistemleri önerilmektedir. Bakteriyel biyosensörler, ağır metallerin sahada saptanması için oldukça büyük potansiyele sahiptirler.

Bu çalışmada, inorganik arsenik ve kadmiyum için iki farklı tam hücre *Escherichia coli* biyoreportör suşları geliştirilmiştir. Ağır metal varlığında artan reportör genin ifadesi floresan sinyali olarak algılanıp, bu sinyal örnekteki metal kirliliği seviyesinin bir ölçüsü olarak gösterilebilmektedir. Klonlama çalışmalarını takiben, arsenik ve kadmiyum bakteriyel biyoreportör suşlarının farklı besiyerlerinde ve indüksiyon planlarında, metal özgünlükleri ve tayin limitleri karakterize edilmiştir. Sıvı deneylerde arsenik biyoreportörü, arsenit ve arsenatı 10 µg/L seviyesinde indüksiyondan 2 saat, kadmiyum biyoreportörü ise 2 µg/L kadmiyum derişimini indüksiyondan 1,5 saat sonra belirleyebilmektedir. Ayrıca arsenik biyoreportörü kirli yeraltı suyundaki biyoerişilebilir arsenik seviyesini tahmin edebilmektedir.

Taşıyabilir cihaza entegre edebilmek için arsenik biyoreportörünün agar ve aljinat biyopolimerlerinde immobilizasyonu çalışılmıştır. Polimer konsantrasyonu ve hücre yoğunluğu parametreleri değerlendirilmiştir. İmmobilize hücreler, farklı besiyerlerindeki metal özgünlükleri ve tayin limitleri açısından karakterize edilmiştir. Agar ve aljinat immobilize biyoreportör sistemleri arsenit ve arsenatı, 25 µg/L ve 150 µg/L derişimlerinde sırasıyla 5 ve 2 saatte belirleyebilmektedir.

Çalışma sonuçları göstermektedir ki bakteriyel arsenik ve kadmiyum biyoreportör suşları çevresel olarak güvenli derişimlerdeki bu iki yaygın ağır metali saptamakta kullanılabilirler.

Anahtar Kelimeler: Ağır Metal Kirliliği, Arsenik, Kadmiyum, Bakteriyel Biyoreportör/Biyosensör, Yeşil Floresan Proteini, Hücre İmmobilizasyonu

To my father and grandfather,

ACKNOWLEDGEMENTS

I would like to express deep appreciation to my advisor, Prof. Dr. Hüseyin Avni Öktem and my co-advisor Prof. Dr. Ayşe Meral Yücel for their encouragement and valuable guidance during my doctoral research. Without their understanding and support, this study would not have been completed. I am deeply grateful to my supervisor, Prof. Dr. Hüseyin Avni Öktem for his guidance, patience, and helpful insights throughout the progression of this research.

I would like to thank the members of my PhD thesis examining committee, Prof. Dr. Füsun İnci Eyidoğan, Prof. Dr. Ayşe Elif Erson Bensan, Prof. Dr. Ayşen Tezcaner, and Asst. Prof. Oya Akça for their helpful criticisms, comments, and directions.

I would like to express my appreciation to Assoc. Prof. Dr. Can Özen and Assoc. Prof. Dr. Çağdaş Devrim Son for their kind help for fluorescence measurements. I would like to thank Konya Food and Agriculture University for kindly providing the groundwater sample.

This study was supported by ÖYP-YÖK Research Capacity Development Funds (Budget No. 38.03.00.01/2/09.4.2.20) and by Nanobiz Technology Inc.

I would like to thank Scientific and Technical Research Council of Turkey (TÜBİTAK) 2522- TÜBİTAK (Turkey) - NRDIO (Hungary) Joint Funding Program; Project No: 217E115.

I also want to thank TÜBİTAK BİDEB for TÜBİTAK 2211 National Graduate Scholarship.

TABLE OF CONTENTS

ABSTRACT	v
ÖZ	vii
ACKNOWLEDGEMENTS	x
TABLE OF CONTENTS	xi
LIST OF TABLES	xvii
LIST OF FIGURES	xviii
LIST OF ABBREVIATIONS	xxvi
CHAPTERS	
1. INTRODUCTION	1
1.1. Heavy Metal Contamination of Environment	1
1.1.1. Pathways of Heavy Metal Contamination	1
1.1.2. Sources of Arsenic Contamination	2
1.1.3. Sources of Cadmium Contamination	3
1.2. Heavy Metal Toxicity	4
1.2.1. Arsenic Toxicity	6
1.2.2. Cadmium Toxicity	8
1.3. Environmental Monitoring of Metal Contamination	9
1.3.1. Physicochemical Methods for Analysis of Metals	9
1.3.2. Biosensing Methods for Analysis of Heavy Metals	10
1.4. Whole-Cell Biosensors	13
1.4.1. Whole-Cell Bacterial Bioreporters	15
1.4.1.1. Principles of Whole-Cell Bacterial (<i>E. coli</i>) Bioreporters	15

1.5. Heavy Metal-Specific Whole-Cell Bacterial Bioreporters	19
1.5.1. Heavy Metal Sensing Modules.....	21
1.5.1.1. Sensing Modules for Arsenic Detection	22
1.5.1.2. Sensing Modules for Cadmium Detection.....	24
1.6. Common Reporter Elements for Biosensor Constructions	26
1.6.1. Green Fluorescent Protein (GFP)	28
1.7. Bioreporter Immobilization Methods.....	29
1.7.1. Entrapment/Encapsulation Methods.....	32
1.7.1.1. Agar immobilization	33
1.7.1.2. Alginate immobilization	34
1.8. Aim of the Study	36
2. MATERIALS AND METHODS	37
2.1. Materials.....	37
2.1.1. Bacterial Strains and Plasmids	37
2.1.2. Growth Media.....	37
2.1.3. Chemicals, Enzymes and Kits	38
2.1.4. Instruments	38
2.2. Molecular Genetics Methods	39
2.2.1. Design of DNA Fragments and Polymerase Chain Reaction (PCR) Primers	39
2.2.2. Bacterial Genomic DNA Isolation	41
2.2.3. Isolation of Plasmid DNA from Bacteria	41
2.2.4. Agarose Gel Electrophoresis of DNA	41
2.2.5. Isolation of DNA Fragments from Agarose Gel	41

2.2.6. Restriction Enzyme Digestions	42
2.2.7. Ligation of DNA Fragments	42
2.2.8. Transformation of Bacteria	43
2.2.8.1. Preparation of Competent <i>E. coli</i> Cells.....	43
2.2.8.2. Transformation of <i>E. coli</i> with Plasmids.....	43
2.2.9. PCR Amplification of Synthetic <i>gfp</i> Gene	44
2.2.10. Cloning of <i>sgfp</i> into pET-17b Expression Vector (pET-sGFP).....	45
2.2.11. Cloning of <i>sGFP</i> into pBR322 Vector (pBR-sGFP)	47
2.2.12. Construction of Arsenic Specific Sensor Plasmid (pBR-arsR773)	48
2.2.13. Construction of Cadmium Specific Sensor Plasmid (pBR-PzntA)	49
2.2.14. Confirmation of Plasmid Constructs.....	51
2.2.14.1. Colony PCR	51
2.2.14.2. Restriction Analysis and DNA Sequencing	52
2.3. Reporter Expression Studies	52
2.3.1. Induction of pET-sGFP Construct	52
2.3.2. Fluorescence Measurements of pET-sGFP.....	53
2.3.3. Induction of pBR-arsR773 and pBR-PzntA Constructs	53
2.3.3.1. Microplate Assays for Arsenic and Cadmium Sensing Bioreporters.....	53
2.3.3.2. Bacterial Growth Effect on Arsenic and Cadmium Sensing Bioreporters.....	53
2.3.3.3. Metal Specificity Test for pBR-arsR773	54
2.3.3.4. Metal Specificity Test for pBR-PzntA.....	54
2.4. Immobilization Studies.....	54
2.4.1. Bacterial Cell Culture Preparation for Immobilization.....	54

2.4.2. Agar Immobilization	55
2.4.3. Alginate Immobilization.....	55
2.4.4. Bioassays for Arsenic Detection of Immobilized Cells	56
2.4.5. Metal Specificity Test for Immobilized Bioreporters	56
2.5. Data Analysis	57
3. RESULTS AND DISCUSSION	59
3.1. Molecular Cloning Studies.....	59
3.1.1. Amplification of Reporter Gene (<i>sgfp</i>)	59
3.1.2. Cloning of <i>sgfp</i> into pET-17b Expression Vector	60
3.1.3. Conformation of pET-sGFP Vector	61
3.1.3.1. Colony PCR Result.....	61
3.1.3.2. Single Enzyme Digest Result	62
3.1.4. Cloning of <i>sgfp</i> into pBR322 Vector.....	63
3.1.5. Confirmation of pBR-sGFP.....	65
3.1.5.1. Colony PCR Result.....	65
3.1.5.2. Single Enzyme Digest Result	65
3.1.6. Cloning of <i>ParsR-arsR</i> into pBR-sGFP	67
3.1.7. Confirmation of pBR-arsR773	68
3.1.7.1. Colony PCR Result.....	68
3.1.7.2. Single Enzyme Digest Result	68
3.1.8. Cloning of <i>PzntA</i> into pBR-sGFP	70
3.1.9. Confirmation of pBR-PzntA	71
3.1.9.1. Colony PCR Result.....	71
3.1.9.2. Single Enzyme Digest Result	72

3.2. Expression Studies	74
3.2.1. Induction of <i>E. coli</i> BL21 (pET-sGFP) Strain.....	74
3.2.2. Induction of <i>E. coli</i> MG1655 (pBR-arsR773) Bioreporter Strain	76
3.2.2.1. Fluorescence Emission Kinetics of Arsenic Bioreporter Strain in M9 Supplemented Medium	78
3.2.2.2. Fluorescence Emission Kinetics of Arsenic Bioreporter Strain in MOPS supplemented medium	83
3.2.2.3. Metal Specificity of Arsenic Bioreporter Strain	88
3.2.2.4. Fluorescence Response of Arsenic Bioreporter Strain at Different Growth Phases.....	89
3.2.2.5. Arsenic Content Determination of Groundwater Sample	96
3.2.3. Induction of <i>E. coli</i> MG1655 (pBR-PzntA) Bioreporter Strain.....	98
3.2.3.1. Fluorescence Emission Kinetics of Cadmium Bioreporter Strain in M9 and MOPS Supplemented Media	99
3.2.3.2. Metal Specificity of Cadmium Bioreporter Strain	103
3.2.3.3. Mercury Sensitivity of Cadmium Bioreporter Strain.....	105
3.2.3.4. Fluorescence Response of Cadmium Bioreporter Strain at Different Growth Phases.....	109
3.3. Immobilization Studies of Arsenic Bioreporter Strain.....	114
3.3.1. Agar Gel Immobilization	116
3.3.1.1. Optimization of Agar Gel Immobilization- Percentage and Cell Density	116
3.3.1.2. Fluorescence Response of Agar Gel Immobilized Biosensor to Arsenite and Arsenate.....	119
3.3.2. Alginate Bead Immobilization.....	122

3.3.2.1. Optimization of Alginate Bead Immobilization- Percentage and Cell Density	122
3.3.2.2. Fluorescence Response of Alginate Bead Immobilized Biosensor to Arsenite and Arsenate.....	126
3.3.3. Metal Specificity of Agar Gel and Alginate Bead Immobilized Bioreporter Cells.....	130
4. CONCLUSION	133
REFERENCES	135
APPENDICES	165
A. COMPOSITIONS OF BACTERIAL CULTURE MEDIA.....	165
B. BUFFERS AND SOLUTIONS	167
C. pGFPuv, ParsR-arsR and PzntA DNA SEQUENCES.....	169
D. GROWTH CURVES	174
E. ONE-WAY ANOVA RESULTS	176
CURRICULUM VITAE.....	187

LIST OF TABLES

TABLES

Table 1.1 Guideline values for heavy metals in drinking water recommended by the WHO and EPA.....	5
Table 1.2 Commonly used reporter genes and their characteristics (French et al., 2011).	27
Table 1.3 Various methods for stabilization of bacterial biosensors (Bjerketorp et al., 2006).	31
Table 2.1 Gene specific primers designed for different cloning vectors.	40
Table 2.2 Optimized PCR condition for amplification of sgfp gene.	45
Table 2.3 Optimized PCR cycling conditions for amplification of sgfp gene.	45
Table 2.4 Optimized PCR conditions for amplification of ParsR-arsR.	49
Table 2.5 Optimized PCR cycling conditions for amplification of ParsR-arsR.	49
Table 2.6 Optimized PCR conditions for amplification of PzntA.	50
Table 2.7 Optimized PCR cycling conditions for amplification of PzntA.	50
Table 2.8 Colony PCR ingredients for detection of recombinants.	51
Table 3.1 Bacterial growth, OD600 values, of pET-17b, pET-sGFP and IPTG added pET-sGFP cultures in LB medium over time.	74
Table 3.2 Fluorescence intensity values of pET-sGFP and IPTG added pET-sGFP cultures over time.	75
Table 3.3 Bacterial growth, OD600 values, of pBR-sGFP and pBR-arsR773 cultures in M9 supplemented medium in presence of arsenite, As(III) and arsenate, As(V) over time.....	77
Table 3.4 Bacterial growth, OD600 values, of pBR-sGFP and pBR-PzntA cultures in M9 supplemented medium in presence of cadmium, Cd(II), over time.	98

LIST OF FIGURES

FIGURES

Figure 1.1 List of 23 metals and metalloids of primary interest (USEPA, 2007).	4
Figure 1.2 Eh-pH diagram for aqueous As species in the system As–O ₂ –H ₂ O at 25 °C and 1 bar total pressure (Smedley & Kinniburgh, 2002).	7
Figure 1.3 Schematic representation of biosensors with a variety of biosensing elements employed (Adapted from Mehta et al., 2016).	12
Figure 1.4 Scheme of <i>E. coli</i> -based biosensor design (Idalia & Bernardo, 2017). ...	17
Figure 1.5 Schematic representation of the types of biosensors. a) “lights-off” biosensor having a constitutive whole-cell sensing system, b) “lights-on” biosensor having an inducible whole-cell sensing system (Date et al., 2010).	18
Figure 1.6 The <i>arsRDABC</i> operon of <i>E. coli</i> plasmid R773. Arsenic enters cells as either As(III) or As(V). As(III) is taken up by the aquaglyceroporin, GlpF, and As(V) is taken up by Pst and Pho phosphate permeases (Chen & Rosen, 2014).	23
Figure 1.7 Regulation of the <i>zntA</i> promoter by the ZntR protein (Adapted from Charrier et al., 2010).	25
Figure 1.8 The instruments for measuring signal output for currently used reporters: fluorescent, bio- or chemiluminescent, and colorimetric (Tecon & van der Meer, 2008).	26
Figure 1.9 Schematic representation of the prevalent methods for immobilization of whole-cell sensing systems (Gupta et al., 2019).	32
Figure 1.10 Ionotropic gelation of alginate solution. a) Chemical structure of alginate and the crosslink between alginate and the counterions (Albuquerque et al., 2016), b) Extrusion method, representing the formation of calcium-alginate beads (Gao et al., 2016).	35
Figure 2.1 Graphical representation of promoterless synthetic gfp DNA fragment..	44

Figure 2.2 Vector map of pET-17b. (AmpR: Ampicillin resistance gene; ori: pBR322 origin; MCS: multiple cloning site).	46
Figure 2.3 Graphical abstract of pET expression system. Addition of IPTG to a growing culture induces T7 RNA polymerase production, which in turn transcribes the target DNA in the plasmid (Novagen pET system manual).	47
Figure 2.4 Vector map of pBR322. (AmpR: Ampicillin resistance gene; TcR: Tetracycline resistance gene; ori: pBR322 origin of replication; rop: regulates plasmid replication, keeps the copy number at about 20 per cell).....	48
Figure 3.1 Agarose gel electrophoresis result of PCR amplification of synthetic gfp gene, with length of 765 bp. 1% agarose gel in 1X TAE solution was run for 60 minutes at 100 volts.	60
Figure 3.2 Vector map of constructed pET-sGFP.....	61
Figure 3.3 Agarose gel electrophoresis result of colony PCR for selected transformants. 1% agarose gel in 1X TAE solution was run for 60 minutes at 90 volts.	62
Figure 3.4 Agarose gel electrophoresis result of BamHI single digests of pET-17b and pET-sGFP. 1% agarose gel in 1X TAE solution was run for 90 minutes at 90 volts.	63
Figure 3.5 Agarose gel electrophoresis result of pBR322 (4361 bp) cloning vector cut with HindIII and Eco88I and loaded in three wells of agarose gel. 1% agarose gel in 1X TAE solution was run for 60 minutes at 90 volts.....	64
Figure 3.6 Agarose gel electrophoresis result of agarose gel purified large fragment of double digested pBR322 and purified double digested sgfp PCR product cut with HindIII and Eco88I. 1% agarose gel in 1X TAE solution was run for 30 minutes at 80 volts.	64
Figure 3.7 Agarose gel electrophoresis result of colony PCR using Col-F and Col-R primers with an amplicon size of 805 bp. 1% agarose gel in 1X TAE solution was run for 60 minutes at 90 volts.....	65

Figure 3.8 Agarose gel electrophoresis result of pBR-sGFP (3703 bp; large fragment of pBR322 (2938 bp) plus sGFP (765 bp) vector digested with BamHI. 1% agarose gel in 1X TAE solution was run for 90 minutes at 90 volts.	66
Figure 3.9 Vector map of constructed promoterless reporter plasmid, pBR-sGFP...	66
Figure 3.10 Agarose gel electrophoresis result of purified double digest products of pBR-sGFP (after cut 3669 bp) vector and ParsR-arsR gene (537 bp). 1% agarose gel in 1X TAE solution was run for 30 minutes at 80 volts.	67
Figure 3.11 Agarose gel electrophoresis result of colony PCR using Col-F and Col-R primers with an amplicon size of 1342 bp. 1% agarose gel in 1X TAE solution was run for 60 minutes at 90 volts.	68
Figure 3.12 Agarose gel electrophoresis result of pBR-arsR773 (4206 bp) vector digested with BamHI. 1% agarose gel in 1X TAE solution was run for 90 minutes at 90 volts.....	69
Figure 3.13 Vector map of constructed arsenic sensing bioreporter plasmid, pBR-arsR773 (Elcin & Öktem, 2019).....	69
Figure 3.14 Agarose gel electrophoresis results of a) isolated genomic DNA from E. coli MG1655 and b) Phusion PCR product of PzntA (379 bp). 1% agarose gel in 1X TAE solution was run for 45 minutes at 90 volts.	70
Figure 3.15 Agarose gel electrophoresis results of double digested and purified a) Phusion PCR product of zntAp (355 bp). b) pBR-sGFP plasmid (after cut 3669 bp). 1% agarose gel in 1X TAE solution was run for 30 minutes at 90 volts.....	71
Figure 3.16 Agarose gel electrophoresis result of colony PCR using Col-F and Col-R primers with right amplicon size of 1160 bp. 1% agarose gel in 1X TAE solution was run for 60 minutes at 90 volts.	72
Figure 3.17 Agarose gel electrophoresis result of pBR-PzntA (4024 bp) vector digested with BamHI. 1% agarose gel in 1X TAE solution was run for 90 minutes at 90 volts.....	73
Figure 3.18 Vector map of constructed Cd sensing bioreporter plasmid, pBR-PzntA.	73

Figure 3.19 Fluorescence micrographs of bacterial cells having a) pET-17b, b) pET-sGFP, and c) pET-sGFP (IPTG induced). Images were taken by using an EVOS Flويد Imaging Station (Thermo Fisher Scientific, USA).	76
Figure 3.20 Fluorescence emission kinetics of arsenic bioreporter cells in response to arsenite, As(III). Bioreporter cells grown in M9 supplemented medium (till OD ₆₀₀ = 0.1) induced with different arsenite concentrations. Data shown as mean ± SD of triplicate wells of each induction. Error bars are shown only when they exceed the size of the symbols.	79
Figure 3.21 Fluorescence microscope images of arsenic bioreporter cells: a) uninduced bioreporters under BF channel, b) uninduced bioreporters under Fluo channel, c) induced bioreporters with 75 µg/L arsenite under BF channel, d) induced bioreporters with 75 µg/L arsenite under Fluo channel. BF: Bright field, Fluo: Fluorescence. Scale: 20µm.	83
Figure 3.22 Fluorescence emission kinetics of arsenic bioreporter cells in response to a) arsenite, As(III), b) arsenate, As(V). Bioreporter cells were grown in MOPS supplemented medium (till OD ₆₀₀ = 0.1). Data shown as mean ± SD of triplicate wells of each induction. Error bars are shown only when they exceed the size of the symbols.	86
Figure 3.23 Overview of bacterial interactions with arsenic. The metalloid is taken up through glycerol or phosphate transporters. Arsenate is reduced to arsenite which may then be extruded from the cell by ArsAB (Kruger et al., 2013).	87
Figure 3.24 Metal specificity of the arsenic bacterial bioreporter. Bioreporter cells were grown either in M9 or in MOPS supplemented medium (till OD ₆₀₀ = 0.1). Control refers to no metal addition. Data shown as mean ± SD of triplicate wells of each induction group and presented at 6-h time point. *p< 0.001.	88
Figure 3.25 The fluorescence intensity values of arsenic bioreporter induced with arsenite at different growth phases. Bioreporter cells were grown in M9 supplemented medium. Data shown as mean ± SD of triplicate wells of each induction group and presented at 6-h time point.	90

Figure 3.26 Fluorescence kinetic profile of arsenic bioreporter with different induction schemes. Bioreporter cells grown in M9 supplemented medium to a) mid-exponential and b) stationary phase induced with different arsenite concentrations. Data shown as mean \pm SD of triplicate wells of each induction.....	91
Figure 3.27 The fluorescence intensity values of arsenic bioreporter induced with a) arsenite and b) arsenate at different growth phases. Bioreporter cells were grown in MOPS supplemented. Data shown as mean \pm SD of triplicate wells of each induction group and presented at 6-h time point.	93
Figure 3.28 Fluorescence kinetic profile of arsenic bioreporter with different induction schemes. Bioreporter cells grown in MOPS supplemented medium to a) mid-exponential and b) stationary phase induced with different arsenite concentrations. Data shown as mean \pm SD of triplicate wells of each induction.	94
Figure 3.29 Fluorescence kinetic profile of arsenic bioreporter with different induction schemes. Bioreporter cells grown in MOPS supplemented medium to a) mid-exponential and b) stationary phase induced with different arsenate concentrations. Data shown as mean \pm SD of triplicate wells of each induction.	95
Figure 3.30 Calibration (standard) curve for arsenite ranging from 0 to 150 $\mu\text{g/L}$ after bioreporter cells were assayed in MOPS medium for 4 hours. Slope linearly interpolated from average of triplicate samples (Elcin & Öktem, 2019).	97
Figure 3.31 Fluorescence emission kinetics of cadmium bioreporter. Bioreporter cells grown in M9 supplemented medium (till $\text{OD}_{600} = 0.1$) induced with different cadmium, Cd(II) concentrations. Data shown as mean \pm SD of triplicate wells of each induction. Error bars are shown only when they exceed the size of the symbols. ..	100
Figure 3.32 Fluorescence emission kinetics of cadmium bioreporter. Bioreporter cells grown in MOPS supplemented medium (till $\text{OD}_{600} = 0.1$) induced with different cadmium, Cd(II) concentrations. Data shown as mean \pm SD of triplicate wells of each induction. Error bars are shown when they exceed the size of the symbols.	101
Figure 3.33 Metal specificity of the cadmium bacterial bioreporter. Bioreporter cells were grown either in M9 or in MOPS supplemented medium (till $\text{OD}_{600} = 0.1$). Control	

refers to no metal addition. Data shown as mean \pm SD of triplicate wells of each induction group and presented at 6-h time point. * $p < 0.001$	104
Figure 3.34 Fluorescence emission kinetics of cadmium bioreporter cells in response to mercury, Hg(II). Bioreporter cells were grown in M9 supplemented medium (till $OD_{600} = 0.1$). Data shown as mean \pm SD of triplicate wells of each induction. Error bars are shown only when they exceed the size of the symbols.	106
Figure 3.35 Fluorescence emission kinetics of cadmium bioreporter cells in response to mercury, Hg(II). Bioreporter cells were grown in MOPS supplemented medium (till $OD_{600}=0.1$). Data shown as mean \pm SD of triplicate wells of each induction. Error bars are shown only when they exceed the size of the symbols.	107
Figure 3.36 Fluorescence microscope images of cadmium bioreporter cells: a, b) uninduced bioreporters under BF and Fluo channel, c, d) induced bioreporters with 100 μ g/L cadmium under BF and Fluo channel, e, f) induced bioreporters with 400 μ g/L mercury under BF and Fluo channel. BF: Bright field; Fluo: Fluorescence. Scale: 20 μ m.	108
Figure 3.37 The fluorescence intensity values of cadmium bioreporter with different induction schemes. Bioreporter cells grown in M9 supplemented medium. Data shown as mean \pm SD of triplicate wells of each induction group and presented at 6-h time point.	110
Figure 3.38 Fluorescence kinetic profile of cadmium bioreporter with different induction schemes. Bioreporter cells grown in M9 supplemented medium to a) mid-exponential and b) stationary phase induced with different cadmium concentrations. Data shown as mean \pm SD of triplicate wells of each induction.....	111
Figure 3.39 The fluorescence intensity values of cadmium bioreporter with different induction schemes. Bioreporter cells grown in MOPS supplemented medium. Data shown as mean \pm SD of triplicate wells of each induction group and presented at 6-h time point.	112
Figure 3.40 Fluorescence kinetic profile of cadmium bioreporter with different induction schemes. Bioreporter cells grown in MOPS supplemented medium to a) mid	

exponential and b) stationary phase induced with different cadmium concentrations. Data shown as mean \pm SD of triplicate wells of each induction.	113
Figure 3.41 Effect of agar percentages of 0.5, 1 and 1.5 (w/v) on the fluorescence response of agar-immobilized arsenic bioreporter prepared in M9 supplemented medium with OD ₆₀₀ = 0.1. The average values of triplicate of each induction were presented for 6-h with standard deviation.	117
Figure 3.42 Effect of cell densities (OD ₆₀₀) of 0.1, 0.4 and 0.7 on the fluorescence response of agar-immobilized arsenic bioreporter prepared in M9 supplemented medium with agar percent of 1.5 (w/v). The average values of triplicate of each induction were presented for 6-h with standard deviation.....	118
Figure 3.43 Kinetic profile of fluorescence emission of agar immobilized arsenic bioreporters formulated with optimal parameters in M9 supplemented medium induced with arsenite, As(III). Data shown as mean \pm SD of triplicate wells of each induction. Error bars are shown only when they exceed the size of the symbols. ..	119
Figure 3.44 Kinetic profile of fluorescence emission of agar immobilized arsenic bioreporter cells formulated with optimal parameters in MOPS supplemented medium induced with a) arsenite, As(III), and b) arsenate, As(V), concentrations. Data shown as mean \pm SD of triplicate wells of each induction.	121
Figure 3.45 Photo images of alginate-immobilized arsenic bioreporter with different alginate percentages a) 1, b) 1.5 and c) 2 (w/v).....	123
Figure 3.46 Effect of alginate percentages of 1, 1.5 and 2 (w/v) on the fluorescence response of alginate-immobilized arsenic bioreporter prepared in M9 supplemented medium with OD ₆₀₀ = 0.1. The average values of triplicate of each induction were presented for 6-h with standard deviation.	124
Figure 3.47 Effect of cell densities (OD ₆₀₀) of 0.1, 0.4 and 0.7 on the fluorescence response of alginate-immobilized arsenic bioreporter prepared in M9 supplemented medium with alginate percent of 1 (w/v). The average values of triplicate of each induction were presented for 6-h with standard deviation.....	125
Figure 3.48 Kinetic profile of fluorescence emission of alginate immobilized arsenic bioreporter formulated with optimal parameters in M9 supplemented medium induced	

with arsenite, As(III). Data shown as mean \pm SD of triplicate wells of each induction. Error bars are shown only when they exceed the size of the symbols.	127
Figure 3.49 The images of alginate-bead immobilized arsenic bioreporters in M9 supplemented medium after 16-h induction, were taken with cellphone camera during excitation under blue channel of EVOS Fluid Imaging Station: a) uninduced beads, b) induced beads with 25 μ g/L of arsenite, c)) induced beads with 150 μ g/L of arsenite.	128
Figure 3.50 Kinetic profile of fluorescence emission of alginate immobilized arsenic bioreporter cells formulated with optimal parameters in MOPS supplemented medium induced with a) arsenite, As(III), and b) arsenate, As(V), concentrations. Data shown as mean \pm SD of triplicate wells of each induction.	129
Figure 3.51 Metal specificity of agar and alginate immobilized immobilized bacterial bioreporter cells prepared in MOPS supplemented medium. Arsenite and arsenate were added in 50 μ g/L, and other metal ions were added in 250 μ g/L. Control refers to no-metal addition. The average values of triplicate of each induction were presented for 8-h with standard deviation. *p< 0.001.	131

LIST OF ABBREVIATIONS

ABBREVIATIONS

ANOVA	Analysis of Variance
As	Arsenic
As(III)	Arsenite
As(V)	Arsenate
bp	Base pair
Cd	Cadmium
dH ₂ O	Distilled Water
DNA	Deoxyribonucleic acid
dNTP	Deoxynucleotide triphosphate
GFP	Green fluorescent protein
Hg	Mercury
IPTG	Isopropyl β-D-1-thiogalactopyranoside
LB	Luria-Bertani Medium
MOPS	3-(N-morpholin-o)propanesulfonicacid
OD	Optical density
PCR	Polymerase chain reaction
RFU	Relative fluorescence unit
sGFP	Synthetic green fluorescent protein
WCB	Whole-cell biosensor
WHO	World Health Organization

CHAPTER 1

INTRODUCTION

1.1. Heavy Metal Contamination of Environment

Heavy metals are defined as metallic elements that have a specific density of more than 5 g/mL and have toxic effects on the environment and organisms. Heavy metals also include metalloids, such as arsenic, since heaviness and toxicity are interrelated. The concern about ecological and global public health has increased due to heavy metal contamination in last decades. As world's population increases rapidly, industrialization and transportation develop, and sources of environmental pollution have increased because of anthropogenic activities (Kim et al., 2018). The industries produce various effluents that are mostly discharged into the environment, hence the resultant dispersion of environmental contaminants and toxic chemicals eventually reach water systems and threaten the human and environmental health. Especially in developing countries, inadequately treated industrial, domestic, and agricultural effluents have excessive levels of heavy metals or metalloids, that are mostly released into the environment. Besides anthropogenic activities, metals can also enter the environment through natural processes (Chowdhury et al., 2016).

1.1.1. Pathways of Heavy Metal Contamination

Heavy metal contamination can originate from both natural/bio-geo processes and anthropogenic activities. Human activities have contributed more to environmental metal pollution due to the perpetual manufacturing of goods to fulfil the demands of growing human population. The foremost anthropogenic sources are mining operations, power plants, electroplating, pharmaceutical industries, metal smelting which releases arsenic, copper, and zinc, disposal of untreated effluents and metal

chelates, immoderate use of inorganic fertilizers and pesticides which release arsenic and cadmium, burning of fossil fuels which release nickel, vanadium, mercury, selenium and tin, and also automobile exhaust which releases lead (Chowdhury et al., 2016; He et al., 2005; Reza & Singh, 2010).

Metals are naturally found in the earth's crust and the natural sources of metal emissions are mainly because of chemical weathering of rock, volcanic eruptions, soil erosion of metal ions, wild forest fires, and biogenic sources. Also, weathering processes and windblown dust and sea salt sprays could cause the release of metals to different environmental districts from their original location (Masindi & Muedi, 2018).

The common metal (or metalloid) species that are considered a heavy/toxic metal pollutant, which may cause detrimental human or environmental effects, are arsenic, cadmium, chromium, copper, lead, mercury, nickel, silver, and zinc (Singh et al., 2011). Among them, arsenic (As) ranks first and cadmium (Cd) ranks seventh place in the priority list of hazardous substances prepared by the Agency for Toxic Substances and Disease Registry (ATSDR) and the Environmental Protection Agency (EPA) in the USA (ATSDR, 2017).

1.1.2. Sources of Arsenic Contamination

Arsenic is a natural crystalline metalloid with features in between metals and nonmetals. Arsenic is the 20th most abundant trace element in the earth's crust and 14th in seawater (Singh et al., 2015). It is usually found in the environment as inorganic arsenic combined with oxygen, chlorine, and sulfur; it can also be found as organic arsenic when combined with carbon and hydrogen. It is ubiquitous and very mobile that is detected in almost every environmental matrix and has been reported worldwide (Argos et al., 2010; Li et al., 2011).

Inorganic arsenic occurs naturally in soil and in many kinds of rock, especially in minerals and ores that contain copper or lead, so arsenic pollution may occur by natural phenomena such as volcanic and natural weathering of geologic material and soil erosion. Moreover, when these ores are heated in smelters, most of the arsenic enters the air as a fine dust having arsenic trioxide (As_2O_3). Organic arsenicals, such as cacodylic acid, disodium methylarsenate, and monosodium methylarsenate, are used as pesticides and copper chromated arsenate as wood preservative. Various organic arsenicals are used as herbicides and as antimicrobial additives for animal and poultry feed. Elemental arsenic is used commercially and industrially as alloying agents in the manufacture of transistors, laser and light-emitting diodes, semiconductors, and lead-acid batteries for automobiles. (ATSDR, 2007; Hughes et al., 2011).

1.1.3. Sources of Cadmium Contamination

Cadmium (Cd) is a heavy metal and widely distributed in the earth's crust. Soluble forms of cadmium can migrate in water, while insoluble forms of cadmium adsorb to sediments. It occurs naturally with zinc, copper, and lead ores (WHO, 2011b).

Natural release of cadmium to environment can occur due to volcanic eruptions, weathering, river transport, forest fires, or generation of sea salt aerosols. The anthropogenic sources of cadmium are non-ferrous metal mining, electroplating onto steel, refining, smelting, manufacture and application of phosphate fertilizers, fossil fuel combustion, incineration of municipal waste, and tobacco smoking. Water sources near cadmium-emitting industries have shown significant elevation of cadmium in water sediments and aquatic organisms. It is also mostly used in rechargeable alkaline batteries as an electrode component and used as metal coatings such as iron and steel to serve as an anticorrosive agent, the rest is used in pigments and plastic stabilizers (ATSDR, 2012; Jaishankar et al., 2014).

1.2. Heavy Metal Toxicity

35 metals pose a human health risk due to residential or occupational exposure, and 23 of them are heavy/toxic metals that are listed in Figure 1.1. Among these metals that are accepted as nutritionally essential in very low concentrations are cobalt, chromium, copper, iron, manganese, molybdenum, selenium, and zinc, while the rest are nutritionally nonessential metals for humans. However, all of them become highly noxious after certain threshold concentrations.

Metals and Metalloids of Primary Interest	
Aluminum	Manganese
Antimony	Mercury (inorganic)
Arsenic	Molybdenum
Barium	Nickel
Beryllium	Selenium
Boron	Silver
Cadmium	Strontium
Chromium	Tin
Cobalt	Thallium
Copper	Vanadium
Iron	Zinc
Lead	

Figure 1.1 List of 23 metals and metalloids of primary interest (USEPA, 2007).

The permissible levels of various heavy metal ions have been proposed by several environmental agencies including World Health Organization (WHO), US Environmental Protection Agency (EPA), and European Environment Agency (EEA) for protection of human health. The guideline values were determined based on the lowest concentration that was reasonably and economically achievable with water treatment technologies, measurable lowest concentration, and the observed effects on human and/or animal health (WHO, 2017).

WHO sets “Guidelines” for a wide range of chemical parameters in drinking water. These are intended to be used on a worldwide basis and are generally in the form of upper concentration limits applied as annual mean values. The WHO recommends that

if the guideline value is exceeded, the proper health authorities should be consulted and action for water quality improvement should be planned, if necessary. The WHO and EPA guideline values for metals and metalloids in drinking water are shown in Table 1.1 below.

Table 1.1 Guideline values for heavy metals in drinking water recommended by the WHO and EPA.

Heavy metal	WHO (mg/L)	EPA (mg/L)
Arsenic (As)	0.010	0.010
Cadmium (Cd)	0.003	0.005
Copper (Cu)	2	1.3
Mercury (Hg)	0.001	0.002
Nickel (Ni)	0.07	0.04
Lead (Pb)	0.010	0.015
Zinc (Zn)	3	5

Heavy metal toxicity is known as non-biodegradable and bioaccumulative. Metal ions interact with cellular components like nucleic acids and nuclear proteins, causing DNA damage and conformational changes that may cause carcinogenesis. They can also displace the essential metal ions to lead cellular dysfunction. Heavy metal toxicity can reduce energy levels of cells, damage the functioning of multiple organs, and cause oxidative stress by producing reactive oxygen species. Long-term exposure can generate physical and neurological degenerative processes similar to diseases such as Alzheimer's disease, multiple sclerosis, Parkinson's disease, and muscular dystrophy (Jaishankar et al., 2014; Tchounwou et al., 2012).

Among the heavy metals, As, Cd, Cr, Hg, and Pb, are of major health concern, because of their high degree of toxicity and presence at relatively high concentrations in

drinking water. According to the International Agency for Research on Cancer (IARC), inorganic As and Cd are classified as Group 1 carcinogens for humans (IARC, 2016).

1.2.1. Arsenic Toxicity

Arsenic (As) has an atomic number of 33 and atomic mass of 74.92 amu and has four oxidation states (-III, 0, +III, and +V). Various forms of arsenic species include organic arsenic compounds, inorganic arsenic compounds, and volatile arsenicals. The forms of arsenic are dependent on the type and amounts of sorbents, pH, redox potential (Eh), physical, chemical, and microbial activities. Among them, arsenite, As(III), and arsenate, As(V), in the form of arsenic oxyanions, are the most dominant ones in aqueous systems. It is mostly found as arsenate if the water is oxygenated (e.g., aerated and well oxygenated surface waters) and found as arsenite under reducing conditions or anoxic conditions (e.g., groundwater, deep lake sediments) (Figure 1.2). Under oxidizing conditions, arsenic usually exists as one of a series of pentavalent (arsenate) forms such as H_3AsO_4^0 , H_2AsO_4^- , HAsO_4^{2-} , AsO_4^{3-} , depending on the Eh and pH conditions. In reducing water, arsenic is present as the trivalent (arsenite) form, which undergoes a similar series of dissociation reactions from H_3AsO_3^0 to H_2AsO_3^- and HAsO_3^{2-} .

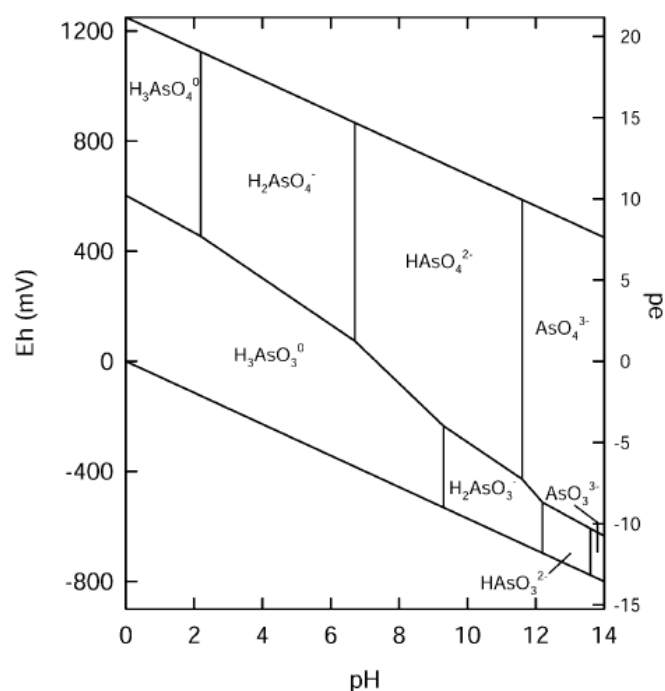


Figure 1.2 Eh-pH diagram for aqueous As species in the system As–O₂–H₂O at 25 °C and 1 bar total pressure (Smedley & Kinniburgh, 2002).

The toxicity and environmental mobility of arsenic depend on their oxidation states and chemical compounds. Inorganic forms are found to be more toxic and mobile than organoarsenicals. Majority of arsenic toxicity cases have been associated with exposure to inorganic arsenic. Furthermore, inorganic trivalent arsenic compounds which are arsenic trioxide, sodium arsenite, and arsenic trichloride are regarded as 2–10 times more toxic than pentavalent inorganic compounds such as arsenic pentoxide, arsenic acid, and arsenates (e.g., lead arsenate and calcium arsenate (WHO, 2011a; Wang & Mulligan, 2006). As(III) suppresses the activity of over 200 enzymes after binding to thiol or sulfhydryl groups on proteins, since affecting numerous organs. As(V) can replace phosphate, which can affect various biochemical pathways (Hong et al., 2014; Hughes, 2002).

Several epidemiological studies have reported that arsenic contamination in drinking water threatens public health for tens of millions of people all over the world,

increasing risks of both carcinogenic and systemic health effects (Ravenscroft et al., 2009). Arsenic poisoning most commonly causes diseases of blood vessels resulting in melanosis, keratosis, hyperkeratosis, dorsum, gangrene (known as black foot disease), and skin cancer. Excessive and long-term human intake of toxic inorganic arsenic causes arsenicosis which leads to cardiovascular, hepatic, renal, gastrointestinal, neurological, and reproductive problems, and malignancies (Chatterjee et al., 2017; Singh et al., 2015). Unfortunately, there are no effective medicinal drugs available for arsenicosis but some preventive measures to fight with the disease such as use of safe drinking water, nutritious food, and vitamins are recommended along with the effective chelation therapies (Majumdar et al., 2014).

1.2.2. Cadmium Toxicity

Cadmium (Cd) has an atomic number of 48 and atomic mass of 112.41 amu. It is found in the environment in only one oxidation state (+II) and does not undergo oxidation-reduction reactions. In groundwaters and surface waters, cadmium can exist as the hydrated ion or as ionic complexes with other inorganic or organic substances. Cadmium and its compounds have high solubility in water and high bioavailability as in inorganic complexes and its mobility depends on several factors such as pH and the presence of organic matter. (ATSDR, 2012).

Cd interacts with iron and decreases hemoglobin concentration leading to anemia, also it interacts with calcium and deposited in bones leading to osteoporosis and hypercalciuria. Cadmium disturbs zinc metabolism by inhibiting enzymes having zinc, and it replaces zinc in metallothionein since they have the same oxidation states (Chakraborty et al., 2013; Jaishankar et al., 2014). Prolonged exposure of humans to cadmium causes renal failure along with the osteoporosis that can lead to painful and debilitating bone disease, Itai-Itai, seen in many occurrences of elderly Japanese people after World War II, exposed to high levels of cadmium in rice and water. Moreover, smokers are more susceptible for cadmium toxicity than non-smokers,

because chronic exposure via inhalation of cadmium particulates is generally associated with cardiovascular and pulmonary diseases (ATSDR, 2012; Goyer & Clarkson, 2001).

1.3. Environmental Monitoring of Metal Contamination

The escalating contamination of environment results in an escalating number of initiatives and scientific attempts to assess metal pollution in water, air, and soil. Especially, limited drinking water sources are continuously contaminated and must be monitored constantly and globally. Their rapid detection is necessary for effective prevention before their public consuming, while being diverted to processing centers for its remediation. There are two main analytical methods for monitoring of chemicals and metals developed in two different directions, namely physicochemical analysis and biosensing methods.

1.3.1. Physicochemical Methods for Analysis of Metals

First approach involves instrument-based analysis represented by chromatographic and spectroscopic techniques. These methods are highly precise and aimed at both identification and quantification of substances. However, they have some disadvantages, including high cost, requirements of sophisticated instrumentation and qualified personnel/operators, complicated procedures, time-consuming sample preparation and pre-concentration, transportation of the sample from the site to the laboratory. Moreover, their use outside the laboratory is not feasible, they cannot perform multiplex analyses and it could take a long time to get results. Furthermore, they fail to provide hazard and toxicological information and synergistic/antagonistic behaviors of metals in mixtures. They also typically over-evaluate the total amount of environmental pollutants and cannot measure the bioavailability of the contaminants which is better to indicate the toxicity and effects of pollutants on living organisms. Nonetheless, they remain today the workhorse of the chemical identification and they are essential for regulatory purposes (Belkin, 2003; Eltzov et al., 2015a).

For the sensitive detection of heavy metals, a number of techniques have been developed and employed, including quantitative techniques inductively coupled plasma with mass spectrometry (ICP-MS), inductively coupled plasma with atomic emission spectrometry (ICP-AES), atomic fluorescence spectrometry (AFS), X-ray fluorescence spectrometry (XRF), neutron activation analysis (NAA) and inductively coupled plasma with optical emission spectrometry (ICP-OES), mostly combined with chromatographic methods such as high-pressure liquid chromatography (HPLC), ion chromatography (IC) and gas chromatography (GC) for speciation determination. By using these techniques, single and/or multiple species at low concentrations can be detected with sensitive quantification of total amounts of elements; however, large sample volumes and pre-treatment steps are required in order to meet the detection range of the instruments (Bansod et al., 2017; Morais et al., 2012).

For determination of arsenic, graphite furnace atomic absorption spectroscopy (GFAAS) with the detection limit of 1 µg/L, hydride generation atomic absorption spectrophotometry (AAS) with the detection limit of 2 µg/L and ICP-MS with a lower detection limit of 0.1 - 10 µg/L. HPLC in combination with ICP-MS can also be used to determine various arsenic species (WHO, 2011a).

For determination of cadmium, ICP-MS with the detection limit of 0.1 - 10 µg/L and AAS using either direct aspiration into a flame (with detection limit of 5 µg/L) or a furnace spectrometric technique (with detection limit of 0.1 µg/L) can be used (WHO, 2011b).

1.3.2. Biosensing Methods for Analysis of Heavy Metals

The second approach involves bioassay-based analysis and biosensors which are recently reviewed by Hassan et al. (2016) and Wang et al. (2014).

For bioassay-based analysis, numerous living systems have been used for water biomonitoring such as aquatic organisms like fish, mussels, water flea, algae, bacteria or plants to detect the acute toxicity of substances such as pesticides and heavy metals as a total systemic effect. Also, human or other mammalian cell lines have been used in toxicity assays to detect the overall effect of the whole mixture of pollutants (Van Wezel et al., 2010). The use of living systems in a variety of environmental bioassays is regarded as a complementary approach in terms of bioavailability and toxicological information to evaluate the toxic risk associated with contaminated water samples even though the contaminants are not clearly identified (Hassan et al., 2016).

Since the development of the first enzymatic biosensor for blood glucose detection, various biosensors have been developed and increasingly employed in different applications, including environmental and food monitoring, and for homeland security. A biosensor can be defined as a self-contained integrated device using a biological recognition element (bioreceptor) retained in direct spatial contact with transduction system, which is capable of providing selective quantitative or semi-quantitative analytical information. Biosensors convert a biological response into a measurable signal proportional to the concentration of the analytes with the help of a transducer. Biosensors are categorized according to types of biological and transduction elements. There are numerous bioreceptors that can be linked to different transducer elements (Figure 1.3). The main classes of bioreceptors are whole cells, enzymes, aptamers, peptides, antibodies and nucleic acids. The basic groups of transduction elements are electrochemical, piezoelectrical, optical, and thermal (Farré et al., 2009; Su et al., 2011).

The use of biosensors provides several advantages over laboratory-based approaches, such as incorporation into portable equipment, low cost, simplicity, specificity, rapid response, and in-situ application as well as online and remote measurement (Justino et al., 2017). They can assess both total and bioavailable metal concentrations with their biological effects like toxicity, cytotoxicity, and genotoxicity. Most importantly,

they offer a possibility for on-site and real-time detection of heavy metals with minimum effort (Mehta et al., 2016; Rodriguez-Mozaz et al., 2006).

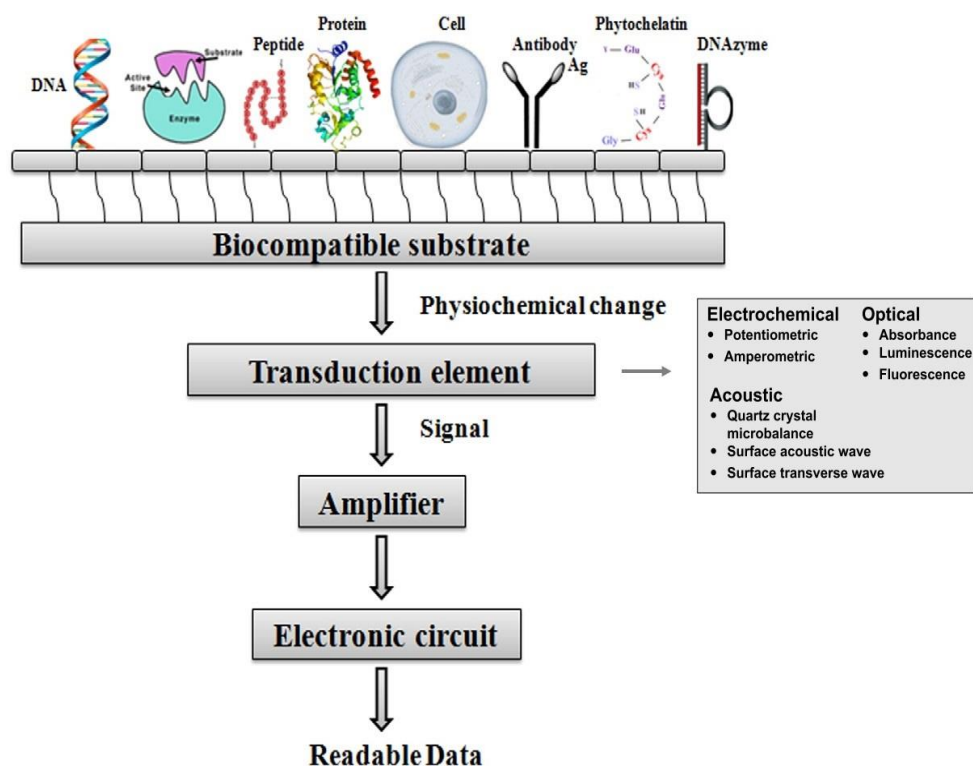


Figure 1.3 Schematic representation of biosensors with a variety of biosensing elements employed (Adapted from Mehta et al., 2016).

The main drawback of biosensors for the current legislations is that they do not give absolute concentration. Also, they are less reproducible than chemical methods since they depend on biological systems. However, they may uncover the presence of unexpected metal contaminants that can be missed by standard methods. On the other hand, since determination of absolute concentrations of toxicants in real-time is very unlikely, the use of biosensors could be suggested for on-line and real-time determination of toxicity levels (Stenuit et al., 2008). Thus, the best methodology to monitor a contaminated area appears to be the combination of an on-line monitoring biosensor system complemented by absolute chemical determinations taken

periodically. Furthermore, biosensors are needed for emergencies such as in the case of accidental spill of toxic metals, or of sudden natural phenomenon where rapid and portable equipment is needed (Farré et al., 2009; Woutersen et al., 2011). Finally, especially in developing countries, standard laboratory technologies may not be accessible, restricting the monitoring of contaminated areas.

Heavy metal biosensors can be classified as cell-free systems such as aptamers, nucleic acids, peptides, enzymes, antibodies, or proteins which act as either catalysts or inhibitors during the interaction with biomolecules, and whole cell-based systems. Diverse biosensors applying different couples of biological and transducer elements have been proposed for heavy metal detection and reviewed by Aragay et al. (2011), Mehta et al. (2016), Turdean (2011) and Verma & Singh (2005).

Although enzymes, antibodies and nucleic acids can detect metals quickly with very high specificity, the expression and purification systems must be optimized. Also, multiple enzymes to generate measurable product and cofactors/coenzymes are needed. Whole cell-based biosensors offer several advantages to overcome costly and time-consuming steps of cell-free systems. Different enzymes and cofactors already exist in cells, they are easily cultivated in inexpensive conditions, and do not require any special techniques for analysis. Besides, information about metal toxicity along with its bioavailability can be obtained, and finally, the requested whole-cell biosensors can be further modified with genetic manipulation (Gui et al., 2017).

1.4. Whole-Cell Biosensors

Microbial biosensors or whole-cell biosensors are analytical devices composed of microbial cells (e.g., bacteria, microalgae, and yeast) as the sensing element, and convert the detected signal into a quantifiable response such as in a biochemical, electrochemical, or physiological manner. Microbial cells are correspondent to “factory” having various enzymes and cofactors that give them the ability to respond

to a variety of compounds (Kim et al., 2018; Su et al., 2011). After 2000s, a large number of whole-cell biosensors have been developed as bio-sentinels to monitor soil, water and air for harmful pollutants ranging from organic matters, xenobiotics, sugars, radiation, metals to general and specific toxicants, which are recently reviewed by Nakamura (2018); Lim et al. (2015) and Xu et al. (2013).

Microbial cells have many advantages compared to higher organisms and other biosensing elements. First, they have a short doubling time and can grow in cheap nutrient media, so they can be produced in vast numbers in a short time using a simple culture process. Second, they can respond rapidly to environmental changes and to various contaminants such as heavy metals, phenolic compounds, organic pollutants, endocrine disruptors, and effluents from industrial activities (Eltzov & Marks, 2011; Hassan et al., 2016; Lei et al., 2006). Third, genetic engineering of microbial cells can be better controlled, and they can be tailored for detection of specific substrates with high selectivity and sensitivity by using advanced recombinant DNA and molecular biology technologies. Also, they can be manipulated by blocking the undesired or inducing the desired metabolic pathway and by adapting the microorganisms to a target chemical through selective cultivation conditions (Zhang & Keasling, 2011). Finally, most biosensors using cell-free system for heavy metal detection measure the total metal ion concentrations rather than the bioavailable concentration. In contrast, as being living entities, whole-cell biosensors can detect the bioavailable proportion of metal ions which is the maximum amount available for cell uptake that is freely available to cross the cellular membrane within a specified period of time. Thus, they not only qualitatively evaluate specific toxicants under a sub-lethal dose but also semi-quantitatively assess their chronic effects instead of the acute impact of global contamination (Kim et al., 2018; Rensing & Maier, 2003).

Despite the multiple advantages of whole-cell biosensors, their widespread use is hindered by some inherent features of microorganisms such as slow response compared to cell-free biosensors, susceptibility to interference by contaminants,

intrinsic cellular heterogeneity, and stochastic protein expression (Bereza-Malcolm et al., 2015; Lim et al., 2015).

1.4.1. Whole-Cell Bacterial Bioreporters

Among prokaryotic and eukaryotic microorganisms, bacteria have been extensively studied due to their benefits over eukaryotic microbial biosensors. They have longer evolutionary history of adaptation to diverse and extreme environmental conditions so that bacterial cells can have the desired metabolism and genetic parts. Bacteria can be genetically tailored easier than eukaryotic cells, and they can respond to specific chemicals or classes of chemicals in a dose-dependent manner. Moreover, due to high growth rates under aerobic and/or anaerobic conditions and short response time, bacterial cells can be easily used as biosensors (Jusoh & Wong, 2014; Struss et al., 2010). Among developed bacterial biosensors, *Escherichia coli* (*E. coli*), *Bacillus subtilis*, *Rhizobium leguminosarum*, and *Pseudomonas* species are widely used in the design whole-cell biosensors.

Of all whole-cell biosensors (WCBs) for detection of heavy metals, nearly 85% are based on prokaryotes mostly bacteria, while the rest 15% have been investigated using eukaryotic cells such as yeast, microalgae, fibroblasts and cardiomyocytes (Mehta et al., 2016). Various microbial designs for detection of heavy metal biosensors are reviewed by Bereza-Malcolm et al. (2015), Hynninen & Virta (2010), Kim et al. (2018) and Teo & Wong (2014).

1.4.1.1. Principles of Whole-Cell Bacterial (*E. coli*) Bioreporters

Over the course of the advancements of bacterial biosensors, the ‘bacterial bioreporter’ term has become the same as a genetically engineered bacteria in which one or more regulatory systems is deployed to produce a detectable and quantifiable signal output. For whole-cell biosensors, especially *E. coli* cells have been most widely used as chassis cells. In the literature, there are diverse reports where *E. coli*-

based biosensors or *E. coli* bioreporters have been custom-engineered for sensing a specific analyte including oxidants, DNA damaging compounds, aromatics, membrane-damaging compounds, protein-damaging compounds, xenobiotics, antibiotics, and so on. (Idalia & Bernardo, 2017; Jouanneau et al., 2017; Robbens et al., 2010). They are constructed by using plasmid or chromosomal elements for the detection of environmental traits or hazards or measuring cellular processes, with a rational design for a genetic circuit adapted from cellular sensory and regulatory systems (van Der Meer & Belkin, 2010).

Most commonly, *E. coli* whole-cell bioreporter systems carry an engineered plasmid by coupling a sensing regulatory element with its promoter/operator DNA sequence linked to a reporter gene that encodes a reporter protein producing the measurable signal (Figure 1.4). These sensing and/or reporter genes can be native or acquired by transformation. (Nivens et al., 2004; Xu et al., 2013).

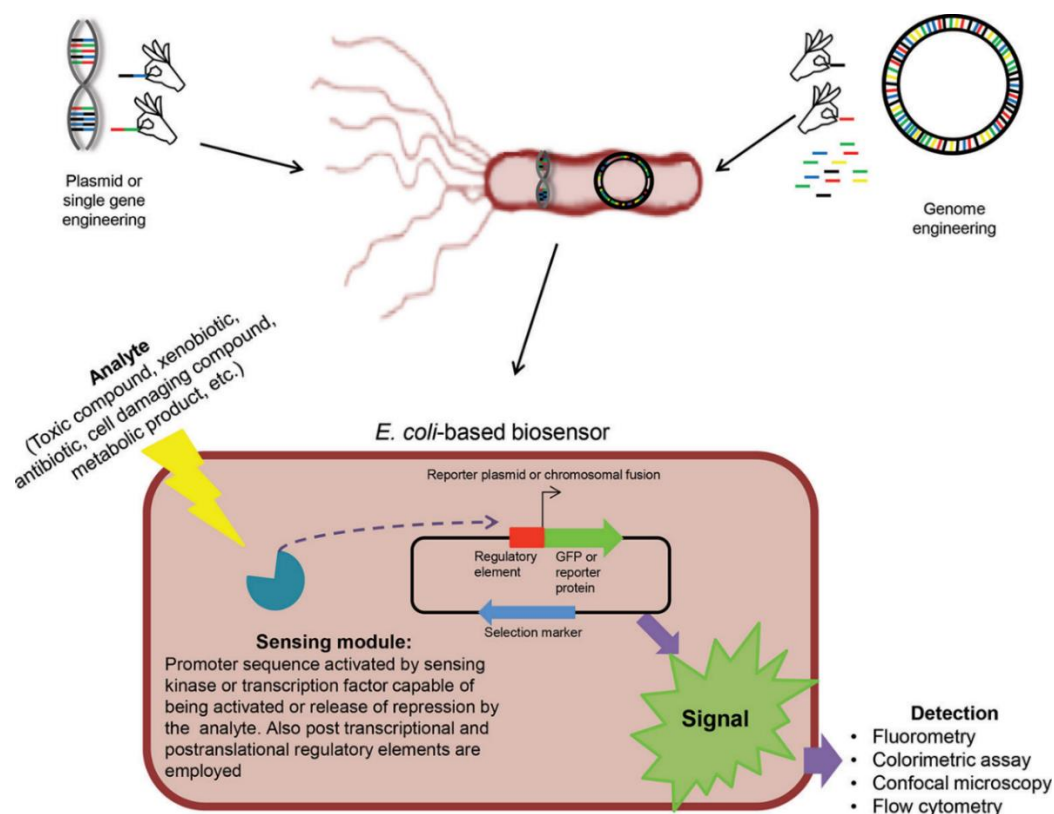


Figure 1.4 Scheme of *E. coli*-based biosensor design (Idalia & Bernardo, 2017).

Gene/operon promoters are specific and sensitive DNA elements present upstream of genes, controlling the translation open reading frames. Promoters are the target sites of regulatory proteins -repressors or activators, and so promoters are responsible for regulation downstream genes related to diverse cell functions such as regulation of temperature, ionic strength, toxins or metabolites, environmental stresses, etc. In the bioreporter cell, the link between promoter and these genes is broken and replaced with a reporter gene. Thus, upon activation by the promoter, reporter gene is transcribed and translated to a reporter protein that emits a measurable signal such as bioluminescent, fluorescent, or colorimetric. The intensity of the signal mostly becomes as a function of the concentration of analyte in the tested sample. To detect bioavailable environmental pollutants, promoterless reporter gene must be artificially brought under the control of a pollutant/toxicant-responsive promoter to measure promoter activity. Reporter proteins with easy detection and quantification, and high

sensitivity properties are preferable, and they are better be not present in the native organism. Thus, an ideal and effective biosensor strain relies on the proper choice of its two components: the promoter and the reporter gene (Paitan et al., 2003; Yagi, 2007).

Based on the signaling mechanisms, they are typically designed either a “lights-off” (constitutive systems) or “lights-on” (inducible systems) biosensors (Figure 1.5).

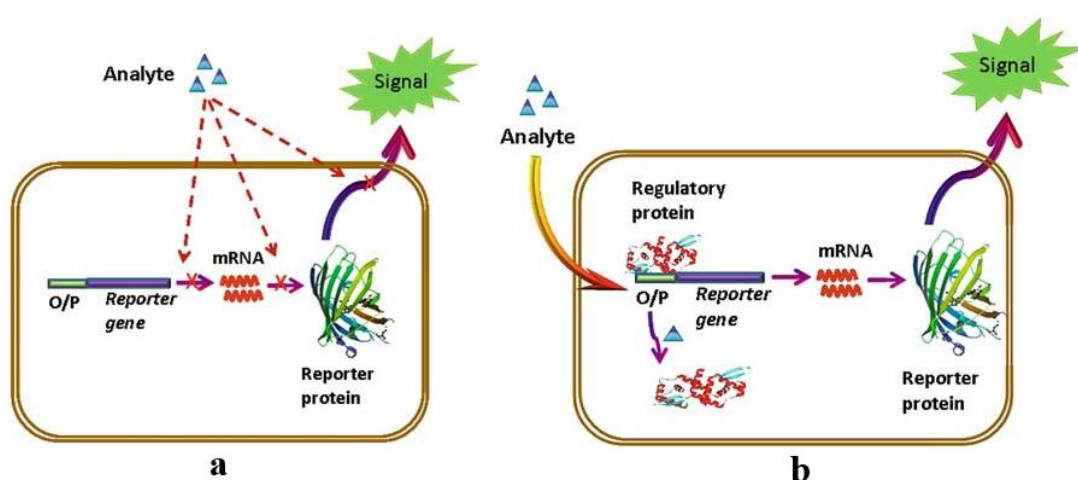


Figure 1.5 Schematic representation of the types of biosensors. a) “lights-off” biosensor having a constitutive whole-cell sensing system, b) “lights-on” biosensor having an inducible whole-cell sensing system (Date et al., 2010).

Based on the specificity of detection, bacterial bioreporters are mainly divided into three categories: non-specific, semi-specific and specific.

Nonspecific bioreporters are used for measuring general toxicity levels of samples and fail to identify the contaminants. They generally have lights-off system that is either natural bacteria (bioluminescent or fluorescent) or built by linking the reporter gene to a constitutive promoter. The toxicity of sample that harms the cell or disrupts cellular metabolism, is measured as a decrease or total inhibition in reporter protein activity in correlation to the degree of toxic interaction. They can be useful for acute

toxic incidences and pre-alarm to the need for further downstream analyses to identify the contaminants (Gu et al., 2004; Xu et al., 2014).

Semi-specific and specific bioreporters generally have lights-on system in which bacteria will not emit any signal until it encounters its designated target(s). Upon exposure, the promoter/reporter gene fusion directly associates with a class of chemicals or a particular chemical, emitting a subsequent signal of which intensity is proportional to the portion of bioavailable chemical (Sørensen et al., 2006). Semi-specific bioreporters are constructed with stress-induced promoters such as the heat shock or the salt overly sensitive (SOS) promoters, that allow the detection of general class of compounds that cause certain cellular responses, such as cytotoxic stress, oxidative stress, osmotic stress, membrane damage or DNA damage without further characterizing the compound (Shin, 2011). Specific bioreporters have a tightly regulated promoter and respond only to the compound in question, permitting a quantitative analysis of the contaminant concentration. The response is usually a measurable increase in reporter protein production. In this manner, specific bacterial bioreporters have been developed for heavy metals and several organic compounds. Binding of a metal ion to the transcription factor induces expression of the reporter gene, thus converting metal sensing into a detectable output signal (Hynninen & Virta, 2010; Yagi, 2007; Xu et al., 2014).

1.5. Heavy Metal-Specific Whole-Cell Bacterial Bioreporters

Many species of bacteria can exist and grow in diverse and extreme environments contaminated by heavy metals, and involve in transformations of metals (Fairbrother et al., 2007). Metal-resistant bacteria have evolved metal-resistance determinants and gene regulation pathways engaged in metal-ion homeostasis and metabolic detoxification. Bacterial resistance mechanisms have been described to be active against low concentrations of toxic metals (Pb, Hg, Cd, As, Sb, Ag, Tl) and very high concentrations of essential metals (Zn, Fe, Ni, Cu, Co, Cr). Significant knowledge of

bacterial metal resistance has been accumulated about genetic and regulatory mechanisms that specifically respond to heavy metals (Chandrangsu et al., 2017; Magrisso et al., 2008; Nies, 1999). The information about nucleotide sequences and genetic circuits of many genetic elements involved in metal resistance can be gathered from microbial genome or metagenome databases. Some of the metal resistance mechanisms are exclusion by cell permeability barrier, intra- and extra-cellular sequestration of metals, active transport of metals by efflux pumps, reducing cellular sensitivity to metal ions, and enzymatic detoxification. A group of bacteria may contain several transport/resistance mechanisms for one metal, whereas other groups may completely lack resistance to the same metal (Das et al., 2016; Olaniran et al., 2013).

The most commonly employed mechanism for development of metal-specific biosensors involves the usage of regulatory regions of genes/operons encoding efflux transporters that actively export the toxic metal ions to the outside of the cell, these pumps may be encoded chromosomally or acquired by mobile resistance factors (Ma et al., 2009). The induction of this particular defense mechanism occurs when metal ions are present at toxic concentrations and often involves a specific transcriptional regulator (metalloregulatory proteins), which activates the transcription of downstream defense related metal-resistance genes (Xu et al., 2013). Metal bioreporter constructs exploit this defense mechanism, redirecting the outcome into expression of the reporter gene. Since heavy metals at nanomolar concentrations are toxic to cells, bacteria can detect very low levels of metals that are also environmentally relevant. The sensing ability of the resistance mechanism determines the specificity (identity) and sensitivity (concentration) of bioreporter strain (Harms, 2007; Hynninen et al., 2010).

1.5.1. Heavy Metal Sensing Modules

Metalloregulatory proteins or metal sensor proteins form specific coordination complexes with metals that subsequently activate operator DNA binding or directly enhances transcriptional activation. Seven major families of metalloregulatory proteins can be divided into two groups (Ma et al., 2009). First group controls the gene expression for metal-ion efflux and/or intracellular storage belong to ArsR/SmtB family, MerR family, CsoR/RcnR family and CopY family, regulating via transcriptional derepression or an activation mechanism. Second group controls gene expression for metal ion uptake belong to Fur family, DtxR family and NikR transcriptional regulator, by binding metal ions as corepressors that causes the repression of the genes that allow for metal ion uptake. Among these, ArsR and MerR are very large families with members sensing a wide range of biologically required metal ions and heavy metals.

The ArsR/SmtB metalloregulators include ArsR (As, Sb), CadC (Cd, Pb), CzcR (Zn), and NmtR (Ni) which act as repressors by binding to the operator region to prevent RNA polymerase binding. Upon binding to specific metals, the binding affinity of the repressor proteins for its specific DNA operator sequence decreases and repressor proteins dissociate exposing promoter region. Consequently, this allows the initiation of transcription from their cognate promoter (Busenlehner et al., 2003).

The MerR family including members such as MerR (Hg), CueR (Cu), ZntR (Zn), and PbrR (Pb), act generally as activators. They bind to RNA polymerase-binding operator regions regardless of metal ion. When metal binds to activators, the DNA bends and twists into a position that opens the DNA structure and allows transcription to start (Brown et al., 2003).

Many types of heavy metal biosensors can be found in literature using sensing modules constructed from various metal-responsive transcription factors

(activators/repressors) along with regulatory regions such as operators, promoters, and ribosomal-binding sites. These can be retrieved from specific bacterial genome databases by BLAST search and transcriptome analysis.

1.5.1.1. Sensing Modules for Arsenic Detection

Some of the family members of ArsR/SmtB metalloregulatory proteins are *Synechococcus sp.* SmtB, *E. coli* ArsR, and *Staphylococcus aureus* pI258 CadC. Biosensor constructions for arsenic detection have exclusively been based on the ArsR protein, which is the transcriptional repressor of the arsenic resistance mechanism conferred by *ars* operon in many bacteria (Wu & Rosen 1993; Suzuki et al., 1998). Very often, research groups have used the *ars* operon derived from plasmid R773 and R46 of *E. coli*, in which case the *arsR* gene is the first in a series of five genes (Figure 1.5). Moreover, bacteria have a chromosomally encoded *arsRBC* operon which confers a moderate level of resistance to arsenic (Carlin et al. 1995).

One of the best characterized resistance systems to arsenic in bacteria is from the conjugative resistance factor R773 of *Escherichia coli* (Chen et al., 1985). It confers resistance against arsenate, arsenite and antimony with the expression of *arsRDABC* operon (Figure 1.6). *arsR* encodes for a transacting repressor protein, ArsR, that binds to the promoter of *ars* operon and inhibiting the transcription of the downstream genes in absence of arsenite, As(III). In its presence, ArsR binds As(III) and dissociates from the *ars* DNA, allowing the expression of the *ars* genes. *arsD* encodes a chaperone protein, ArsD, that binds and transfer As(III) to the catalytic subunit of the ArsAB efflux pump. ArsD also functions weak repressor of the *ars* operon, independent of inducer. *arsA* gene produces an oxyanion-stimulated ATPase, ArsA, interacting with ArsB to form an As(III) efflux pump energized by ATP hydrolysis. *arsB* encodes for an integral membrane protein, ArsB, that pumps arsenite out of the cell, thus diminishing arsenite accumulation. *arsC* encodes for arsenate reductase

enzyme, ArsC, that is able to reduce arsenate, As(V) to As(III), prior to extrusion of the latter oxyanion (Yang et al., 2012; Fekih et al., 2018).

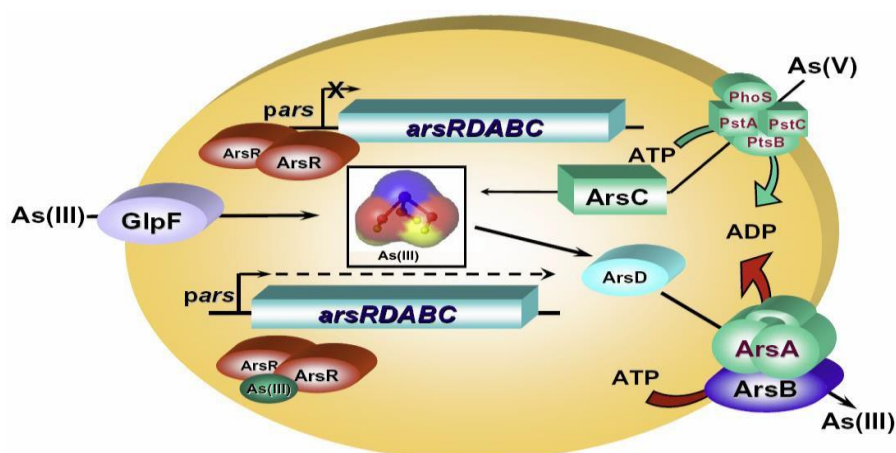


Figure 1.6 The *arsRDABC* operon of *E. coli* plasmid R773. Arsenic enters cells as either As(III) or As(V). As(III) is taken up by the aquaglyceroporin, GlpF, and As(V) is taken up by Pst and Pho phosphate permeases (Chen & Rosen, 2014).

The *ars* control switch has been applied many times for the construction of bioreporter bacteria, but exclusively in its native form with *arsR* as first gene under the control of its own promoter, followed by the reporter gene. Constant production of ArsR from its own promoter ensures that the system is turned off when arsenite is removed the cell, in which case non-As(III) bound ArsR represses the promoter. Bioreporters that employ the native configuration of the *ars* control system suffer from high background signals, which are the result of the low transcription rate that is necessary to produce ArsR and the read-through in the reporter gene.

Various arsenic sensor plasmids constructed by different sensing and reporter elements have been reviewed by Diesel et al. (2009), Merulla et al. (2013) and Kaur et al. (2015).

1.5.1.2. Sensing Modules for Cadmium Detection

Some of the family members of MerR metalloregulatory proteins members of the MerR family are MerR (as various mobile elements), *Streptomyces sp.* TipA, and *E. coli* SoxR, CueR and ZntR. There are various genetic circuit constructions for cadmium detection and one of them is based on the ZntR protein, which was the first described *E. coli* MerR-like metalloregulator (Brown et al., 2003). The *zntR* gene is physically separate from *zntA* promoter on the *E. coli* genome. The product of *zntR* gene, ZntR, is a regulator of *zntA* gene and binds *zntA* promoter in the absence of a class of heavy metals. In *E. coli*, *zntA* gene encodes an integral membrane protein of the CPx-type ATPase family that is responsible for active efflux of divalent metal ions such as Zn(II), Cd(II), Hg(II), Pb(II), Co(II) and Ni(II). Upon binding of these divalent metal ions, the conformation of ZntR changes and allows the RNA polymerase to transcribe *zntA* gene (Figure 1.7) (Brocklehurst et al., 1999; Rensing et al., 1997; Outten et al., 1999). Upregulation of *zntA* expression is induced mainly by zinc, cadmium, lead, and also mercury (Binet & Poole, 2000; Noll & Lutsenko, 2000).

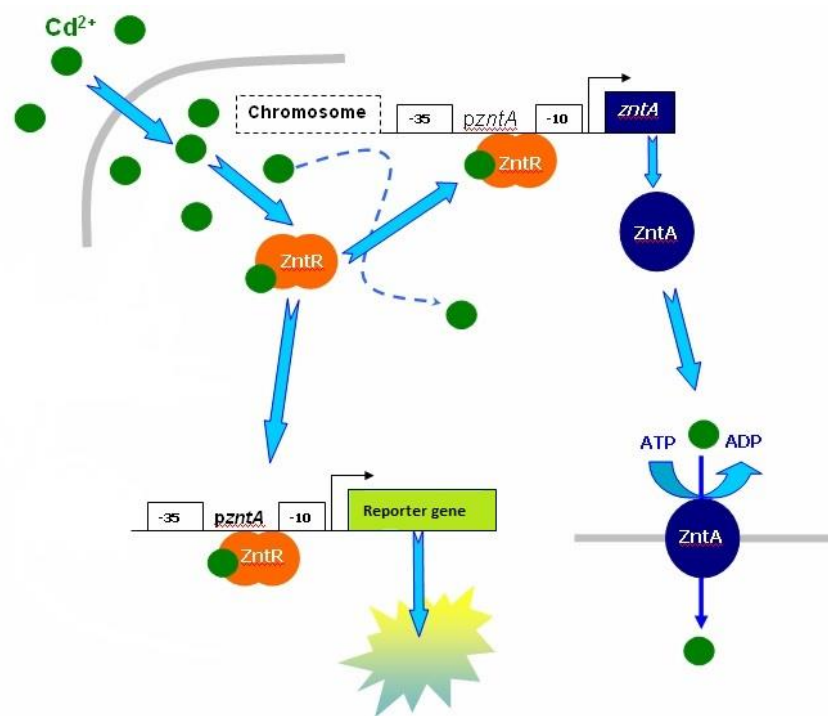


Figure 1.7 Regulation of the *zntA* promoter by the ZntR protein (Adapted from Charrier et al., 2010).

Especially, for the design of cadmium sensing plasmid, the *zntA* gene can be replaced by a reporter gene since cadmium induces expression of *zntA* at much lower concentrations than divalent metal ions. Bioreporters constructed using ZntR and the promoter of the *zntA* gene are most sensitive to Cd, but they are also induced by much higher concentrations of Pb, Zn and Hg (Kim & Yoon, 2016; Biran et al., 2000; Gireesh-Babu & Chaudhari, 2012; Ivask et al., 2002; Riether et al., 2001). Metal-activated transcription factors usually sense several different heavy metal ions with similar properties due to the limited possibilities for coordinate binding between proteins and metal ions. Thus, in practice it is not possible to construct a bioreporter strain that senses only one metal. Owing to variation in the binding affinities of metals, different metals can be sensed at different concentrations. Also, metal specificities can differ by different species of bacterial hosts (Hynninen & Virta, 2010).

1.6. Common Reporter Elements for Biosensor Constructions

Various reporter genes have been described that are isolated from naturally occurring microorganisms and classified based on their method of detection (Daunert et al., 2000; Köhler et al. 2000; van der Meer & Belkin, 2010). Among detection techniques, electrochemical and optical are most widely used for whole-cell biosensors (Close et al., 2009; Su et al., 2011). Particularly, optical detection is massively employed by using reporter proteins resulting in color development, bioluminescence, and fluorescence (Figure 1.8) (Pasco et al., 2011; Tecon & van der Meer, 2008; Yagi, 2007). Optical sensing techniques are mostly preferred in high throughput screening for monitoring multiple analytes simultaneously.

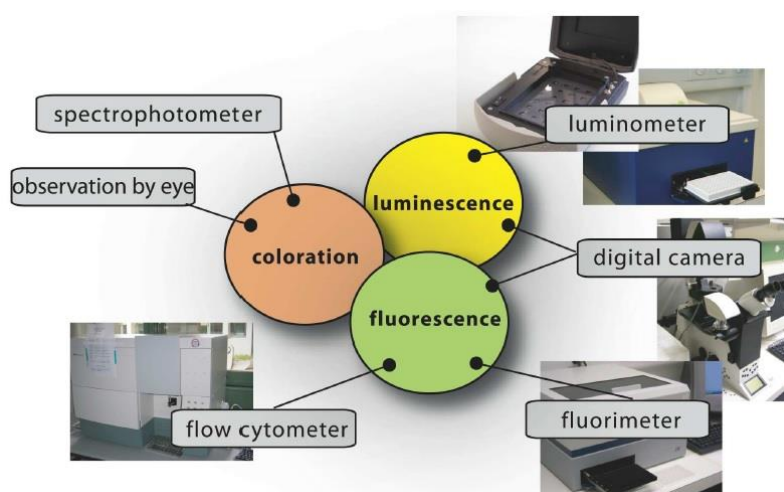


Figure 1.8 The instruments for measuring signal output for currently used reporters: fluorescent, bio- or chemiluminescent, and colorimetric (Tecon & van der Meer, 2008).

Commonly used reporter proteins for optical detection are β -galactosidase encoded by the *E. coli lacZ* gene generating coloration, fluorescent proteins such as GFP encoded by *Aequorea victoria*, and luciferases (firefly luciferase, Luc, and bacterial luciferase, Lux) encoded by eukaryotic *lucF* gene, and the bacterial *luxCDABE* genes (Table 1.2).

Table 1.2 Commonly used reporter genes and their characteristics (French et al., 2011).

Reporter	Characteristics
<i>lacZ</i> (β-galactosidase)	Chromogenic (X-gal, <i>o</i> -nitrophenyl galactoside) and chemiluminescent substrates are available. In <i>E. coli</i> host strains with the <i>lacZ</i> Δ <i>M15</i> mutation, only a small peptide representing the missing N-terminus, designated <i>lacZ'</i> α , is required.
<i>luxAB</i> (bacterial luciferase)	Blue bioluminescence in the presence of added substrate (a long-chain aldehyde, usually decanal).
<i>luxCDABE</i> (bacterial luciferase)	As above; presence of <i>luxCDE</i> allows biosynthesis of the substrate so that it need not be added to the reaction.
Firefly or click-beetle luciferase	Bioluminescence in the presence of added substrate (D-luciferin). Quantum yield is higher than for bacterial luciferase, but the substrate is much more expensive. Luminescence is normally green, but color variants are available.
Fluorescent proteins	Fluorescence when stimulated by ultraviolet or visible light. The original green fluorescent protein (GFP), still widely used, is stimulated best by ultraviolet; enhanced green fluorescent protein responds well to blue light, and numerous color variants are available.

The ideal reporter proteins should be easy to detect in small quantities, and not need addition of any reagents for generation of signal. Furthermore, it should be better to detect reporter activity using diverse instrumentation enabling measurements by different systems without having to modify the bioreporters. Ideally, a reporter protein is not naturally present in the host cell for the reporter construction because this may dramatically increase the background activity. Then, the reporter protein should obviously not be toxic for the producer cell or else its presence disturbs the reaction one wishes to measure and interpret. Finally, a reporter protein should allow non-

invasive measurement of its activity or presence to minimize disturbance to the study system. As a consequence, many reporter proteins are available and probably not a single one is ideal for all purposes (van der Meer, 2010).

1.6.1. Green Fluorescent Protein (GFP)

Green fluorescent protein, encoded by *gfp* gene, is one of the most popular reporters due to its good stability and sensitivity, and the fluorescence signal can be easily detected by different optical equipment without cell lysis (Su et al., 2011). The ability to autofluoresce allows for near real-time sensing and makes GFP bioreporters an effective method for heavy metal monitoring.

GFP is part of a family of natural and recombinant photoproteins isolated from the jellyfish *Aequorea victoria*. The small size of GFP (238 amino acids) provides a straightforward cloning procedure. GFP is an autofluorescent protein so that it does not require any exogenous substrate or ATP, which reduces the burden on the cell, and it isn't influenced by the kinetics of cellular uptake of substrate. It is also resistant to heat, alkaline pH fluctuations, chaotropic salts, organic solvents, and many proteases (Close et al., 2009). Moreover, GFP bioreporters are amenable to various techniques such as single-cell analysis by epifluorescence microscopy (EFM), laser-induced fluorescence confocal spectroscopy (LIF-CS) and fluorescence flow cytometry (FFM) (Kohlmeier et al., 2007). GFP emits a signal at 509 nm upon excitation with ultraviolet or blue light. Consequently, GFP-based bioreporters must always be connected to an instrument to deliver the excitation wavelength and measuring the emission wavelength (Xu et al., 2014).

Some of the limitations of GFP are its oxygen requirement but only of a limited amount, and difficulty in distinguishing GFP-specific fluorescence from the background autofluorescence when the GFP is poorly localized or expressed (Zimmer, 2002). GFP keeps accumulating in cell for hours and continues even after cell death

due to its high stability (Tombolini et al., 1997). This can hamper the dynamic real-time biosensing potential, but it can be particularly relevant because long-lived GFP expressed from weak promoters or under conditions of low metabolic activity can be useful for detection over time (Feliciano et al., 2006).

The specific amino acid substitutions in GFP can alter fluorescent characteristics, and there are many fluorescent variants with altered excitation and emission maxima such as in the red, yellow, cyan, and orange fluorescent proteins (Müller-Taubenberger & Anderson, 2007; Shaner et al., 2005). The presence of selectable colors gives the opportunity to develop bioreporters capable of sensing multiple analytes by linking individual promoters to differently colored fluorescent reporter genes. Due to their differently colored light emission outputs, they provide the ability of simultaneous detection of multiple targets that can be implemented in dual-color formats where each color indicates a separate event (Hever & Belkin, 2006). After the first isolation and characterization of GFP in 1970s, its genetic manipulations and applications have expanded greatly resulting in a wide range of mutant *gfp* genes encoding variants with different useful characters such as thermostability, enhanced fluorescence intensity, shifted excitation and emission spectra, no dimerization at high concentration, faster chromophore folding and optimized codon usage for expression in different hosts (Fukuda et al., 2000; Zacharias & Tsien, 2006).

1.7. Bioreporter Immobilization Methods

Irrespective of its sophisticated genetic engineering, practical application of a bacterial bioreporter outside the laboratory boundaries is only possible when they become miniaturized and portable biosensing device. This autonomous biosensors for on-line and real-time applications should allow long-term storage and maintenance of cells, sample introduction, and signal transduction. For efficient application of bacterial biosensors, the viability as well as activity and analytical performance of the cells should be preserved to obtain a reasonable “shelf-life” by either keeping their activity

at an optimum level over a long time or to restore the cells in active state at the time of sample exposure (Belkin, 2006; Roggo & van der Meer, 2017).

To overcome these challenges, different techniques for maintenance and preservation of biosensor cells have been proposed. One approach is to lyophilize by freeze/vacuum drying, second one is continuous cultivation by sustaining a constant pool of actively growing cells, third one is to immobilize them in biocompatible organic/inorganic polymers (Bjerketorp et al. 2006; Date et al., 2010). These methods with their advantages and disadvantages are given in Table 1.3.

Proper immobilization of bioreporter cells has several advantages such that it prevents wash out from flow cell while enabling efficient communication with the surrounding, gives better correlation to target concentration, provides essentially the same local aqueous microenvironment while preventing self-aggregation, occupies less space compared to free-cells, easier to handle, and can be used repeatedly. Moreover, whole cells could be associated intimately with the transducer/detecting platforms, instead of passive culture flasks, can convert the fluorescence light signal into electrical quantity to be processed and enable the measurement of many cellular parameters in a precise and quantifiable manner (Close et al., 2009; Gupta et al., 2019; Xu & Ying, 2011).

Table 1.3 Various methods for stabilization of bacterial biosensors (Bjerketorp et al., 2006).

Preservation method	Advantages	Disadvantages
Freeze drying (lyophilization)	Conserves formulation structure Proven industrial performance record Easily rehydrated product	Costly and complex technique Product sensitive to moisture
Vacuum drying	Yields potentially high survival rates and long-term stability Relatively low production costs Possible alternative for freeze-sensitive microorganisms	Less well-proven performance record Harsher drying conditions than freeze drying
Continuous culture	Provides a biocompatible static environment and fresh, active bacteria	Complex and labour-intensive maintenance Risk of genetic drift Risk of contamination
Encapsulation in organic polymers (e.g. hydrogels)	Immobilisation, physical shielding and isolation Allows solute diffusion	Biodegradable Bacterial growth may occur Opacity may hinder optical signal detection
Encapsulation in inorganic polymers (e.g. sol-gel)	Immobilisation, physical shielding and isolation Mechanical rigidity and good optical properties Allows solute diffusion Limits bacterial growth	Less well-proven performance record Tested for a limited variety of microorganisms

The immobilization methods have been improved with the time (D'Souza, 2001) and several immobilization strategies have been utilized for supporting bioreporter cells onto solid platforms. Frequently used methods are shown in Figure 1.9. As a result of immobilization onto portable devices, optical fibers, and high-throughput platforms such as 2D and 3D cellular microarrays, multi-well microtiter plates, microfluidics platforms, integrated circuits and 3D-printed cell minicartridges can be obtained (Ben-Yoav et al., 2011; Cevenini et al., 2016; Hong et al., 2017; Shin, 2011).

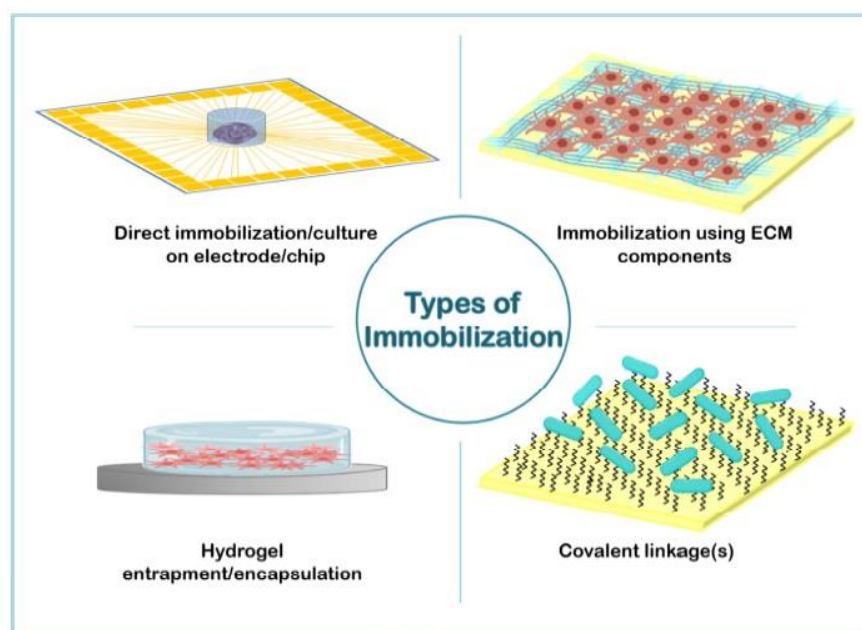


Figure 1.9 Schematic representation of the prevalent methods for immobilization of whole-cell sensing systems (Gupta et al., 2019).

The choice of the immobilization technique is critical and determined by the criteria of biological activity, sensor stability and durability, sensing specificity, proximity of the biological layer to the transducer, and measurement rate (i.e. the diffusion characteristics of a support (Date et al., 2010; Eltzov & Marks, 2011).

1.7.1. Entrapment/Encapsulation Methods

One of the most widely used and the least disruptive methods for immobilization is encapsulation or entrapment of bioreporters (Zhu, 2007). It can be achieved by the retention of the cells in close proximity of the transducer surface using dialysis or filter membrane or in biopolymers (e.g., agar, carrageenan, or alginate), proteins (e.g., gelatin, collagen, or egg white), synthetic polymers (polyacrylamide, polydimethylsiloxane (PDMS), sol-gel silica glass, photo cross-linkable resin, polyethylene glycol (PEG) (Lei et al., 2006; Michelini & Roda, 2012; Xu & Ying, 2011).

Entrapping and encapsulation bacteria in a hydrogel is straightforward, rapid, and mild process and functional at ambient temperature. In theory, encapsulated cells should remain viable but not growing which is very important when immobilized cells have to be stored for long periods of time without loss of viability. Hydrogels (such as collagen, fibrin, alginate, and PEG) are extensively used as biomaterials to mimic extracellular matrix (ECM) due to their cytocompatibility, moldability, tunability in mechanical properties, highwater content, and controlled porosity, which can provide a suitable environment for diffusion of oxygen and nutrients and samples. Usually, the application of substances to the bioreporter requires mixing the cell culture with a liquid polymer (Ben-Yoav et al., 2011; Chen et al., 2016; Michelini & Roda, 2012).

1.7.1.1. Agar immobilization

Agar is a commonly used hydrogel polymer. It is a dried colloid extracted from the cell wall of certain macroalgae of the *Rhodophyceae* class. Agar is a mixture of polysaccharides and has two major fractions, agarose and agarpectin. Chemically, it is made up of alternating D- and L-galactopyranose units. It has also been widely studied and applied in the biomedical field because of its good biocompatibility, biodegradability, nontoxicity. Agar entrapment has certain advantages such as easy preparation, low cost, good mechanical and acid stability. Agar is insoluble in cold water and melts around 85 °C. For 1.5% agar solution, gelation starts when its temperature drops below 45 °C (Albuquerque et al., 2016; Rinaudo, 2008).

One example of agar application in bacterial bioreporter, cell chip or a multi-well plate preparation by dispersing the cell–agar mixture. Then the toxicity assessment of sample water was done by measuring bioluminescence change using a highly sensitive cooled charge-coupled device camera. (Lee et al., 2007).

1.7.1.2. Alginate immobilization

Alginate or alginic acid is another widely used biocompatible hydrogel biopolymer derived from marine brown algae. It is an anionic linear polysaccharide consisting of 1,4-linked β -D-mannuronic acid (M) and α -L-guluronic acid (G), present in varying amounts. Its physical properties in aqueous medium are determined by both the M/G ratio and the distribution of M and G units along the chain (Rinaudo, 2008). It can form gel (crosslinked network) in the presence of divalent cations such as calcium, Ca^{2+} , and the higher content of G units form stable crosslinked junctions with divalent counterions (Figure 1.10a). This spontaneous ionic gelation of alginates is attractive for cell entrapment (Albuquerque et al., 2016). The resultant insoluble calcium alginate beads are recognized as rapid, nontoxic, inexpensive, and versatile form of immobilization.

These beads can be formed by extrusion or emulsification techniques. In the extrusion method, the cells are suspended in sodium alginate (2–4% w/v) solution and added dropwise into a calcium chloride (20–100 mM) hardening solution (Figure 1.10b). In the emulsification method, the cell/alginate suspension is dispersed into an oil phase and gelation then occurs when calcium is added.

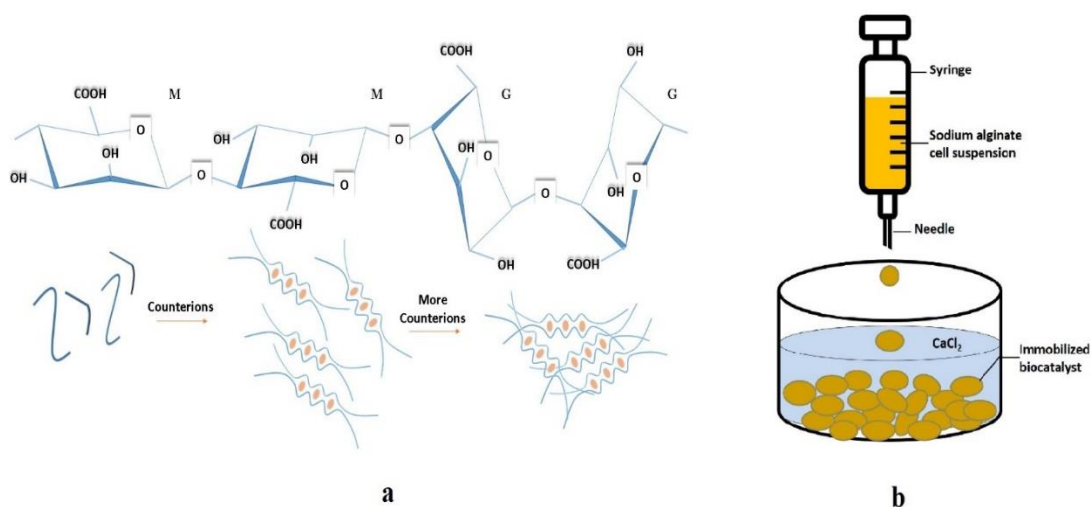


Figure 1.10 Ionotropic gelation of alginate solution. a) Chemical structure of alginate and the crosslink between alginate and the counterions (Albuquerque et al., 2016), b) Extrusion method, representing the formation of calcium-alginate beads (Gao et al., 2016).

The factors affecting the bead properties like gel strength, size, stability, and subsequently cell activity include the type of alginate (viscosity, monomeric composition, block structure, and molecular size), alginate concentration, CaCl_2 concentration and cell/alginate ratio (Zhu, 2007). Alginate bead preparation is a rapid and mild process that can be carried out at room temperature and physiological pH. Moreover, calcium alginate beads are biocompatible, inexpensive, transparent, permeable, highly porous and having high-water absorption capacity and high mechanical strength and stability (de-Bashan & Bashan, 2010; Ulah et al., 2015).

As an example, Polyak et al. (2001) immobilized their bioluminescent *E. coli* bioreporter cells onto unclad optic fiber tips by using alginate for detection of genotoxic compounds. After coated tips were dipped into a water sample, the response was read by a photon counter at the other end of the fiber.

1.8. Aim of the Study

The main aim was to construct fluorescent *E. coli* whole cell bioreporters to be used for the detection of highly toxic and prominent heavy metals, namely inorganic arsenic and cadmium. The studies included generation of heavy metal specific *E. coli* strains and their evaluation in terms of metal specificity and detection limits as bioreporter systems. Their fluorescence performances were characterized under different conditions including growth phase of induction and growth media.

The second aim was to convert the liquid assay format into reproducible solid format later to be integrated into portable biosensor devices enabling in-field detection. To this end, immobilization of arsenic bioreporter strain was investigated in different biocompatible polymers, agar and alginate, by optimizing their entrapment parameters. Then, immobilized arsenic bioreporters were evaluated in terms of their specificity and limits of detection.

CHAPTER 2

MATERIALS AND METHODS

2.1. Materials

2.1.1. Bacterial Strains and Plasmids

E. coli DH5 α was used as the host for recombinant DNA protocols (for recombinant plasmid constructions). pET-17b (Novagen, Madison, WI) was used as an expression vector which has medium copy number with T7 inducible promoter. *E. coli* BL21 (DE3) pLysS (Novagen, Madison, WI) cells were used as expression host for pET-sGFP construct. pBR322 (Promega, USA) was used as a cloning vector. *E. coli* MG1655 (ATCC 700926) strain was used as the whole cell bioreporter host.

2.1.2. Growth Media

E. coli strains were grown in Luria-Bertani (LB) Broth (Appendix A) for cloning purposes. M9 supplemented medium and MOPS supplemented medium (Appendix A) were used for heavy metal detection assays. Ampicillin (100 μ g/mL) was added to the culture for plasmid maintenance and positive selection.

E. coli strains were maintained in LB-Amp petri dishes and as freezer stocks in 20% glycerol and stored at -80 °C. Prior to use stocks were cultured in Luria-Bertani media, inoculated flasks were incubated at 37 °C on a rotary shaker at 125 rpm. Once exponential growth was achieved, a 100 μ L aliquot was transferred into a flask containing 25 mL of shaken minimal medium. After the first transfer into minimal medium, 200 μ L were transferred to a flask containing 50 mL shaken minimal medium.

2.1.3. Chemicals, Enzymes and Kits

Compositions of solutions and buffers were given in Appendix B. All solutions were prepared by using sterile distilled water. All the enzymes used for DNA manipulations, PCR and cloning were purchased from New England Biolabs (USA) and Thermo-Scientific (USA). Bacterial genomic DNA was isolated using Bacterial Genomic DNA Isolation Kit, for Gram-negative bacteria (Nanobiz, Turkey). Plasmid DNA was isolated from bacterial strains using Zippy Plasmid Miniprep Kit (ZymoResearch, USA). DNA purifications were carried by using DNA Clean& Concentrator-5 (ZymoResearch, USA). Plasmid DNA fragment was isolated from agarose gel by using Zymoclean™ Gel DNA Recovery Kit (ZymoResearch, USA). AgNO₃, CdCl₂, CoCl₂, CuSO₄, FeCl₃, HgCl₂, MgCl₂, MnCl₂, Na₂MoO₄, NaAsO₂, Na₂HAsO₄·7H₂O, NiCl₂, Pb(CH₃CO₂)₂·3H₂O and ZnCl₂ metal salts were supplied from Merck, Sigma-Aldrich and Applichem. Agar (05039) and alginic acid sodium salt (71238-for immobilization of microorganisms) were purchased from Sigma-Aldrich.

2.1.4. Instruments

The cell growth was measured using Multiskan GO UV/Visible Microplate and Cuvette Spectrophotometer (Thermo Fisher Scientific, U.S.A.) at 600 nm. Purity and concentration of DNA were measured by a Biodrop Duo UV/Vis Spectrophotometer (Isogen Life Science, the Netherlands). For 96-well microplate experiments, fluorescence measurements were done by using fluorescence microplate readers. For fluorescence measurements of liquid assay of arsenic bioreporter, Spectramax Paradigm (Molecular Devices, USA) was used. For fluorescence measurements of liquid assay of cadmium bioreporter and of immobilized arsenic bioreporter, Varioskan Lux multimode microplate reader (Thermo Fisher Scientific, USA) was used at $\lambda_{\text{excitation}}$: 395 nm and $\lambda_{\text{emission}}$: 509 nm with a bandwidth value of 12 nm.

For large scale induction cultures including groundwater test with arsenic bioreporter and pET expression cultures, the emitted fluorescence was measured using Nanodrop 3300 Fluorospectrometer (Thermo Fisher Scientific, USA) at excitation λ : 365 ± 10 nm (UV LED) and emission λ : 509 nm.

After cells were pelleted and resuspended with 1X PBS (Appendix B), fluorescence images were taken by using EVOS Fluid Imaging Station (Thermo Fisher Scientific, USA) under illumination of blue channel with excitation of 390 ± 40 nm and emission of 446 ± 33 nm and fluorescence microscope, Leica DM6000 M Fully Automated Upright Microscope at bright field and fluorescence channel with fluorescence I3 filter (excitation range: blue, excitation filter: BP 450-490), with 1 minute of exposure time and 100X total magnification.

2.2. Molecular Genetics Methods

2.2.1. Design of DNA Fragments and Polymerase Chain Reaction (PCR) Primers

The reporter protein was chosen as GFPuv which is a mutant variant of wild type GFP; however, throughout this study the reporter protein is referred as synthetic GFP (sGFP). The sequence of promoterless *sgfp* gene fragment is based on the *gfpuv* gene in pGFPuv (GenBank Accession Number U62636.1) (Appendix C). It was synthesized by Integrated DNA Technologies (USA) and amplified using oligonucleotides sGFP-F and sGFP-R (Table 2.1) as primers. *BamHI* restriction site in the original *gfpuv* gene was disabled and a new *BamHI* site was created upstream of the synthetic *gfp* DNA fragment for insertion of promoter regions. Also, extra stop codons were added downstream of the stop codon of original *gfpuv* gene. This *sgfp* DNA fragment has no promoter region such that following restriction of cloning sites there is an immediate start codon.

The arsenic sensing DNA fragment consisting of the promoter/operator of the *arsR* operon and *arsR* gene from *E. coli* resistance plasmid R773 (GenBank Accession

Number X16045.1) (Appendix C) was synthesized by PRZ Biotech (Turkey) and amplified using oligonucleotides arsR773-F and arsR773-R (Table 2.1).

The cadmium sensing DNA fragment consisting of the promoter/operator of the *zntA* gene (Gene ID number: 947972) (Appendix C) was amplified from *E. coli* K12 MG1655 genomic DNA using oligonucleotides zntAp-F and zntAp-R (Table 2.1).

For specificity of designed oligonucleotides, NCBI/Primer-BLAST web tool (<http://www.ncbi.nlm.nih.gov/tools/primer-blast/>) was used. T_m values of primer pairs were checked in T_m calculator web tool.

Table 2.1 Gene specific primers designed for different cloning vectors.

Primer name	Oligonucleotide Sequence	Restriction enzyme
sGFP-F (pBR322)	5'-GCAGAA <u>AAGCTT</u> GTCTGGATCCATG-3'	<i>HindIII</i>
sGFP-R (pBR322)	5'-TGCTTCCCGAGTTATCATTATTT-3'	<i>Eco88I</i>
sGFP-F (pET-17b)	5'-GCATGAGGATCCATGAGTAAAGGAGAAGAAC-3'	<i>BamHI</i>
sGFP-R (pET-17b)	5'-GCATGAGAATTCTTATTTGTAAGCTCATCCATG-3'	<i>EcoRI</i>
arsR773-F (pBR-sGFP)	5'-GTTGTAGAATTCAGCGGATCAGTTCCAGCAG-3'	<i>EcoRI</i>
arsR773-R (pBR-sGFP)	5'-GCAGTTGGATCCTTAAGTCAAATGTTCTTACT-3'	<i>BamHI</i>
zntAp-F (pBR-sGFP)	5'-GTGACAGAATTCGCGCTGTTACTGGCGATTATC-3'	<i>EcoRI</i>
zntAp-R (pBR-sGFP)	5'-GTATGTGGATCCATCCTCCGGTTAAGTTTTTTC-3'	<i>BamHI</i>

-Restriction sites are underlined.

2.2.2. Bacterial Genomic DNA Isolation

E. coli K12 MG1655 genomic DNA was isolated for promoter amplification. Genomic DNA isolation was performed by using Nanobiz DNA4U Bacterial Genomic DNA Isolation Kit for Gram-negative bacteria. Purity and integrity of the plasmid DNA were confirmed by Biodrop Duo spectrophotometer and gel electrophoresis, respectively. The isolated genomic DNA was stored at -20°C until use.

2.2.3. Isolation of Plasmid DNA from Bacteria

Miniprep plasmid DNA isolation was performed by using Zippy Plasmid Miniprep Kit (ZymoResearch, USA) according to the manufacturer's instructions. Purity and integrity of the plasmid DNA were confirmed by Biodrop Duo spectrophotometer and gel electrophoresis, respectively. The isolated plasmid DNA was stored at - 20 °C until use.

2.2.4. Agarose Gel Electrophoresis of DNA

Plasmid molecules and PCR products were visualized on agarose gel which was performed according to Sambrook & Russel (2001). Different gel concentrations (0.8-2 % w/v) were prepared in 1X TAE electrophoresis buffer solutions. The samples to be loaded were mixed with 6X DNA gel loading dye (Thermo Fisher Scientific, USA) and applied into the wells. Together with the samples, commercial DNA size marker Thermo-Scientific GeneRuler 1 kb DNA Ladder (SM0311) was loaded into separate wells to determine approximate size of samples. Then the electrophoresis tank was connected to a power supply and run under constant voltage of 90-100 volts. The resolved gels were visualized and documented with UVP gel imaging system.

2.2.5. Isolation of DNA Fragments from Agarose Gel

PCR products, restriction enzyme digested DNAs and plasmid DNAs were loaded on 2% agarose gel run at 90 V and visualized under the UV light. Desired DNA fragment

bands were excised from the gel as quickly as possible and gel piece was transferred into 2-mL tube and weighed. The volume of the sliced gel was determined by its weight and Zymoclean™ Gel DNA Recovery Kit (ZymoResearch, USA) was used for isolation of DNA fragment from gel.

2.2.6. Restriction Enzyme Digestions

Restriction enzymes from Thermo-Scientific (USA) were used for all restriction enzyme digestion reactions. Double digestion reactions were preformed according to DoubleDigest™ web tool (<https://www.thermofisher.com/tr/en/home/brands/thermo-scientific/molecular-biology/thermo-scientific-restriction-modifying-enzymes/restriction-enzymes-thermo-scientific/double-digest-calculator-thermo-scientific.html>) which supplies selection of recommended buffer for double digestion reaction. Plasmid DNA (~ 100 ng) and/or PCR products (~ 50 ng) were digested with restriction enzymes (10 U/μL) in a reaction mixture including proper enzyme buffers in recommended final concentration. Total reaction volume was completed to 20 μL with nuclease-free water and incubated at 37° C in thermocycler for 14 hours for complete digestion. Digested products were then either column purified using DNA Clean& Concentrator-5 (ZymoResearch, USA) or gel purified using Zymoclean™ Gel DNA Recovery Kit (ZymoResearch, USA).

2.2.7. Ligation of DNA Fragments

T4 DNA ligase (NEB) was used for ligation reactions according to manufacturer's recommendation. Concentration of the plasmid and insert DNA was determined by using Biodrop Duo spectrophotometer and by comparing the relative band intensities of products with the bands in prescribed amount of DNA ladder. Ligation mixture contains 1:3 molar ratio of plasmid:insert DNA. The ligation mixture was incubated for 16 hours at 16°C for complete ligation and then T4 ligase was heat denaturated at 65 °C for 10 mins. Ligation reaction mixture was then transformed into the competent *E. coli* DH5α cells.

2.2.8. Transformation of Bacteria

The cloning and expression vectors used were transferred to competent *E. coli* cells via the heat shock method.

2.2.8.1. Preparation of Competent *E. coli* Cells

E. coli DH5 α and *E. coli* MG1655 strains from the glycerol stock were streaked onto LB agar plate and were grown overnight at 37°C. A single colony of bacterial strain was inoculated into 5 mL of LB medium and incubated overnight at 37°C with shaking at 250 rpm. From this, subculture was made by diluting 1:100 into LB medium and grown until reach to exponential phase ($OD_{600} = 0.3 - 0.5$). The culture was incubated on ice for 15 minutes and from this point, the cells were kept on ice during procedure. The cells were centrifuged at 3500 xg for 10 minutes at 4°C in Sigma Laboratory Centrifuge Model 3-16PK, Germany, using a pre-chilled rotor. The pellet was resuspended in 0.4 volume (100 mL for 250 mL culture) transformation buffer I (Appendix B) and incubated on ice for 15 minutes. The cells were lastly centrifuged at 3500 xg for 10 minutes at 4°C and supernatant was discarded. The second resuspension was made with 0.04 volumes (10 mL for 250 mL culture) of transformation buffer II (Appendix B). The cells were finally dispensed in 100- μ L aliquots of cells into 2-mL tubes. Tubes were flash frozen in liquid nitrogen and stored at -80°C.

2.2.8.2. Transformation of *E. coli* with Plasmids

Ligation products or plasmids were added into competent *E. coli* cells which were thawed on ice for 5 mins. This cell and DNA mixture was incubated on ice for 30 minutes and then a heat shock at 42°C for 60 seconds was applied to facilitate the entrance of ligation products or plasmids into the cells. The mixture was immediately incubated on ice for 5 minutes. Then, 900 μ L of room temperature LB medium was added on bacteria cell suspension and grown at 37°C for 70 minutes. Finally, 150 μ L

transformed bacterial cells were spread onto pre-warmed LB agar plates with ampicillin (100 µg/mL) which were inverted and incubated overnight at 37°C for 18 hours for bacterial colony formation.

2.2.9. PCR Amplification of Synthetic *gfp* Gene

PCR amplification of synthesized *gfp* DNA fragment with gene specific forward and reverse primers (for either pET-17b or pBR322) was performed by using *Phusion* DNA polymerase. PCR conditions and program used for PCR amplification are given in Table 2.2 and Table 2.3, respectively. *Phusion* polymerase is a high-fidelity DNA polymerase with 3'→5' exonuclease activity and generates blunt-ended products. After all other components were added to PCR tube, *Phusion* DNA polymerase enzyme was added to the mixture and contents were mixed by tapping the tube gently and briefly spinning the tubes once in a microfuge. PCR reaction on the above mixture was carried out as per reaction conditions given in Table 2.3. At the end of the reaction the tubes were removed from thermocycler, and the PCR mix was electrophoresed as described. For determining the size of the DNA band of interest, a maker was also electrophoresed. At the end of electrophoresis, the gel was photographed as described. Amplified fragment was purified using DNA Clean & Concentrator-5 (ZymoResearch, USA).



Figure 2.1 Graphical representation of promoterless synthetic *gfp* DNA fragment.

Table 2.2 Optimized PCR condition for amplification of *sgfp* gene.

Reagents	Stock	Amount	Final conc.
dNTPs	5 mM	1 μ L	250 μ M each
HF Buffer	5X	4 μ L	1X
Forward gene specific primer	10 μ M	1 μ L	0.5 μ M
Reverse gene specific primer	10 μ M	1 μ L	0.5 μ M
Synthesized DNA fragment	10 ng/ μ L	1 μ L	0.5 ng/ μ L
<i>Phusion</i> DNA Pol	2 units/ μ L	0.2 μ L	0.02 units/ μ L
dH ₂ O		11.8 μ L	
Total		20 μL	

Table 2.3 Optimized PCR cycling conditions for amplification of *sgfp* gene.

PCR Steps		Temperature	Time	Cycle
Initial denaturation		96 °C	30 sec	1
Amplification	Denaturation	97 °C	20 sec	10
	Annealing	62 °C	20 sec	
	Extension	72 °C	25 sec (15-30 sec/ 1 kb)	
Final Extension		72 °C	4 min	1

2.2.10. Cloning of *sgfp* into pET-17b Expression Vector (pET-sGFP)

The pET-17b vector carries an N-terminal 11aa T7 Tag sequence followed by a region of useful cloning sites (Figure 2.2). Target genes are cloned in pET plasmids under control of strong bacteriophage T7 transcription and translation signals; plasmids are transferred into expression hosts having a chromosomal copy of the T7 RNA polymerase gene under *lacUV5* control, and expression is induced by the addition of

isopropyl β -D-1-thiogalactopyranoside (IPTG) following manufacturer's instructions (Figure 2.3).

The *sgfp* DNA fragment was *Phusion* amplified by using oligonucleotides sGFP-F (pET-17b) and sGFP-R (pET-17b) (Table 2.1). Both *sgfp* PCR product and pET-17b plasmid were double digested with *EcoRI* and *BamHI* restriction enzymes overnight at 37 °C and ligated by T4 DNA ligase. Thus, *sgfp* gene was introduced into multiple cloning sites in pET-17b and the construct was named as 'pET-sGFP'. Then ligation product was transformed to competent *E. coli* DH5 α cells. After finding the right transformant, pET-sGFP was transformed into *E. coli* BL21 (DE3) pLysS competent cells for expression. Transformation was done according to manufacturer's instructions.

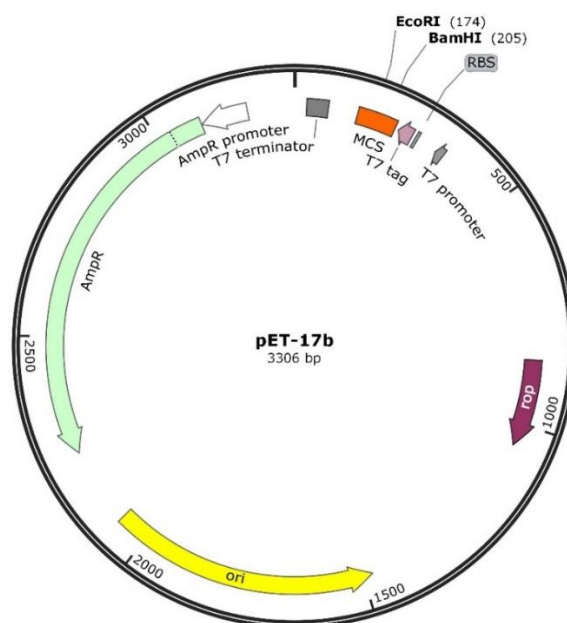


Figure 2.2 Vector map of pET-17b. (AmpR: Ampicillin resistance gene; ori: pBR322 origin; MCS: multiple cloning site).

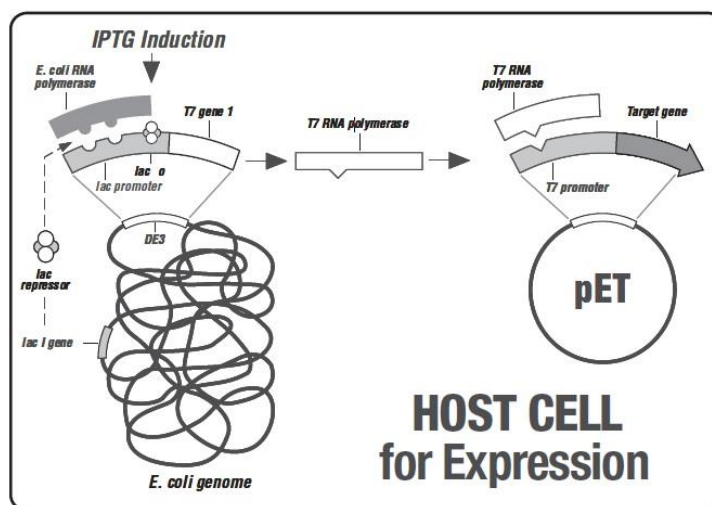


Figure 2.3 Graphical abstract of pET expression system. Addition of IPTG to a growing culture induces T7 RNA polymerase production, which in turn transcribes the target DNA in the plasmid (Novagen pET system manual).

2.2.11. Cloning of *sGFP* into pBR322 Vector (pBR-sGFP)

For template vector of reporter plasmids, *E. coli* cloning vector, pBR322 (GenBank Accession Number J01749.1) was used. Promoterless *sgfp* gene was *Phusion* PCR amplified by using oligonucleotides sGFP-F (pBR322) and sGFP-R (pBR322) (Table 2.1). The amplified DNA fragment and pBR322 were double digested with *HindIII* and *Eco88I* (*AvaI*). The large fragment of digested pBR322 was extracted from gel by using Zymoclean™ Gel DNA Recovery Kit (ZymoResearch, USA) and digested *sgfp* product was purified with DNA Clean & Concentrator-5 (ZymoResearch, USA). Then digested fragments were ligated and ligation product was transformed to competent *E. coli* DH5α cells. The construct was designated as ‘pBR-sGFP’ and transformed into *E. coli* MG1655 competent cells for expression studies to serve as blank.

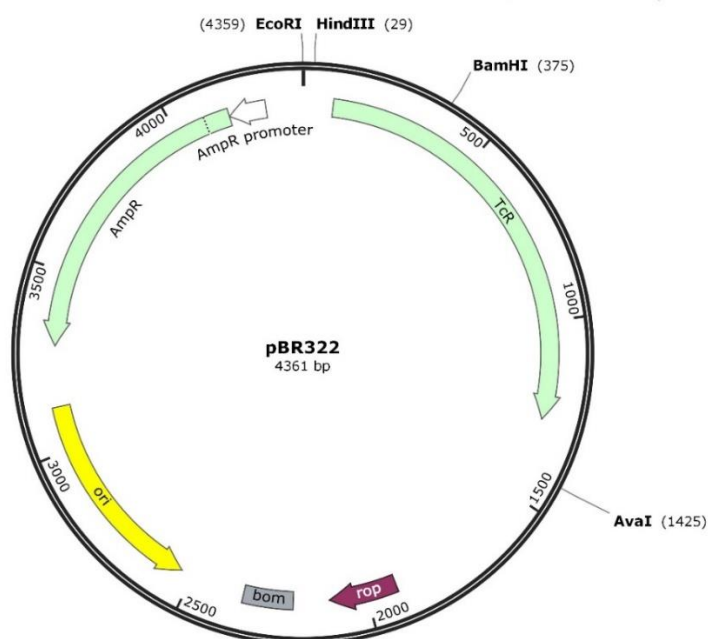


Figure 2.4 Vector map of pBR322. (AmpR: Ampicillin resistance gene; TcR: Tetracycline resistance gene; ori: pBR322 origin of replication; rop: regulates plasmid replication, keeps the copy number at about 20 per cell).

2.2.12. Construction of Arsenic Specific Sensor Plasmid (pBR-arsR773)

The arsenic sensing DNA sequence consisting of the promoter region of the *arsR* operon and *arsR* gene obtained from *E. coli* plasmid *R773* (GenBank Accession Number X16045.1) (Appendix C) was synthesized by Integrated DNA Technologies (USA). High fidelity PCR amplification of *ParsR-arsR* was carried out (Table 2.4, Table 2.5) using oligonucleotides *arsR773-F* and *arsR773-R* (Table 2.1). The amplified DNA fragment and promoterless plasmid (pBR-sGFP) were digested with *EcoRI* and *BamHI* and the sticky ends were ligated. Ligation product was transformed to competent *E. coli* DH5 α cells and positive transformant was chosen by colony PCR. The resulting sensor plasmid named as ‘pBR-arsR773’ was transformed into competent *E. coli* MG1655 cells for expression studies.

Table 2.4 Optimized PCR conditions for amplification of *ParsR-arsR*.

Reagents	Stock	Amount	Final conc.
dNTPs	5 mM	1.5 µL	250 µM each
HF Buffer	5X	6 µL	1X
Forward specific primer	10 µM	1,5 µL	0.5 µM
Reverse specific primer	10 µM	1,5 µL	0.5 µM
Gene fragment	10 ng/µL	2 µL	1 ng/µL
<i>Phusion</i> DNA Pol	2 units/µL	0.3 µL	0.02 units/µL
dH ₂ O		17.2 µL	
Total		30 µL	

Table 2.5 Optimized PCR cycling conditions for amplification of *ParsR-arsR*.

PCR Steps		Temperature	Time	Cycle
Initial denaturation		97 °C	30 sec	1
Amplification	Denaturation	97 °C	25 sec	
	Annealing	59 °C	20 sec	22
	Extension	72 °C	19 sec (15-30 sec/1 kb)	
Final Extension		72 °C	3 min	1

2.2.13. Construction of Cadmium Specific Sensor Plasmid (pBR-PzntA)

The cadmium sensing DNA sequence information consisting of the promoter region of the *zntA* gene (Appendix C) was obtained from *E. coli* MG1655 genome (GenBank Accession Number U00096.3). High fidelity PCR amplification of *PzntA* was carried out (Table 2.6, Table 2.7) with oligonucleotides *zntAp-F* (pBR-sGFP) and *zntAp-R* (pBR-sGFP) (Table 2.1) using *E. coli* MG1655 genomic DNA. The amplified DNA fragment was then digested with *EcoRI* and *BamHI* and inserted at the same restriction sites into promoterless plasmid (pBR-sGFP). Ligation product was transformed to

competent *E. coli* DH5 α cells and positive transformant was chosen by colony PCR. The resulting sensor plasmid named as ‘pBR-PzntA’ was transformed into competent *E. coli* MG1655 cells for expression studies.

Table 2.6 Optimized PCR conditions for amplification of *PzntA*.

Reagents	Stock	Amount	Final conc.
dNTPs	5 mM	1.5 μ L	250 μ M each
HF Buffer	5X	6 μ L	1X
Forward specific primer	10 μ M	1,5 μ L	0.5 μ M
Reverse specific primer	10 μ M	1,5 μ L	0.5 μ M
Genomic DNA	2 ng/ μ L	6 μ L	0.4 ng/ μ L
<i>Phusion</i> DNA Pol	2 units/ μ L	0.3 μ L	0.02 units/ μ L
dH ₂ O		13.2 μ L	
Total		30 μ L	

Table 2.7 Optimized PCR cycling conditions for amplification of *PzntA*.

PCR Steps		Temperature	Time	Cycle
Initial denaturation		98 °C	1 min	1
Amplification	Denaturation	97 °C	35 sec	22
	Annealing	61 °C	20 sec	
	Extension	72 °C	14 sec (15-30 sec/1 kb)	
Final Extension		72 °C	4 min	1

2.2.14. Confirmation of Plasmid Constructs

2.2.14.1. Colony PCR

To verify the presence and orientation of the DNA insert into recombinant clones, colony PCR, restriction analysis and sequencing were performed depending on the purpose. Colonies which were grown overnight at 37°C were randomly selected and colony PCR method was firstly applied for the detection of recombinants. The following protocol was used for colony screening by PCR (Table 2.8) with vector specific forward primer Col-F (5'-ATCACGAGGCCCTTTCGTCTTCAAGAATTC-3') and gene specific reverse primer Col-R (5'-ACGCTGCCCCGAGTTATCATTATTTGTAGAGCTC-3'). Individual colony was picked and resuspended in 14 µL of the nuclease-free water and burst at 98 °C for 10 minutes. PCR master mix without water was prepared in PCR tube on ice and dispensed into colony lysates. PCR was performed as; 97°C, 2 min; 95°C, 35 s, 58°C, 20 s, 72°C 1 min/kb; 27 cycles. The PCR products were analyzed on 1% agarose gel.

Table 2.8 Colony PCR ingredients for detection of recombinants.

Component	Amount
10X <i>Taq</i> buffer	2.0 µL
dNTP mix, 5 mM each	1.0 µL
MgCl ₂ , 25 mM	1.5 µL
Forward sequencing primer, 10 µM	1 µL
Reverse gene specific primer, 10 µM	1 µL
<i>Taq</i> DNA polymerase 5 U/µL	0.3 µL
Water, nuclease-free	13.2 µL
Total volume	20.0 µL

2.2.14.2. Restriction Analysis and DNA Sequencing

Positive colonies were grown in liquid culture and plasmid DNA was isolated from an overnight bacterial culture. Following plasmid isolation, restriction analysis was performed using appropriate restriction endonuclease enzymes. All constructed plasmids (~50 ng) containing inserted fragment were digested with 1 µL of restriction enzyme (10 U/µL) in a reaction mixture including appropriate enzyme buffers in 1X final concentration. Reaction mixture was rolled up to 20 µL of final volume with nuclease-free water and incubated at 37° C for 2 hours. The size of construct was confirmed using gel electrophoresis.

If the colony carries the DNA insert, plasmid was sequenced. All constructs, except pET-sGFP, were sent to RefGen Biyoteknoloji Ltd. Şti. (Ankara, Turkey) or Poyraz Biyoteknoloji Ltd. Şti. (Ankara, Turkey) for 5' and 3' sequencing using the oligonucleotides Col-F and Col-R (2.2.14.1) as primers.

2.3. Reporter Expression Studies

2.3.1. Induction of pET-sGFP Construct

Induction protocol for *E. coli* BL21 (pET-sGFP) was followed according to Novagen pET system manual, retrieved from, http://kirschner.med.harvard.edu/files/protocols/Novagen_petsystem.pdf. A single colony from a freshly streaked plate was picked and inoculated 50 mL LB containing the appropriate antibiotic(s) for the plasmid and host strain in a 250 mL Erlenmeyer flask. For good aeration, medium up to only 20% of the total flask volume was added. Culture was incubated with vigorous shaking at 37 °C until OD₆₀₀ reached to 0.6 as recommended, about 3 h. After initial growth, sample for the uninduced control was removed and to the remainder, IPTG from a 100 mM stock to a final concentration of 0.4 mM was added. After IPTG was added, fluorescence measurements were taken up to 24 h with incubation at 37 °C with vigorous shaking.

2.3.2. Fluorescence Measurements of pET-sGFP

In order to follow bacterial growth, OD₆₀₀ measurements were done at determined time periods for 24 h. After induction of pET-sGFP culture with IPTG, at every 3 h, 1 mL of culture was taken and centrifuged at 3000 xg for 5 min at RT. Bacterial pellet was resuspended in 1 mL of 1X PBS (Appendix B) solution. Then, fluorescence measurements were taken by using Nanodrop 3300 Fluorospectrometer. As a blank measurement, *E. coli* BL21 (pET-17b) culture was used.

2.3.3. Induction of pBR-arsR773 and pBR-PzntA Constructs

2.3.3.1. Microplate Assays for Arsenic and Cadmium Sensing Bioreporters

The cultures were then added in 190-μL aliquots to wells of a 96-well black microplate (Fluotrac, Greiner Bio-One). Dilution series of metal ions, for arsenic bioreporter, As(III) and As(V) (ranging from 0.133 μM to 2 μM) and for cadmium bioreporter, Cd(II) (ranging from 0.018 μM to 0.89 μM) including a metal-free control, were added in 10 μL aliquots. Fluorescence intensities were measured by the fluorescence microplate reader, for arsenic bioreporter, Spectramax Paradigm (Molecular Devices, USA) and, for cadmium bioreporter, Varioskan Lux Multimode Microplate Reader (Thermo Fisher Scientific, USA) were used. Fluorescence microplate readers were programmed to measure fluorescence with excitation/emission wavelength of 395 nm/509 nm for every 30-min during 12 hours with continuous incubation at 35 °C and with orbital pulsed shaking before each measurement.

2.3.3.2. Bacterial Growth Effect on Arsenic and Cadmium Sensing Bioreporters

The overnight culture of bioreporter cells was diluted with fresh medium at a 1:100 ratio and grown to early exponential phase (OD₆₀₀ = 0.1), mid exponential phase (OD₆₀₀ = 0.4 - 0.6) and stationary phase (OD₆₀₀ = 1.5 - 2.0). The bioreporter cells were assayed in M9 supplemented medium and in MOPS supplemented medium. The measurements were taken using the procedure described in Section 2.3.3.1.

2.3.3.3. Metal Specificity Test for pBR-arsR773

The induction of the sensing system by various metal ions, including Ag(I), As(III), As(V), Cd(II), Co(II), Cu(II), Fe(II), Hg(II), Mg(II), Mn(II), Mo(VI), Ni(II), and Zn(II), was studied. Final metal ion concentrations of arsenite and arsenate were 50 µg/L, while other metals were 500 µg/L. The bioreporter cells in early growth phase were assayed in M9 and MOPS supplemented medium. The measurements were taken using the procedure described in Section 2.3.3.1.

2.3.3.4. Metal Specificity Test for pBR-PzntA

The induction of the sensing system by various metal ions, including Ag(I), As(III), As(V), Cd(II), Co(II), Cu(II), Fe(II), Hg(II), Mn(II), Ni(II), Pb(II) and Zn(II), was studied. Cadmium was added in 50 µg/L, whereas all other metal salts were added in 250 µg/L of final metal ion concentration. The bioreporter cells in early growth phase were assayed in M9 and MOPS supplemented medium. The measurements were taken using the procedure described in Section 2.3.3.1.

2.4. Immobilization Studies

2.4.1. Bacterial Cell Culture Preparation for Immobilization

The bioreporter cells grown in M9 medium overnight were used for inoculation into fresh M9 or MOPS medium at a 1:50 (v/v) ratio. Exponentially growing cells were centrifuged at 3000 xg and 25 °C for 5 mins. Cell pellets were then resuspended in calculated amount of fresh media (M9 or MOPS) to adjust cell concentration.

For gel concentration optimization tests, final bacterial cell density of $OD_{600} = 0.1$ was used in the matrix. For cell density optimization tests, final cell densities of OD_{600} values of 0.1, 0.4 and 0.7 were tested in the matrices. The optical density of cells was measured using Multiskan GO UV/Vis Microplate and Cuvette Spectrophotometer (Thermo Fisher Scientific, USA) at 600 nm.

2.4.2. Agar Immobilization

For agar immobilization, to assess the effect of agar concentration, aqueous agar solutions with different percentages (1, 2 and 3 % (w/v)) were autoclaved at 121 °C for 15 min and then kept at 70 °C. Before immobilization, temperature of agar solution was decreased to 42 °C in water bath. Bacterial culture prepared in M9 supplemented medium at given OD₆₀₀ value was mixed with the agar matrix in 1:1 (v/v) ratio and gently pipetted for homogenization. The procedure was carried out in temperature-controlled heat-block at 40 °C. The cell culture and immobilization matrix mixtures were immediately pipetted into the wells of the 96-well microplate in 100 µL aliquots and left to solidify at room temperature for 30 mins. The microplate was then covered and stored at 4°C in an airtight container to prevent evaporation until use, which was always the next day. To assess parameters of optimum cell density and agar percentages, immobilized cells were induced with final 25 and 100 µg/L of As(III) concentrations.

2.4.3. Alginate Immobilization

For alginate immobilization, to the assess effect of alginate concentration, aqueous alginate solutions with different percentages (2, 3 and 4 % (w/v)) were prepared one day before making beads for polymer stabilization. Bacterial cultures prepared in M9 supplemented medium at given OD₆₀₀ value were mixed with the alginate matrix in 1:1 (v/v) ratio and stirred for complete homogenization. With a syringe pump (Goldman AR-03, Turkey) connected to a 10 mL syringe with a 2 mm inner diameter spout, the alginate/bacteria solution was dripped at a flow rate of 3 mL/min into a 0.2 M CaCl₂ solution in a beaker glass, spontaneously forming spherical beads. The beads were stirred for additional 30 mins for hardening and to assure the completion of the gelling process and rinsed with sterile dH₂O to remove excess calcium chloride. Three beads were then placed into the wells of the 96-well microplate. The microplate was then covered and stored at 4°C in an airtight container to prevent evaporation until use, which was always the next day. To assess parameters of optimum cell density and

alginate percentages, immobilized cells were induced with final 25 and 100 $\mu\text{g/L}$ of As(III) concentrations.

2.4.4. Bioassays for Arsenic Detection of Immobilized Cells

For the arsenic dose response tests, bioreporter cells were prepared in either M9 supplemented or MOPS supplemented medium at determined optimal cell density and matrix concentration. Dilution series of As(III) and As(V) were prepared in sterile deionized water to obtain final arsenic (MW: 75 g/mol) ion concentrations of 10, 25, 50, 75, 100, 150 and 200 $\mu\text{g/L}$ (ranging from 0.133 μM to 2.66 μM of As) within wells. The microplates were removed from 4°C storage and incubated at room temperature for one hour to allow the cells to recover. Then arsenic dilutions including an arsenic-free control (deionized water) were added in 25 μL aliquots for agar and in 100 μL aliquots for alginate matrices into each well. Fluorescence measurements were performed using Varioskan Lux multimode microplate reader (Thermo Fisher Scientific, USA) which was programmed to measure fluorescence for every 30-min up to 16 h during continuous incubation at 30 °C ambient temperature. For the reporter protein, sGFP, the excitation and emission wavelengths were selected as 395 nm and 509 nm, respectively.

2.4.5. Metal Specificity Test for Immobilized Bioreporters

The induction of the immobilized sensing systems by various metal ions other than As(III) and As(V) including Ag(I), Cd(II), Co(II), Cu(II), Fe(II), Hg(II), Mn(II), Ni(II), Pb(II) and Zn(II) were studied. Arsenite and arsenate were tested at 50 $\mu\text{g/L}$, whereas all other metal ions were tested at 250 $\mu\text{g/L}$ final concentration. Both agar and alginate immobilized bioreporter cells were assayed in MOPS supplemented medium employed with their respective optimal parameters. The fluorescence measurements were taken using the procedure described above.

2.5. Data Analysis

All the statistical analyses in this study were conducted using Microsoft Excel and the IBM SPSS Statistics 25.0 software package for Windows. Raw fluorescence intensities were expressed in the instrument's arbitrary relative fluorescence units (RFU). These units vary with different fluorimeters. The stable background fluorescence emitted from *E. coli* carrying promoterless plasmid (as blank) was subtracted from all averages of fluorescence values at the corresponding time points. The response of bioreporter cells to different concentrations of metals was shown by fluorescence intensity, RFU values. All analyses were performed in triplicate and results were expressed as mean \pm standard deviation (SD) which were represented by error bars in the figures. The one-way analysis of variance (one-way ANOVA) was performed with the significance level of 0.05 ($p < .05$) between induced samples and uninduced sample (negative control) to determine the detection limit followed by Tukey's post hoc comparison test to test for differences between data. Standard curve fits were done by linear regression analysis.

CHAPTER 3

RESULTS AND DISCUSSION

In order to detect environmental arsenic and cadmium contamination, arsenic and cadmium sensing *E. coli* bioreporter strains were constructed by engineering sensing *E. coli* plasmids. The plasmids were obtained by genetically fusing the arsenic and cadmium sensing regulatory regions and/or gene upstream of promoterless reporter gene, *sgfp*. These two different heavy metal sensing fluorescent bacterial strains were characterized in terms of their metal specificities and detection limits in different induction schemes. Finally, arsenic specific bioreporter strain were immobilized in different hydrogel polymers and their characterization studies were carried out.

3.1. Molecular Cloning Studies

3.1.1. Amplification of Reporter Gene (*sgfp*)

Wild-type green fluorescent protein (GFP) is a 27 kDa protein of 238 amino acids in length. Wild-type GFP fluoresces maximally when excited at 395 nm, with a minor peak at 475 nm, and emits at 509 nm. GFPuv was chosen as a reporter protein in this study which is the “cycle 3” variant of GFP described by Crameri et al. (1996). Compared to wild-type GFP, GFPuv has three amino acid substitutions and three silent mutations. These substitutions involved the replacement of hydrophobic residues with more hydrophilic residues, which resulted in reduced aggregation and increased chromophore activation. Thus, GFPuv has been optimized for brighter fluorescence when excited by ultraviolet (UV) light at 395nm with a maximum emission spectrum of 509nm, similar to that of wild-type GFP. GFPuv is 18 times brighter than wild-type GFP under excitation and can easily be detected by the eye without the need for specialized equipment.

The promoterless *sgfp* gene was obtained with restrictions sites at both ends by high-fidelity amplification of synthesized gene fragment. The purified PCR product's integrity and band size (expected size: 765 bp) were confirmed on agarose gel (Figure 3.1).

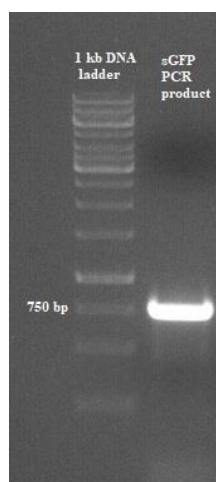


Figure 3.1 Agarose gel electrophoresis result of PCR amplification of synthetic *gfp* gene, with length of 765 bp. 1% agarose gel in 1X TAE solution was run for 60 minutes at 100 volts.

3.1.2. Cloning of *sgfp* into pET-17b Expression Vector

Before using synthetic *gfp* as a reporter gene, verification of promoterless *sgfp* gene that should produce functional fluorescent protein was confirmed by cloning it into pET-17b expression vector. To that end, the amplified *sgfp* fragment was digested with *EcoRI* and *BamHI* and inserted at the same restriction sites into pET-17b vector (Figure 3.2).

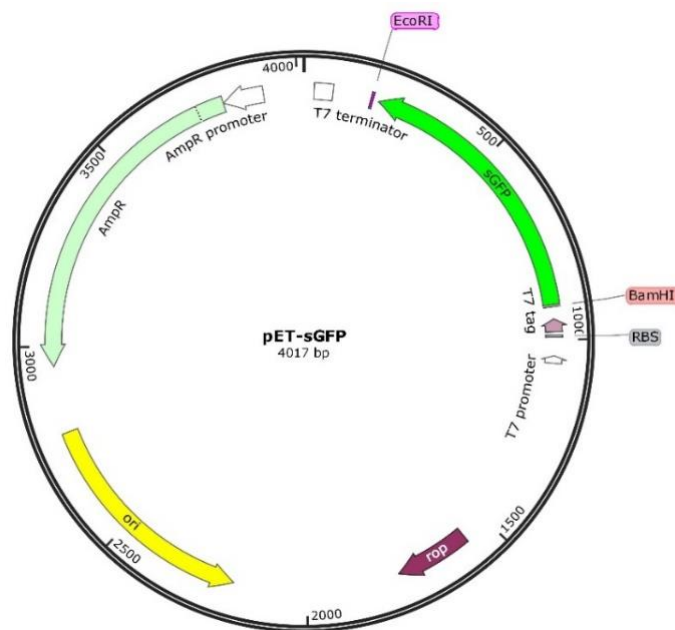


Figure 3.2 Vector map of constructed pET-sGFP.

3.1.3. Conformation of pET-sGFP Vector

3.1.3.1. Colony PCR Result

After ligation and transformation into *E. coli* DH5 α cells, to obtain the right colony having gene insertion, colony PCR was performed. Colony PCR was done using gene specific primers, sGFP-F (pET-17b) and sGFP-R (pET-17b). Colony PCR conditions was previously described in the Section 2.2.10. The colony PCR amplification products that belong to *sgfp* gene were visualized on 1% agarose gel.

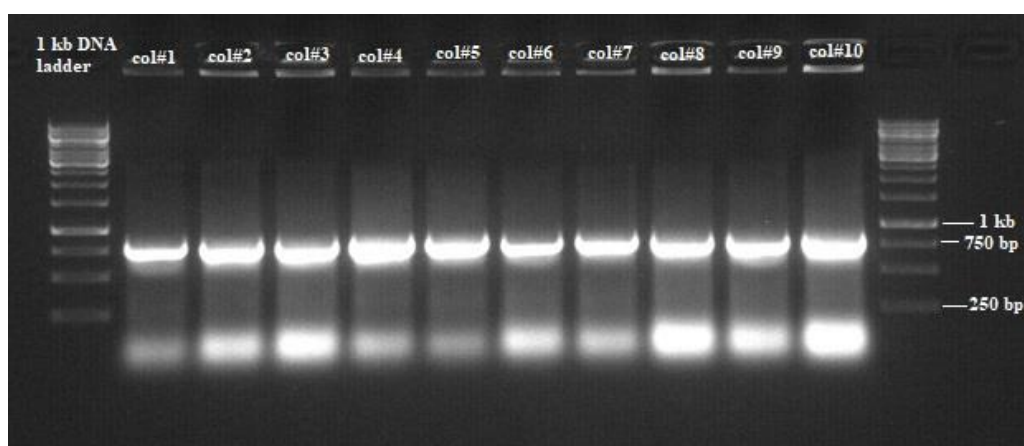


Figure 3.3 Agarose gel electrophoresis result of colony PCR for selected transformants. 1% agarose gel in 1X TAE solution was run for 60 minutes at 90 volts.

As seen in Figure 3.3, all the colonies picked showed gene insertion, so that one of them was streaked into a fresh LB-agar and further verified by ‘diagnostic digestion’ procedure.

3.1.3.2. Single Enzyme Digest Result

To show the final plasmid size after gene insertion, the plasmid isolation was done from the bacteria on newly streaked plate. The recombinant plasmid (pET-sGFP) and pET-17b plasmid were digested with *Bam*HI restriction enzyme to show the size difference. The plasmid size of pET-17b is 3306 bp and after gene insertion, expected plasmid size of pET-sGFP, 4017 bp was obtained as shown in Figure 3.4.

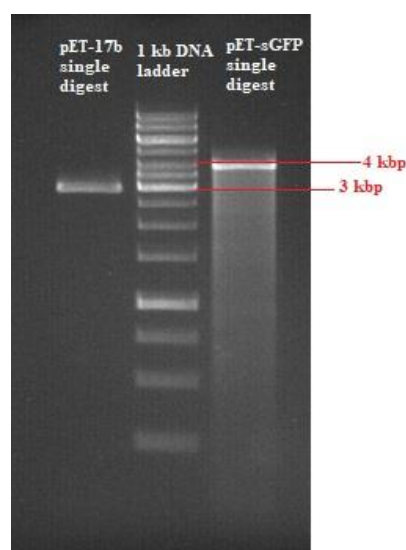


Figure 3.4 Agarose gel electrophoresis result of *Bam*HI single digests of pET-17b and pET-sGFP. 1% agarose gel in 1X TAE solution was run for 90 minutes at 90 volts.

After verification of cloning, the pET-sGFP vector was transformed into *E. coli* BL21 (DE3) pLysS competent cells. After visible GFP production was confirmed as referred in Section 3.2.1, the cloning studies were continued for construction of bioreporter plasmids.

3.1.4. Cloning of *sgfp* into pBR322 Vector

For construction of promoterless reporter plasmid, promoterless *sgfp* was cloned into pBR322 plasmid. *E. coli* plasmid, pBR322, was chosen since it has a medium copy number and for biosensing applications, either low or medium plasmid copy number was preferred to control the behavior of the reporter systems. For cloning of *sgfp* into pBR322 plasmid, *sgfp* was amplified as described in Section 2.2.11. Both isolated pBR322 plasmid and *sgfp* were double digested with *Hind*III and *Eco*88I (*Ava*I) restriction enzymes. After digestion, *sgfp* PCR product was purified by using PCR purification kit. However, after double digestion of pBR322, it produced two large fragments that the smaller fragment of 1423 bp, including *TcR* gene, (Figure 3.5) that

cannot be eliminated by kit purification. So, the desired fragment of 2938 bp was excised from the gel and agarose gel purified by using kit.

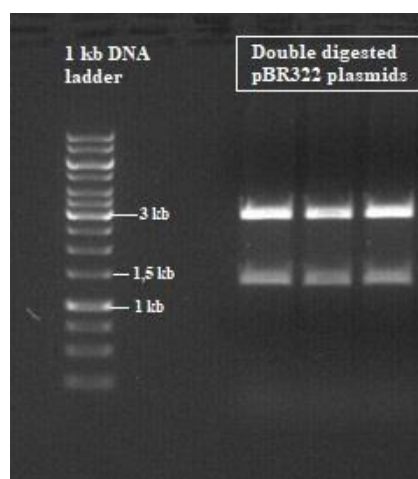


Figure 3.5 Agarose gel electrophoresis result of pBR322 (4361 bp) cloning vector cut with *HindIII* and *Eco88I* and loaded in three wells of agarose gel. 1% agarose gel in 1X TAE solution was run for 60 minutes at 90 volts.

After purifications, digested gene and plasmid products were loaded in agarose gel to check for their integrity, purity and concentration (Figure 3.6).

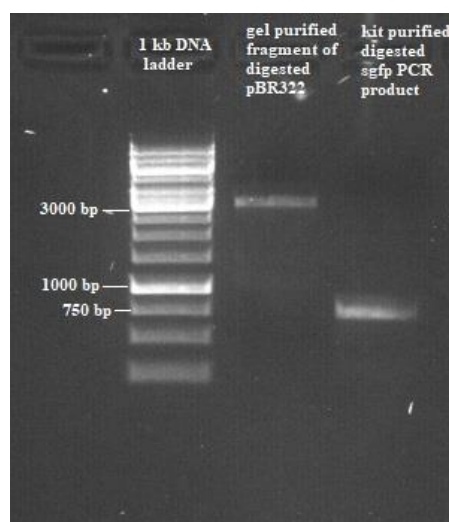


Figure 3.6 Agarose gel electrophoresis result of agarose gel purified large fragment of double digested pBR322 and purified double digested *sgfp* PCR product cut with *HindIII* and *Eco88I*. 1% agarose gel in 1X TAE solution was run for 30 minutes at 80 volts.

3.1.5. Confirmation of pBR-sGFP

3.1.5.1. Colony PCR Result

After ligation and transformation into *E. coli* DH5 α cells, to obtain the right colony having gene insertion, colony PCR was performed. Colony PCR was performed using gene and plasmid specific primers, Col-F and Col-R.

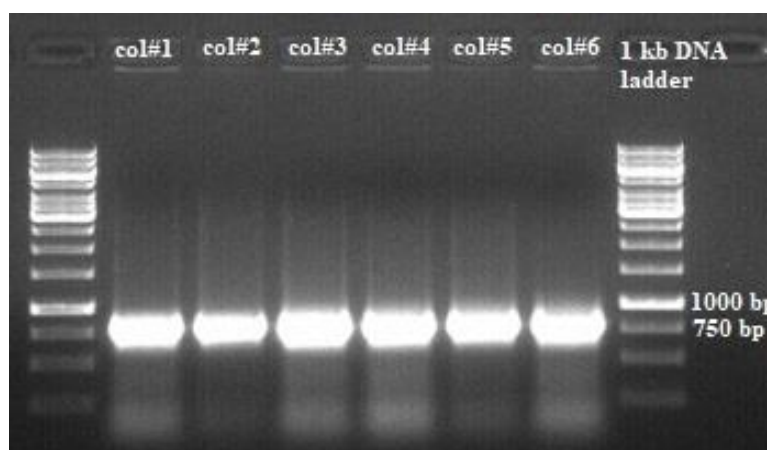


Figure 3.7 Agarose gel electrophoresis result of colony PCR using Col-F and Col-R primers with an amplicon size of 805 bp. 1% agarose gel in 1X TAE solution was run for 60 minutes at 90 volts.

As seen in Figure 3.7, all the colonies picked showed gene insertion, so that one of them was streaked into a fresh LB-agar and further verified by ‘diagnostic digestion’ procedure.

3.1.5.2. Single Enzyme Digest Result

To show the final plasmid size after gene insertion, the plasmid isolation was done from the newly streaked plate. The recombinant plasmids, pBR-sGFP (Figure 3.9) were digested with *Bam*HI restriction enzyme. The plasmid size of pBR322 is 4361 bp and after digestion and gene insertion, expected plasmid size of pBR-sGFP, 3703 bp were obtained as shown in Figure 3.8.

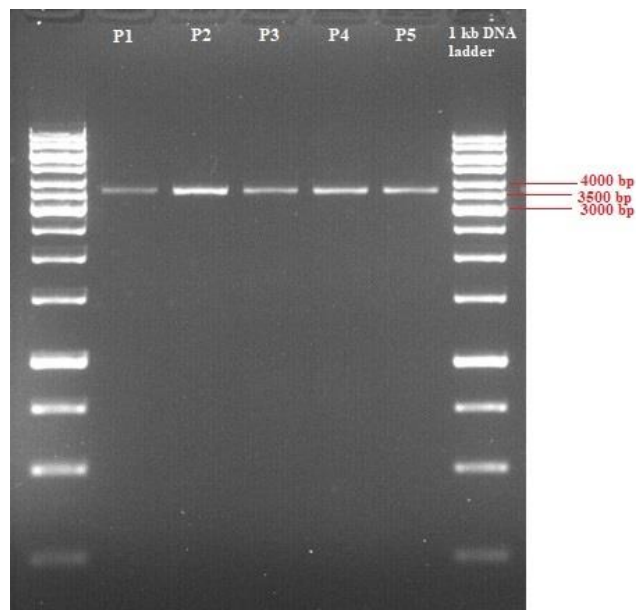


Figure 3.8 Agarose gel electrophoresis result of pBR-sGFP (3703 bp; large fragment of pBR322 (2938 bp) plus sGFP (765 bp) vector digested with BamHI. 1% agarose gel in 1X TAE solution was run for 90 minutes at 90 volts.

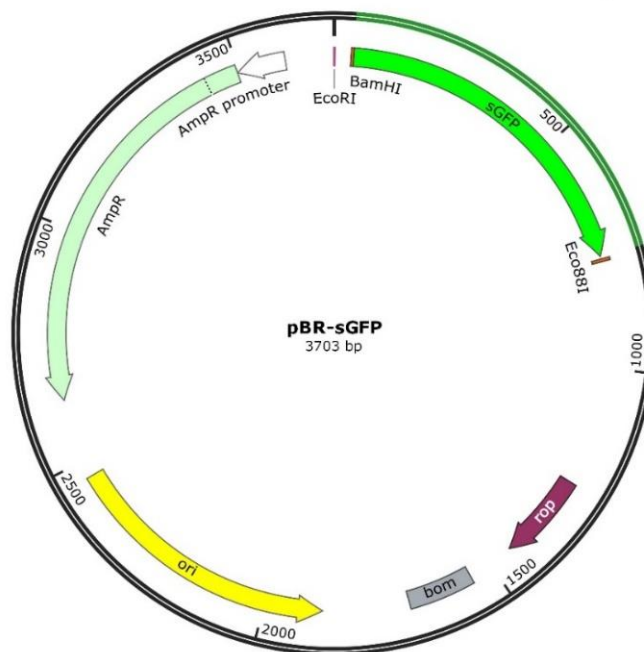


Figure 3.9 Vector map of constructed promoterless reporter plasmid, pBR-sGFP.

After isolation of pBR-sGFP, the plasmid was sent to RefGen Biyoteknoloji Ltd. Şti. (Ankara, Turkey) for sequencing and the results showed that it has the right orientation and base pairing. Then this plasmid was used to insert promoter sequences in orientation of *EcoRI* restriction site at 5' end and *BamHI* site at 3' end.

3.1.6. Cloning of *ParsR-arsR* into pBR-sGFP

In order to construct arsenic sensing bioreporter plasmid, synthesized DNA sequence consisting of the promoter region of the *arsR* operon and *arsR* gene was amplified and cloned upstream of the promoterless *sgfp* gene in pBR-sGFP. At the best T_m value for primer annealing, high fidelity PCR was performed with *Phusion* DNA polymerase to amplify the sensing DNA element, *ParsR-arsR*. After double digestions of PCR product and plasmid with *BamHI* and *EcoRI* restriction enzymes, PCR purified *ParsR-arsR* PCR product and pBR-sGFP plasmid were checked on agarose gel to determine their integrity, purity, and concentration for ligation (Figure 3.10).

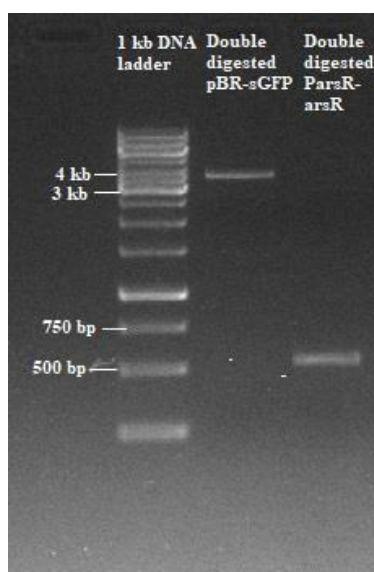


Figure 3.10 Agarose gel electrophoresis result of purified double digest products of pBR-sGFP (after cut 3669 bp) vector and *ParsR-arsR* gene (537 bp). 1% agarose gel in 1X TAE solution was run for 30 minutes at 80 volts.

3.1.7. Confirmation of pBR-arsR773

3.1.7.1. Colony PCR Result

After ligation and transformation into *E. coli* DH5 α cells, to obtain the right colony having gene insertion, colony PCR was performed by using gene and plasmid specific primers, Col-F and Col-R.

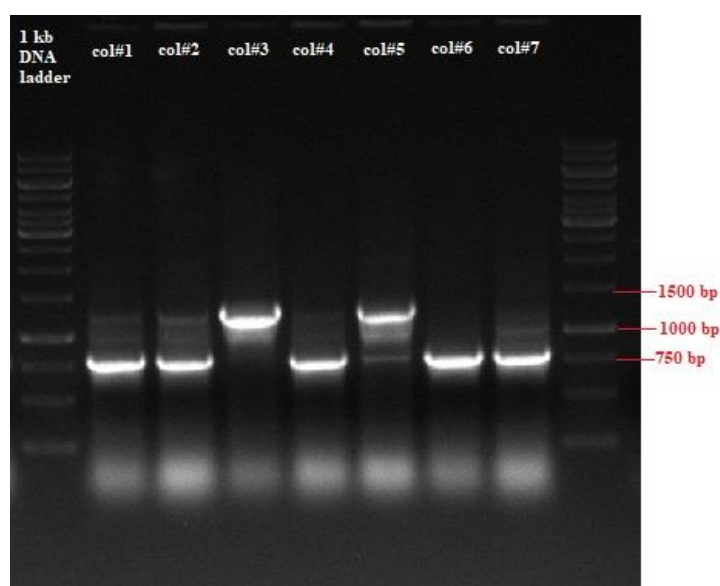


Figure 3.11 Agarose gel electrophoresis result of colony PCR using Col-F and Col-R primers with an amplicon size of 1342 bp. 1% agarose gel in 1X TAE solution was run for 60 minutes at 90 volts.

As seen in Figure 3.11, col#3 and col#5 showed gene insertion, and they were streaked into a fresh LB-agar and further verified by ‘diagnostic digestion’ procedure.

3.1.7.2. Single Enzyme Digest Result

To show the final plasmid size after gene insertion, the plasmid isolations were performed from the newly streaked plate. The recombinant plasmids, pBR-arsR773 (Figure 3.13) were digested with *Bam*HI restriction enzyme. The expected plasmid size of pBR-arsR773 is 4206 bp was obtained as shown in Figure 3.12.

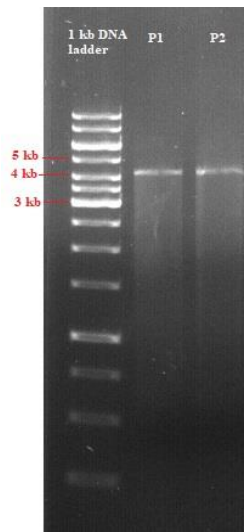


Figure 3.12 Agarose gel electrophoresis result of pBR-arsR773 (4206 bp) vector digested with BamHI. 1% agarose gel in 1X TAE solution was run for 90 minutes at 90 volts.

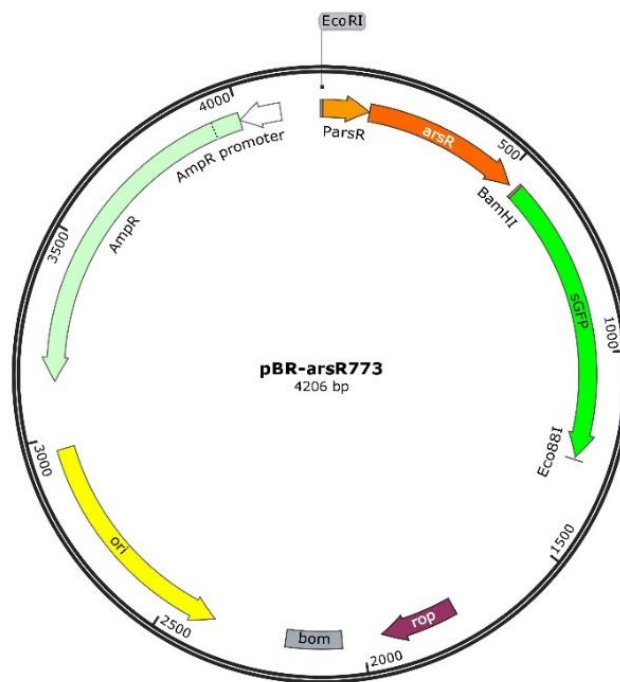


Figure 3.13 Vector map of constructed arsenic sensing bioreporter plasmid, pBR-arsR773 (Elcin & Öktem, 2019).

After isolation of pBR-arsR773, the plasmid was sent to Poyraz Biyoteknoloji Ltd. Şti. (Ankara, Turkey) for sequencing and the results showed that it had the right orientation and base pairing.

3.1.8. Cloning of *PzntA* into pBR-sGFP

In order to construct cadmium sensing bioreporter plasmid, the DNA sequence consisting of the promoter region of the *zntA* gene was amplified and cloned the upstream of the promoterless *sgfp* gene in pBR-sGFP. Since *zntA* promoter region was to be amplified from genomic DNA, first *E. coli* MG1655 cells were grown in LB medium, its genomic DNA was isolated, and its integrity was checked (Figure 3.14a). By using primers specific for promoter region of *zntA* gene, gradient PCR was performed with genomic DNA as template to determine optimal annealing temperature of primers. At the best T_m value for primer annealing, high fidelity PCR was performed with *Phusion* DNA polymerase to amplify the sensing DNA element, *PzntA* (Figure 3.14b).

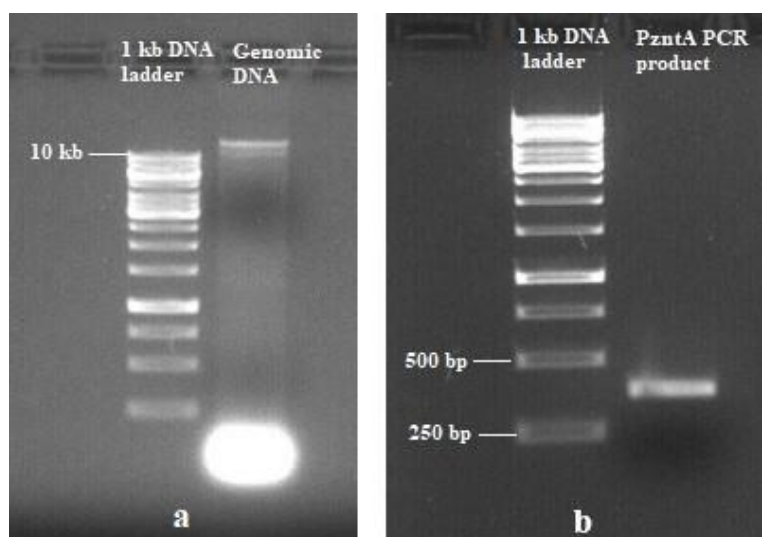


Figure 3.14 Agarose gel electrophoresis results of a) isolated genomic DNA from *E. coli* MG1655 and b) *Phusion* PCR product of *PzntA* (379 bp). 1% agarose gel in 1X TAE solution was run for 45 minutes at 90 volts.

After double digestions of the PCR product and plasmid with *Bam*HI and *Eco*RI restriction enzymes, PCR purification kit purified *PzntA* PCR product (Figure 3.15a) and pBR-sGFP (Figure 3.15b) were checked on agarose gel to determine their integrity, purity, and concentration for ligation.

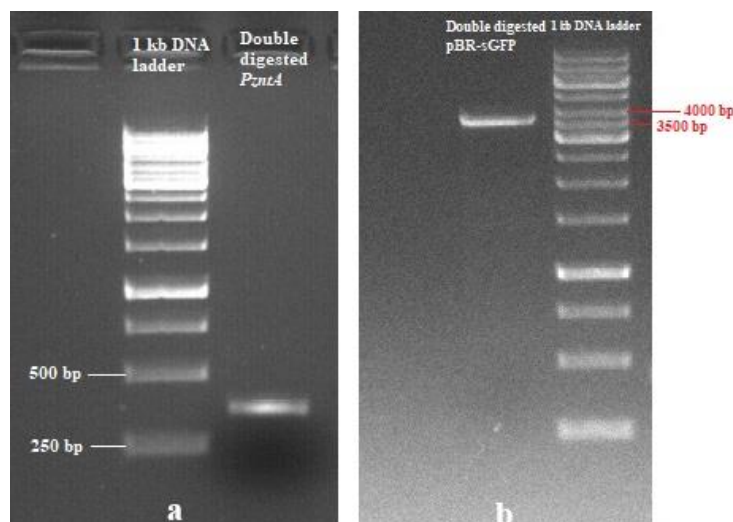


Figure 3.15 Agarose gel electrophoresis results of double digested and purified a) *Phusion* PCR product of *zntAp* (355 bp). b) pBR-sGFP plasmid (after cut 3669 bp). 1% agarose gel in 1X TAE solution was run for 30 minutes at 90 volts.

3.1.9. Confirmation of pBR-PzntA

3.1.9.1. Colony PCR Result

After ligation and transformation into *E. coli* DH5 α cells, to obtain the right colony having gene insertion, colony PCR was performed. Colony PCR was performed using gene and plasmid specific primers, Col-F and Col-R.

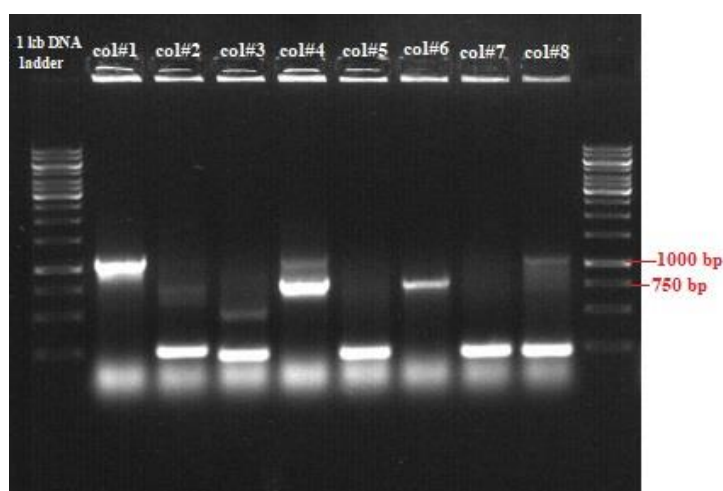


Figure 3.16 Agarose gel electrophoresis result of colony PCR using Col-F and Col-R primers with right amplicon size of 1160 bp. 1% agarose gel in 1X TAE solution was run for 60 minutes at 90 volts.

As seen in Figure 3.16, col#1 and col#8 showed gene insertion, and they were streaked into a fresh LB-agar and further verified by ‘diagnostic digestion’ procedure.

3.1.9.2. Single Enzyme Digest Result

To show the final plasmid size after gene insertion, the plasmid isolations were performed from the newly streaked plate. The recombinant plasmids, pBR-PzntA (Figure 3.18) were digested with *Bam*HI restriction enzyme. The expected plasmid size of pBR-PzntA is 4024 bp was obtained as shown in Figure 3.17.

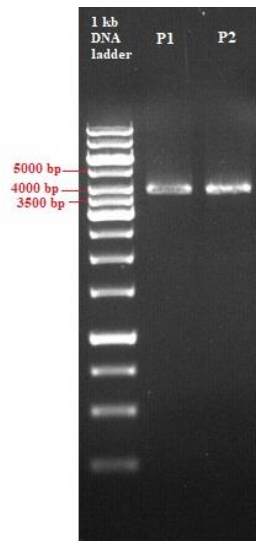


Figure 3.17 Agarose gel electrophoresis result of pBR-PzntA (4024 bp) vector digested with BamHI. 1% agarose gel in 1X TAE solution was run for 90 minutes at 90 volts.

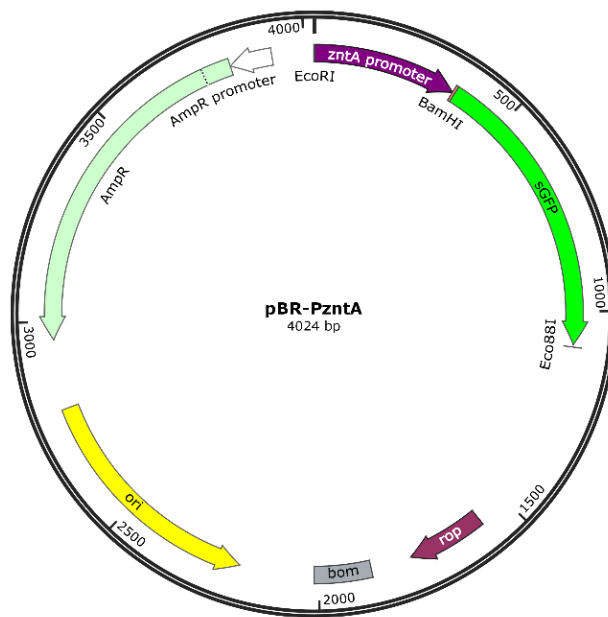


Figure 3.18 Vector map of constructed Cd sensing bioreporter plasmid, pBR-PzntA.

After isolation of pBR-PzntA, the plasmid was sent to Poyraz Biyoteknoloji Ltd. Şti. (Ankara, Turkey) for sequencing and the results showed that it has the right orientation and base pairing.

3.2. Expression Studies

3.2.1. Induction of *E. coli* BL21 (pET-sGFP) Strain

To elucidate functional reporter protein expression, pET-sGFP plasmid, in which *sgfp* gene was under the control of *lac* promoter, was induced with IPTG according to manufacturer's instructions.

Induction of *E. coli* BL21 (pET-sGFP) strain along with blank (pET-17b) and negative control were done in LB medium. During the expression studies, bacterial growth was measured at 3rd, 6th, 9th, and 24th hours of bacterial culture. The optical density results of bacterial cultures at 600 nm are shown in Table 3.1.

Table 3.1 Bacterial growth, OD600 values, of pET-17b, pET-sGFP and IPTG added pET-sGFP cultures in LB medium over time.

OD/hour	pET-17b	pET-sGFP (no IPTG)	pET-sGFP (0.4 mM IPTG)
3	0.67 ± 0.07	0.69 ± 0.06	
6	1.40 ± 0.09	1.3 ± 0.08	1.37 ± 0.04
9	1.98 ± 0.1	1.83 ± 0.09	1.83 ± 0.07
24	2.66 ± 0.15	2.52 ± 0.13	2.46 ± 0.11

-The average values of replicates are presented with standard deviation (n = 3).

According to manufacturer's instruction, pET-sGFP bacterial culture was induced with final 0.4 mM of IPTG in late exponential phase (at 3th hours of growth). At the indicated hours, the cultures were drawn, and the fluorescence intensities were

measured as described in Section 2.3.2. The fluorescence intensity values of samples are shown in Table 3.2.

Table 3.2 Fluorescence intensity values of pET-sGFP and IPTG added pET-sGFP cultures over time.

RFU/hour	pET-sGFP (no IPTG)	pET-sGFP (0.4 mM IPTG)
3	59.83 ± 1.31	NA
6	92.3 ± 1.44	117.33 ± 5.43
9	122.9 ± 5.62	197.5 ± 2.08
24	586.36 ± 8.2	776.6 ± 10.03

- The average values of replicates are presented with standard deviation (n = 3).

-NA: Not applicable.

As seen in Table 3.2, IPTG induced culture showed increased GFP expression, although uninduced pET-sGFP culture also showed GFP expression, probably due to high basal expression or leakage of *lac* promoter. The samples were taken from blank culture (pET-sGFP), uninduced culture (pET-sGFP) and induced culture after 24 hours of growth and visualized by using cell imaging station (Figure 3.19).

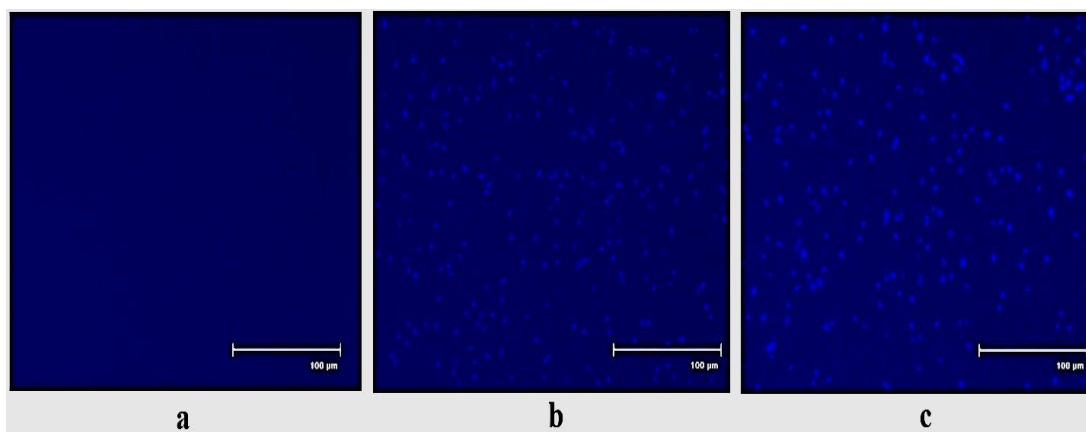


Figure 3.19 Fluorescence micrographs of bacterial cells having a) pET-17b, b) pET-sGFP, and c) pET-sGFP (IPTG induced). Images were taken by using an EVOS Floid Imaging Station (Thermo Fisher Scientific, USA).

Under UV illumination, blank culture showed no GFP expression while pET-sGFP and IPTG induced pET-sGFP culture showed fluorescent bacteria. Thus, reporter protein expression was confirmed and then the metal sensing plasmids were constructed.

3.2.2. Induction of *E. coli* MG1655 (pBR-arsR773) Bioreporter Strain

For expression studies, arsenic sensor plasmid, pBR-arsR773, was isolated from *E. coli* DH5 α and transformed into *E. coli* MG1655 strain. Before 96-well microplate experiments, the growth of *E. coli* MG1655 (pBR-arsR773) strain was tested under low and high concentrations of arsenite and arsenate to confirm the healthy bacterial growth under metal exposure. The growth curves for up to 48-h are given in Appendix D.

Table 3.3 Bacterial growth, OD600 values, of pBR-sGFP and pBR-arsR773 cultures in M9 supplemented medium in presence of arsenite, As(III) and arsenate, As(V) over time.

OD/hour	pBR-sGFP	NC	As(III) 100 µg/L	As(III) 400 µg/L	As(V) 100 µg/L	As(V) 400 µg/L
3	0.32 ± 0.03	0.35 ± 0.02	0.32 ± 0.04	0.30 ± 0.03	0.33 ± 0.02	0.32 ± 0.01
6	0.98 ± 0.07	0.99 ± 0.03	0.97 ± 0.08	0.92 ± 0.01	0.95 ± 0.06	0.94 ± 0.02
9	1.32 ± 0.08	1.36 ± 0.05	1.37 ± 0.04	1.35 ± 0.06	1.37 ± 0.05	1.32 ± 0.04
24	2.00 ± 0.1	2.20 ± 0.13	2.09 ± 0.08	2.11 ± 0.14	2.19 ± 0.19	2.10 ± 0.09

- The average values of replicates are presented with standard deviation (n = 3).

- NC: Negative control (pBR-arsR773 culture with no addition of arsenic)

The growth results did not show any bacterial growth impairment (Table 3.3), and then the expression studies were performed. Induction of GFP expression from *ParsR-arsR* will occur by As(III) along with the dissociation of ArsR transcriptional repressor protein from its cognate promoter, *ParsR*.

The applicability of bioreporter was assessed by inducing the cells with arsenite and arsenate in different media and different induction schemes. The concentrations of arsenic ions between 0 and 150 µg/L were chosen in relation to Turkey's current regulation of drinking water quality standard maximum of 10 µg/L, and surface water quality standards permissible limit value of 50 µg/L. Moreover, surface waters containing arsenic concentrations above 100 µg/L are regarded to be highly contaminated (T.C., 2013, 2015).

M9 itself is a minimal and low osmolarity defined media for *E. coli*, resulting in slower growth rate of these cells and the recipe was taken from Maniatis et al. (1982). Bacterial growth could be controlled by changing medium composition in order to enhance reproducibility and sensitivity of biosensors, since bacteria reproduce very fast in nutrient rich media (doubling time: 20 minutes, at 37 °C) (Sezonov et al., 2007). Thus, it is important to keep the number of bioreporter cells as stable as possible during the period of sensing to minimize the risk of growth-dependent variations in

GFP production. The reason for using supplemented M9 medium is because it is supplemented with amino acids which is crucial for biosynthesis of reporter protein, enhancing the response of whole-cell bioreporters.

3.2.2.1. Fluorescence Emission Kinetics of Arsenic Bioreporter Strain in M9 Supplemented Medium

To characterize the arsenic bioreporter cells in response to different concentrations of arsenite and arsenate, 96-well plate assays were performed with M9 supplemented medium as an induction medium. The detection limit was determined using statistically significant change ($p < 0.05$) in RFU compared with no induction (negative) control RFU.

Fluorescence against time curves were drawn for 6-h induction time for clarity, since it presented adequately high fluorescent signal to differentiate between dose–response curves. One-way ANOVA result for M9 supplemented medium showed that the arsenic bioreporter induction by all of the tested concentrations of As(III) compared to uninduced sample was significant after 2 hours, $p = .000$. Also, 150 $\mu\text{g/L}$ (2 μM) of arsenite was detected after 30-min incubation and 10 $\mu\text{g/L}$ (133 nM) of arsenite was detected after 2 hours of induction with a statistically significant change ($p < 0.05$), thus the bioreporter's detection limit was higher in the beginning and it decreased with time. The fluorescence signal increased continuously with time as GFP tend to accumulate in cell. The background fluorescence exhibited by the uninduced biosensor did not have any statistically significant fluorescent change during the incubation period. Moreover, a linear dynamic range was obtained between 0 and 150 $\mu\text{g/L}$ of arsenite concentrations (Figure 3.20). In order to determine the significance levels of induction groups, Tukey's HSD (honestly significant difference) test was performed for 2-h time point; the descriptive statistics table, ANOVA table and post hoc test results are given at Section A in Appendix E.

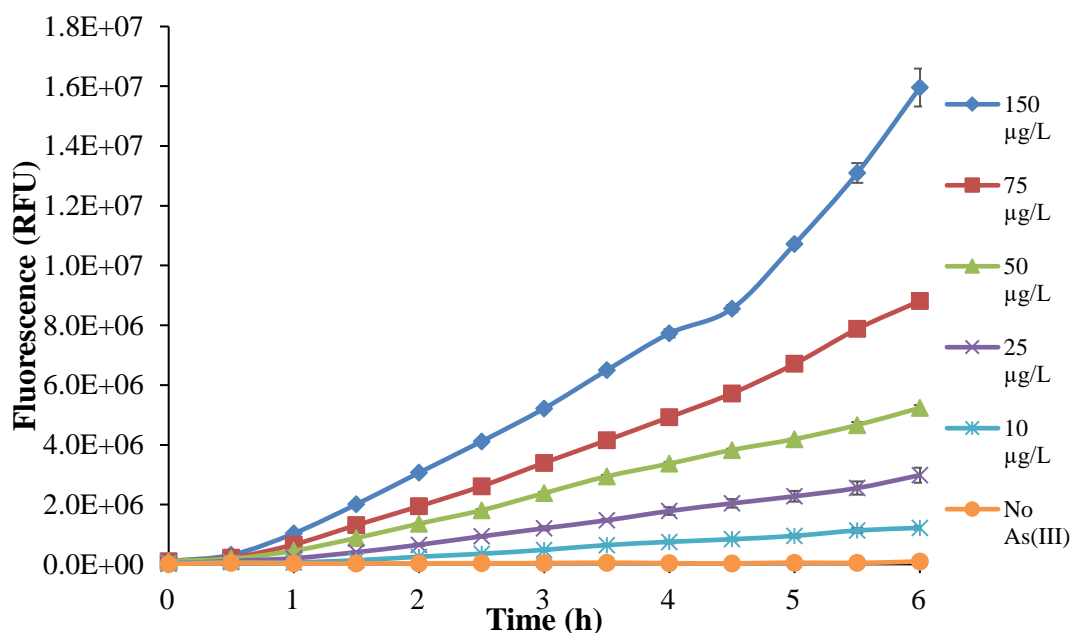


Figure 3.20 Fluorescence emission kinetics of arsenic bioreporter cells in response to arsenite, As(III). Bioreporter cells grown in M9 supplemented medium (till $OD_{600} = 0.1$) induced with different arsenite concentrations. Data shown as mean \pm SD of triplicate wells of each induction. Error bars are shown only when they exceed the size of the symbols.

Bacterial biosensors for As(III) have previously been developed using various reporter genes, such as *lacZ*, *luxCDABE*, *luc*, and *gfp* with various induction patterns and sensitivities for detecting As(III).

Liao and Ou (2005) described a construction of *E. coli* whole-cell biosensor for the detection of bioavailable As(III), As(V), and Sb(III) by employing red-shifted GFP (rs-GFP) as a reporter protein. The sensor plasmid, pVLAS1, is based on the expression of rs-GFP under the control of the *ars* promoter and the *arsR* gene of the *S. aureus* plasmid pI258. The detection limit for As(III) was 0.4 μ M (30 μ g/L) and for As(V) was 1 μ M (75 μ g/L) after 2-h exposure time in LB medium. When the induction time was increased to 8 h, the lowest detection limit for As(III) and As(V) was 0.1 μ M (7.5 μ g/L).

Tani et al. (2009) used an *E. coli* DH5 α for plasmid construction. Design of oligonucleotides used for PCR was based on the nucleotide sequences of K12 chromosome DNA deposited at GenBank/EMBL/DDBJ accession numbers NC000913. They attempted fluorescent microplate method to detect arsenic using recombinant *Escherichia coli* cells transformed with plasmids harboring three tandem copies of the *ars* promoter/operator—the gene for green fluorescent protein (*gfp*). They detected 10 $\mu\text{g/L}$ of arsenite at the response time of 6 h in LB medium.

Theytaz et al. (2009) designed and tested microfluidic chips with fluorescent (GFP) *E. coli* bacteria that respond to arsenic, *E. coli* DH5 α pProbe-gfp(tagless)-arsR-ABS. This particular strain was engineered in order to generate a fluorescent signal, due to the production of GFP in response to arsenite. They were engineered to produce the ArsR protein, which normally controls the synthesis of a set of proteins implicated in arsenite resistance, but now represses expression of the gene for GFP. The response time to detect 50 $\mu\text{g/L}$ of arsenite was 90 minutes in minimal medium.

Hu et al. (2010) proposed an arsenic-resistant promoter and the regulatory gene *arsR*. This was obtained by PCR from the genome of *E. coli* DH5 α , and then ligated to the reporter protein gene *phiYFP*. The construction was introduced into *E. coli* DH5 α to convert this bacterium as an arsenic whole-cell biosensor (WCB-11) in which *phiYFP* produced good results for the first time. They detected 375 $\mu\text{g/L}$ of arsenite and arsenate with a response time of 2 h in LB medium.

Li et al. (2015) constructed an arsenite-inducible vector with GFP as the reporter gene, pUC18-ars-gfp. Then, iteratively, multirounds of directed evolution were applied to improve the arsenite-sensing element and looked for the improved mutants. Induction response of a final mutant ep3, *E. coli* (pUC18-ep3ars-gfp) was obtained with more than 12-fold fluorescence intensity compared with that of the wild-type control, *E. coli* (pUC18-ars-gfp). They had improved the detection limit of As(III) from 3 to 0.75

µg/L within 1 hour and also the evolved ep3 arsenite biosensor could detect 10 µg/L As(III) within 45 min in TB (terrific broth) medium.

Huang et al. (2015a) proposed a DNA fragment comprising the promoter/operator of the *ars* operon (*Pars*) and *arsR* gene, which was amplified by PCR from the pI258 plasmid isolated from *Staphylococcus aureus* (NCTC 50581; National Collection of Type Cultures, Colindale, London, UK). The amplified DNA fragment was subsequently inserted upstream of the promoterless *lacZ* gene in the vector pTZ110 for creating pAs-lacZ fusion plasmid. The recombinant plasmid pAs-lacZ was then transformed to *E. coli* DH5α. The developed bacterial biosensor demonstrated a quantitative range from 10 to 500 µg/L of arsenite in 3-h reaction time in LB medium.

Prévéral et al. (2017) constructed the transcriptional fusion between the bacterial luciferase operon *lux* and an arsenite-inducible promoter *Pars* controlled by the transcriptional repressor ArsR. The genetic construct pArs-lux was hosted in *E. coli* W3110. The detection of 0.1–0.2 µM (7.5–15 µg/L) of arsenite was achieved after 60-min upon arsenite addition in LB medium.

Pola-López et al. (2018) constructed a bacterial biosensor named arsenic biosensor POLA (ABP) made with three genetic modules. These modules consisted of a promoter, a gene expression amplifier, and a reporter gene, into an *Escherichia coli* MG1655k12, with the goal of reaching higher sensitivity for arsenite detection in water. The plasmid backbone and polymerase used were pSB1A2 and T7 RNAP, respectively. The detection range changed from 5 to 140 µg/L of arsenite with response time of 1 h in LB medium.

By comparing our arsenic bioreporter with these reports, it can be concluded that the sensitivity of arsenic bioreporter developed in this study is comparable to or more sensitive than other gfp-based arsenic bioreporters. On the other hand, any of the tested arsenate concentrations had no effect on GFP expression of arsenic bioreporter even

after 6 hours, $p = .088$. However, only 150 $\mu\text{g/L}$ or higher concentrations of arsenate showed induction after 10-hour induction time, while much higher arsenate concentrations resulted in induction less than 10 hours (data not shown). This may result from high inorganic phosphate content of M9 minimal medium outcompeting arsenate ions, and only after phosphate was used by cells with time, arsenate can be taken by the cell so that induction can occur. Thus, arsenic bioreporter cells showed higher sensitivity toward arsenite rather than arsenate in M9 supplemented medium.

Rothert et al. (2005) reported a bioreporter strain *E. coli* AW10 (pSD10). It carries a reporter plasmid with a transcriptional fusion between the o/p sequence of the *ars* operon and *arsR* gene isolated from plasmid pBGD23 and the gene encoding *gfpuv* isolated from plasmid pBAD-GFPuv. They also used M9 minimal assay medium and reported the higher detection limit for arsenite of 8 μM (600 $\mu\text{g/L}$) with a response time of 30 min and no induction by arsenate. They concluded that *ars* operon is not induced by similar anions referring to arsenate which is not the case for *ars* operon. Roberto et al. (2002) proposed an O/P region, as well as the entire *arsR* gene and initial region of *arsD*. These were amplified by PCR from pIRC120 using oligonucleotide primers designed based on the published sequence of the R46 *ars* operon. They detected 1 $\mu\text{g/L}$ of arsenite with a longer response time of 12 h. They also described threefold lower fluorescence response at 10 ppm (10 $\mu\text{g/L}$) arsenate compared to arsenite of their *arsR-gfp* reporter system in M9 minimal medium after 12-h induction time.

Figure 3.21 shows the fluorescence microscopy images of uninduced and As(III)-induced bioreporter cells assayed in M9 supplemented medium after 6 hours of induction. Images were taken by using Leica DM6000 M Fully Automated Upright Microscope.

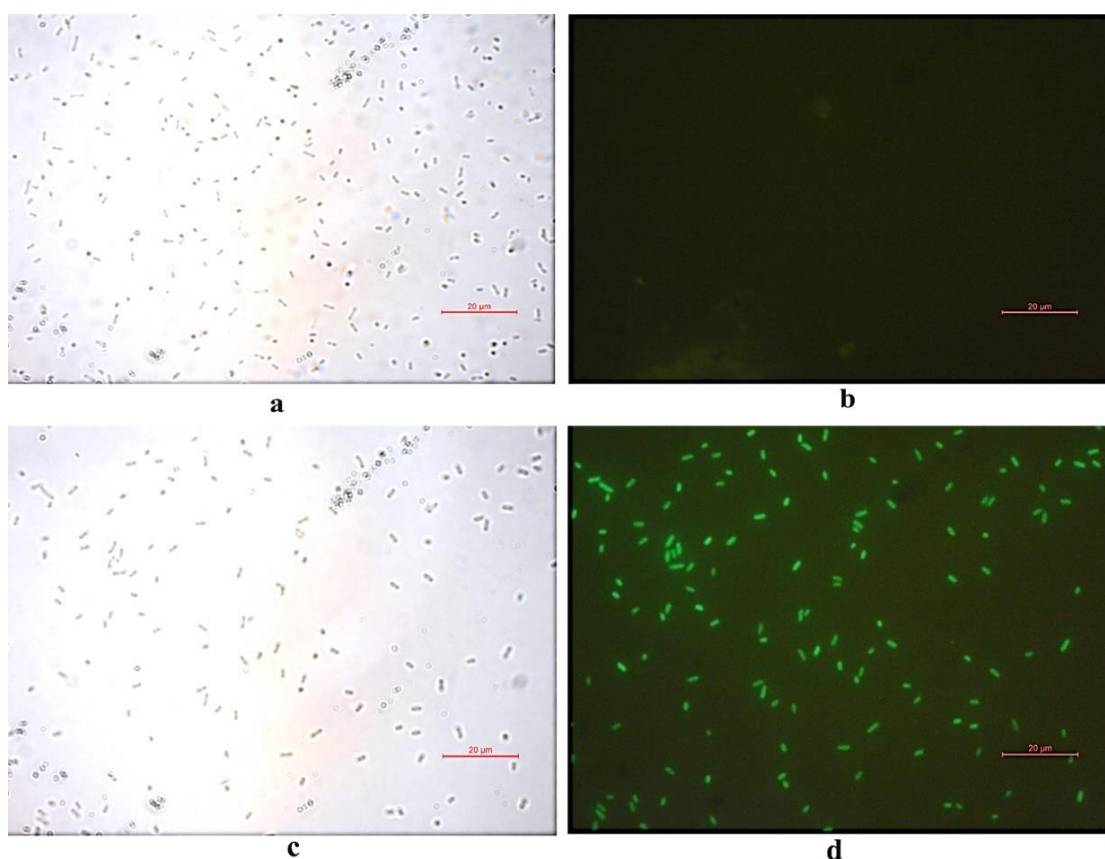


Figure 3.21 Fluorescence microscope images of arsenic bioreporter cells: a) uninduced bioreporters under BF channel, b) uninduced bioreporters under Fluo channel, c) induced bioreporters with 75 µg/L arsenite under BF channel, d) induced bioreporters with 75 µg/L arsenite under Fluo channel. BF: Bright field, Fluo: Fluorescence. Scale: 20µm.

3.2.2.2. Fluorescence Emission Kinetics of Arsenic Bioreporter Strain in MOPS supplemented medium

Nearly all the bacterial biosensors developed so far were focused on the detection of arsenite based on the argument that arsenite is around tens of times more toxic than arsenate (Akter et al., 2005).

Few studies reported bacterial bioreporters' response to environmentally relevant concentrations of arsenate, which is the next most toxic form after arsenite. It is very important to detect dominant forms of arsenic species in water which are both

available to millions of people around the world. Some well-documented examples include Bangladesh, India, Thailand, and Vietnam (Singh et al., 2015), also Turkey, in the region of Simav plain (Kütahya) (Gunduz et al., 2010). Arsenite and arsenate are readily interconverted and therefore often found together, and the speciation between these might take place depending on the conditions such as the redox potential, pH, oxygen enrichment status, organic and other dissolved matter contents, and microbial activity (Panagiotaras & Nikolopoulos, 2015). Furthermore, biotransformation of inorganic arsenic has been shown to occur in both animals and humans. Reduction of arsenate and oxidation of arsenite *in vivo* have been demonstrated in experimental animals (Fowler et al., 2015). Thus, determining the abundance of different forms of arsenic ions is helpful in assessing the potential toxicity levels of water bodies.

Composition of induction medium affects the sensitivity and specificity of bioreporter cells by changing the bioavailability of heavy metals and metalloids. Defined media like a minimal medium confer bioreporter cells a higher sensitivity than a complex media like LB medium (Hynninen & Virta, 2010). For arsenic bioassays, commonly used media is LB (Tani et al. 2009; Liao & Ou, 2005); however, arsenic bioreporter cells in this study didn't exhibit an efficient fluorescence performance in LB medium instead a weak fluorescence response was observed for high concentrations (150-750 µg/L) of arsenite and arsenate overnight. However, this arsenic bioreporter cells showed striking change of response to arsenate when assayed in MOPS supplemented medium which is rarely used medium for arsenic bioassays. MOPS supplemented medium was different from M9 supplemented medium in a way that phosphate compounds were substituted by MOPS for buffering purpose.

One-way ANOVA result for MOPS supplemented medium showed that the arsenic bioreporter induction by the all of the tested concentrations of As(III) compared to uninduced sample was significant after 3.5 hours, $p = .000$. Also, 150 µg/L of arsenite

was detected after 1-hour incubation and 10 µg/L of arsenite was detected after 3.5 hours of incubation with a statistically significant change ($p<0.05$) (Figure 3.22a).

One-way ANOVA result for MOPS supplemented medium showed that the arsenic bioreporter induction by all of the tested concentrations of As(V) compared to uninduced sample was significant after 2 hours, $p= .000$. Also, 150 µg/L of arsenate was detected after 1-hour incubation and 10 µg/L of arsenate was detected after 2 hours of incubation with a statistically significant change ($p<0.05$) of GFP expression (Figure 3.22b).

The fluorescence increased with time and linearly with increasing arsenite/arsenate concentrations up to 150 µg/L. In order to determine the significance levels of induction groups, Tukey's HSD tests were run for arsenite at 3.5-h time point and for arsenate at 2-h time point; the descriptive statistics tables, ANOVA tables and post hoc test results are given at Section B and C, respectively in Appendix E.

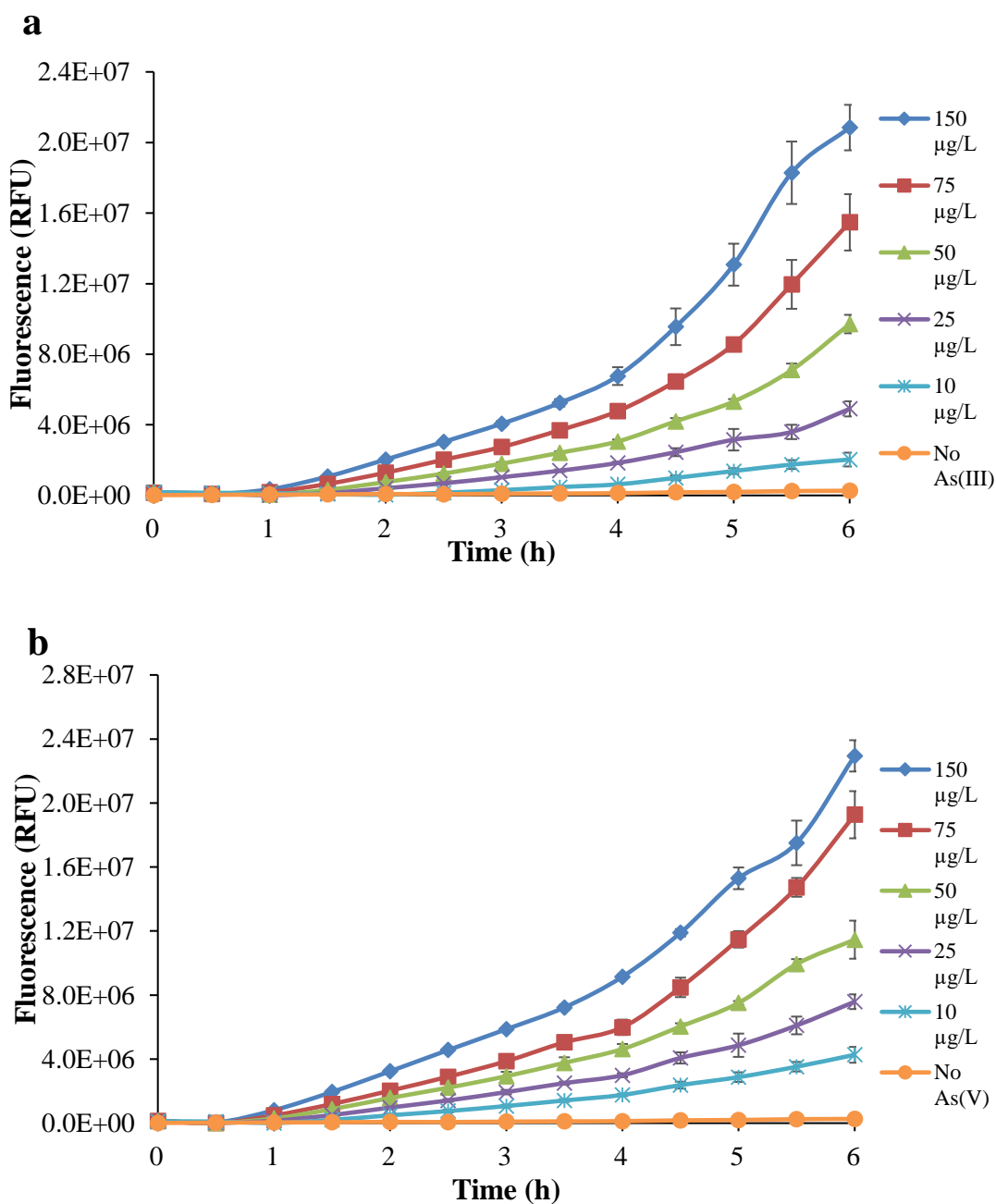


Figure 3.22 Fluorescence emission kinetics of arsenic bioreporter cells in response to a) arsenite, As(III), b) arsenate, As(V). Bioreporter cells were grown in MOPS supplemented medium (till $OD_{600} = 0.1$). Data shown as mean \pm SD of triplicate wells of each induction. Error bars are shown only when they exceed the size of the symbols.

The reason for the dramatic increase in sensitivity toward arsenate compared to M9 medium might be explained by the absence of phosphate ions in MOPS medium resulting an increase in bioavailability of arsenate. Dissolved As(III) most likely enters the cell by diffusion in its trioxyanion form through a glycerol channel and As(V) via phosphate transporters followed by its reduction to As(III) (Figure 3.23). Arsenate complexes (H_2AsO_4^-) and inorganic phosphate (H_2PO_4^-) are chemical analogs, and in *E. coli*, arsenate is taken up by two major phosphate transport systems: Pst and Pit (Willsky & Malamy, 1980). The Pit system is the major uptake system for arsenate, while the Pst system has a higher affinity for phosphate than for arsenate but induced by phosphate starvation. Therefore, phosphate depletion favors arsenate uptake by the cells, and they become sensitive to arsenate (Yang et al., 2012). Once inside of cells, As(V) is reduced to As(III) by one of several different As(V) reductases in addition to ArsC reductase. In bacteria, two unrelated ArsC enzymes reduce As(V) using either glutathione and a small thiol protein glutaredoxin 2 or another small thiol protein thioredoxin (Garbinski et al., 2019).

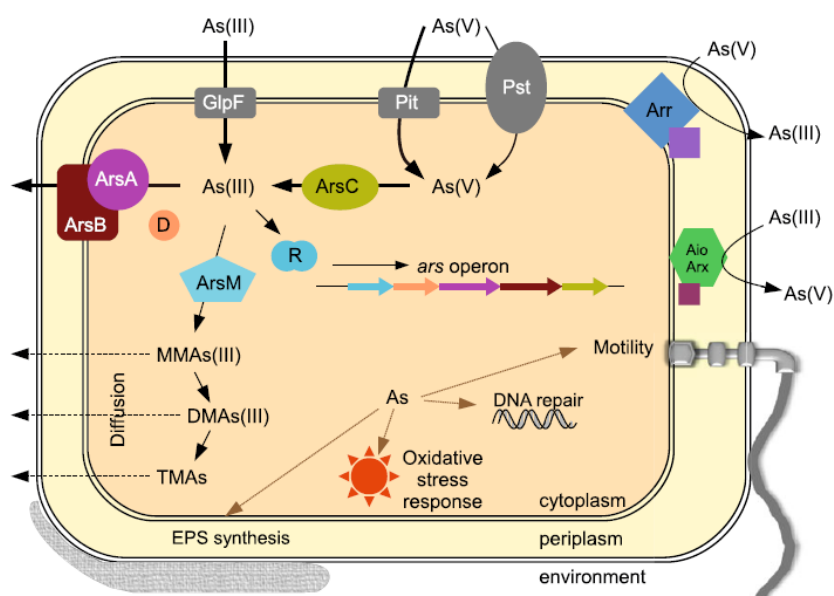


Figure 3.23 Overview of bacterial interactions with arsenic. The metalloid is taken up through glycerol or phosphate transporters. Arsenate is reduced to arsenite which may then be extruded from the cell by ArsAB (Kruger et al., 2013).

This was the first study (Elcin & Öktem, 2019) to describe the effect of media on arsR-gfp-based bacterial bioreporter to evaluate response to arsenate concentrations. The results suggest that while M9 medium is suitable for detection of low concentrations of arsenite, MOPS medium can be used to detect both arsenite and arsenate with higher sensitivity toward arsenate. Thus, by comparing the detected arsenic content in both media, relative content of different arsenic species in a sample can be determined semi-quantitatively.

3.2.2.3. Metal Specificity of Arsenic Bioreporter Strain

In natural waters, other metal ions are generally found in combination with arsenic, which may produce a non-specific induction of fluorescence. To evaluate specificity of the constructed arsenic bioreporter, the response to some of the most common metals that are of public health concern was tested at 500 µg/L while arsenic concentrations tested at 50 µg/L in M9 and MOPS supplemented media (Figure 3.24).

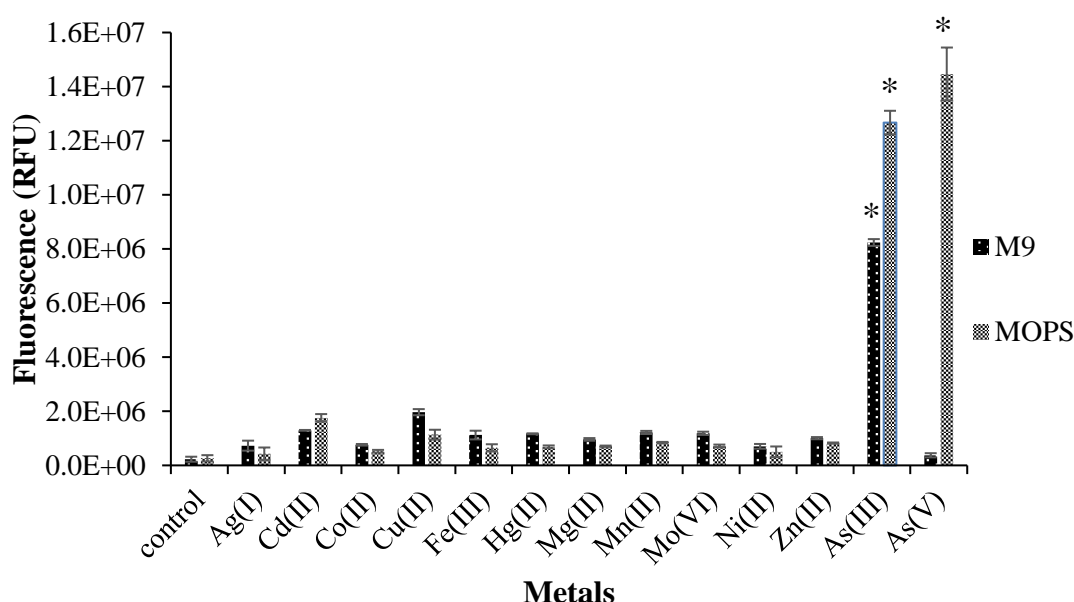


Figure 3.24 Metal specificity of the arsenic bacterial bioreporter. Bioreporter cells were grown either in M9 or in MOPS supplemented medium (till $OD_{600} = 0.1$). Control refers to no metal addition. Data shown as mean \pm SD of triplicate wells of each induction group and presented at 6-h time point. * $p < 0.001$.

The arsenic biosensor gave no significant change of fluorescence response towards tested metals in both media indicating the arsenic bioreporter had high affinity to arsenic species but no apparent affinity to other metals. This indicates the high specificity of arsenic biosensor which is commonly reported feature of the *arsR*-based bacterial bioreporters.

3.2.2.4. Fluorescence Response of Arsenic Bioreporter Strain at Different Growth Phases

Physiological status of the cells considerably affects the performance of the whole-cell metal bioreporters. Cells that are in the exponential growth phase have often been used in bioreporter assays. However, the best growth phase of each bacterial bioreporter strain should be determined for specific genetic construction and induction protocol for better reliability and reproducibility of results.

In this study, different bacterial cultures in terms of growth phases were tested to evaluate the effect of growth stage on the sensitivity of arsenic bioreporter. Assays were conducted in both M9 and MOPS supplemented media. Apart from early exponential cells, mid exponential cells ($OD_{600} = 0.4\text{--}0.6$) and stationary cells (overnight culture, $OD_{600} = 1.5\text{--}2.0$) were used for induction. Early exponential phase was chosen for dose-response assays because, in preliminary experiments with cells taken from exponential and stationary culture, higher variability in fluorescence response was observed.

When the arsenite-induced fluorescent responses were compared for M9 supplemented medium, higher fluorescence response for all arsenite concentrations were obtained for stationary phase cells. However, stationary cells also had the highest background fluorescence due to large number of cells and so the detection of $10\text{ }\mu\text{g/L}$ arsenite within 2 hours was less significant, probably due to lower bioavailability arsenite due to crowded cell population. Moreover, the fluorescence response reached

plateau earlier than other phases (Figure 3.26b). At concentrations of arsenite higher than 10 $\mu\text{g/L}$, the bacterial cultures in mid-exponential and stationary phase cells showed higher fluorescence values than early exponential phase cells with higher standard deviations (Figure 3.25).

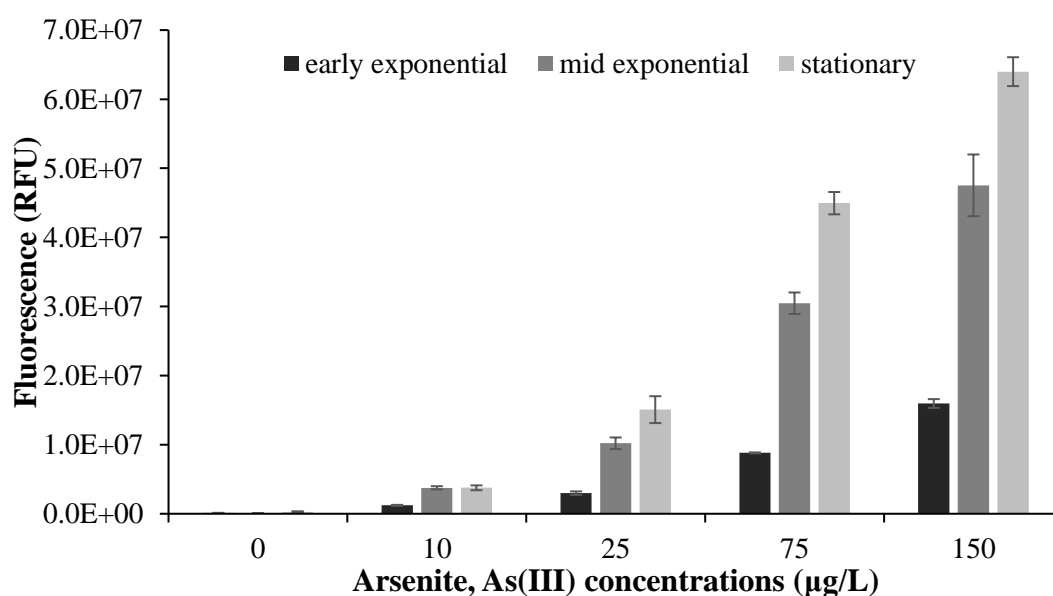


Figure 3.25 The fluorescence intensity values of arsenic bioreporter induced with arsenite at different growth phases. Bioreporter cells were grown in M9 supplemented medium. Data shown as mean \pm SD of triplicate wells of each induction group and presented at 6-h time point.

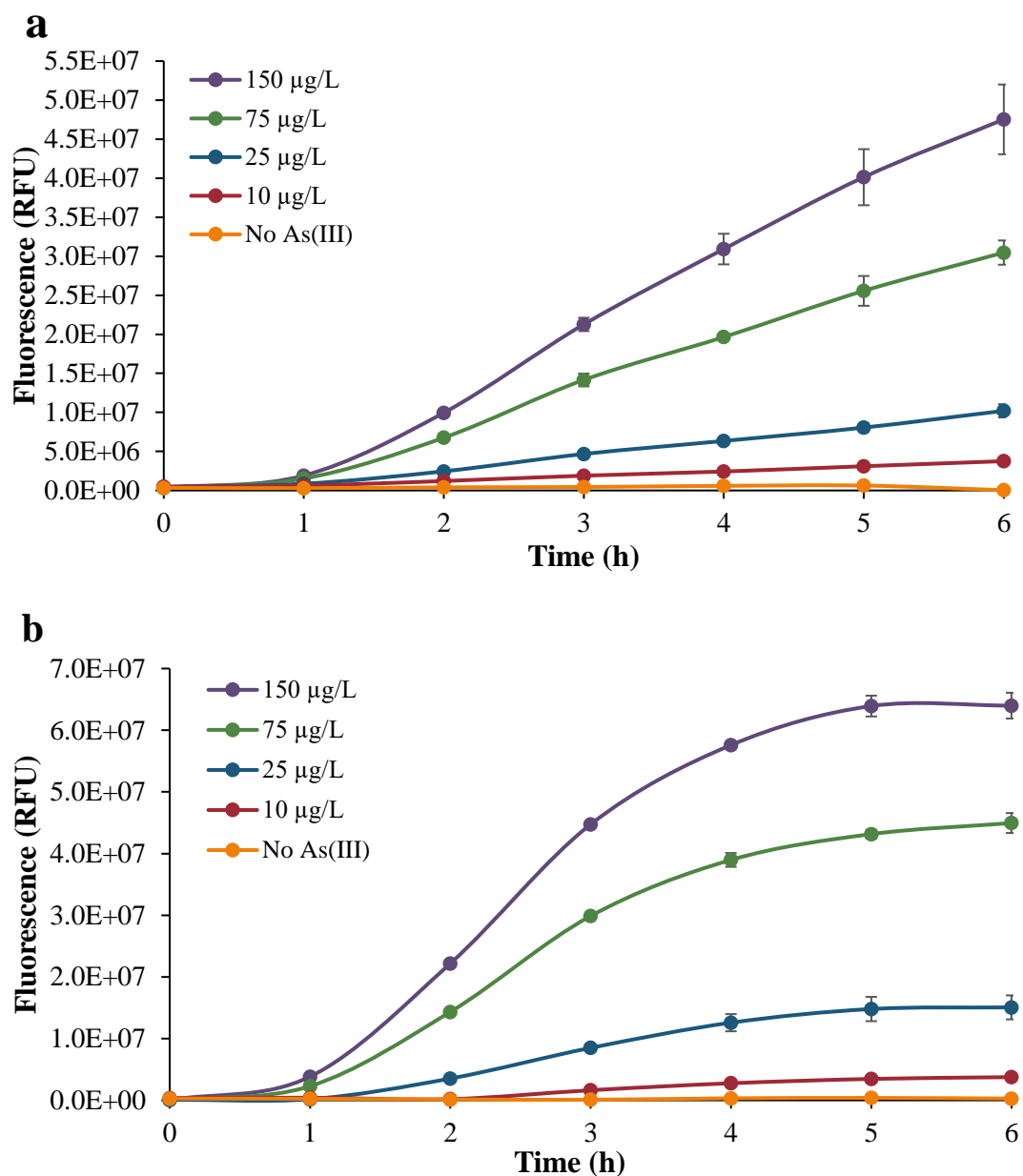


Figure 3.26 Fluorescence kinetic profile of arsenic bioreporter with different induction schemes. Bioreporter cells grown in M9 supplemented medium to a) mid-exponential and b) stationary phase induced with different arsenite concentrations. Data shown as mean \pm SD of triplicate wells of each induction.

To detect arsenite in M9 supplemented medium, both mid exponential or stationary cells could be used if the cell growth and induction parameters can be tightly controlled to reduce the deviation and standardize the biosensor application. On the

other hand, using overnight culture directly is more practical and simple experimental procedure than preparation of exponentially growing cells such that mid exponential phase cells in M9 medium can be reached after 4 hours of incubation.

For bioreporters cultured in MOPS supplemented medium, for arsenite (Figure 3.27a) and arsenate (Figure 3.27b), mid exponential phase cells exhibited higher fluorescence values for all concentrations than others with higher standard deviations. Again, stationary cells had the highest background fluorescence due to large number of cells and the fluorescence response reached plateau earlier than other phases (Figure 3.28, Figure 3.29). The fluorescence performance of stationary cells in MOPS medium was worse than that in M9 medium. The reason could be that cells in M9 medium were healthier since M9 medium has sufficient inorganic phosphate which is an essential nutrient for cells. Moreover, the detection limit of arsenite increased to 25 µg/L for stationary cells.

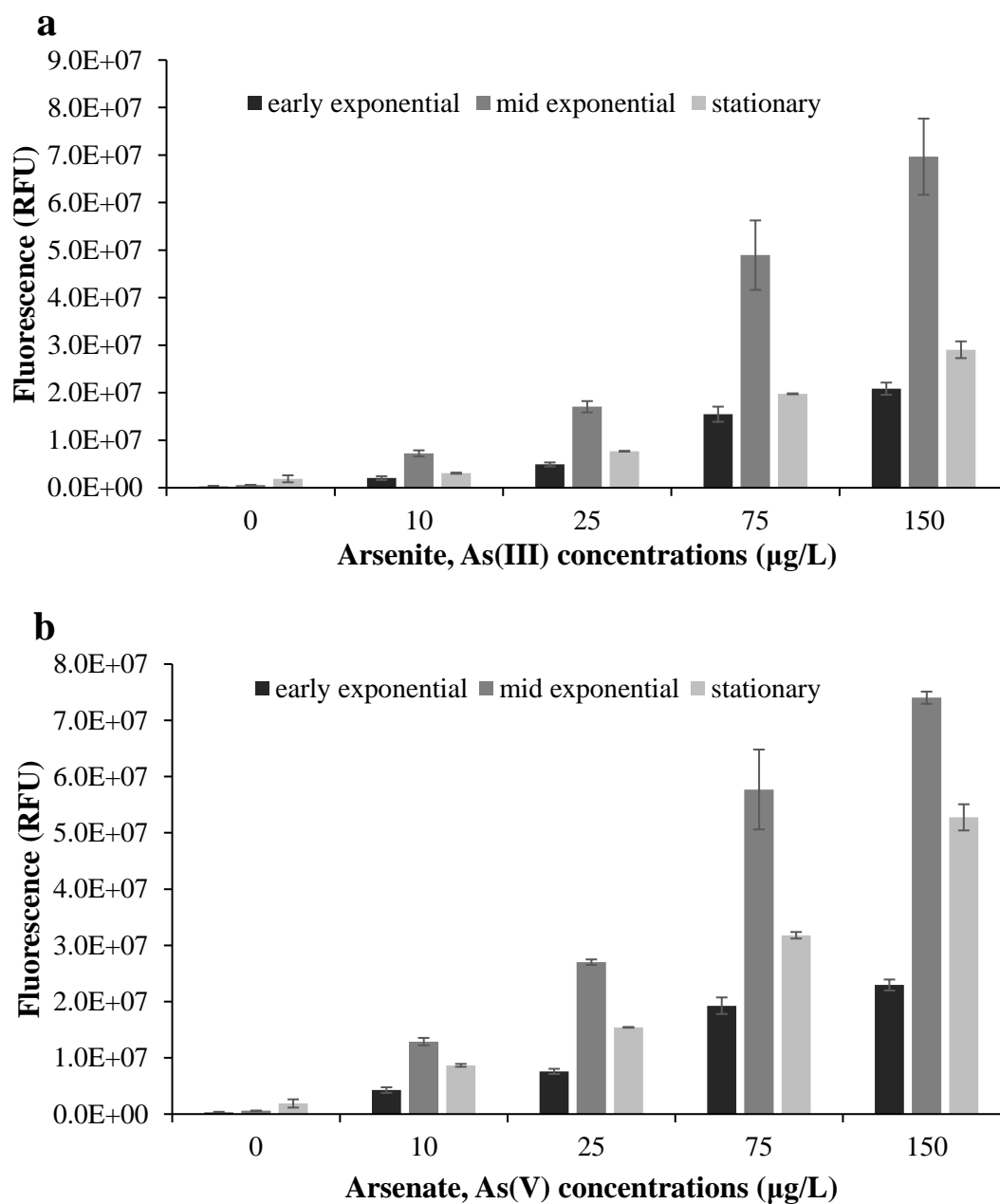


Figure 3.27 The fluorescence intensity values of arsenic bioreporter induced with a) arsenite and b) arsenate at different growth phases. Bioreporter cells were grown in MOPS supplemented. Data shown as mean \pm SD of triplicate wells of each induction group and presented at 6-h time point.

To detect arsenite/arsenate in MOPS supplemented medium, mid exponential cells could be used instead of early exponential cells if the cell growth and induction

parameters can be tightly controlled to reduce the deviation and standardize the biosensor application.

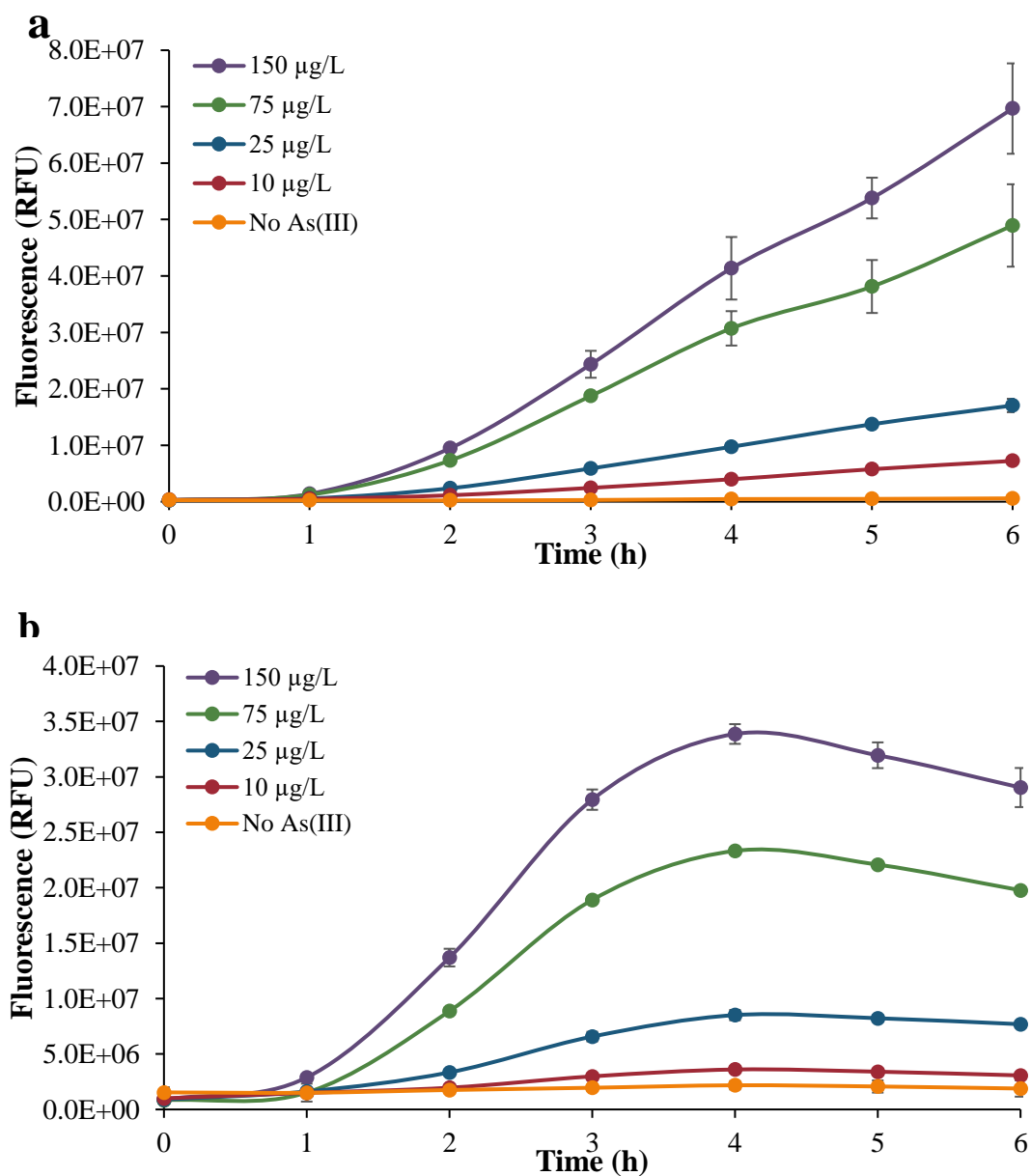


Figure 3.28 Fluorescence kinetic profile of arsenic bioreporter with different induction schemes. Bioreporter cells grown in MOPS supplemented medium to a) mid-exponential and b) stationary phase induced with different arsenite concentrations. Data shown as mean \pm SD of triplicate wells of each induction.

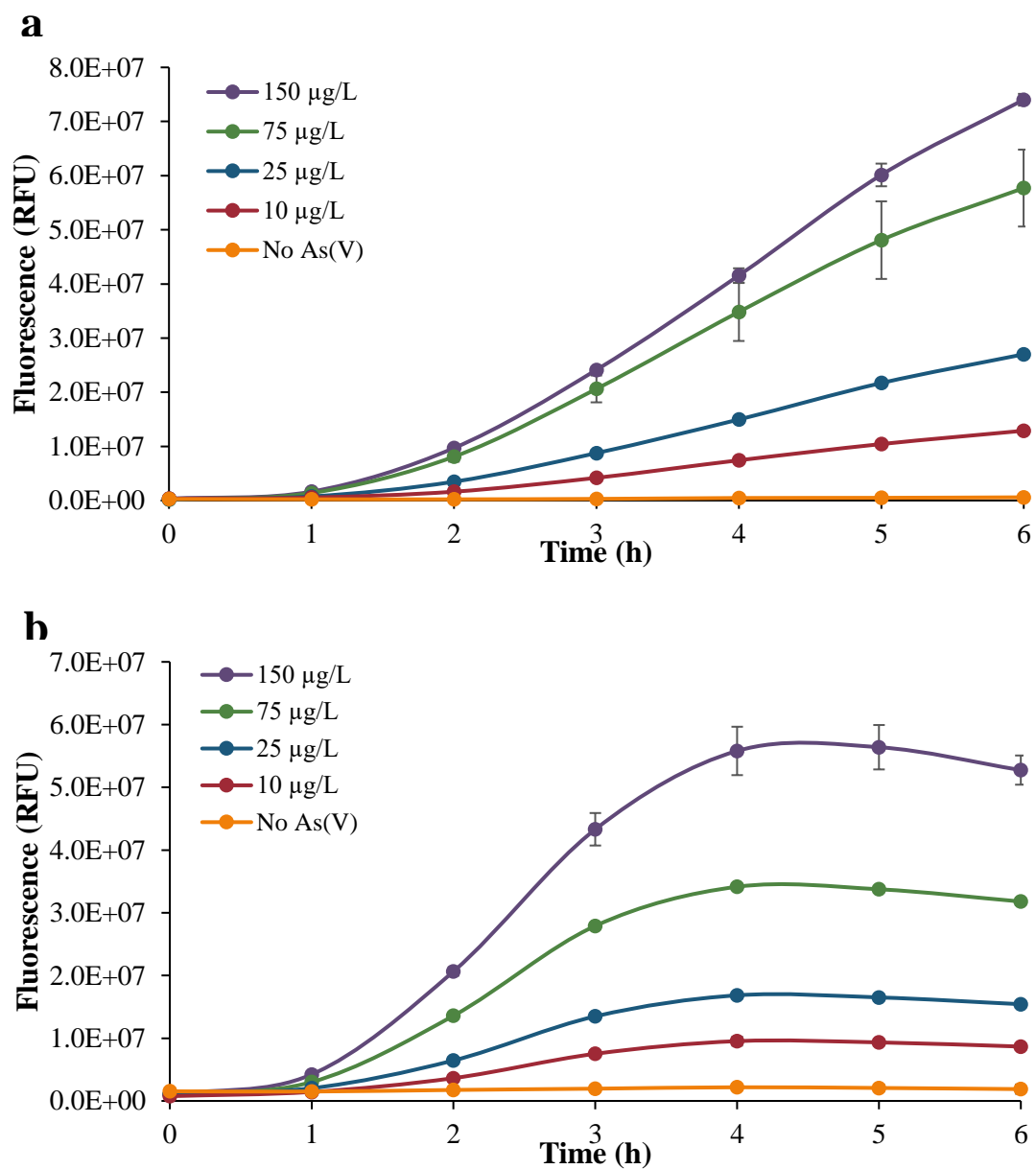


Figure 3.29 Fluorescence kinetic profile of arsenic bioreporter with different induction schemes. Bioreporter cells grown in MOPS supplemented medium to a) mid-exponential and b) stationary phase induced with different arsenate concentrations. Data shown as mean \pm SD of triplicate wells of each induction.

3.2.2.5. Arsenic Content Determination of Groundwater Sample

To test the applicability of arsenic biosensor to real life samples, a groundwater sample was obtained from an arsenic polluted tube well in Central Anatolia region, Turkey. For quantitative assessment of the total inorganic As concentration in groundwater, bioreporter cells were cultured in MOPS supplemented medium and a standard curve was generated from known concentrations of arsenite, As(III), in deionized water by linear analysis and a good linear response to arsenite occurred between 0 and 150 $\mu\text{g/L}$ (Figure 3.30). Calculated arsenite concentration from the standard curve was $93.24 \pm 13.08 \mu\text{g/L}$. After taking the dilution factor of the groundwater sample into account as MOPS culture medium and groundwater were mixed in 1:1 (v/v) ratio, the estimated concentration of arsenite in the groundwater were $186.48 \pm 26.16 \mu\text{g/L}$.

To further verify the concentration, groundwater sample was spiked with a known concentration of As(III) (50 $\mu\text{g/L}$) to eliminate possible inhibitory effects caused by compounds other than arsenic in the groundwater. For As(III) spiked groundwater, the fluorescence intensity was similar to that of a positive control in standard curve containing the same final concentration of arsenite ($\sim 150 \mu\text{g/L}$) in deionized water. Since groundwater samples have mostly arsenite due to their anoxic conditions, the total arsenic ion concentration calculated was mostly attributed to arsenite.

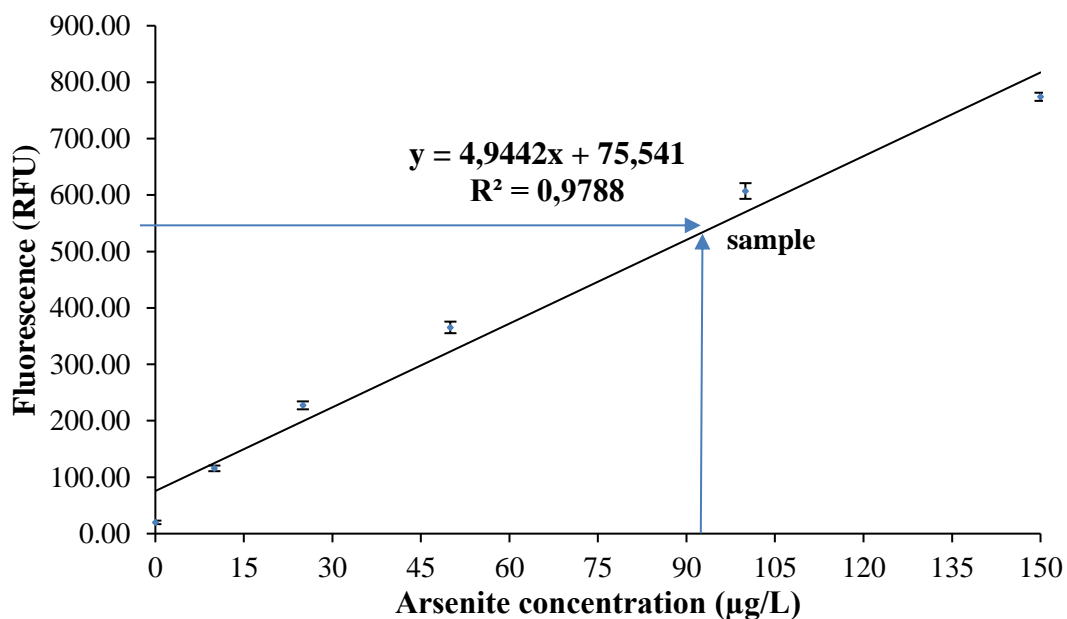


Figure 3.30 Calibration (standard) curve for arsenite ranging from 0 to 150 µg/L after bioreporter cells were assayed in MOPS medium for 4 hours. Slope linearly interpolated from average of triplicate samples (Elcin & Öktem, 2019).

According to laboratory analysis with ICP-MS and groundwater sample's natural content of total arsenic was reported as 240 µg/L. The values obtained with the arsenic biosensor were lower than the data obtained by ICP-MS analysis, indicating the bioavailable portion of arsenic was lower than the total arsenic content. This may result from the presence of water-insoluble arsenic in the form of complexes with organic matter and adsorbed onto Al- and Fe-oxyhydroxides, and phyllosilicates (Aide et al., 2016). Moreover, presence of phosphates and reduction by sulfides and other metals influence the speciation and bioavailability of arsenic (Jonnalagadda & Rao, 1993). Given the notion that metal toxicity to organisms is related to bioavailable portion rather than the total metal concentration (Olaniran et al., 2013), this bioreporter system gives comparable results with analytical techniques and bioavailable arsenic content in order to determine the acute toxicity risks. Thus, according to both ICP-MS and arsenic biosensor results, the tube well must be closed immediately because the arsenic concentration was higher than 50 µg/L.

3.2.3. Induction of *E. coli* MG1655 (pBR-PzntA) Bioreporter Strain

For expression studies, Cd sensor plasmid, pBR-PzntA, was isolated from *E. coli* DH5 α and transformed into *E. coli* MG1655 strain. Before 96-well microplate experiments, the growth of *E. coli* MG1655 (pBR-PzntA) strain was tested under low and high cadmium concentrations to confirm the healthy bacterial growth under metal exposure. The growth curves for up to 48-h is given in Appendix D.

Table 3.4 Bacterial growth, OD600 values, of pBR-sGFP and pBR-PzntA cultures in M9 supplemented medium in presence of cadmium, Cd(II), over time.

OD/hour	pBR-sGFP	NC	Cd (II) 100 μ g/L	Cd (II) 500 μ g/L
3	0.31 \pm 0.02	0.31 \pm 0.01	0.34 \pm 0.03	0.30 \pm 0.01
6	0.92 \pm 0.07	1.02 \pm 0.06	1.16 \pm 0.13	1.0 \pm 0.01
9	1.33 \pm 0.05	1.39 \pm 0.09	1.46 \pm 0.08	1.35 \pm 0.08
24	2.2 \pm 0.08	2.1 \pm 0.09	2.23 \pm 0.09	2.12 \pm 0.1

- The average values of replicates are presented with standard deviation (n = 3).

- NC: Negative control (pBR-PzntA culture with no addition of cadmium)

The growth results did not show any bacterial growth impairment (Table 3.4), and then the expression studies were performed. Induction of GFP expression from *PzntA* will occur by Cd(II) along with the activation of ZntR transcriptional regulator protein to allow expression from its cognate promoter, *zntA*.

The applicability of bioreporter was assessed by inducing the cells with cadmium in different media and different induction schemes. The concentrations of cadmium ions between 0 and 200 μ g/L were chosen. According to current regulation in Turkey, maximum of 5 μ g/L of cadmium was employed as allowable limit for drinking water and for surface water quality standards. Moreover, surface waters containing cadmium concentrations above 7 μ g/L are regarded to be highly contaminated (T.C 2013, 2015).

3.2.3.1. Fluorescence Emission Kinetics of Cadmium Bioreporter Strain in M9 and MOPS Supplemented Media

To characterize the cadmium bioreporter cells in response to different concentrations of cadmium, 96-well plate assays were performed with M9 supplemented medium as an induction medium. The detection limit was determined using statistically significant changes ($p < 0.05$) in RFU compared with no induction (negative) control RFU.

Fluorescence against time curves were drawn for 6-h induction time for clarity, since it presented adequately high fluorescent signal to differentiate between dose–response curves. One-way ANOVA result for M9 supplemented medium showed that the cadmium bioreporter induction by tested concentrations of Cd(II) compared to uninduced sample was significant after 3.5 hours, $p = .000$. Also, 50 and 100 $\mu\text{g/L}$ of cadmium was detected after 1.5 hours incubation and 5 $\mu\text{g/L}$ (44 nM) of cadmium was detected after 3.5 hours of induction with a statistically significant change ($p < 0.05$), thus the bioreporter's detection limit was higher in the beginning and it decreased with time. In M9 supplemented medium, 2 $\mu\text{g/L}$ (18 nM) of cadmium couldn't be detected within assay time. The fluorescence signal increased continuously with time and increasing metal concentration and the background fluorescence exhibited by the uninduced biosensor did not have any statistically significant fluorescent change during the incubation period (Figure 3.31). In order to determine the significance levels of induction groups, Tukey's HSD test was performed for 3.5-h time point; the descriptive statistics table, ANOVA table and post hoc test results are given at Section D in Appendix E.

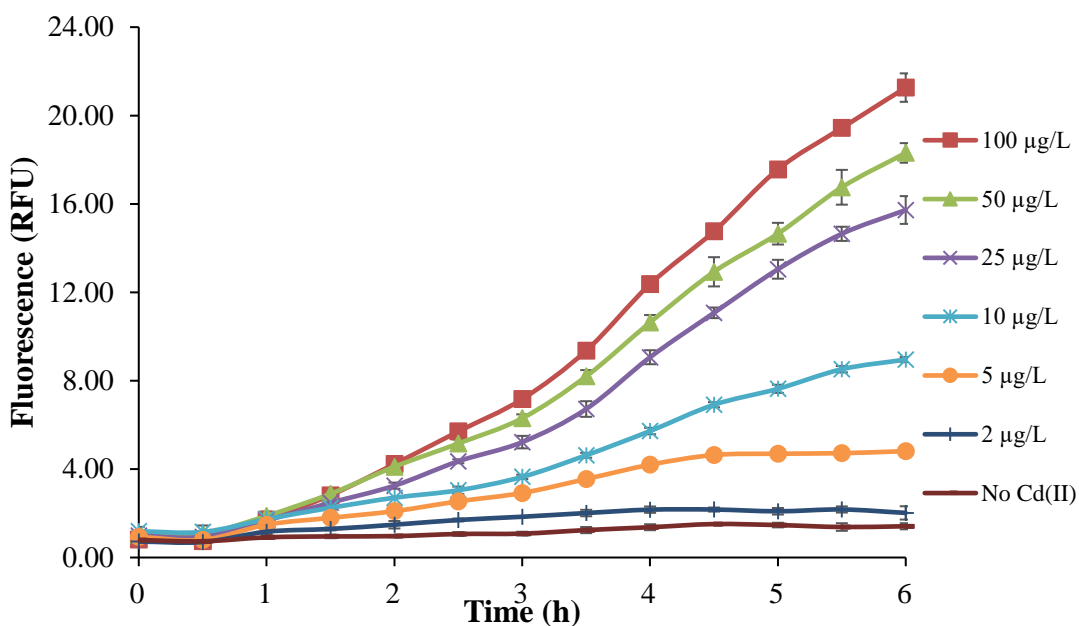


Figure 3.31 Fluorescence emission kinetics of cadmium bioreporter. Bioreporter cells grown in M9 supplemented medium (till $OD_{600} = 0.1$) induced with different cadmium, Cd(II) concentrations. Data shown as mean \pm SD of triplicate wells of each induction. Error bars are shown only when they exceed the size of the symbols.

One-way ANOVA result for MOPS supplemented medium showed that the cadmium bioreporter induction by all of the tested concentrations of Cd(II) compared to uninduced sample was significant after 1.5 hours, $p = .000$. Also, both 2 and 100 $\mu\text{g/L}$ of cadmium could be detected after 1.5 hours incubation with a statistically significant change ($p < 0.05$). The background fluorescence exhibited by the uninduced biosensor did not have any statistically significant fluorescent change during the incubation period. The fluorescence signal increased continuously with time and increasing metal concentration except for 2 $\mu\text{g/L}$ of cadmium (Figure 3.32). In order to determine the significance levels of induction groups, Tukey's HSD test was run for 1.5-h time point; the descriptive statistics table, ANOVA table and post hoc test results are given at Section E in Appendix E.

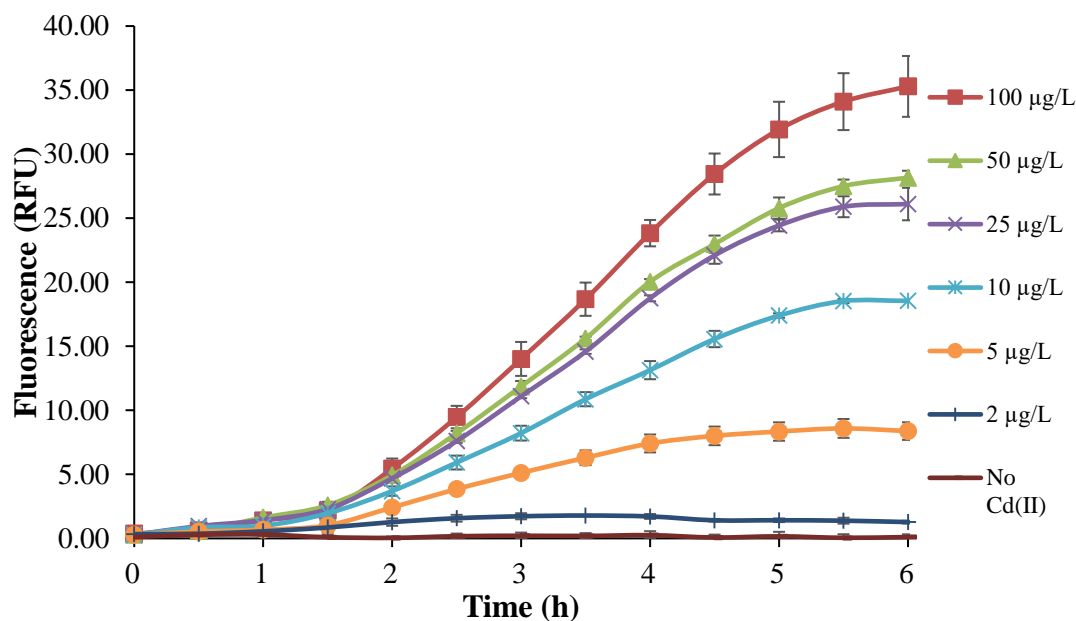


Figure 3.32 Fluorescence emission kinetics of cadmium bioreporter. Bioreporter cells grown in MOPS supplemented medium (till $OD_{600} = 0.1$) induced with different cadmium, $Cd(II)$ concentrations. Data shown as mean \pm SD of triplicate wells of each induction. Error bars are shown when they exceed the size of the symbols.

According to the results, the fluorescence values in MOPS medium were higher than that of M9 medium, suggesting that cadmium bioreporter cells were more sensitive to cadmium in MOPS supplemented medium. The reason for the increased sensitivity may be attributed to the increased bioavailability of cadmium ions, since inorganic polyphosphate causes extracellular precipitation of metal-phosphate complexes in the medium. It is also known that one of the passive mechanisms of bacterial tolerance to heavy metals is intracellular chelation of heavy metals by anionic polyphosphate that the amount of polyphosphate in a cell correlates with cellular tolerance to heavy metals (Keasling & Hupf, 1996).

Biran et al. (2000) constructed a biosensor for cadmium in *E. coli* RBE23-17 that consists of the *lacZ* gene expressed under the control of the cadmium-responsive promoter of *zntA*. They reported that under optimized conditions, using cells growing exponentially in rich medium (LB), 50 nM Cd^{2+} was the lowest concentration that

could be detected after 30 min, and 25 nM (2.8 µg/L) Cd²⁺ could be detected after 1 hour.

Riether et al. (2001) constructed *lux* transcriptional fusion to the *zntA* gene to create heavy metal luminescent reporter strain, *E. coli* MG1655 (pZNT::lux). This strain proved to be sensitive to Cd(II), Pb(II), Zn(II), and Hg(II). Metal concentrations that caused the highest luminescence induction were 0.3 µM CdCl₂, 1 µM Pb(NO₃)₂, and 30 µM HgCl₂ and ZnSO₄ after 80-min incubation. The strongest inducer of this strain was cadmium with the lowest detection threshold and significant luminescence induction at 10 nM, (1.1 µg/L) in modified glycerol-glycerophosphate medium (GGM) (glucose 0.5%, 40 mM MOPS, 1 mM MgCl₂, 18 mM NH₄Cl, 13 mM KCl, 5 mM K₂SO₄, 0.07 mM CaCl₂, 5 mM disodium β-glycerophosphate). They also concluded that the sensitivity of the *zntAp*::lux biosensor in LB compared to GGM medium was reduced probably due to metal chelation or precipitation by medium components such as inorganic phosphates.

Charrier et al. (2010) constructed *lux* transcriptional fusion to the *zntA* promoter and formed an *E. coli* DH1 pBzntlux strain. They reported that eight metals were detected by *E. coli* DH1 pBzntlux. Detection limits for cadmium and mercury were 5 nM and other heavy metals like lead, zinc, tin, cobalt, nickel, and chromium (VI) were detected at 5 or 50 µM. They used an acetate medium with a C/N/P ratio of 100/10/1 for growth and biosensor applications.

Gireesh-Babu & Chaudhari (2012) constructed *E. coli* DH5α (pPROBE- *zntR*-*zntA*) by cloning *zntA* gene promoter and *zntR* regulatory gene of *E. coli znt* operon amplified from *E. coli* DH5α genomic DNA into upstream to the *gfp* gene in pPROBE-KT vector. The detection limit for Cd(II), Hg(II) and Zn(II) was 5 µg/L, 2 µg/L and 20 mg/L, respectively, after 16 hours of incubation.

Hou et al. (2015) constructed *E. coli* (pzntRluc) sensor by cloning *Pznt* promoter to the upstream of *luc* in pUC18luc. The detection limit reported for Cd(II) was 0.1 μ M (11.2 μ g/L) and for Pb(II) was 0.05 μ M after 2.5 hours of incubation time.

Yoon et al. (2016) constructed the metal-sensing plasmids pZntA-eGFP and pZntA-mCherry, consisting of the promoter region of *zntA* (*zntAp*) in *E. coli* and *egfp* or *mcherry* as a sensing and reporter domain, respectively. *E. coli* DH5 α was used as the host strain for plasmids and LB was used for assay medium. *E. coli* (pZntA-eGFP) strain detected 0.1 mg/L of Cd(II) after 1 hour while *E. coli* (pZntA-mCherry) strain showed slower and weaker response that 1 mg/L of Cd(II) was detected after 2 hours.

3.2.3.2. Metal Specificity of Cadmium Bioreporter Strain

Since *zntA* gene is a pump for heavy metals, besides Zn(II) and Cd(II), ZntA exports also other divalent ions such as Pb(II), Hg(II), Co(II) and Ni(II) from the cell (Beard et al., 1997). In order to evaluate specificity of the constructed cadmium bioreporter, the response to major heavy metal contaminants of territorial environments and mostly divalent metal ions was tested at 250 μ g/L while cadmium was tested at 50 μ g/L concentration both in M9 and MOPS supplemented medium (Figure 3.33).

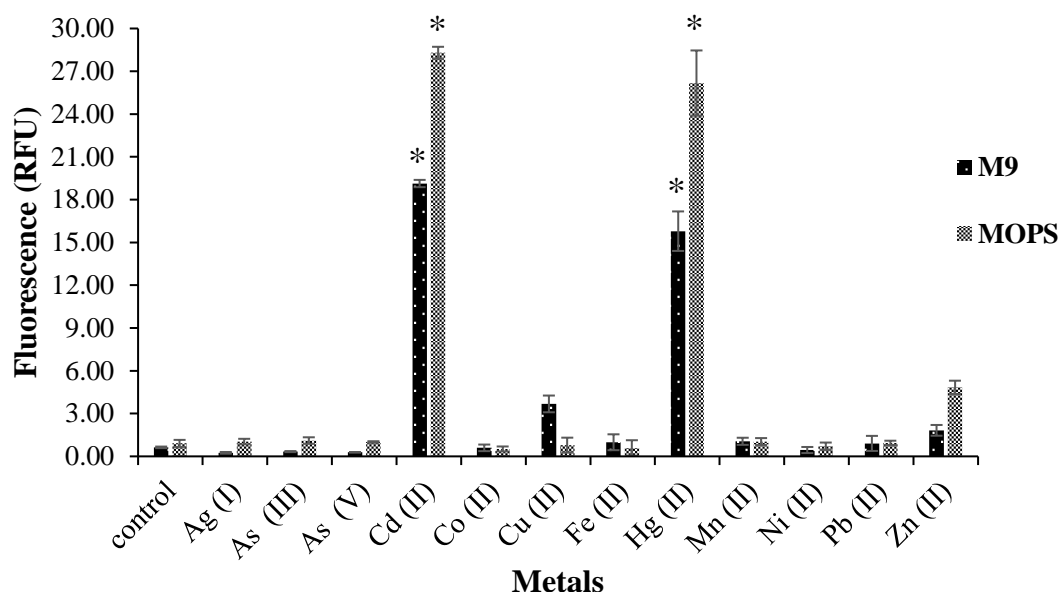


Figure 3.33 Metal specificity of the cadmium bacterial bioreporter. Bioreporter cells were grown either in M9 or in MOPS supplemented medium (till $OD_{600} = 0.1$). Control refers to no metal addition. Data shown as mean \pm SD of triplicate wells of each induction group and presented at 6-h time point. * $p < 0.001$.

Among all tested metals, except Cd(II), only Hg(II) showed a high fluorescence response especially in MOPS medium rather than M9 medium. Moreover, In M9 medium, Cu(II) showed a little higher response than in MOPS medium while Zn(II) showed higher response in MOPS medium rather than M9 medium (Figure 3.33).

Biran et al. (2000) stated that their biosensor was specific to $CdCl_2$, although a weak response to $HgCl_2$ and an even weaker response to $ZnCl_2$ were obtained at a higher concentration (100 times).

Riether et al. (2001) also reported that *E. coli* MG1655 (pZNT::lux) strain proved to be sensitive to a lesser degree to Co(II), Ni(II), SbO_2^- , CrO_4^{2-} , and $Cr_2O_7^{2-}$. They said that the other metal ions except Cd(II) were detected at higher concentrations in the following order: $Pb(II) > Hg(II) > Zn(II) > Co(II) > Ni(II) = SbO_2^- > CrO_4^{2-} = Cr_2O_7^{2-}$.

Charrier et al. (2010) also concluded that their *E. coli* DH1 pBzntlux strain detects large number of heavy metals and consequently it cannot be used as a specific sensor, rather it should still be considered as a general warning system for heavy metal water pollution.

Yoon et al. (2016) stated that the WCB harboring pZnt-eGFP and pZnt-mCherry showed the same metal selectivity and showed highest induction coefficient toward Cd(II) among tested metal(loid)s with a lesser extent to Pb(II), Cr(II) and Zn(II). They speculated the reason why the WCB employing *zntAp* was more sensitive to cadmium than the other metals tested was that Cd(II) would associate with ZntR more tighter than others, and since it has larger atomic and covalent radii, the Cd(II)-ZntR complex would be more stable. They concluded that the quantification of bioavailable cadmium using WCBs was logical given that the interaction of the endogenous ZntR in *E. coli* with Cd(II) was predicted to be stronger than any other metal ions, including zinc.

Gireesh-Babu and Chaudhari (2012) stated that the concentrations of Hg(II), Cd(II) and Zn(II) needed for the induction of the *zntR-zntA* based sensor differed remarkably, the amount of Hg(II) being 700 and the amount of Cd(II) being 450 times lower than the respective concentration of Zn(II). Most importantly, the concentrations of mercury, cadmium and zinc inducing the biosensor are in good correlation with the toxicities of these metals. For example, for crustacean *Daphnia magna* the 24 h LC50 (lethal concentration) values for Hg(II) (0.01 mg/L) and for Cd(II) (0.64 mg/L; 24) are 760 and 12 times lower than for Zn(II) (7.6 mg/L; 25). The correlation of the sensitivities with toxicities of the metals is quite expected as the ‘sensing’ elements of the current biosensors originate from living organisms.

3.2.3.3. Mercury Sensitivity of Cadmium Bioreporter Strain

The cadmium biosensor showed a fluorescence response toward 250 µg/L of mercury, Hg(II) which is very high according to water quality standards. In Turkey, if mercury

concentration exceeds 2 $\mu\text{g/L}$, the surface water is marked as highly polluted (T.C., 2015). Also, drinking water safety limit for mercury is 1 $\mu\text{g/L}$ (T.C., 2013). To check for the specificity and sensitivity to mercury, the lower concentrations of Hg(II) of 1, 5, 10, 25, 50, 100 and 200 $\mu\text{g/L}$ were tested in both M9 and MOPS supplemented media. The general trend for both media was that the bioreporter's fluorescence response was lower towards mercury than that of cadmium indicating lower sensitivity towards mercury.

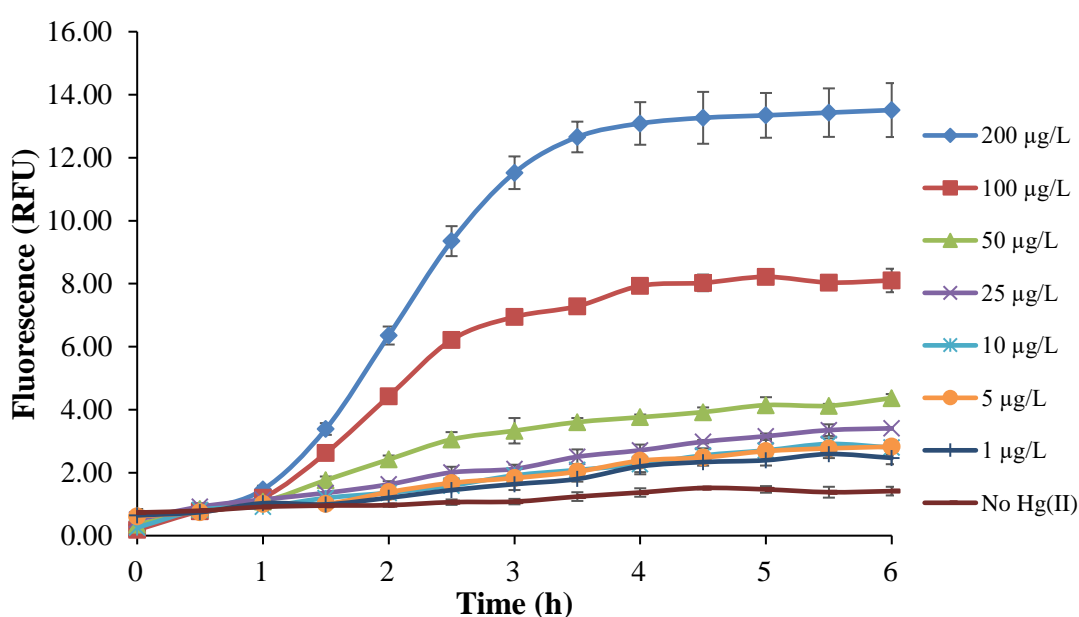


Figure 3.34 Fluorescence emission kinetics of cadmium bioreporter cells in response to mercury, Hg(II). Bioreporter cells were grown in M9 supplemented medium (till $OD_{600} = 0.1$). Data shown as mean \pm SD of triplicate wells of each induction. Error bars are shown only when they exceed the size of the symbols.

In M9 supplemented medium, cadmium bioreporter cells can detect 100 and 200 $\mu\text{g/L}$ after 1.5 hours, and 50 $\mu\text{g/L}$ of Hg(II) after 3 hours. It can detect maximum Hg(II) concentration of 25 $\mu\text{g/L}$ after 10 hours while it couldn't detect concentrations of 1, 5 and 10 $\mu\text{g/L}$ of Hg(II). The fluorescence values for all tested Hg(II) were lower compared to that of the same cadmium concentrations and the fluorescence response didn't increase continuously during the assay time and reached plateau (Figure 3.34).

The fluorescence response increased with time for 100 and 200 µg/L of Hg(II) while for 50 µg/L or lower it didn't increase.

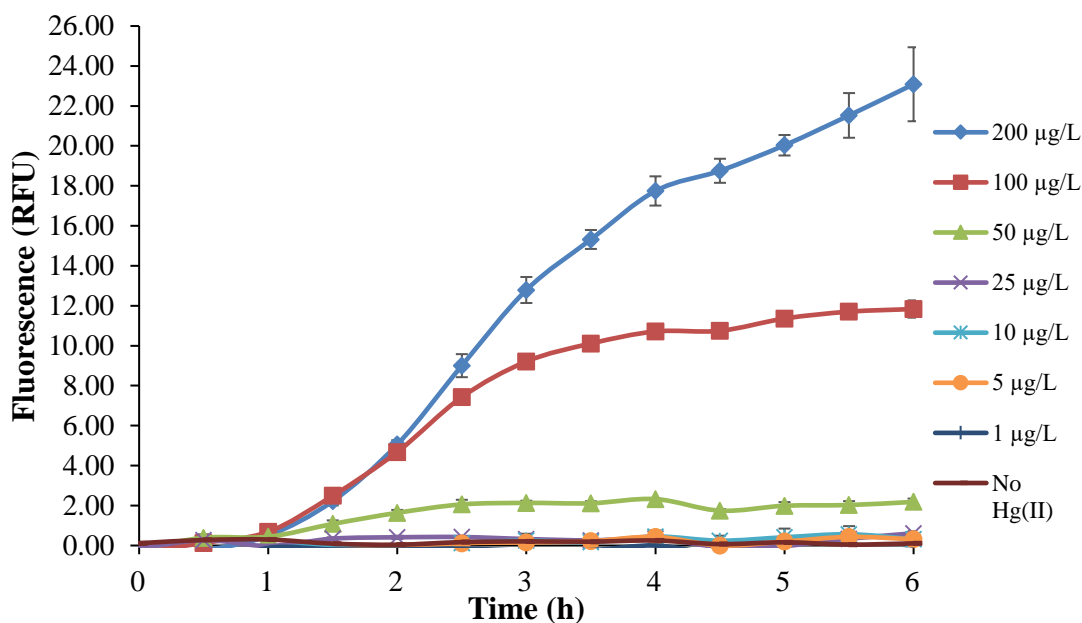


Figure 3.35 Fluorescence emission kinetics of cadmium bioreporter cells in response to mercury, Hg(II). Bioreporter cells were grown in MOPS supplemented medium (till $OD_{600}=0.1$). Data shown as mean \pm SD of triplicate wells of each induction. Error bars are shown only when they exceed the size of the symbols.

In MOPS supplemented medium, cadmium bioreporter cells can detect 50, 100 and 200 µg/L after 2 hours. Here, it cannot detect 25, 10, 5 and 1 µg/L of Hg(II) during the assay period. Again, the fluorescence values for all tested Hg(II) were lower compared to that of the same cadmium concentrations. The fluorescence response increased with time for 100 and 200 µg/L of Hg(II) while for 50 µg/L it didn't increase (Figure 3.35).

To conclude, the bioreporter's sensitivity to mercury in both media was limited to 50 µg/L which was very high compared to cadmium which was 2 µg/L. Also, as in the case of cadmium, the fluorescence performance was higher in MOPS medium compared to M9 medium.

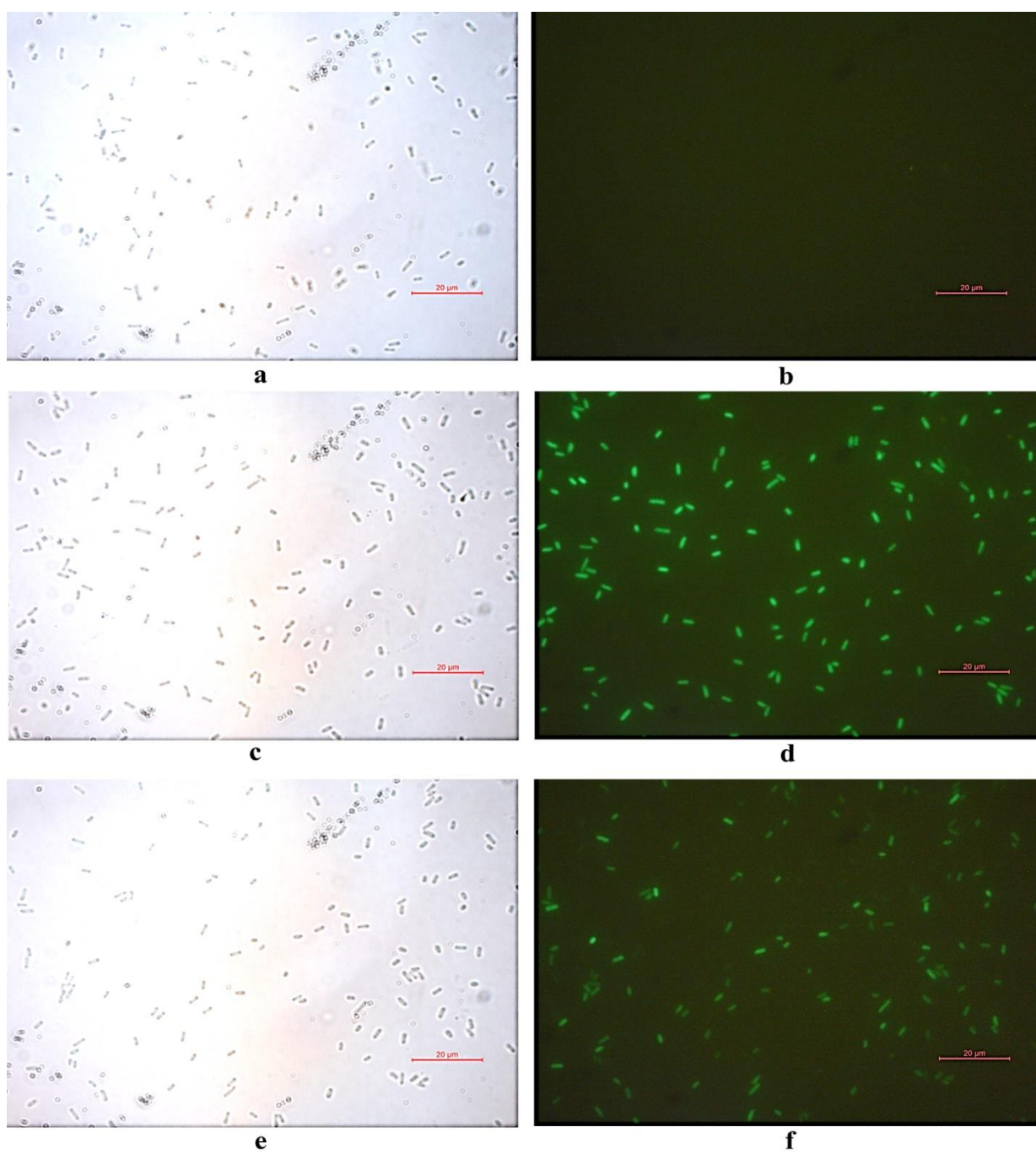


Figure 3.36 Fluorescence microscope images of cadmium bioreporter cells: a, b) uninduced bioreporters under BF and Fluo channel, c, d) induced bioreporters with 100 $\mu\text{g/L}$ cadmium under BF and Fluo channel, e, f) induced bioreporters with 400 $\mu\text{g/L}$ mercury under BF and Fluo channel. BF: Bright field; Fluo: Fluorescence. Scale: 20 μm .

Figure 3.36 shows the fluorescence microscopy images of the uninduced, Cd(II) and Hg(II)-induced cadmium bioreporter cells assayed in M9 supplemented medium after 6 hours. Images were taken by using Leica DM6000 M Fully Automated Upright Microscope.

3.2.3.4. Fluorescence Response of Cadmium Bioreporter Strain at Different Growth Phases

For cadmium bioreporter, the best growth phase of this strain with better cadmium sensitivity was determined. Assays were conducted in both M9 and MOPS supplemented media. Apart from early exponential cells, mid exponential cells ($OD_{600} = 0.4-0.6$) and stationary cells (overnight culture, $OD_{600} = 1.5-2.0$) were used for induction. Early exponential phase was chosen for dose-response assays because, in preliminary experiments and the results of growth effect experiments with cells taken from exponential and stationary culture, poor fluorescence performance and higher variability in fluorescence response were observed.

When the cadmium bioreporter's fluorescent responses were compared for M9 supplemented medium, the higher fluorescence responses were obtained for 5 and 25 $\mu\text{g/L}$ of Cd(II) concentrations in exponential growth phase cells. For 100 $\mu\text{g/L}$ of Cd(II), early exponential phase cells were more sensitive than other phases (Figure 3.37).

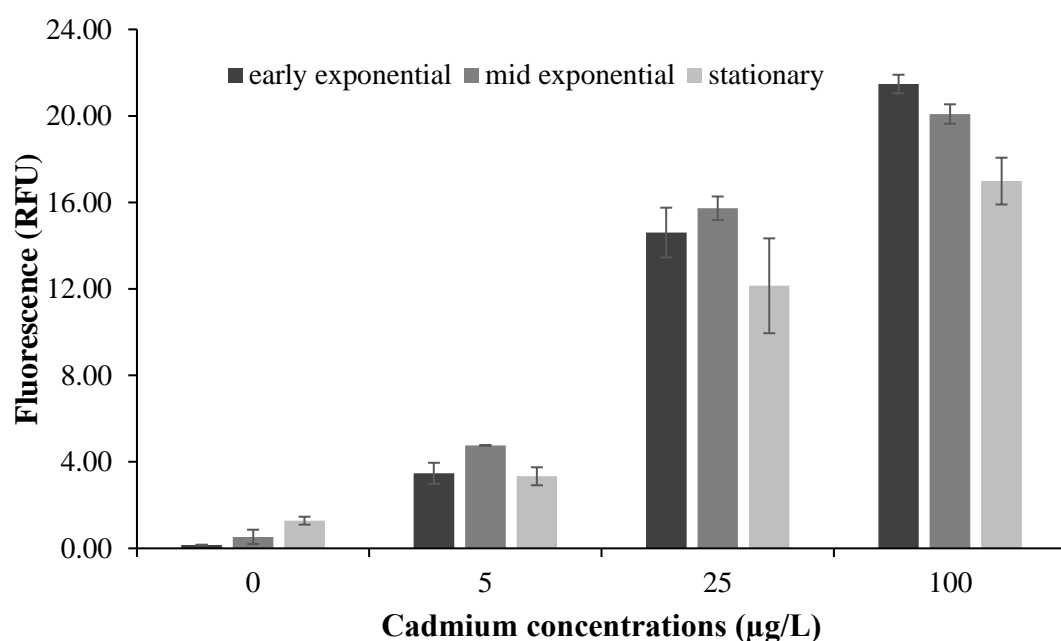


Figure 3.37 The fluorescence intensity values of cadmium bioreporter with different induction schemes. Bioreporter cells grown in M9 supplemented medium. Data shown as mean \pm SD of triplicate wells of each induction group and presented at 6-h time point.

As in the case of arsenic bioreporter cells, stationary phase cells had the highest background fluorescence and highest standard deviation due to large number of cells. For both mid exponential and stationary growth phases the fluorescence response reached plateau earlier than early phase cells (Figure 3.38).

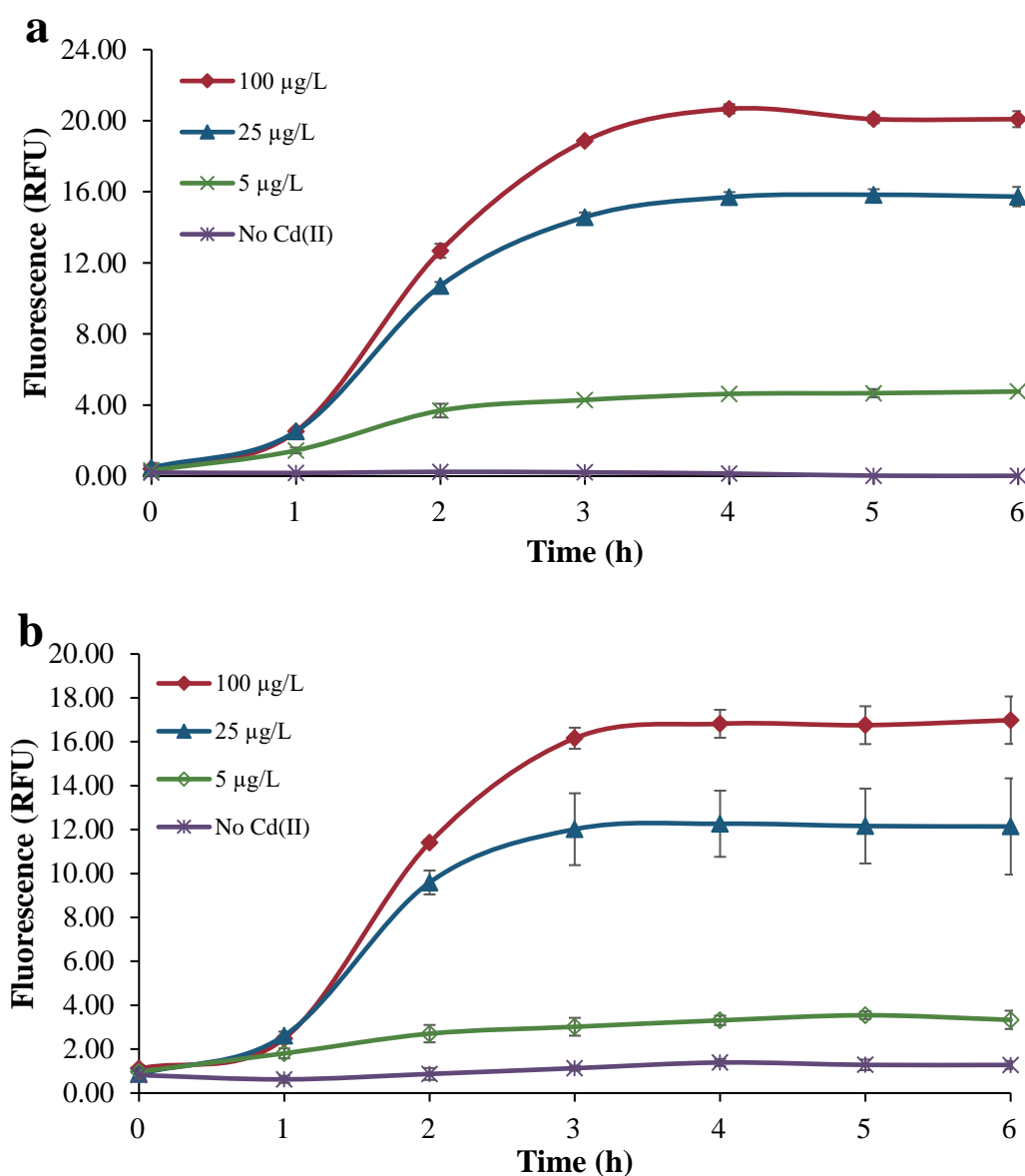


Figure 3.38 Fluorescence kinetic profile of cadmium bioreporter with different induction schemes. Bioreporter cells grown in M9 supplemented medium to a) mid-exponential and b) stationary phase induced with different cadmium concentrations. Data shown as mean \pm SD of triplicate wells of each induction.

To detect cadmium in M9 supplemented medium, both early and mid exponential cells could be used if the cell growth and induction parameters can be tightly controlled to reduce the deviation and standardize the biosensor application. On the other hand,

using overnight culture may not be good since the cells perform worse in this phase with less sensitivity.

For cadmium bioreporter cultures cultured in MOPS supplemented medium, early exponential phase cells exhibited higher fluorescence values for all concentrations than other phases (Figure 3.39). The stationary cells had very high background fluorescence and it did not have sensitivity to any of the tested cadmium concentrations (Figure 3.40b). Mid exponential cells were better than stationary cells, but the dose response was absent for increasing concentrations (Figure 3.40a). The reason for poor fluorescence performance of later phases can be that the cells in M9 medium were healthier due to presence of inorganic phosphates which are the essential nutrients for bacteria.

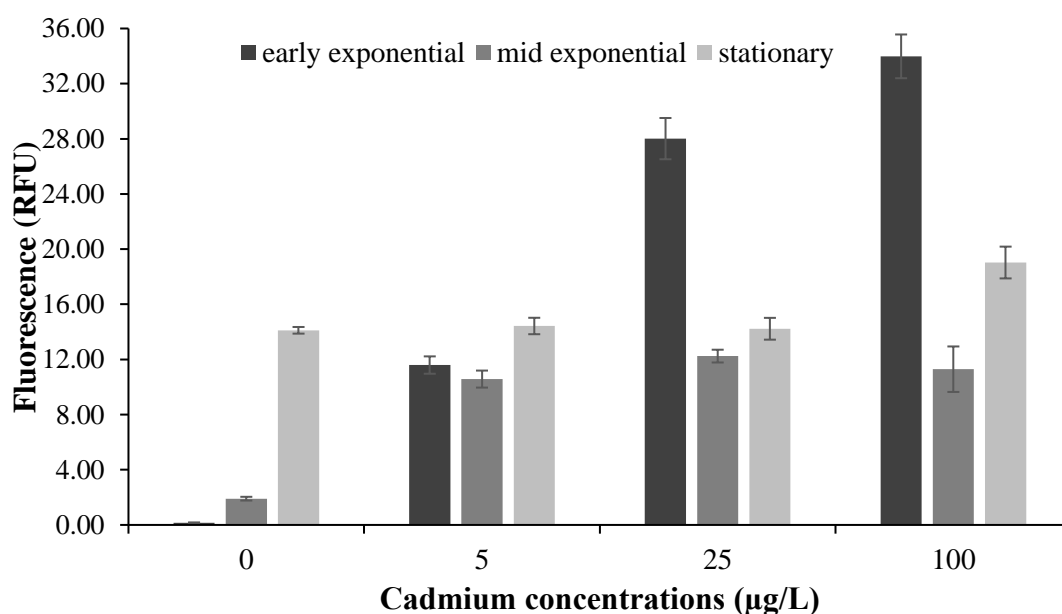


Figure 3.39 The fluorescence intensity values of cadmium bioreporter with different induction schemes. Bioreporter cells grown in MOPS supplemented medium. Data shown as mean \pm SD of triplicate wells of each induction group and presented at 6-h time point.

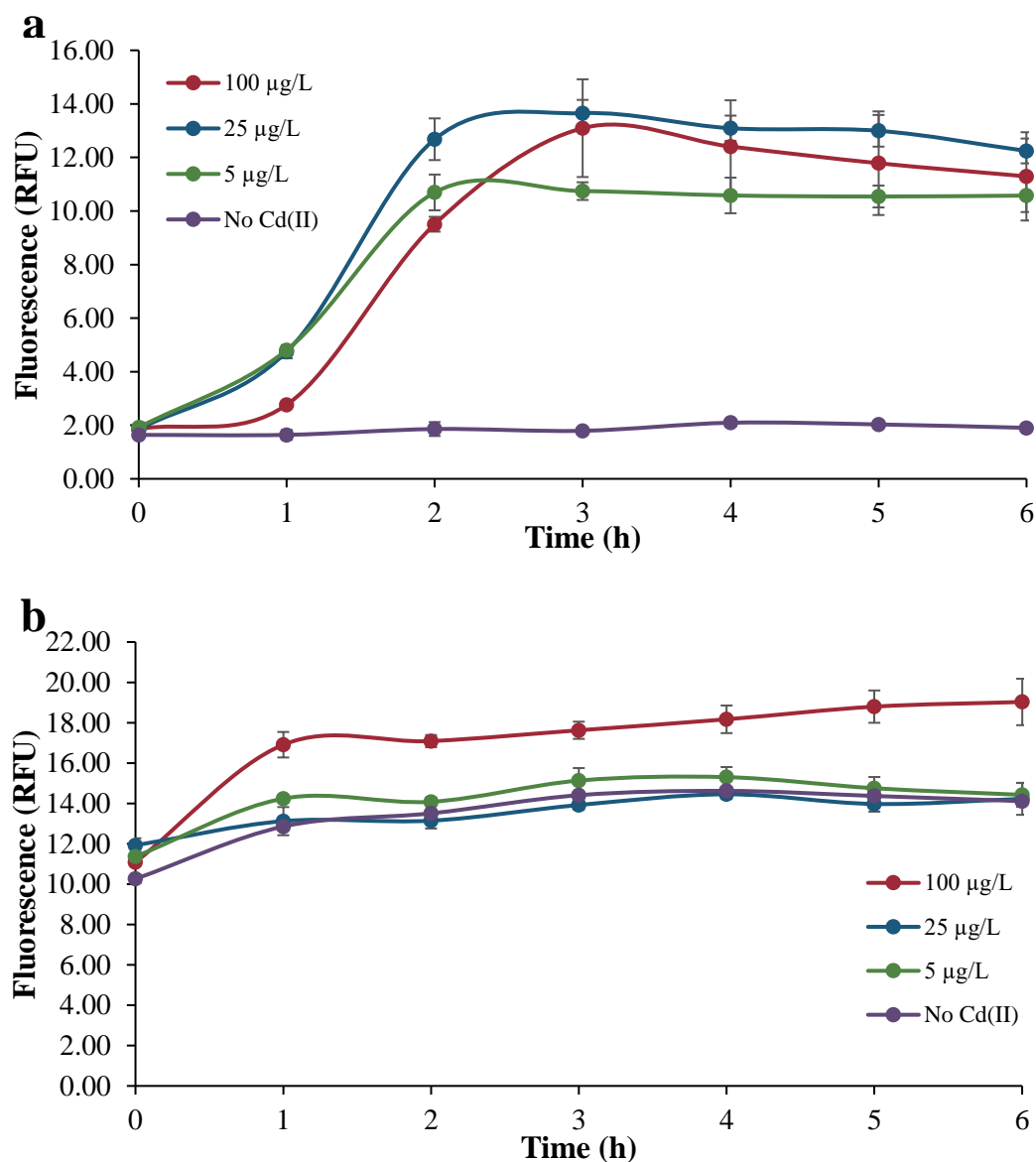


Figure 3.40 Fluorescence kinetic profile of cadmium bioreporter with different induction schemes. Bioreporter cells grown in MOPS supplemented medium to a) mid exponential and b) stationary phase induced with different cadmium concentrations. Data shown as mean \pm SD of triplicate wells of each induction.

To detect cadmium in MOPS supplemented medium, early exponential cells should be used since exponentially growing and stationary cells had very poor sensitivity compared to early phase cells.

Similar results were shown by Riether et al. (2001) that the best performance of the *luxCDABE*-expressing Cu and Zn reporters (*E. coli*) in cells grown in rich LB media was obtained at early exponential growth. That study also showed that the response of the bioreporters decreased at higher cell densities, most likely due to the absorption of metals by cell wall components or to light absorption due to the turbidity of the bacterial suspension. A similar effect has been shown with bioluminescent Hg-sensing *E. coli*, *P. putida*, and *Enterobacter aerogenes*, where reducing cell density by two orders of magnitude increased the sensitivity of the assay by two orders of magnitude (Rasmussen et al., 1997; Fu et al., 2008). In the case of *Bacillus subtilis*, the lowest concentrations of the target metals were sensed in the early stages of growth when cell density was low (Tauriainen et al., 1997). However, Harkins et al. (2004) reported a maximum of bioluminescence in exponential phase for their bioluminescent mercury bioreporter. Also, Charrier et al. (2010) stated that the induction of their *E. coli* DH1 pBzntlux strain by Cd(II) was extremely reliant on the growth phase. The induction ratio of *E. coli* DH1 pBzntlux was at maximum during the stationary phase (beginning and end of the growth). They explained this phenomenon by the fact that the ZntR regulator from the MerR family (specific to heavy metals and considered as stress-sensitive factors) is mainly expressed during the stationary phase of the growth.

These disparities between different studies could be explained by the genetic construction, reporter proteins and the use of different induction protocols and conditions. Thus, it is important to perform growth phase experiments since the mentioned factors significantly affect the bioreporter's performance and sensitivity.

3.3. Immobilization Studies of Arsenic Bioreporter Strain

To be used as a portable on-site monitoring device, the bioreporter cells should be preserved in a way for supporting long-term cell viability and biological activity, obtaining a rigid network tight enough for preventing wash-out from flow cell while enabling efficient exchange with the surrounding. For that, in this study, whole-cell

fluorescent arsenic bacterial bioreporter was immobilized/entrapped in the interstices of naturally occurring biocompatible gel polymers, agar and alginate, to convert the liquid assay into reproducible solid assay format.

Despite of various arsenic bioreporter systems reported with good sensing properties with low detection limits, there are relatively few studies for formulation of bacterial bioreporter specific to arsenic. These studies include bioreporters in lyophilized form (Charrier et al., 2011; Kuppardt et al., 2009; Prévéral et al., 2017), agarose embedded form (Jouanneau et al., 2012; Buffi et al., 2011) and alginate embedded fibre-optic form (Ivask et al., 2007). However, there are no alginate immobilization in bead format. Moreover, mostly bioreporter's response to arsenite was investigated but not to arsenate which the second most abundant ionic form of arsenic. In this study, agar gel and alginate bead immobilizations of the fluorescent arsenic bioreporter strain, *E. coli* MG1655 (pBR-arsR773), were investigated in terms of sensitivities of both systems towards two ionic forms of arsenic. To date, this is the first study to describe the agar hydrogel and alginate bead immobilized fluorescent arsenic bacterial bioreporter systems that can detect both arsenite and arsenate at a safe drinking water limit.

For immobilization experiments, exponential phase cells were used for immobilization studies since it was found that (Section 3.2.2.4) mid exponential cells showed higher fluorescence performance both in M9 and MOPS supplemented media than other phases. Although they have higher standard deviation than early exponential cells, entrapped cells showed lower deviation than free cells probably because of limited growth of cells due to lower metabolism in a restricted area.

For both matrices parameters such as gel (polymer) concentration and cell density in the final mixture were evaluated to optimize fluorescence performance in terms of sensitivity and reliability. Formulations with different media were evaluated to be used as both arsenite and arsenate biosensor by fluorescence response. Metal specificity of

the bioreporter systems to arsenic species was also determined. All bioassays were performed at 30 °C in order to further slow the growth of bacteria in the matrix (optimum growth at 37 °C) to keep cell number constant and also to mimic outdoor conditions.

3.3.1. Agar Gel Immobilization

Agar hydrogel was chosen as one of the immobilization matrices since it is an advantageous well-known polymer for entrapment of bacterial cells due to its ease of preparation, low cost, good mechanical stability (Albuquerque et al., 2016).

3.3.1.1. Optimization of Agar Gel Immobilization- Percentage and Cell Density

For agar gel optimization studies, the bioreporter cells prepared in M9 supplemented medium were used and induced with arsenite solution. Agar gel matrix was prepared by adding cell culture to agar solution at the temperature close to the setting point of the agar while minimizing heat damage to the bacterial cells. The volume of the agar-cell mixture within the wells was chosen as 100 µL since it has provided a homogenous distribution of added arsenic solution throughout the matrix. Three different final agar percentages of 0.5, 1 and 1.5 (w/v) were tested to assess the effect of agar concentration on the fluorescence response. Final cell density $OD_{600} = 0.1$ was kept constant for different agar concentrations. The agar percentages between 0.5 and 1.5 (w/v) were chosen since final agar percent higher than 1.5 was too viscous to mix with the cell culture and requires high working temperature (higher than 42 °C) that can damage the cells; agar percent lower than 0.5 was not solid enough to support the cells.

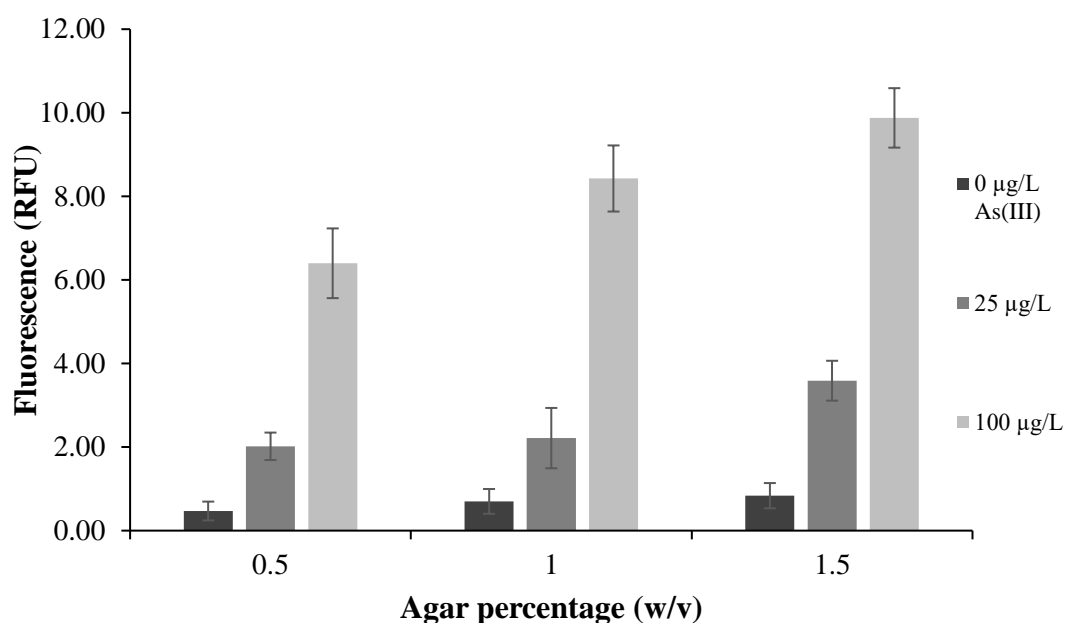


Figure 3.41 Effect of agar percentages of 0.5, 1 and 1.5 (w/v) on the fluorescence response of agar-immobilized arsenic bioreporter prepared in M9 supplemented medium with $OD_{600} = 0.1$. The average values of triplicate of each induction were presented for 6-h with standard deviation.

Figure 3.41 shows that increasing agar concentration in the matrix resulted in increase of fluorescence response to arsenite concentrations. Final agar concentration of 1.5 % (w/v) had highest fluorescence response to low (25 µg/L) and high (100 µg/L) arsenite concentrations which also had better mechanical rigidity compared to lower percentages. Thus, final agar concentration of 1.5% (w/v) was employed for further experiments. Similar result was also reported by Mitchell & Gu (2006) that the best agar concentration for their stress-responsive bioluminescent bacterial strains was 1.5%.

The effect of concentration of entrapped cells within agar gel was also determined. Final optical cell densities (OD_{600}) of 0.1, 0.4 and 0.7 (0.1 unit of $OD_{600} = 1 \times 10^8$ cells/mL) were tested in agar-1.5% (w/v) matrix. When the cell concentration increased within the matrix, relative fluorescence value of induced samples to the uninduced sample decreased since the fluorescence of uninduced cells drastically increased (Figure 3.42). The fluorescence intensity increase of uninduced cells can be

attributed to ‘leakage’ of the *ars* promoter, i.e., incomplete binding of the ArsR repressor protein in the absence of metal. Slight leakage at low cell densities might have become more prominent when cell concentration was increased. For cell densities of 0.4 and 0.7, the sensitivity of bioreporter-agar matrix decreased with increasing cell density such that 25 µg/L As(III) could not be distinguished from uninduced sample but rather 100 µg/L As(III) was detected.

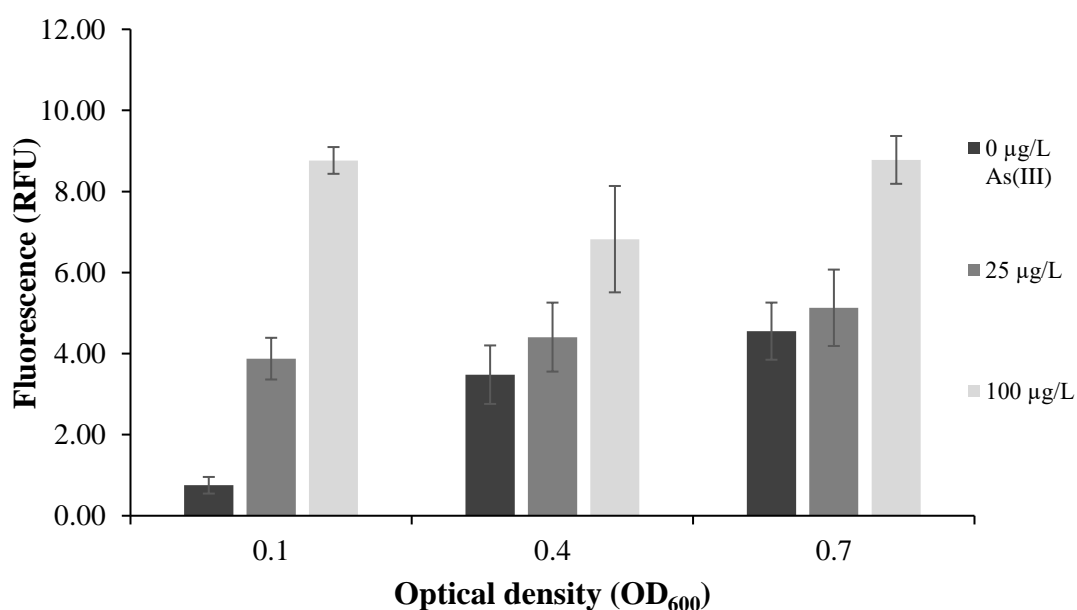


Figure 3.42 Effect of cell densities (OD₆₀₀) of 0.1, 0.4 and 0.7 on the fluorescence response of agar-immobilized arsenic bioreporter prepared in M9 supplemented medium with agar percent of 1.5 (w/v). The average values of triplicate of each induction were presented for 6-h with standard deviation.

Final optical cell density (OD₆₀₀) of 0.1 was found to have better fluorescence response compared to higher cell densities. This result can be explained by the negative effects of the crowded cell population such as shading, quenching and lowered chemical mass transfer. Some cells may die in the immobilization matrix where a barrier was formed destroying the mass transfer of both metabolites and inducers. Reduced oxygen diffusion and availability to the deeper bacterial layers in the agar matrix may also be a reason since oxygen is an essential component for

fluorescence emission (Kim & Gu, 2003). Thus, final OD₆₀₀ = 0.1 of cell concentration within agar matrix was chosen for further experiments since it provided the best sensitivity and dose-dependent increase in response to arsenite.

3.3.1.2. Fluorescence Response of Agar Gel Immobilized Biosensor to Arsenite and Arsenate

After determining optimal agar concentration (1.5% (w/v)) and cell density (OD₆₀₀ = 0.1), these parameters were employed for agar immobilization of arsenic bioreporter cells which were then induced with a concentration range between 0 and 150 µg/L of arsenite and arsenate for determination time dependent dose response profile. Fluorescence emission curves are shown up to 8 hours.

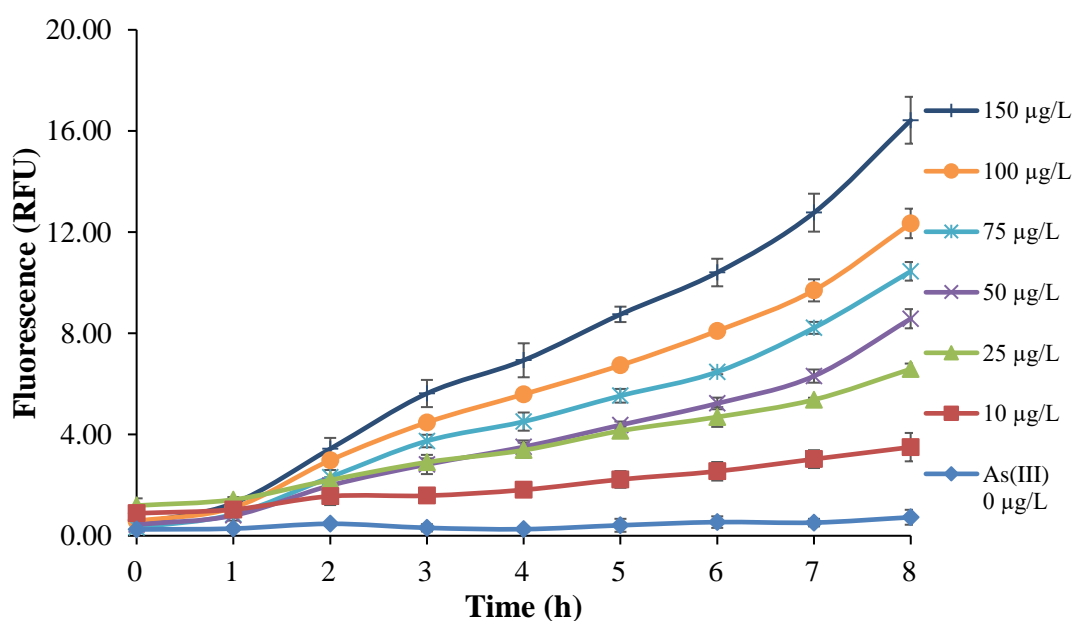


Figure 3.43 Kinetic profile of fluorescence emission of agar immobilized arsenic bioreporters formulated with optimal parameters in M9 supplemented medium induced with arsenite, As(III). Data shown as mean \pm SD of triplicate wells of each induction. Error bars are shown only when they exceed the size of the symbols.

When bioreporter cells in M9 supplemented medium were immobilized in agar matrix, arsenite concentration of 150 $\mu\text{g/L}$ was detected after 1.5 hours incubation and detection limit decreases to 10 $\mu\text{g/L}$ after 3 h-incubation time with a statistically significant change ($p < 0.05$) (Figure 3.43). Compared to free cells, immobilized cells responded arsenite an hour later, possibly due to slow diffusion rate of arsenite through agar gel. One-way ANOVA analysis was performed for 3-h time point; the descriptive statistics table, ANOVA table and post hoc test results were given at Section F in Appendix E. Arsenate concentrations between 0 and 150 $\mu\text{g/L}$ did not yield any significant fluorescence response within assay time as in the case of free bioreporter cells (data not shown).

The effect of medium used in immobilization procedure was tested by using MOPS supplemented medium, which has limited inorganic phosphate increasing the bioavailability of arsenate ions. For agar immobilized bioreporter cells prepared in MOPS medium, arsenite concentration of 150 $\mu\text{g/L}$ was detected after 2 hours, 25 $\mu\text{g/L}$ after 6 hours and 10 $\mu\text{g/L}$ after 7 hours of incubation (Figure 3.44a). Arsenate concentration of 150 $\mu\text{g/L}$ was detected after 2 hours and 10 $\mu\text{g/L}$ after 5 hours of incubation time with a statistically significant change ($p < 0.05$) (Figure 3.44b). Generally, for effective detection of lower concentrations of arsenic longer incubation period was required and higher concentrations of arsenic could elicit faster induction as early as an hour. Compared to free cells, immobilized cells responded 150 $\mu\text{g/L}$ of arsenite an hour later; although they responded 10 $\mu\text{g/L}$ of arsenite and arsenate 4.5 hours and 3.5 hours later than free cells, respectively. In fact, 100 $\mu\text{g/L}$ of arsenite and arsenate can be detected within 3 hours and it is helpful enough to assess the acute toxicity in a short period of time.

The fluorescence increases with time and linearly with increasing arsenite/arsenate concentrations up to 150 $\mu\text{g/L}$. In order to determine the significance levels of induction groups, Tukey's HSD tests were run for arsenite at 6-h time point and for

arsenate at 5-h time point; the descriptive statistics tables, ANOVA tables and post hoc test results are given at Section G and H, respectively in Appendix E.

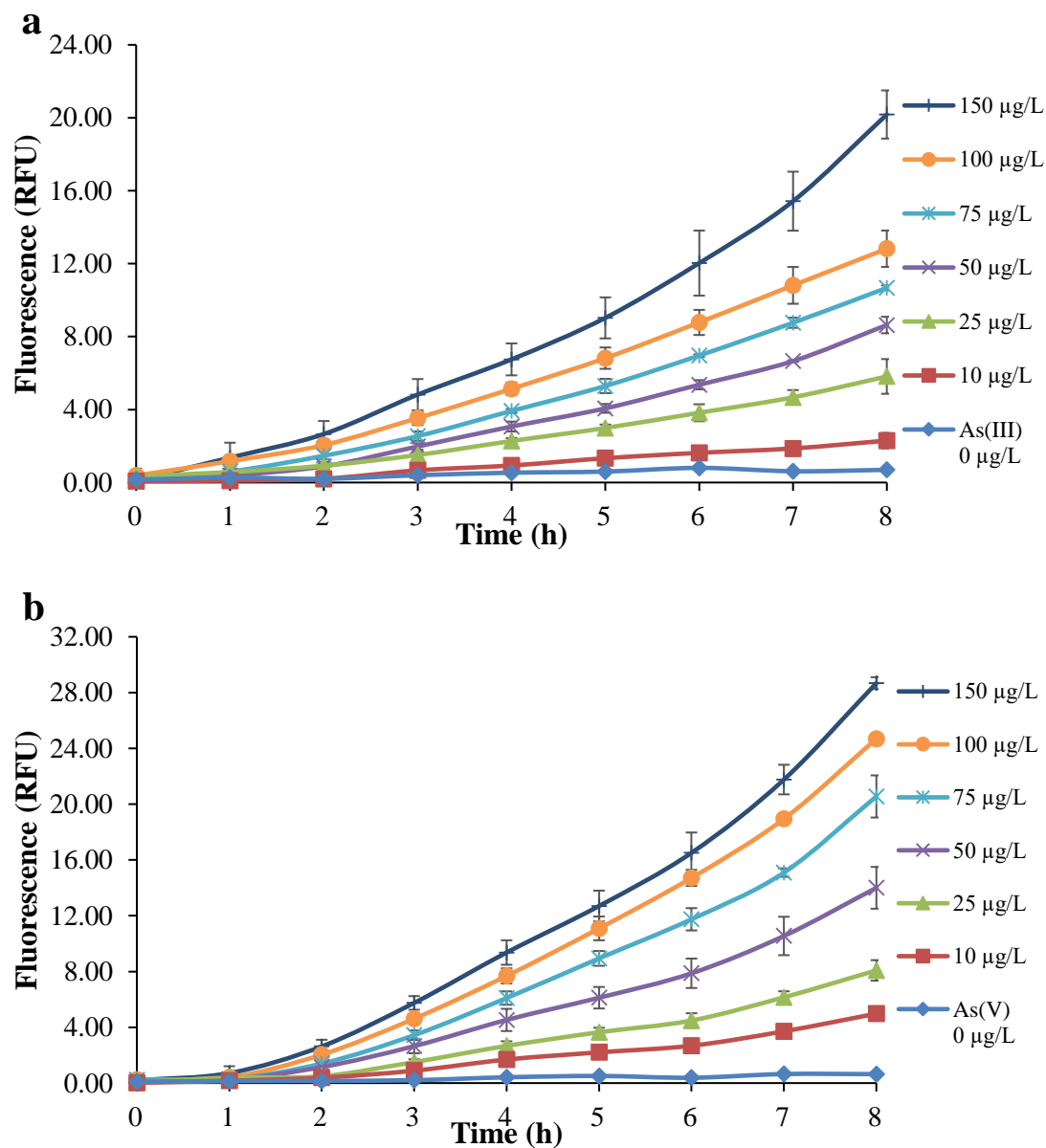


Figure 3.44 Kinetic profile of fluorescence emission of agar immobilized arsenic bioreporter cells formulated with optimal parameters in MOPS supplemented medium induced with a) arsenite, As(III), and b) arsenate, As(V), concentrations. Data shown as mean \pm SD of triplicate wells of each induction.

For agar immobilization prepared with M9 supplemented medium, none of the tested arsenate concentrations could be detected but arsenite concentration of 10 µg/L was detected after 3 hours of induction. Since bioreporter cell culture and aqueous agar gel solution were mixed with 1:1 (v/v) ratio, the cell resuspension medium influenced the bioreporter's sensitivity and selectivity. In MOPS media formulated agar matrix, bioreporter cells showed remarkable change of response to arsenate that arsenate concentration as low as 10 µg/L could be detected after 5 hours. In a similar study of Elad et al. (2011), which bioluminescent *arsR* reporter was immobilized in 1.5% LB-agar and assayed at a microtiter plate at 37 °C, they reported minimal response ratio for 0.02 mg/L arsenic (As(III)) after 2 hours. Another example is the immobilization of bioluminescent *E. coli* DH1 (pBarslux) strain in final 2% agarose and OD₆₂₀ = 0.1 in acetate medium assayed at a microtiter plate at 30 °C (Charrier et al., 2011). They reported 1 µM (75 µg/L) detection limit for arsenite after 2 hours.

3.3.2. Alginate Bead Immobilization

Alginate gel, one of the most common encapsulation matrices, was chosen as another immobilization matrix for arsenic bioreporter cells. It is attractive for cell entrapment because of its ionic gelation between divalent cations, especially Ca²⁺, which is simple and mild process. Calcium-alginate beads are biocompatible, pliable, transparent, permeable and have high mechanical strength and stability (Axelrod et al., 2016; Selimoglu & Elibol, 2010).

3.3.2.1. Optimization of Alginate Bead Immobilization- Percentage and Cell Density

For alginate bead optimization studies, the bioreporter cells suspended in M9 supplemented medium were used and induced with arsenite solution. The number of the beads inside well of microplate was three since it fitted better than higher number of beads and provided more reliable and reproducible results than a smaller number

of beads. Average number of beads formed from 1 mL of alginate-cell matrix mixture were 30.

Three different final alginate percentages 1, 1.5 and 2 (w/v) were tested to assess the effect of alginate concentration on bioreporter fluorescence response. Final cell density $OD_{600} = 0.1$ were kept constant for different alginate concentrations. For tested alginate percentages 1, 1.5 and 2 (w/v), the size of the beads increased as the concentration of alginate increased such that 1% (w/v) alginate matrix solution resulted in beads of average diameter of 3-mm while 2% (w/v) alginate matrix solution resulted in average diameter of 4-mm (Figure 3.45). Moreover, the beads lost their transparency and appeared to be white as the alginate concentration was increased. This is due to more tightly crosslinked gels at higher concentrations with more calcium binding sites (Chandramouli et al., 2004).

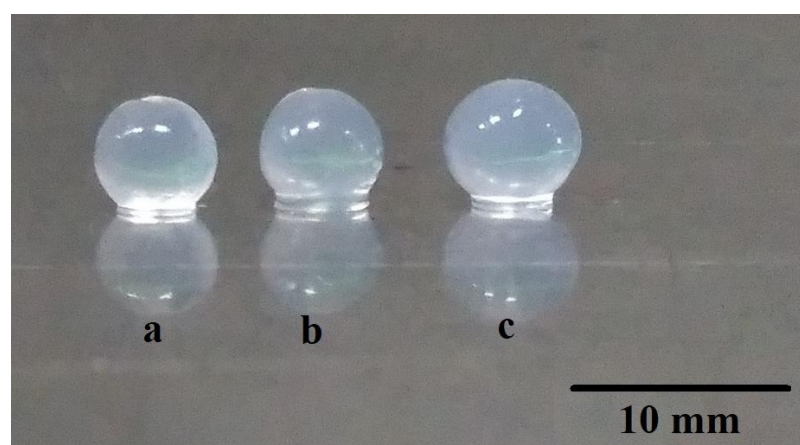


Figure 3.45 Photo images of alginate-immobilized arsenic bioreporter with different alginate percentages a) 1, b) 1.5 and c) 2 (w/v).

For alginate-Ca beads, the concentration of calcium chloride solution is an important factor for the formation of round shape beads. For tested calcium concentrations, lower than 0.02 M did not provide spherical beads whilst 0.2 M provided good round shaped-beads (data not shown). Higher calcium concentrations were not preferred

since it resulted in harder beads (Wasito et al., 2019) resulting in slower interaction between environment and bioreporter cells.

As final alginate concentration was increased, the background fluorescence increased possibly due to increased number of cells, since the size of beads increased with the increasing alginate concentration which can accommodate higher number of cells. Moreover, higher alginate concentration resulted in higher standard deviation that may result from nonuniform encapsulation and distribution of cells to the beads due to high viscosity of higher alginate concentrations. It was reported that higher alginate concentration results in fewer number of pores with smaller pore size (Bilal & Asgher, 2015). It could be deduced that 1% concentration allowed higher diffusion rate of arsenite inside matrix leading to higher arsenic bioavailability and induction. Hence, the optimal alginate concentration was found to be 1% (w/v) having higher fluorescence response and sensitivity (Figure 3.46).

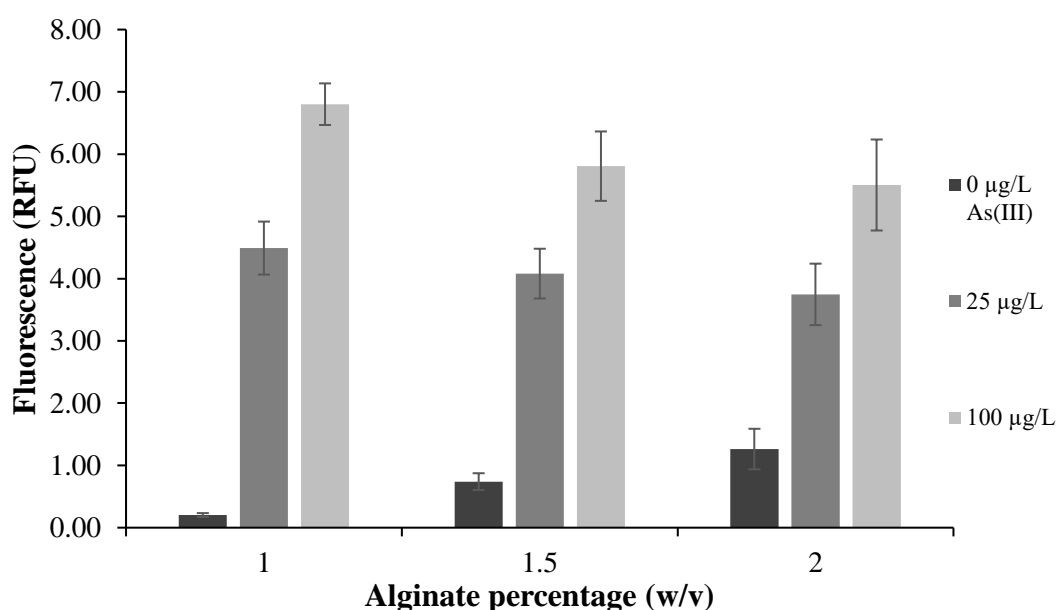


Figure 3.46 Effect of alginate percentages of 1, 1.5 and 2 (w/v) on the fluorescence response of alginate-immobilized arsenic bioreporter prepared in M9 supplemented medium with $OD_{600} = 0.1$. The average values of triplicate of each induction were presented for 6-h with standard deviation.

Similar result was also found by Eltzov et al., (2015b) that the optimal alginate concentration was 0.5% (w/v) for their bioluminescent bacterial strains detecting general toxicity of water.

The effect of the entrapped cell concentration within alginate bead on fluorescence response was also determined. Final optical densities (OD_{600}) of 0.1, 0.4 and 0.7 were tested in alginate-1% (w/v) matrix. When the cell concentration was increased within the matrix, fluorescence signal output increased (Figure 3.47).

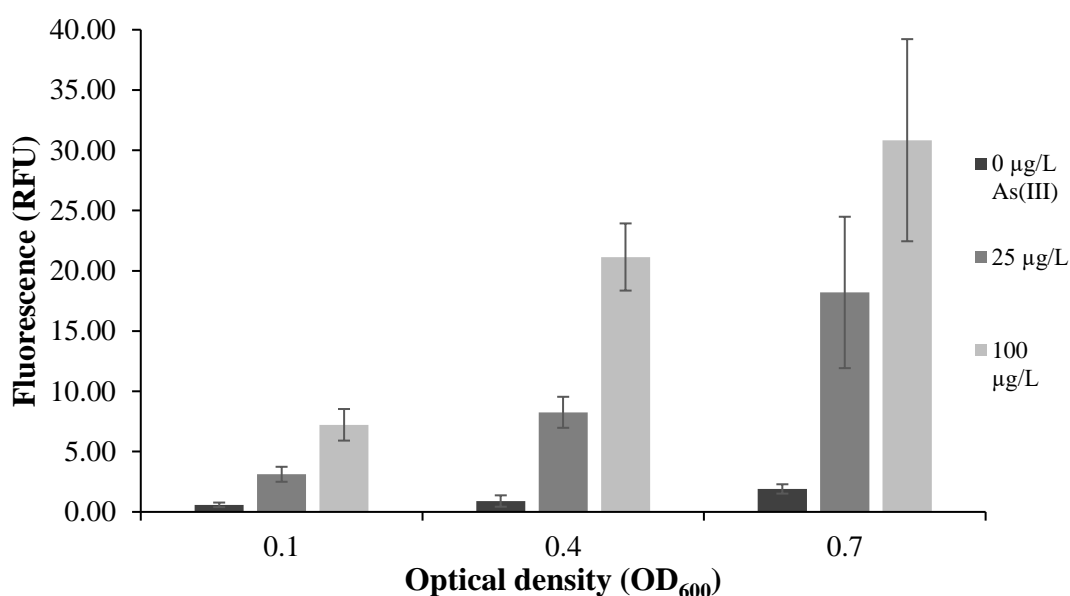


Figure 3.47 Effect of cell densities (OD_{600}) of 0.1, 0.4 and 0.7 on the fluorescence response of alginate-immobilized arsenic bioreporter prepared in M9 supplemented medium with alginate percent of 1 (w/v). The average values of triplicate of each induction were presented for 6-h with standard deviation.

Unlike agar gel matrix, for alginate bead form, increase in cell concentration resulted in increasing fluorescence response suggesting that bioreporter cell density is one of the important parameters for immobilized bioreporter system development. Although cell density of $OD_{600} = 0.7$ had the highest fluorescence response, it had a huge standard deviation that would disrupt the reliability and reproducibility of results. This

high deviation from the mean may result from the variation of cell numbers in beads and uneven diffusion of oxygen and arsenic solution to cells to deeper bacterial layers in alginate bead. Thus, final cell density $OD_{600} = 0.4$ was adopted and used in the next experiments producing highest bacterial fluorescence responses than $OD_{600} = 0.1$ and much lower standard deviation than $OD_{600} = 0.7$.

3.3.2.2. Fluorescence Response of Alginate Bead Immobilized Biosensor to Arsenite and Arsenate

Alginate bead immobilized arsenic bioreporter system was induced with the same concentration range of arsenite and arsenate for determination time dependent dose response profile of bioreporter cells employing optimal alginate matrix concentration (1% (w/v)) and cell density ($OD_{600} = 0.4$). Fluorescence emission curves are shown up to 8 hours.

For alginate immobilized bioreporter cells in M9 supplemented medium, arsenite concentration of 150 $\mu\text{g/L}$ was detected after 2 hours while detection limit decreased to 25 $\mu\text{g/L}$ after 5 hours and then 10 $\mu\text{g/L}$ after 7 hours of incubation time with a statistically significant change ($p < 0.05$) (Figure 3.48). One-way ANOVA analysis was performed for 5-h time point; the descriptive statistics table, ANOVA table and post hoc test results were given at Section I in Appendix E. Arsenate concentrations between 0 and 100 $\mu\text{g/L}$ did not yield significant fluorescence emission within assay time; however, 150 $\mu\text{g/L}$ of As(V) resulted in a slight induction after 11 hours (data not shown).

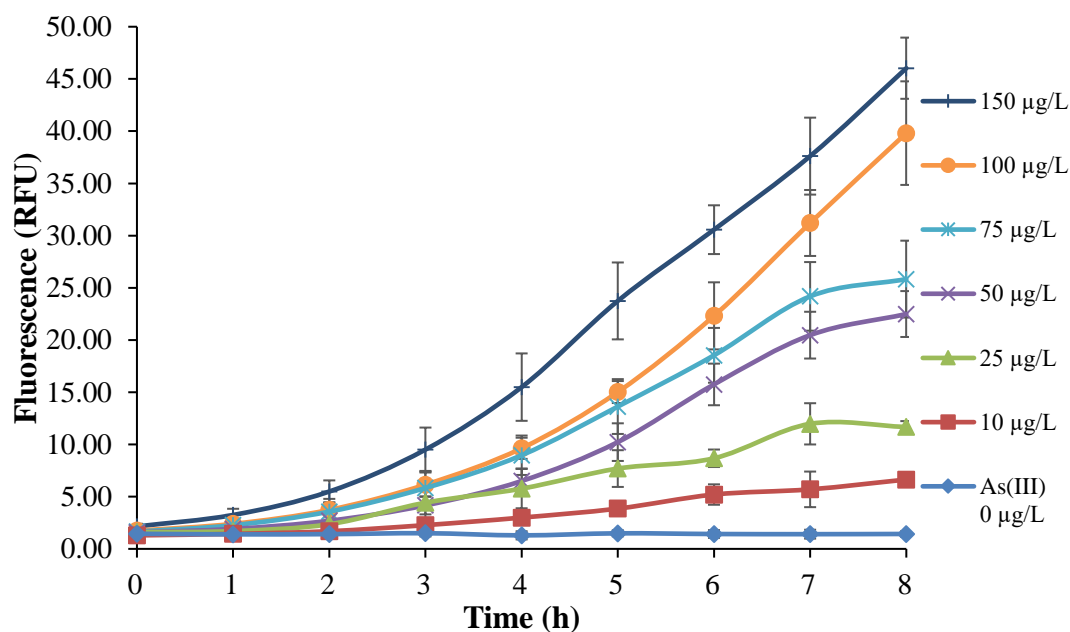


Figure 3.48 Kinetic profile of fluorescence emission of alginate immobilized arsenic bioreporter formulated with optimal parameters in M9 supplemented medium induced with arsenite, As(III). Data shown as mean \pm SD of triplicate wells of each induction. Error bars are shown only when they exceed the size of the symbols.

After microplate assay was completed, the alginate beads were taken out and excited under UV channel with excitation 390 ± 40 nm and emission 446 ± 33 nm. It can be seen from Figure 3.49 that while uninduced beads did not give any GFP response, arsenite induced beads gave green fluorescent emissions. Induction with higher arsenite concentration resulted in more intense fluorescent light.

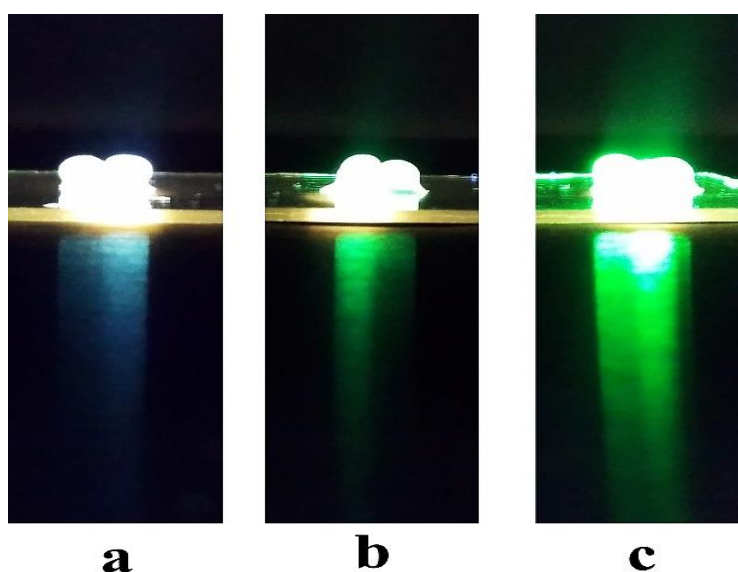


Figure 3.49 The images of alginate-bead immobilized arsenic bioreporters in M9 supplemented medium after 16-h induction, were taken with cellphone camera during excitation under blue channel of EVOS Fluid Imaging Station: a) uninduced beads, b) induced beads with 25 µg/L of arsenite, c) induced beads with 150 µg/L of arsenite.

When bioreporter cells were immobilized in alginate beads with MOPS medium, arsenate concentration of 150 µg/L was detected after 1.5 hours and 25 µg/L after 5 hours incubation time (Figure 3.50b); arsenite concentration of 150 µg/L was detected after 2 hours incubation and 25 µg/L after 5-hour incubation time (Figure 3.50a) with a significance level of 0.05. For both arsenite and arsenate of 10 µg/L, they could be detected after 6 hours induction time. Fluorescence values increased with induction time and proportional to the exposed arsenic concentration.

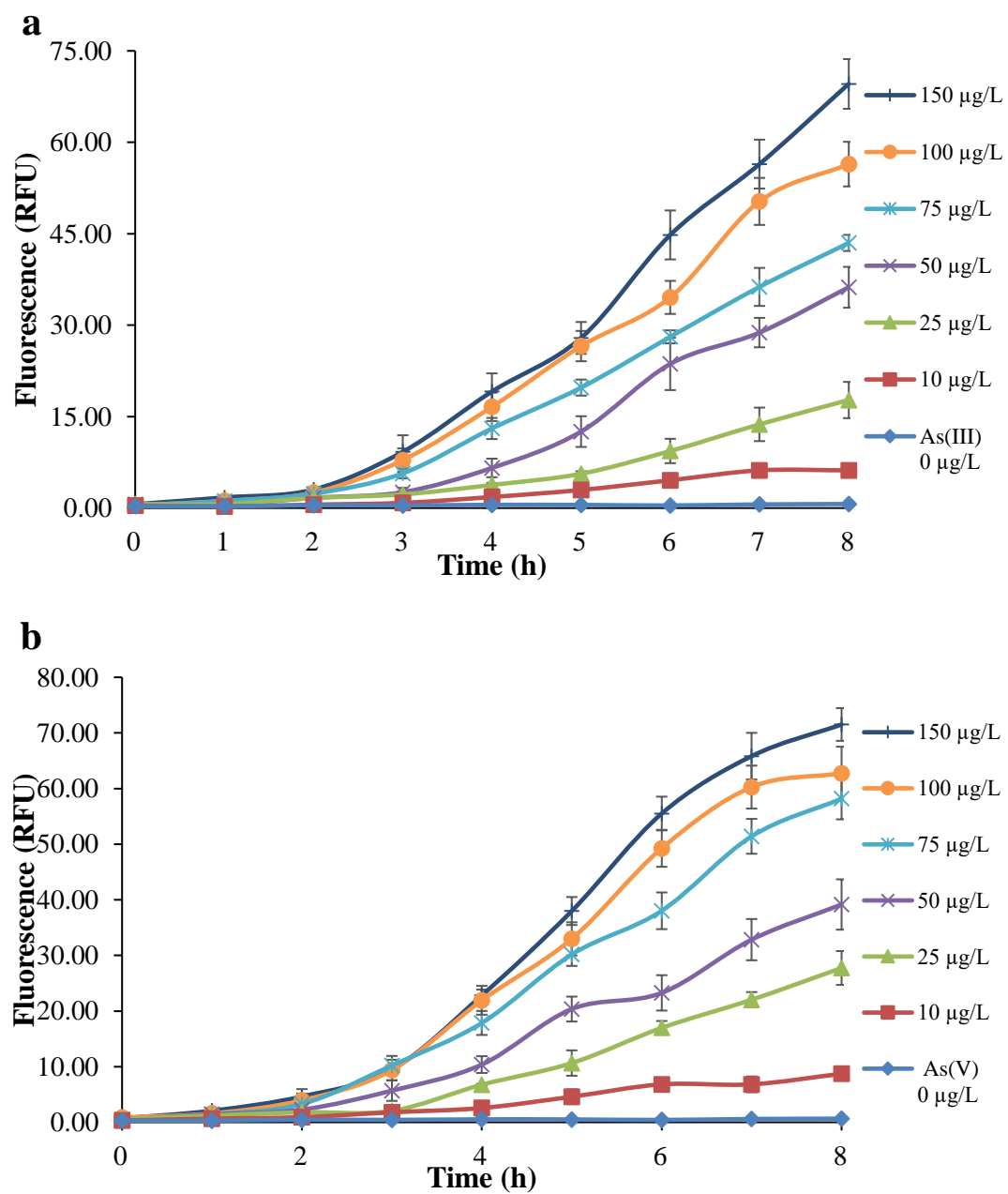


Figure 3.50 Kinetic profile of fluorescence emission of alginate immobilized arsenic bioreporter cells formulated with optimal parameters in MOPS supplemented medium induced with a) arsenite, As(III), and b) arsenate, As(V), concentrations. Data shown as mean \pm SD of triplicate wells of each induction.

The fluorescence increased with time and increasing arsenite/arsenate concentrations up to 150 µg/L. In order to determine the significance levels of induction groups, Tukey's HSD tests were run for arsenite at 5-h time point and for arsenate at 5-h time point; the descriptive statistics tables, ANOVA tables and post hoc test results are given at Section J and K, respectively in Appendix E.

Compared to free cells, immobilized cells responded to 150 µg/L of arsenic species an hour later and responded to 10 µg/L of arsenic about two times slower than free cells. However, immobilized bioreporter could detect 100 µg/L of arsenite and arsenate within 3 hours and it is helpful enough to assess the acute toxicity in a small period.

3.3.3. Metal Specificity of Agar Gel and Alginate Bead Immobilized Bioreporter Cells

As metal specificity of agar and alginate immobilized bioreporter is concerned, 10 metals including Ag(I), Cd(II), Co(II), Cu(II), Fe(II), Hg(II), Mn(II), Ni(II), Pb(II) and Zn(II) were tested. These tested metals were chosen since they are listed as primary interest for their potential to harm human health (U.S. EPA., 2007) and they are commonly found in soils and groundwaters. In order to evaluate specificity of the immobilized arsenic bioreporter, the response to some of the common metals found in groundwaters and that are of public health concern were tested at 250 µg/L while arsenic concentrations tested at 50 µg/L in MOPS supplemented medium.

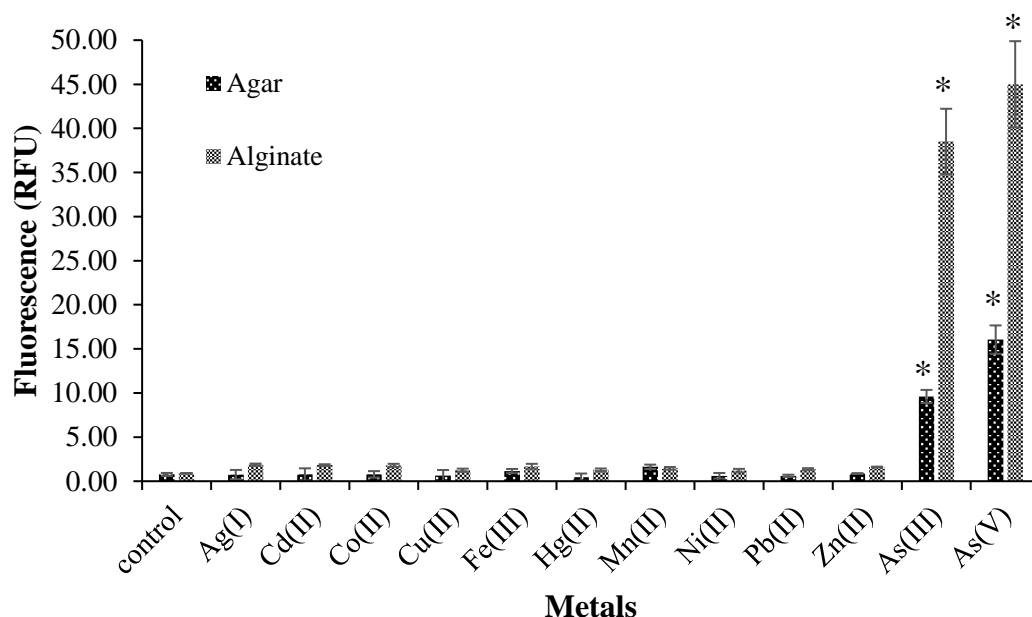


Figure 3.51 Metal specificity of agar and alginate immobilized immobilized bacterial bioreporter cells prepared in MOPS supplemented medium. Arsenite and arsenate were added in 50 $\mu\text{g/L}$, and other metal ions were added in 250 $\mu\text{g/L}$. Control refers to no-metal addition. The average values of triplicate of each induction were presented for 8-h with standard deviation. * $p < 0.001$.

As shown in Figure 3.51, immobilized arsenic bioreporter cells in both agar and alginate gave no significant change of fluorescence response to tested metal ions indicating the immobilized arsenic bioreporters had high specificity towards arsenic species as in the case of free cells. It can be concluded that, for the experiments with natural water samples, metal ions are generally found in combination with arsenic, will not produce a non-specific induction of fluorescence.

Two most important characteristics of bacterial bioreporters are their specificity (the range of detected chemicals) and sensitivity (the detection limit). Several factors may influence the sensitivity of the biosensor for detecting arsenic. These factors include the exposure time, the bacterial culture medium composition, the growth phase of the harvested bacteria, and the number of bacteria per measurement (Hansen & Sørensen, 2001; Hynninen & Virta, 2010; Huang et al., 2015b). Moreover, factors including the

sensor plasmid, the host strain, the reporter gene, the analytical detection method, the fluorescent transducer used, and the methods used to define the detection limit in the biosensor assays may also contribute to varying sensitivities of arsenic detection. As it is difficult to directly compare the biosensor developed in the current study with other biosensor constructs due to the factors described above, the sensitivity of the immobilized arsenic bacterial biosensor in this study is comparable with other reports (Elad et al., 2011; Prévéral et al., 2017; Truffer et al., 2014).

The WHO guidelines for drinking-water quality and the water quality standards in Turkey is 10 µg/L as the provisional guideline value and maximum permissible concentration of 50 µg/L arsenic were established. The countries employ different allowable national standards for arsenic such as 50 µg/L in India and Bangladesh (Rahman et al., 2015), 25 µg/L in Mexico, and 10 µg/L in most European countries and the USA (Fisher et al., 2017). The experiments indicated that the genetic constitution and arrangement of *Pars*, *arsR*, and *sgfp* established in this study with immobilization studies have greatly promoted the development of the practical biosensor module for the fluorescent microplate assay that can detect low levels of arsenic in a relatively short time. This arsenic biosensor can be employed for primary screening of naturally polluted water once the procedure is standardized. As a rule of thumb, for chemical detection accuracy with bioreporters, it is important to standardize the experimental conditions, detection techniques as well as method of data analysis. Therefore, the future challenge lies in using such biosensors to develop portable, inexpensive, single-use tools for monitoring environmental heavy metal toxicity.

CHAPTER 4

CONCLUSION

In this study, as an alternative to conventional techniques, whole-cell bacterial biosensors were proposed for practical environmental detection of prominent heavy metal pollutants which are arsenic and cadmium.

Firstly, green fluorescent protein based whole cell *E. coli* bioreporter (pBR-arsR773) was constructed for the measurement of dominant inorganic arsenic species, arsenite and arsenate. The expression studies of liquid assays in M9 supplemented medium showed that the arsenic bioreporter strain could detect arsenic at safe drinking water quality standard of 10 µg/L of arsenite after 2 hours incubation. It has been shown that the bioreporter has much higher sensitivity towards arsenate ions in inorganic phosphate limiting minimal medium compared to phosphate rich minimal medium. In phosphate limiting medium, it could detect 10 µg/L of arsenate after 2 hours of incubation. Also, the bioreporter has a high metal specificity towards arsenic species. The groundwater test suggests that this fluorescent arsenic biosensor could be used in quantitative measurement of bioavailable portion of arsenic complementing the traditional analytical methods which give total content of arsenic.

Secondly, green fluorescent protein based whole cell *E. coli* bioreporter (pBR-PzntA) was constructed for the measurement of inorganic cadmium. The expression studies of liquid assays in M9 supplemented medium showed that the cadmium bioreporter strain could detect cadmium safe drinking water quality standard of 5 µg/L of cadmium after 3.5 hours of induction. In MOPS supplemented medium, it has higher sensitivity that 2 µg/L of cadmium could be detected after 1.5 hours of induction. The growth phase test showed that it has higher detection sensitivity when it is induced at

early exponential phase. Furthermore, it has been shown that it can detect very high concentrations of mercury which is not an environmentally relevant case.

Thirdly, arsenic bioreporter was immobilized in agar and alginate biopolymer matrices. Different entrapment parameters were evaluated for optimization of fluorescence performance.

When optimal parameters were applied, agar immobilized bioreporter could detect arsenite of 10 $\mu\text{g/L}$ after 3 hours in M9 supplemented medium and, arsenate of 10 $\mu\text{g/L}$ after 5 hours in MOPS supplemented medium. Alginate immobilized bioreporter could detect arsenite of 10 $\mu\text{g/L}$ after 7 hours in M9 supplemented medium and, arsenite and arsenate of 10 $\mu\text{g/L}$ after 6 hours in MOPS supplemented medium. Although the time required for detection of 10 $\mu\text{g/L}$ seems to be long, these immobilized systems can detect 100 $\mu\text{g/L}$ of inorganic arsenic species after 2 hours of induction, which is enough time for near real time monitoring and early warning purposes. As a result, similar to free cells, the immobilized arsenic bacterial bioreporter is also applicable in determining the concentrations of the two abundant ionic forms of arsenic at safe drinking water limits.

The results of this study will be leading to further investigations for developing fast, specific and sensitive and low-cost portable biosensor device for detection of arsenic and cadmium content of environmental samples. Either agar gels and alginate beads can be lyophilized by using appropriate cryoprotectants and stored at vials in room temperature that could provide longer shelf-life. Also, they can be used in different microarray platforms that can be stored at 4 °C later to be integrated into transducer device. In various ways of packaging, they would be used as an alternative and/or complementary method to conventional analytical methods. They could be used for in-field applications by everyone to determine the bioavailable content of heavy metal along with its forms, which would give an insight about the risk of toxicity and planning of treatment or removal processes.

REFERENCES

- Aide, M., Beighley, D., & Dunn, D. (2016). Arsenic in the soil environment: a soil chemistry review. *International Journal of Applied Agricultural Research*, 11, 1–28.
- Akter, K. F., Owens, G., Davey, D. E., & Naidu, R. (2005). Arsenic Speciation and Toxicity in Biological Systems. *Reviews of Environmental Contamination and Toxicology*, 97–149. https://doi.org/10.1007/0-387-27565-7_3
- Albuquerque, P. B. S., Coelho, L. C. B. B., Teixeira, J. A., & Carneiro-da-Cunha, M. G. (2016). Approaches in biotechnological applications of natural polymers. *AIMS Molecular Science*, 3(3), 386–425. <https://doi.org/10.3934/molsci.2016.3.386>
- Aragay, G., Pons, J., & Merkoçi, A. (2011). Recent Trends in Macro-, Micro-, and Nanomaterial-Based Tools and Strategies for Heavy-Metal Detection. *Chemical Reviews*, 111(5), 3433–3458. <https://doi.org/10.1021/cr100383r>
- Argos, M., Kalra, T., Rathouz, P. J., Chen, Y., Pierce, B., Parvez, F., Islam, T., Ahmed, A., Rakibuz-Zaman, M., Hasan, R., Sarwar, G., Slavkovich, V., van Geen, A., Graziano, J., & Ahsan, H. (2010). Arsenic exposure from drinking water, and all-cause and chronic-disease mortalities in Bangladesh (HEALS): A prospective cohort study. *Lancet*, 376(9737), 252–258. [https://doi.org/10.1016/S0140-6736\(10\)60481-3](https://doi.org/10.1016/S0140-6736(10)60481-3)
- ATSDR (2007). Toxicological Profile for Arsenic. Agency for Toxic Substances and Disease Registry, Center for Disease Control, Atlanta, Georgia. Retrieved from <https://www.atsdr.cdc.gov/toxprofiles/tp2.pdf>

ATSDR (2012). Toxicological Profile for Cadmium. Agency for Toxic Substances and Disease Registry, Center for Disease Control, Atlanta, Georgia. Retrieved from <https://www.atsdr.cdc.gov/toxprofiles/tp5.pdf>

ATSDR (2017). PHS Priority list of hazardous substances. Agency for Toxic Substances and Disease Registry, Center for Disease Control, Atlanta, Georgia. Retrieved from <https://www.atsdr.cdc.gov/spl/>

Axelrod, T., Eltzov, E., & Marks, R. S. (2016). Bioluminescent bioreporter pad biosensor for monitoring water toxicity. *Talanta*, 149, 290–297. <https://doi.org/10.1016/j.talanta.2015.11.067>

Bansod, B. K., Kumar, T., Thakur, R., Rana, S., & Singh, I. (2017). A review on various electrochemical techniques for heavy metal ions detection with different sensing platforms. *Biosensors and Bioelectronics*, 94, 443–455. <https://doi.org/10.1016/j.bios.2017.03.031>

Beard, S. J., Hashim, R., Membrillo-Hernández, J., Hughes, M. N., & Poole, R. K. (1997). Zinc(II) tolerance in *Escherichia coli* K-12: evidence that the *zntA* gene (o732) encodes a cation transport ATPase. *Molecular Microbiology*, 25(5), 883–891. <https://doi.org/10.1111/j.1365-2958.1997.mmi518.x>

Belkin, S. (2003). Microbial whole-cell sensing systems of environmental pollutants. *Current Opinion in Microbiology*, 6(3), 206–212. [https://doi.org/10.1016/S1369-5274\(03\)00059-6](https://doi.org/10.1016/S1369-5274(03)00059-6)

- Belkin, S. (2006). Genetically Engineered Microorganisms for Pollution Monitoring. In I, Twardowska, H. E, Allen, M. M, Häggblom, & S, Stefaniak (Eds.). *Soil and Water Pollution Monitoring, Protection and Remediation*. NATO Science Series, (vol 69, pp. 147-160). Dordrecht: Springer.
- Ben-Yoav, H., Melamed, S., Freeman, A., Shacham-Diamand, Y., & Belkin, S. (2011). Whole-cell biochips for bio-sensing: Integration of live cells and inanimate surfaces. *Critical Reviews in Biotechnology*, 31(4), 337–353. <https://doi.org/10.3109/07388551.2010.532767>
- Bereza-Malcolm, L. T., Mann, G., & Franks, A. E. (2015). Environmental Sensing of Heavy Metals Through Whole Cell Microbial Biosensors: A Synthetic Biology Approach. *ACS Synthetic Biology*, 4, 535–546. <https://doi.org/10.1021/sb500286r>
- Bilal, M., & Asgher, M. (2015). Dye decolorization and detoxification potential of Ca-alginate beads immobilized manganese peroxidase. *BMC Biotechnology*, 15, 111. <https://doi.org/10.1186/s12896-015-0227-8>
- Binet, M. R., & Poole, R. K. (2000). Cd(II), Pb(II) and Zn(II) ions regulate expression of the metal-transporting P-type ATPase ZntA in *Escherichia coli*. *FEBS Letters*, 473(1), 67–70. [https://doi.org/10.1016/s0014-5793\(00\)01509-x](https://doi.org/10.1016/s0014-5793(00)01509-x)
- Biran, I., Babai, R., Levkov, K., Rishpon, J., & Ron, E. Z. (2000). Online and in situ monitoring of environmental pollutants: electrochemical biosensing of cadmium. *Environmental Microbiology*, 2(3), 285–290. <https://doi.org/10.1046/j.1462-2920.2000.00103.x>

- Bjerketorp, J., Håkansson, S., Belkin, S., & Jansson, J. K. (2006). Advances in preservation methods: Keeping biosensor microorganisms alive and active. *Current Opinion in Biotechnology*, 17(1), 43–49. <https://doi.org/10.1016/j.copbio.2005.12.005>
- Brocklehurst, K. R., Hobman, J. L., Lawley, B., Blank, L., Marshall, S. J., Brown, N. L., & Morby, A. P. (1999). ZntR is a Zn(II)-responsive MerR-like transcriptional regulator of zntA in *Escherichia coli*. *Molecular Microbiology*, 31(3), 893–902. <https://doi.org/10.1046/j.1365-2958.1999.01229.x>
- Brown, N. L., Stoyanov, J. V., Kidd, S. P., & Hobman, J. L. (2003). The MerR family of transcriptional regulators. *FEMS Microbiology Reviews*, 27(2-3), 145–163. [https://doi.org/10.1016/s0168-6445\(03\)00051-2](https://doi.org/10.1016/s0168-6445(03)00051-2)
- Buffi, N., Merulla, D., Beutier, J., Barbaud, F., Beggah, S., van Lintel, H., Renaud, P., & van der Meer, J. R. (2011). Development of a microfluidics biosensor for agarose-bead immobilized *Escherichia coli* bioreporter cells for arsenite detection in aqueous samples. *Lab on a Chip*, 11(11), 2369–2377. <https://doi.org/10.1039/c1lc20274j>
- Busenlehner, L. S., Pennella, M. A., & Giedroc, D. P. (2003). The SmtB/ArsR family of metalloregulatory transcriptional repressors: Structural insights into prokaryotic metal resistance. *FEMS Microbiology Reviews*, 27(2–3), 131–143. [https://doi.org/10.1016/S0168-6445\(03\)00054-8](https://doi.org/10.1016/S0168-6445(03)00054-8)
- Cai, J., & DuBow, M. S. (1997). Use of a luminescent bacterial biosensor for biomonitoring and characterization of arsenic toxicity of chromated copper arsenate (CCA). *Biodegradation*, 8(2), 105–111. <https://doi.org/10.1023/A:1008281028594>

- Carlin, A., Shi, W., Dey, S., & Rosen, B. P. (1995). The *ars* operon of *Escherichia coli* confers arsenical and antimonial resistance. *Journal of Bacteriology*, 177(4), 981–986. <https://doi.org/10.1128/jb.177.4.981-986.1995>
- Cevenini, L., Calabretta, M. M., Tarantino, G., Michelini, E., & Roda, A. (2016). Smartphone-interfaced 3D printed toxicity biosensor integrating bioluminescent “sentinel cells.” *Sensors and Actuators, B: Chemical*, 225, 249–257. <https://doi.org/10.1016/j.snb.2015.11.017>
- Chakraborty, S., Dutta, A. R., Sural, S., Gupta, D., & Sen, S. (2013). Ailing bones and failing kidneys: a case of chronic cadmium toxicity. *Annals of Clinical Biochemistry: An International Journal of Biochemistry and Laboratory Medicine*, 50(5), 492–495. <https://doi.org/10.1177/0004563213481207>
- Chandramouli, V., Kailasapathy, K., Peiris, P., & Jones, M. (2004). An improved method of microencapsulation and its evaluation to protect *Lactobacillus spp.* in simulated gastric conditions. *Journal of Microbiological Methods*, 56(1), 27–35. <https://doi.org/10.1016/j.mimet.2003.09.002>
- Chandrangsu, P., Rensing, C., & Helmann, J. D. (2017). Metal homeostasis and resistance in bacteria. *Nature Reviews Microbiology*, 15(6), 338–350. <https://doi.org/10.1038/nrmicro.2017.15>
- Charrier, T., Durand, M. J., Affi, M., Jouanneau, S., Thouand, G., & Jouanneau, S. (2010). Bacterial Bioluminescent Biosensor Characterisation for On-line Monitoring of Heavy Metals Pollutions in Waste Water Treatment Plant Effluents. In P. A., Serra, (Ed.). *Biosensors*, (pp. 179–206). Vienna: INTECH. <https://doi.org/10.5772/7210>

- Charrier, T., Durand, M. J., Jouanneau, S., Dion, M., Perneti, M., Poncelet, D., & Thouand, G. (2011). A multi-channel bioluminescent bacterial biosensor for the on-line detection of metals and toxicity. Part I: Design and optimization of bioluminescent bacterial strains. *Analytical and Bioanalytical Chemistry*, 400(4), 1051–1060. <https://doi.org/10.1007/s00216-010-4353-9>
- Chatterjee, S., Datta, S., & Gupta, D. K. (2017). Studies on Arsenic and Human Health. In D. K. Gupta, & S. Chatterjee (Eds.), *Arsenic Contamination in the Environment* (pp. 37–66). Switzerland: Springer Nature.
- Chen, C. M., Mobley, H. L. T., & Rosen, B. P. (1985). Separate resistances to arsenate and arsenite (antimonate) encoded by the arsenical resistance operon of R factor R773. *Journal of Bacteriology*, 161(2), 758–763.
- Chen, J., & Rosen, B. P. (2014). Biosensors for inorganic and organic arsenicals. *Biosensors*, 4(4), 494–512. <https://doi.org/10.3390/bios4040494>
- Chen, P., Wang, S., Inci, F., Güven, S., Tasoglu, S., & Demirci, U. (2016). Cell-Encapsulating Hydrogels for Biosensing. In L. Kang, & S. Majd (Eds.). *Gels Handbook* (pp. 327–356). https://doi.org/10.1142/9789813140417_0012
- Chowdhury, S., Mazumder, M. A. J., Al-Attas, O., & Husain, T. (2016). Heavy metals in drinking water: Occurrences, implications, and future needs in developing countries. *Science of the Total Environment*, 569–570, 476–488. <https://doi.org/10.1016/j.scitotenv.2016.06.166>
- Close, D. M., Ripp, S., & Sayler, G. S. (2009). Reporter proteins in whole-cell optical bioreporter detection systems, biosensor integrations, and biosensing applications. *Sensors*, 9(11), 9147–9174. <https://doi.org/10.3390/s91109147>

- Crameri, A., Whitehorn, E. A., Tate, E., & Stemmer, W. P. C. (1996). Improved green fluorescent protein by molecular evolution using DNA shuffling. *Nature Biotechnology*, *14*, 315–319. <https://doi.org/10.1038/nbt0396-315>
- Das, S., Dash, H. R., & Chakraborty, J. (2016). Genetic basis and importance of metal resistant genes in bacteria for bioremediation of contaminated environments with toxic metal pollutants. *Applied Microbiology and Biotechnology*, *100*(7), 2967–2984. <https://doi.org/10.1007/s00253-016-7364-4>
- Date, A., Pasini, P., & Daunert, S. (2010). Fluorescent and Bioluminescent Cell-Based Sensors: Strategies for Their Preservation. In S, Belkin, & M, Gu (Eds.). *Whole Cell Sensing Systems I. Advances in Biochemical Engineering/Biotechnology* (vol 117). Berlin, Heidelberg: Springer.
- Daunert, S., Barrett, G., Feliciano, J. S., Shetty, R. S., Shrestha, S., & Smith-Spencer, W. (2000). Genetically Engineered Whole-Cell Sensing Systems: Coupling Biological Recognition with Reporter Genes. *Chemical Reviews*, *100*(7), 2705–2738. <https://doi.org/10.1021/cr990115p>
- de-Bashan, L. E., & Bashan, Y. (2010). Immobilized microalgae for removing pollutants: review of practical aspects. *Bioresource Technology*, *101*(6), 1611–1627. <https://doi.org/10.1016/j.biortech.2009.09.043>
- Diesel, E., Schreiber, M., & van Der Meer, J. R. (2009). Development of bacteria-based bioassays for arsenic detection in natural waters. *Analytical and Bioanalytical Chemistry*, *394*(3), 687–693. <https://doi.org/10.1007/s00216-009-2785-x>

- D'Souza, S. F. (2001). Immobilization and Stabilization of Biomaterials for Biosensor Applications. *Applied Biochemistry and Biotechnology*, 96(1-3), 225–238. <https://doi.org/10.1385/abab:96:1-3:225>
- Elad, T., Almog, R., Yagur-Kroll, S., Levkov, K., Melamed, S., Shacham-Diamand, Y., & Belkin, S. (2011). Online monitoring of water toxicity by use of bioluminescent reporter bacterial biochips. *Environmental Science and Technology*, 45(19), 8536–8542. <https://doi.org/10.1021/es202465c>
- Elcin, E., & Öktem, H. A. (2019). Whole-cell fluorescent bacterial bioreporter for arsenic detection in water. *International Journal of Environmental Science and Technology*, 16(10), 5489–5500. <https://doi.org/10.1007/s13762-018-2077-0>
- Eltzov, E., & Marks, R. S. (2011). Whole-cell aquatic biosensors. *Analytical and Bioanalytical Chemistry*, 400(4), 895–913. <https://doi.org/10.1007/s00216-010-4084-y>
- Eltzov, E., Slobodnik, V., Ionescu, R. E., & Marks, R. S. (2015a). On-line biosensor for the detection of putative toxicity in water contaminants. *Talanta*, 132, 583–590. <https://doi.org/10.1016/j.talanta.2014.09.032>
- Eltzov, E., Yehuda, A., & Marks, R. S. (2015b). Creation of a new portable biosensor for water toxicity determination. *Sensors and Actuators, B: Chemical*, 221, 1044–1054. <https://doi.org/10.1016/j.snb.2015.06.153>
- Fairbrother, A., Wenstel, R., Sappington, K., & Wood, W. (2007). Framework for Metals Risk Assessment. *Ecotoxicology and Environmental Safety*, 68(2), 145–227. <https://doi.org/10.1016/j.ecoenv.2007.03.015>

- Farré, M., Kantiani, L., Pérez, S., & Barceló, D. (2009). Sensors and biosensors in support of EU Directives. *Trends in Analytical Chemistry*, 28(2), 170–185. <https://doi.org/10.1016/j.trac.2008.09.018>
- Fekih, I. B., Zhang, C., Li, Y. P., Zhao, Y., Alwathnani, H. A., Saquib, Q., Rensing, C., & Cervantes, C. (2018). Distribution of arsenic resistance genes in prokaryotes. *Frontiers in Microbiology*, 9, 1–11. <https://doi.org/10.3389/fmicb.2018.02473>
- Feliciano, J., Pasini, P., Deo, S. K., Daunert, S. (2006). Photoproteins as Reporters in Whole-cell Sensing. In S. Daunert, & S. K. Deo (Eds.). *Photoproteins in Bioanalysis*. Weinheim: Wiley-VCH Verlag GmbH & Co. KGaA.
- Fisher, A. T., López-Carrillo, L., Gamboa-Loira, B., & Cebrián, M. E. (2017). Standards for arsenic in drinking water: implications for policy in Mexico. *Journal of Public Health Policy*, 38(4), 395–406. <https://doi.org/10.1057/s41271-017-0087-7>
- Fowler, B. A., Selene, C.-H., Robert, J. C., Dexter, L. J., Sullivan Jr, W., & Chen, C.-J. (2015). Arsenic. In G. F., Nordberg, B. A., Fowler, & M., Nordberg (Eds.). *Handbook on the Toxicology of Metals* (4th ed., pp. 581–624). Academic Press. <https://doi.org/10.1016/b978-0-444-59453-2.00028-7>
- French, C. E., de Mora, K., Joshi, N., Elfick, A., Haseloff, J., & Ajioka, J. (2011). Synthetic biology and the art of biosensor design. In: Institute of Medicine (US) Forum on Microbial Threats. *The Science and Applications of Synthetic and Systems Biology: Workshop Summary*. Washington (DC): National Academies Press (US).

- Fu, Y.-J., Chen, W.-L., & Huang, Q.-Y. (2008). Construction of two lux-tagged Hg²⁺-specific biosensors and their luminescence performance. *Applied Microbiology and Biotechnology*, 79(3), 363–370. <https://doi.org/10.1007/s00253-008-1442-1>
- Fukuda, H., Arai, M., & Kuwajima, K. (2000). Folding of Green Fluorescent Protein and the Cycle3 Mutant. *Biochemistry*, 39(39), 12025–12032. <https://doi.org/10.1021/bi000543l>
- Gao, H., Khera, E., Lee, J.K., & Wen, F. (2016). Immobilization of Multi-Biocatalysts in Alginate Beads for Cofactor Regeneration and Improved Reusability. *The Journal of Visualized Experiments*, 110, e53944. <https://doi.org/10.3791/53944>
- Garbinski, L. D., Rosen, B. P., & Chen, J. (2019). Pathways of arsenic uptake and efflux. *Environment International*, 126, 585–597. <https://doi.org/10.1016/j.envint.2019.02.058>
- Gireesh-Babu, P., & Chaudhari, A. (2012). Development of a broad-spectrum fluorescent heavy metal bacterial biosensor. *Molecular Biology Reports*, 39(12), 11225–11229. <https://doi.org/10.1007/s11033-012-2033-x>
- Goyer, R.A., & Clarkson, T.W. (2001). Toxic Effects of Metals. In C. D, Klaasen (Ed.), *Casarett and Doull's Toxicology: The Basic Science of Poisons*, (6th ed., pp. 861-867). New York, NY, McGraw-Hill.

- Gu, M. B., Mitchell, R. J., & Kim, B. C. (2004). Whole-Cell-Based Biosensors for Environmental Biomonitoring and Application. In J. J. Zhong (Ed.). *Advances in Biochemical Engineering* (vol 87, pp.269-305). Berlin, Heidelberg: Springer.
- Gui, Q., Lawson, T., Shan, S., Yan, L., & Liu, Y. (2017). The Application of Whole Cell-Based Biosensors for Use in Environmental Analysis and in Medical Diagnostics. *Sensors*, 17(7), 1623. <https://doi.org/10.3390/s17071623>
- Gunduz, O., Simsek, C., & Hasozbek, A. (2009). Arsenic Pollution in the Groundwater of Simav Plain, Turkey: Its Impact on Water Quality and Human Health. *Water, Air, and Soil Pollution*, 205(1-4), 43–62. <https://doi.org/10.1007/s11270-009-0055-3>
- Gupta, N., Renugopalakrishnan, V., Liepmann, D., Paulmurugan, R., & Malhotra, B. D. (2019). Cell-based biosensors: Recent trends, challenges and future perspectives. *Biosensors and Bioelectronics*, 141, 111435. <https://doi.org/10.1016/j.bios.2019.111435>
- Hansen, L. H., & Sørensen, S. J. (2001). The use of whole-cell biosensors to detect and quantify compounds or conditions affecting biological systems. *Microbial Ecology*, 42(4), 483–494. <https://doi.org/10.1007/s00248-001-0025-9>
- Harkins, M., Porter, A. J. R., & Paton, G. I. (2004). The role of host organism, transcriptional switches and reporter mechanisms in the performance of Hg-induced biosensors. *Journal of Applied Microbiology*, 97(6), 1192–1200. <https://doi.org/10.1111/j.1365-2672.2004.02421.x>

- Harms, H. (2007). Biosensing of Heavy Metals. In D. H. Nies, & S. Silver (Eds). *Molecular Microbiology of Heavy Metals (Microbiology Monographs)* (vol 6, pp. 143-157). Berlin, Heidelberg: Springer.
- Hassan, S. H. A., Van Ginkel, S. W., Hussein, M. A. M., Abskharon, R., & Oh, S. E. (2016). Toxicity assessment using different bioassays and microbial biosensors. *Environment International*, 92–93, 106–118. <https://doi.org/10.1016/j.envint.2016.03.003>
- He, Z. L., Yang, X. E., & Stoffella, P. J. (2005). Trace elements in agroecosystems and impacts on the environment. *Journal of Trace Elements in Medicine and Biology*, 19(2–3), 125–140. <https://doi.org/10.1016/j.jtemb.2005.02.010>
- Hever, N., & Belkin, S. (2006). A Dual-Color Bacterial Reporter Strain for the Detection of Toxic and Genotoxic Effects. *Engineering in Life Sciences*, 6(3), 319–323. <https://doi.org/10.1002/elsc.200620132>
- Hong, Y. S., Song, K. H., & Chung, J. Y. (2014). Health effects of chronic arsenic exposure. *Journal of Preventive Medicine and Public Health*, 47(5), 245–252. <https://doi.org/10.3961/jpmph.14.035>
- Hong, H. J., Koom, W. S., & Koh, W. G. (2017). Cell microarray technologies for high-throughput cell-based biosensors. *Sensors (Switzerland)*, 17(6). <https://doi.org/10.3390/s17061293>
- Hughes, M. F. (2002). Arsenic toxicity and potential mechanisms of action. *Toxicology Letters*, 133(1), 1–16. [https://doi.org/10.1016/s0378-4274\(02\)00084-x](https://doi.org/10.1016/s0378-4274(02)00084-x)

- Hou, Q., Ma, A., Wang, T., Lin, J., Wang, H., Du, B., Zhuang, X., & Zhuang, G. (2015). Detection of bioavailable cadmium, lead, and arsenic in polluted soil by tailored multiple *Escherichia coli* whole-cell sensor set. *Analytical and Bioanalytical Chemistry*, 407(22), 6865–6871. <https://doi.org/10.1007/s00216-015-8830-z>
- Hu, Q., Li, L., Wang, Y., Zhao, W., Qi, H., & Zhuang, G. (2010). Construction of WCB-11: A novel *phi*YFP arsenic-resistant whole-cell biosensor. *Journal of Environmental Sciences*, 22(9), 1469–1474. [https://doi.org/10.1016/s1001-0742\(09\)60277-1](https://doi.org/10.1016/s1001-0742(09)60277-1)
- Huang, C-W., Wei, C.-C., & Liao, V. H-C. (2015a). A low cost color-based bacterial biosensor for measuring arsenic in groundwater. *Chemosphere*, 141, 44–49. <https://doi.org/10.1016/j.chemosphere.2015.06.011>
- Huang, C. W., Yang, S. H., Sun, M. W., & Liao, V. H. C. (2015b). Development of a set of bacterial biosensors for simultaneously detecting arsenic and mercury in groundwater. *Environmental Science and Pollution Research*, 22(13), 10206–10213. <https://doi.org/10.1007/s11356-015-4216-1>
- Hughes, M. F., Beck, B. D., Chen, Y., Lewis, A. S., & Thomas, D. J. (2011). Arsenic exposure and toxicology: A historical perspective. *Toxicological Sciences*, 123(2), 305–332. <https://doi.org/10.1093/toxsci/kfr184>
- Hynninen, A., & Virta, M. (2010). Whole-Cell Bioreporters for the Detection of Bioavailable Metals. In S., Belkin, & M., Gu (Eds.). *Whole Cell Sensing System II: Applications. Advances in Biochemical Engineering / Biotechnology* (vol 118, pp. 31-63). Berlin, Germany, Springer-Verlag.

- Hynninen, A., Tönismann, K., & Virta, M. (2010). Improving the sensitivity of bacterial bioreporters for heavy metals. *Bioengineered Bugs*, 1(2), 132–138. <https://doi.org/10.4161/bbug.1.2.10902>
- IARC (2016). IARC monographs on the identification of carcinogenic hazards to humans. International Agency for Research on Cancer. Retrieved from <https://monographs.iarc.fr/list-of-classifications-volumes/>
- Idalia, V.-M. N., & Bernardo, F. (2017). *Escherichia coli* as a Model Organism and Its Application in Biotechnology. *Escherichia coli* - Recent Advances on Physiology, Pathogenesis and Biotechnological Applications. *IntechOpen*. <https://doi.org/10.5772/67306>
- Ivask, A., Virta, M., & Kahru, A. (2002). Construction and use of specific luminescent recombinant bacterial sensors for the assessment of bioavailable fraction of cadmium, zinc, mercury and chromium in the soil. *Soil Biology and Biochemistry*, 34(10), 1439–1447. [https://doi.org/10.1016/s0038-0717\(02\)00088-3](https://doi.org/10.1016/s0038-0717(02)00088-3)
- Ivask, A., Green, T., Polyak, B., Mor, A., Kahru, A., Virta, M., & Marks, R. (2007). Fibre-optic bacterial biosensors and their application for the analysis of bioavailable Hg and As in soils and sediments from Aznalcollar mining area in Spain. *Biosensors and Bioelectronics*, 22(7), 1396–1402. <https://doi.org/10.1016/j.bios.2006.06.019>
- Jaishankar, M., Tseten, T., Anbalagan, N., Mathew, B. B., & Beeregowda, K. N. (2014). Toxicity, mechanism and health effects of some heavy metals. *Interdisciplinary Toxicology*, 7(2), 60–72. <https://doi.org/10.2478/intox-2014-0009>

- Jonnalagadda, S. B., & Rao, P. V. V. P. (1993). Toxicity, bioavailability and metal speciation. *Comparative Biochemistry and Physiology Part C: Pharmacology, Toxicology and Endocrinology*, 106(3), 585–595. [https://doi.org/10.1016/0742-8413\(93\)90215-7](https://doi.org/10.1016/0742-8413(93)90215-7)
- Jouanneau, S., Durand, M. J., & Thouand, G. (2012). Online detection of metals in environmental samples: Comparing two concepts of bioluminescent bacterial biosensors. *Environmental Science and Technology*, 46(21), 11979–11987. <https://doi.org/10.1021/es3024918>
- Jouanneau, S., Durand, M. J., Assaf, A., Bittel, M., & Thouand, G. (2017). Bacterial Bioreporter Applications in Ecotoxicology: Concepts and Practical Approach. In C., Cravo-Laureau, C., Cagnon, B., Lauga, & R., Duran (Eds.). *Microbial Ecotoxicology* (pp. 283-311). Cham, Switzerland: Springer Nature.
- Jusoh, W. N. A. W., & Wong, L. S. (2014). Exploring the Potential of Whole Cell Biosensor: A Review in Environmental Applications. *International Journal of Chemical, Environmental & Biological Sciences*, 2(1), 52–56.
- Justino, C. I. L., Duarte, A. C., & Rocha-Santos, T. A. P. (2017). Recent progress in biosensors for environmental monitoring: A review. *Sensors*, 17(12), 2918. <https://doi.org/10.3390/s17122918>
- Kaur, H., Kumar, R., Babu, J. N., & Mittal, S. (2015). Advances in arsenic biosensor development—A comprehensive review. *Biosensors and Bioelectronics*, 63, 533–545. <https://doi.org/10.1016/j.bios.2014.08.003>
- Kim, B. C., & Gu, M. B. (2003). A bioluminescent sensor for high throughput toxicity classification. *Biosensors and Bioelectronics*, 18(8), 1015–1021. [https://doi.org/10.1016/S0956-5663\(02\)00220-8](https://doi.org/10.1016/S0956-5663(02)00220-8)

- Kim, S., & Yoon, Y. (2016). Assessing bioavailability and genotoxicity of heavy metals and metallic nanoparticles simultaneously using dual-sensing *Escherichia coli* whole-cell bioreporters. *Applied Biological Chemistry*, 59(4), 661–668. <https://doi.org/10.1007/s13765-016-0206-3>
- Kim, H. J., Jeong, H., & Lee, S. J. (2018). Synthetic biology for microbial heavy metal biosensors. *Analytical and Bioanalytical Chemistry*, 410(4), 1191–1203. <https://doi.org/10.1007/s00216-017-0751-6>
- Kohlmeier, S., Mancuso, M., Tecon, R., Harms, H., van der Meer, J. R., & Wells, M. (2007). Bioreporters: gfp versus lux revisited and single-cell response. *Biosensors and Bioelectronics*, 22(8), 1578–1585. <https://doi.org/10.1016/j.bios.2006.07.005>
- Köhler, S., Belkin, S., & Schmid, R. D. (2000). Reporter gene bioassays in environmental analysis. *Fresenius' Journal of Analytical Chemistry*, 366(6-7), 769–779. <https://doi.org/10.1007/s002160051571>
- Kruger, M. C., Bertin, P. N., Heipieper, H. J., & Arsène-Ploetze, F. (2013). Bacterial metabolism of environmental arsenic - Mechanisms and biotechnological applications. *Applied Microbiology and Biotechnology*, 97(9), 3827–3841. <https://doi.org/10.1007/s00253-013-4838-5>
- Kuppardt, A., Chatzinotas, A., Breuer, U., Van Der Meer, J. R., & Harms, H. (2009). Optimization of preservation conditions of As(III) bioreporter bacteria. *Applied Microbiology and Biotechnology*, 82(4), 785–792. <https://doi.org/10.1007/s00253-009-1888-9>

- Lee, J. H., Youn, C. H., Kim, B. C., & Gu, M. B. (2007). An oxidative stress-specific bacterial cell array chip for toxicity analysis. *Biosensors and Bioelectronics*, 22(9–10), 2223–2229. <https://doi.org/10.1016/j.bios.2006.10.038>
- Lei, Y., Chen, W., & Mulchandani, A. (2006). Microbial biosensors. *Analytica Chimica Acta*, 568(1–2), 200–210. <https://doi.org/10.1016/j.aca.2005.11.065>
- Li, G., Sun, G.-X., Williams, P. N., Nunes, L., & Zhu, Y.-G. (2011). Inorganic arsenic in Chinese food and its cancer risk. *Environment International*, 37(7), 1219–1225. <https://doi.org/10.1016/j.envint.2011.05.007>
- Li, L., Liang, J., Hong, W., Zhao, Y., Sun, S., Yang, X., Xu, A., Hang, H., Wu, L., & Chen, S. (2015). Evolved bacterial biosensor for arsenite detection in environmental water. *Environmental Science and Technology*, 49(10), 6149–6155. <https://doi.org/10.1021/acs.est.5b00832>
- Liao, V. H-C., & Ou, K. L. (2005). Development and testing of a green fluorescent protein-based bacterial biosensor for measuring bioavailable arsenic in contaminated groundwater samples. *Environmental Toxicology and Chemistry*, 24(7), 1624–1631. <https://doi.org/10.1897/04-500R.1>
- Lim, J. W., Ha, D., Lee, J., Lee, S. K., & Kim, T. (2015). Review of Micro/Nanotechnologies for Microbial Biosensors. *Frontiers in Bioengineering and Biotechnology*, 3(61), 1–13. <https://doi.org/10.3389/fbioe.2015.00061>
- Ma, Z., Jacobsen, F. E., & Giedroc, D. P. (2009). Coordination Chemistry of Bacterial Metal Transport and Sensing. *Chemical Reviews*, 109(10), 4644–4681. <https://doi.org/10.1021/cr900077w>

- Magrisso, S., Erel, Y., & Belkin, S. (2008). Microbial reporters of metal bioavailability. *Microbial Biotechnology*, 1(4), 320–330. <https://doi.org/10.1111/j.1751-7915.2008.00022.x>
- Majumdar, K. K., Ghose, A., Ghose, N., Biswas, A., & Mazumder, D. N. G. (2014). Effect of Safe Water on Arsenicosis: A Follow-up Study. *Journal of Family Medicine and Primary Care*, 3(2), 124–128. <https://doi.org/10.4103/2249-4863.137626>
- Maniatis, T., Fritsch, E. F., & Sambrook, J. (1982). *Molecular cloning: A laboratory manual*. Cold Spring Harbor, N.Y: Cold Spring Harbor Laboratory.
- Masindi, V., & Muedi, K. L. (2018). Environmental Contamination by Heavy Metals. In H. E. M, Saleh, & R. F, Aglan (Eds.). *Heavy Metals*. IntechOpen. <https://doi.org/10.5772/intechopen.76082>
- Mehta, J., Bhardwaj, S. K., Bhardwaj, N., Paul, A. K., Kumar, P., Kim, K. H., & Deep, A. (2016). Progress in the biosensing techniques for trace-level heavy metals. *Biotechnology Advances*, 34(1), 47–60. <https://doi.org/10.1016/j.biotechadv.2015.12.001>
- Merulla, D., Buffi, N., Beggah, S., Truffer, F., Geiser, M., Renaud, P., & van der Meer, J. R. (2013). Bioreporters and biosensors for arsenic detection. Biotechnological solutions for a world-wide pollution problem. *Current Opinion in Biotechnology*, 24(3), 534–541. <https://doi.org/10.1016/j.copbio.2012.09.002>

- Michelini, E., & Roda, A. (2012). Staying alive: New perspectives on cell immobilization for biosensing purposes. *Analytical and Bioanalytical Chemistry*, 402(5), 1785–1797. <https://doi.org/10.1007/s00216-011-5364-x>
- Mitchell, R. J., & Gu, M. B. (2006). Characterization and optimization of two methods in the immobilization of 12 bioluminescent strains. *Biosensors and Bioelectronics*, 22(2), 192–199. <https://doi.org/10.1016/j.bios.2005.12.019>
- Morais, S., e Costa, F. G., & Pereir, M. L. (2012). Heavy Metals and Human Health. *Environmental Health - Emerging Issues and Practice*. Jacques Oosthuizen, IntechOpen. <https://doi.org/10.5772/29869>
- Müller-Taubenberger, A., & Anderson, K. I. (2007). Recent advances using green and red fluorescent protein variants. *Applied Microbiology and Biotechnology*, 77(1), 1–12. <https://doi.org/10.1007/s00253-007-1131-5>
- Nakamura, H. (2018). Current status of water environment and their microbial biosensor techniques – Part II: Recent trends in microbial biosensor development. *Analytical and Bioanalytical Chemistry*, 410(17), 3967–3989. <https://doi.org/10.1007/s00216-018-1080-0>
- Nies, D. H., (1999). Microbial heavy-metal resistance. *Applied Microbiology and Biotechnology*, 51(6), 730–750. <https://doi.org/10.1007/s002530051457>
- Nivens, D. E., McKnight, T. E., Moser, S. A., Osbourn, S. J., Simpson, M. L., & Sayler, G. S. (2004). Bioluminescent bioreporter integrated circuits: Potentially small, rugged and inexpensive whole-cell biosensors for remote environmental monitoring. *Journal of Applied Microbiology*, 96(1), 33–46. <https://doi.org/10.1046/j.1365-2672.2003.02114.x>

- Noll, M. & Lutsenko, S. (2000). Expression of ZntA, a Zinc-Transporting P 1 -Type ATPase, is Specifically Regulated by Zinc and Cadmium. *IUBMB Life (International Union of Biochemistry and Molecular Biology: Life)*, 49, 297–302. <https://doi.org/10.1080/15216540050033168>
- Olaniran, A. O., Balgobind, A., & Pillay, B. (2013). Bioavailability of heavy metals in soil: Impact on microbial biodegradation of organic compounds and possible improvement strategies. *International Journal of Molecular Sciences*, 14(5), 10197–10228. <https://doi.org/10.3390/ijms140510197>
- Outten, C. E., Outten, F. W., & O'Halloran, T. V. (1999). DNA Distortion Mechanism for Transcriptional Activation by ZntR, a Zn(II)-responsive MerR Homologue in *Escherichia coli*. *Journal of Biological Chemistry*, 274(53), 37517–37524. <https://doi.org/10.1074/jbc.274.53.37517>
- Paitan, Y., Biran, D., Biran, I., Shechter, N., Babai, R., Rishpon, J., & Ron, E. Z. (2003). On-line and in situ biosensors for monitoring environmental pollution. *Biotechnology Advances*, 22(1–2), 27–33. <https://doi.org/10.1016/j.biotechadv.2003.08.014>
- Panagiotaras, D., & Nikolopoulos, D. (2015). Arsenic occurrence and fate in the environment; a geochemical perspective. *Journal of Earth Science and Climatic Change*, 6, 269. <https://doi.org/10.4172/2157-7617.1000269>
- Pasco, N. F., Weld, R. J., Hay, J. M., & Gooneratne, R. (2011). Development and applications of whole cell biosensors for ecotoxicity testing. *Analytical and Bioanalytical Chemistry*, 400(4), 931–945. <https://doi.org/10.1007/s00216-011-4663-6>

- Pola-López, L. A., Camas-Anzueto, J. L., Martínez-Antonio, A., Luján-Hidalgo, M. C., Anzueto-Sánchez, G., Ruíz-Valdiviezo, V. M., Grajales-Coutino, R., & González, J. H. C. (2018). Novel arsenic biosensor “POLA” obtained by a genetically modified *E. coli* bioreporter cell. *Sensors and Actuators, B: Chemical*, 254, 1061–1068. <https://doi.org/10.1016/j.snb.2017.08.006>
- Polyak, B., Bassis, E., Novodvoretz, A., Belkin, S., & Marks, R. S. (2001). Bioluminescent whole cell optical fiber sensor to genotoxics: System optimization. *Sensors and Actuators B: Chemical*, 74(1-3), 18–26. [https://doi.org/10.1016/S0925-4005\(00\)00707-3](https://doi.org/10.1016/S0925-4005(00)00707-3)
- Prévéral, S., Brutesco, C., Descamps, E. C. T., Escoffier, C., Pignol, D., Ginet, N., & Garcia, D. (2017). A bioluminescent arsenite biosensor designed for inline water analyzer. *Environmental Science and Pollution Research*, 24(1), 25–32. <https://doi.org/10.1007/s11356-015-6000-7>
- Rahman, M. M., Dong, Z., & Naidu, R. (2015). Concentrations of arsenic and other elements in groundwater of Bangladesh and West Bengal, India: potential cancer risk. *Chemosphere*, 139, 54–64. <https://doi.org/10.1016/j.chemosphere.2015.05.051>
- Rasmussen, L. D., Turner, R. R., & Barkay, T. (1997). Cell-density-dependent sensitivity of a mer-lux bioassay. *Applied and Environmental Microbiology*, 63, 3291–3293.
- Ravenscroft, P., Brammer, H., & Richards, K. (2009). *Arsenic Pollution: A Global Synthesis* (pp.318–485). UK: Wiley-Blackwell. <https://doi.org/10.1002/9781444308785>

- Rensing, C., Mitra, B., & Rosen, B. P. (1997). The *zntA* gene of *Escherichia coli* encodes a Zn(II)-translocating P-type ATPase. *Proceedings of the National Academy of Sciences*, 94(26), 14326–14331. <https://doi.org/10.1073/pnas.94.26.14326>
- Rensing, C., & Maier, R. M. (2003). Issues underlying use of biosensors to measure metal bioavailability. *Ecotoxicology and Environmental Safety*, 56(1), 140–147. [https://doi.org/10.1016/s0147-6513\(03\)00057-5](https://doi.org/10.1016/s0147-6513(03)00057-5)
- Reza, R., & Singh, G. (2010). Heavy metal contamination and its indexing approach for river water. *International Journal of Environmental Science and Technology*, 7(4), 785–792. <https://doi.org/10.1007/BF03326187>
- Riether, K., Dollard, M.-A., & Billard, P. (2001). Assessment of heavy metal bioavailability using *Escherichia coli* *zntAp::lux* and *copAp::lux*-based biosensors. *Applied Microbiology and Biotechnology*, 57(5-6), 712–716. <https://doi.org/10.1007/s00253-001-0852-0>
- Rinaudo, M. (2008). Main properties and current applications of some polysaccharides as biomaterials. *Polymer International*, 57(3), 397–430. <https://doi.org/10.1002/pi.2378>
- Robbens, J., Dardenne, F., Devriese, L., De Coen, W., & Blust, R. (2010). *Escherichia coli* as a bioreporter in ecotoxicology. *Applied Microbiology and Biotechnology*, 88(5), 1007–1025. <https://doi.org/10.1007/s00253-010-2826-6>
- Roberto, F. F., Barnes, J. M., & Bruhn, D. F. (2002). Evaluation of a GFP reporter gene construct for environmental arsenic detection. *Talanta*, 58(1), 181–188. [https://doi.org/10.1016/S0039-9140\(02\)00266-7](https://doi.org/10.1016/S0039-9140(02)00266-7)

- Rodriguez-Mozaz, S., Lopez De Alda, M. J., & Barceló, D. (2006). Biosensors as useful tools for environmental analysis and monitoring. *Analytical and Bioanalytical Chemistry*, 386(4), 1025–1041. <https://doi.org/10.1007/s00216-006-0574-3>
- Roggo, C., & van der Meer, J. R. (2017). Miniaturized and integrated whole cell living bacterial sensors in field applicable autonomous devices. *Current Opinion in Biotechnology*, 45, 24–33. <https://doi.org/10.1016/j.copbio.2016.11.023>
- Rothert, A., Deo, S. K., Millner, L., Puckett, L. G., Madou, M. J., & Daunert, S. (2005). Whole-cell-reporter-gene-based biosensing systems on a compact disk microfluidics platform. *Analytical Biochemistry*, 342(1), 11–19. <https://doi.org/10.1016/j.ab.2004.10.048>
- Sambrook, J. & Russel, D. W. (2001). Molecular cloning: a laboratory manual. Cold Spring Harbor, N.Y: Cold Spring Harbor Laboratory Press.
- Selimoglu, S. M., & Elibol, M. (2010). Alginate as an immobilization material for MAb production via encapsulated hybridoma cells. *Critical Reviews in Biotechnology*, 30(2), 145–159. <https://doi.org/10.3109/07388550903451652>
- Sezonov, G., Joseleau-Petit, D., & D'Ari, R. (2007). *Escherichia coli* Physiology in Luria-Bertani Broth. *Journal of Bacteriology*, 189(23), 8746-8749. <https://doi.org/10.1128/JB.01368-07>
- Shaner, N. C., Steinbach, P. A., & Tsien, R. Y. (2005). A guide to choosing fluorescent proteins. *Nature Methods*, 2(12), 905–909. <https://doi.org/10.1038/nmeth819>

- Shin, H. J. (2011). Genetically engineered microbial biosensors for in situ monitoring of environmental pollution. *Applied Microbiology and Biotechnology*, 89(4), 867–877. <https://doi.org/10.1007/s00253-010-2990-8>
- Singh, R., Gautam, N., Mishra, A., & Gupta, R. (2011). Heavy metals and living systems: An overview. *Indian Journal of Pharmacology*, 43(3), 246–253. <https://doi.org/10.4103/0253-7613.81505>
- Singh, R., Singh, S., Parihar, P., Singh, V. P., & Prasad, S. M. (2015). Arsenic contamination, consequences and remediation techniques: A review. *Ecotoxicology and Environmental Safety*, 112, 247–270. <https://doi.org/10.1016/j.ecoenv.2014.10.009>
- Smedley, P. L., & Kinniburgh D.G. (2002). A review of the source, behaviour and distribution of arsenic in natural waters. *Applied Geochemistry*, 17, 517–568.
- Sørensen, S. J., Burmølle, M., & Hansen, L. H. (2006). Making bio-sense of toxicity: New developments in whole-cell biosensors. *Current Opinion in Biotechnology*, 17(1), 11–16. <https://doi.org/10.1016/j.copbio.2005.12.007>
- Stenuit, B., Eysers, L., Schuler, L., Agathos, S. N., & George, I. (2008). Emerging high-throughput approaches to analyze bioremediation of sites contaminated with hazardous and/or recalcitrant wastes. *Biotechnology Advances*, 26(6), 561–575. <https://doi.org/10.1016/j.biotechadv.2008.07.004>

- Stocker, J., Balluch, D., Gsell, M., Harms, H., Feliciano, J., Daunert, S., Khurseed, A. M., & van der Meer, J. R. (2003). Development of a set of simple bacterial biosensors for quantitative and rapid measurements of arsenite and arsenate in potable water. *Environmental Science and Technology*, 37(20), 4743–4750. <https://doi.org/10.1021/es034258b>
- Struss, A. K., Pasini, P., & Daunert, S. (2010). Biosensing Systems Based on Genetically Engineered Whole Cells. In M., Zourob (Ed.). *Recognition Receptors in Biosensors* (pp. 565-598). New York, NY: Springer.
- Su, L., Jia, W., Hou, C., & Lei, Y. (2011). Microbial biosensors: A review. *Biosensors and Bioelectronics*, 26(5), 1788–1799. <https://doi.org/10.1016/j.bios.2010.09.005>
- Suzuki, K., Wakao, N., Kimura, T., Sakka, K., & Ohmiya, K. (1998). Expression and regulation of the arsenic resistance operon of *Acidiphilium multivorum* AIU 301 plasmid pKW301 in *Escherichia coli*. *Applied and Environmental Microbiology*, 64(2), 411–418.
- Tani, C., Inoue, K., Tani, Y., Harun-ur-Rashid, M., Azuma, N., Ueda, S., Yoshida, K., & Maeda, I. (2009). Sensitive fluorescent microplate bioassay using recombinant *Escherichia coli* with multiple promoter- reporter units in tandem for detection of arsenic. *Journal of Bioscience and Bioengineering*, 108(5), 414–420. <https://doi.org/10.1016/j.jbiosc.2009.05.014>
- Tauriainen, S., Karp, M., Chang, W., & Virta, M. (1997). Recombinant luminescent bacteria for measuring bioavailable arsenite and antimonite. *Applied and Environmental Microbiology*, 63, 4456– 4461.

- T.C. Orman ve Su İşleri Bakanlığı (2015). Yerüstü su kalitesi yönetmeliğinde değişiklik yapılmasına dair yönetmelik. RG No. 29327
- T.C. Sağlık Bakanlığı. Türkiye Halk Sağlığı Kurumu (2013). İnsani tüketim amaçlı sular hakkında yönetmelikte değişiklik yapılmasına dair yönetmelik. RG No:28580
- Tchounwou, P. B., Yedjou, C. G., Patlolla, A. K., & Sutton, D. J. (2012). Heavy metal toxicity and the environment. *Experientia Supplementum*, 101, 133–164. https://doi.org/10.1007/978-3-7643-8340-4_6
- Tecon, R., & Van Der Meer, J. R. (2008). Bacterial biosensors for measuring availability of environmental pollutants. *Sensors*, 8(7), 4062–4080. <https://doi.org/10.3390/s8074062>
- Teo, S. C., & Wong, L. S. (2014). Whole Cell-based Biosensors for Environmental Heavy Metals Detection. *Annual Research & Review in Biology*, 4(17), 2663–2674. <https://doi.org/10.9734/ARRB/2014/9472>
- Theytaz, J., Braschler, T., van Lintel, H., Renaud, P., Diesel, E., Merulla, D., & van der Meer, J. (2009). Biochip with *E. coli* bacteria for detection of arsenic in drinking water. *Procedia Chemistry*, 1(1), 1003–1006. <https://doi.org/10.1016/j.proche.2009.07.250>
- Tombolini, R., Unge, A., Davey, M. E., Bruijn, F. J., & Jansson, J. K. (1997). Flow cytometric and microscopic analysis of GFP-tagged *Pseudomonas fluorescens* bacteria. *FEMS Microbiology Ecology*, 22(1), 17–28. <https://doi.org/10.1111/j.1574-6941.1997.tb00352.x>

- Truffer, F., Buffi, N., Merulla, D., Beggah, S., van Lintel, H., Renaud, P., van der Meer, J. R., & Geiser, M. (2014). Compact portable biosensor for arsenic detection in aqueous samples with *Escherichia coli* bioreporter cells. *Review of Scientific Instruments*, 85(1), 20–24. <https://doi.org/10.1063/1.4863333>
- Turdean, G. L. (2011). Design and Development of Biosensors for the Detection of Heavy Metal Toxicity. *International Journal of Electrochemistry*, 2011, 1–15. <https://doi.org/10.4061/2011/343125>
- Ullah, F., Othman, M. B. H., Javed, F., Ahmad, Z., & Akil, H. M. (2015). Classification, processing and application of hydrogels: A review. *Materials Science and Engineering: C*, 57, 414–433. <https://doi.org/10.1016/j.msec.2015.07.053>
- U.S. EPA. (2007). Framework for Metals Risk Assessment. EPA 120/R-07/001. United States Environmental Protection Agency, Office of the Science 454 Advisor, Washington, DC.
- van der Meer, J. R. (2010). Bacterial Sensors: Synthetic Design and Application Principles. *Synthesis Lectures on Synthetic Biology*, 2. <https://doi.org/10.2200/S00312ED1V01Y201011SBI002>
- van Der Meer, J. R., & Belkin, S. (2010). Where microbiology meets microengineering: Design and applications of reporter bacteria. *Nature Reviews Microbiology*, 8(7), 511–522. <https://doi.org/10.1038/nrmicro2392>
- Van Wezel, A., Mons, M., & Van Delft, W. (2010). New methods to monitor emerging chemicals in the drinking water production chain. *Journal of Environmental Monitoring*, 12(1), 80–89. <https://doi.org/10.1039/b912979k>

- Verma, N., & Singh, M. (2005). Biosensors for heavy metals. *Biometals*, 18(2), 121–129. <https://doi.org/10.1007/s10534-004-5787-3>
- Wang, S., & Mulligan, C. N. (2006). Occurrence of arsenic contamination in Canada: Sources, behavior and distribution. *Science of the Total Environment*, 366(2–3), 701–721. <https://doi.org/10.1016/j.scitotenv.2005.09.005>
- Wang, X., Lu, X., & Chen, J. (2014). Development of biosensor technologies for analysis of environmental contaminants. *Trends in Environmental Analytical Chemistry*, 2, 25–32. <https://doi.org/10.1016/j.teac.2014.04.001>
- Wasito, H., Fatoni, A., Hermawan, D., & Susilowati, S. S. (2019). Immobilized bacterial biosensor for rapid and effective monitoring of acute toxicity in water. *Ecotoxicology and Environmental Safety*, 170, 205–209. <https://doi.org/10.1016/j.ecoenv.2018.11.141>
- WHO (2011a). Arsenic in drinking-water, in Background Document for Development of WHO Guidelines for Drinking-Water Quality. World Health Organization, Geneva. Retrieved from www.who.int/en; WHO/SDE/WSH/03.04/75/Rev/1.
- WHO (2011b). Cadmium in drinking- water, in Background Document for Development of WHO Guidelines for Drinking-Water Quality. World Health Organization, Geneva. Retrieved from www.who.int/en; WHO/SDE/WSH/03.04/80/Rev/1.
- WHO (2017). Guidelines for Drinking-water Quality. Fourth Edition Incorporating the First Addendum, ISBN-13: 978-92-4-154995-0. World Health Organization, Geneva.

- Willsky, G. R., & Malamy, M. H. (1980). Effect of arsenate on inorganic phosphate transport in *Escherichia coli*. *Journal of Bacteriology*, 144, 366–374.
- Woutersen, M., Belkin, S., Brouwer, B., Van Wezel, A. P., & Heringa, M. B. (2011). Are luminescent bacteria suitable for online detection and monitoring of toxic compounds in drinking water and its sources? *Analytical and Bioanalytical Chemistry*, 400(4), 915–929. <https://doi.org/10.1007/s00216-010-4372-6>
- Wu, J., & Rosen, B. P. (1993). Metalloregulated expression of the ars operon. *Journal of Biological Chemistry*, 268(1), 52–58.
- Xu, X., & Ying, Y. (2011). Microbial biosensors for environmental monitoring and food analysis. *Food Reviews International*, 27(3), 300–329. <https://doi.org/10.1080/87559129.2011.563393>
- Xu, T., Close, D. M., Sayler, G. S., & Ripp, S. (2013). Genetically modified whole-cell bioreporters for environmental assessment. *Ecological Indicators*, 28, 125–141. <https://doi.org/10.1016/j.ecolind.2012.01.020>
- Xu, T., Perry, N., Chuahan, A., Sayler, G., & Ripp, S. (2014). Microbial Indicators for Monitoring Pollution and Bioremediation. In S. Das (Ed.). *Microbial Biodegradation and Bioremediation* (115–136). Elsevier.
- Yagi, K. (2007). Applications of whole-cell bacterial sensors in biotechnology and environmental science. *Applied Microbiology and Biotechnology*, 73(6), 1251–1258. <https://doi.org/10.1007/s00253-006-0718-6>
- Yang, H. C., Fu, H. L., Lin, Y. F., & Rosen, B. P. (2012). Pathways of arsenic uptake and efflux. *Current Topics in Membranes*, 69, 325–358. <https://doi.org/10.1016/B978-0-12-394390-3.00012-4>

- Yoon, Y., Kim, S., Chae, Y., Kang, Y., Lee, Y., Jeong, S. W., & An, Y. J. (2016). Use of tunable whole-cell bioreporters to assess bioavailable cadmium and remediation performance in soils. *PLoS ONE*, *11*(5), 1–16. <https://doi.org/10.1371/journal.pone.0154506>
- Zacharias, D. A., & Tsien, R. Y. (2006). Molecular Biology and Mutation of Green Fluorescent Protein. In M, Chalfie, & S. R, Kain (Eds.). *Green Fluorescent Protein: Properties, Applications, and Protocols*, (2nd ed., pp.83-120). Hoboken, New Jersey: John Wiley & Sons, Inc.
- Zhang, F., & Keasling, J. (2011). Biosensors and their applications in microbial metabolic engineering. *Trends in Microbiology*, *19*(7), 323–329. <https://doi.org/10.1016/j.tim.2011.05.003>
- Zimmer, M. (2002). Green fluorescent protein (GFP): Applications, structure, and related photophysical behavior. *Chemical Reviews*, *102*(3), 759-781.
- Zhu, Y. (2007). Immobilized Cell Fermentation for Production of Chemicals and Fuels. In S-T, Yang (Ed.). *Bioprocessing for Value-Added Products from Renewable Resources*, New Technologies and Applications (pp. 373–396). Elsevier.

APPENDICES

A. COMPOSITIONS OF BACTERIAL CULTURE MEDIA

Luria-Bertani Broth (1 L)

Yeast extract 5 g
Tryptone 10 g
NaCl 10 g
Bacterial agar 15 g (for solid medium)

-The pH of the medium is adjusted to 7.4 and autoclaved at 121°C for 20 minutes.

M9 supplemented medium (500 ml)

5X M9 Minimal Salts 100 ml
Filter sterilized stock solutions added,
MgSO₄·7H₂O stock, 1 M 1 ml
CaCl₂·2H₂O stock, 1M 500 µl
Casaminoacids stock, 10% v/v) 5 ml
Glucose stock, 20% (v/v) 10 ml

-The pH of the medium is adjusted to 7.0. Complete to 500 ml with sterile distilled water.

M9 Minimal salts, 5X (1 L)

Na₂HPO₄ 30 g
KH₂PO₄ 15 g
NaCl 2.5 g
NH₄Cl 5 g

-Autoclaved at 121°C for 20 minutes.

MOPS supplemented medium (500 ml)

MOPS sodium salt	4.9 g
NaCl	0.25 g
NH ₄ Cl	0.5 g
Na ₂ HPO ₄	0.025 g
KH ₂ PO ₄	0.025 g

The pH is adjusted to 7.0 by addition of NaOH and completed to 483.5 ml with distilled water. Autoclaved at 121°C for 20 minutes.

Filter sterilized stock solutions added,

MgSO ₄ .7H ₂ O stock, 1 M	1 ml
CaCl ₂ .2H ₂ O stock, 1M	500 µl
Casaminoacids stock, 10% v/v)	5 ml
Glucose stock, 20% (v/v)	10 ml

B. BUFFERS AND SOLUTIONS

50X Tris-Acetate-EDTA (TAE) Buffer (1 L)

Component	Quantity
Tris Base	242 g
Glacial Acetic Acid	57.1 mL
0.5 M EDTA (pH: 8.0)	100 mL

-For 1X working solution, 50X stock is diluted in 1:50 ratio with dH₂O.

Transformation buffer I (200 mL)

Compound	Amount	Final molarity
Potassium acetate	0.588 g	30 mM
Rubidium chloride	2.42 g	100 mM
Calcium chloride	0.294 g	10 mM
Glycerol 30 ml 87% v/v		

Transformation buffer II (100 mL)

Compound	Amount	Final molarity
MOPS	0.21 g	10 mM
Calcium chloride	1.1 g	75 mM
Rubidium chloride	0.121 g	10 mM
Glycerol 15 ml 87% v/v		

-The pH of the buffers is adjusted to 6.5 and performed filter sterilization.

1X Phosphate-buffered saline (PBS) (1 L)

Compound	Amount	Final molarity
NaCl	8 g	137 mM
KCl	0.2 g	2.7 mM
Na ₂ HPO ₄	1.44 g	10 mM
KH ₂ PO	0.24 g	1.8 mM

-The pH of the solution is adjusted to 7.4 with HCl. Autoclaved at 121°C for 20 minutes and performed filter sterilization.

C. PGFPUV, PARSR-ARSR AND PZNTA DNA SEQUENCES

Cloning vector *pGFPuv*, Partial Sequence

```

LOCUS          CVU62636                      3337 bp      DNA      linear      SYN
14-AUG-1996
DEFINITION     Cloning vector pGFPuv, complete sequence.
ACCESSION      U62636
VERSION        U62636.1
SOURCE         Cloning vector pGFPuv
ORGANISM       Cloning vector pGFPuv
               other sequences; artificial sequences; vectors.
REFERENCE      1  (bases 1 to 3337)
AUTHORS        Kitts,P.A.
TITLE          pGFPuv complete sequence
JOURNAL        Unpublished
REFERENCE      2  (bases 1 to 3337)
AUTHORS        Kitts,P.A.
TITLE          Direct Submission
JOURNAL        Submitted (28-JUN-1996) CLONTECH Laboratories, Inc.,
1020 East Meadow Circle, Palo Alto, CA 94303-4230, USA
FEATURES
  source        Location/Qualifiers
                1..3337
                /organism="Cloning vector pGFPuv"
                /mol_type="genomic DNA"
                /db_xref="taxon:49914"
  gene          289..1005
                /gene="gfpuv"
  CDS           289..1005
                /gene="gfpuv"
                /note="green fluorescent protein variant;
GFPuv is the GFP variant called 'cycle 3'"
                /codon_start=1
                /transl_table=11
                /product="GFPuv"
                /protein_id="AAB06048.1"

/translation="MSKGEELFTGVVPILVELDGDVNGHKFSVSGEGEGDATYGKLTLL
KFICTTGKLPVPWPPTLVTTFSYGVQCFSRYPDHMKRHDFFKSAMPEGYVQERTISFKD
DGNYKTRAEVKFEGDTLVNRIELKGIDFKEDGNILGHKLEYNYNshNVYITADKQKNG
IKANFKIRHNIEDGSVQLADHYQQNTPIGDGPVLLPDNHYLSTQSALSKDPNEKRDHM
VLLEFVTAAGITHGMDELYK"
  gene          1537..2397
                /gene="bla"
  CDS           1537..2397
                /gene="bla"
                /function="confers resistance to ampicillin"

```

```

/codon_start=1
/transl_table=11
/product="beta-lactamase"
/protein_id="AAB06049.1"

/translation="MSIQHFRVALIPFFFAAFCLPVFAHPETLVKVKDAEDQLGARVGY
IELDLNSGKILESFRPEERFPMSTFKVLLCGAVLSRIDAGQEQLGRRIHYSQNDLVE
YSPVTEKHLTDGMTVRELCSAAITMSDNTAANLLLTIGGPKELTAFLHNMGDHVTRL
DRWEPELNEAIPNDERDRTMPVAMATTLRKLLTGELLTLASRQQLIDWMEADKVAGPL
LRSALPAGWFIADKSGAGERGSRGIIAALGPDGKPSRIVVIYTTGSQATMDERNRQIA
EIGASLIKHW"
ORIGIN
    1 agcgcccaat acgcaaaccg cctctccccg cgcgttggcc gattcattaa
tgcagctggc .....
   241 catgcctgca ggtcgactct agaggatccc cgggtaccgg tagaaaaaat
gagtaaagga
   301 gaagaacttt tctactggagt tgtcccaatt cttgttgaat tagatgggtga
tgttaatggg
   361 cacaaatfff ctgtcagtgg agagggtgaa ggtgatgcaa catacggaaa
acttaccctt
   421 aaatftatft gcactactgg aaaactacct gttccatggc caacacttgt
cactactttc
   481 tcttatgggtg ttcaatgctt ttcccgttat ccggatcata tgaaacggca
tgactttttc
   541 aagagtgcc a tgcccgaagg ttatgtacag gaacgcacta tatctttcaa
agatgacggg
   601 aactacaaga cgcgtgctga agtcaagttt gaagggtgata cccttggttaa
tcgtatcgag
   661 ttaaaaggta ttgattttta agaagatgga aacattctcg gacacaaact
cgagtacaac
   721 tataactcac acaatgtata catcacggca gacaaacaaa agaatggaat
caaagctaac
   781 ttcaaaattc gccacaacat tgaagatgga tccgttcaac tagcagacca
ttatcaacaa
   841 aatactcaa ttggcgatgg ccctgtcctt ttaccagaca accattacct
gtcgacacaa
   901 tctgcccttt cgaaagatcc caacgaaaag cgtgaccaca tggtccttct
tgagtttgta
   961 actgctgctg ggattacaca tggcatggat gagctctaca aataatgaat
tccaactgag
  1021 cgccgggtcg taccattacc aacttgtctg gtgtcaaaaa taataggcct
actagtccgc
  1081 cgtacggggc ctttcgtctc gcgcgtttcg gtgatgacgg tgaacacctc
tgacacatgc
  1141 agtccccgga gacggtcaca gcttgtctgt aagcggatgc cgggagcaga
caagcccgtc.....
  3301 accgagcgca gcgagtcagt gagcgaggaa gcggaag
//

```

***ParsR-arsR* DNA Sequence**

***E. coli* R-factor R773 *arsR* gene**

LOCUS X16045 727 bp DNA linear BCT
18-APR-2005
DEFINITION *E. coli* R-factor R773 *arsR* gene.
ACCESSION X16045
VERSION X16045.1
KEYWORDS arsenical resistance; *arsR* gene; ArsR protein; DNA-binding protein;
regulatory protein; resistance gene.
SOURCE *Escherichia coli*
ORGANISM [Escherichia coli](#)
Bacteria; Proteobacteria; Gammaproteobacteria;
Enterobacteriales;
Enterobacteriaceae; *Escherichia*.
REFERENCE 1 (bases 1 to 727)
AUTHORS San Francisco,M.J., Hope,C.L., Owolabi,J.B., Tisa,L.S.
and
Rosen,B.P.
TITLE Identification of the metalloregulatory element of the
plasmid-encoded arsenical resistance operon
JOURNAL Nucleic Acids Res. 18 (3), 619-624 (1990)
PUBMED [2408017](#)
REFERENCE 2 (bases 1 to 727)
AUTHORS Rosen,B.P.
TITLE Direct Submission
JOURNAL Submitted (09-AUG-1989) Rosen B.P., Department of
Biochemistry,Wayne State University, School of Medicine, 54- E
Canfield Avenue, Detroit MI 48201, U S A
FEATURES Location/Qualifiers
source 1..727
/organism="Escherichia coli"
/mol_type="genomic DNA"
/db_xref="taxon:[562](#)"
/clone="pWSU1"
/clone_lib="pBR322"
regulatory 73..79
/regulatory_class="promoter"
/note="pot. -35 region"
regulatory 96..102
/regulatory_class="promoter"
/note="pot. -10 region"
misc_feature 107
/note="transcriptional start site"
regulatory 114..118
/regulatory_class="ribosome_binding_site"
/note="pot. ribosome binding site"
CDS 125..478
/note="unnamed protein product; ArsR protein
(AA 1 - 117)"
/codon_start=1

```

        /transl_table=11
        /protein_id="CAA34168.1"
        /db_xref="GOA:P15905"
        /db_xref="InterPro:IPR001845"
        /db_xref="InterPro:IPR011991"
        /db_xref="InterPro:IPR018334"
        /db_xref="UniProtKB/Swiss-Prot:P15905"

/translation="MLQLTPLQLFKNLSDETRLGIVLLLREMGELCVCDLCMALDQSQ
PKISRHLAMLRESGILLDRKQGKQVHYRLSPHIPSWAAQIIEQAWLSQQDDVQVIARK
        regulatory 482..511
                        /regulatory_class="terminator"
                        /note="pot. stem-loop structure"

ORIGIN
      1 gaattccaag ttatctcacc taccttaagg taatagtgtg attaatacata
tgcgtttttg
     61 gttatgtggt gtttgactta atatcagagc cgagagatac ttgttttcta
caaaggagag
    121 ggaaatgttg caactaacac cacttcagtt atttaaaaac ctgtccgatg
aaacccgttt
    181 gggatatctg ttgttgctca gggagatggg agagttgtgc gtgtgtgatc
tttgcattgg
    241 actggatcaa tcacagccca aaatatcccg tcattctggcg atgctacggg
aaagtgggaat
    301 ccttctggat cgtaaacagg gaaaatgggt tcactaccgc ttatcaccgc
atattccttc
    361 atgggctgcc cagattattg agcaggcctg gttaagccaa caggacgacg
ttcagggtcat
    421 cgcacgcaag ctggcttcag ttaactgctc cggtagcagt aaggctgtct
gcatctaaaa
    481 aatttgctg aacatatatg ttttatcaaa tgcgagggtat ttaagatgaa
aacgttaatg
    541 gtatttgacc cggcgatgtg ttgcagcacc ggcgtctgcg gtacagatgt
tgatcaggct
    601 ctggtcgatt tttctacaga tgtgcaatgg ctcaaacaat gcggtgtaca
aattgagcgt
    661 ttcaatcttg cgcaacaacc gatgagcttt gtacagaacg agaagggtcaa
agcgtttatt
    721 gaagctt
//

```

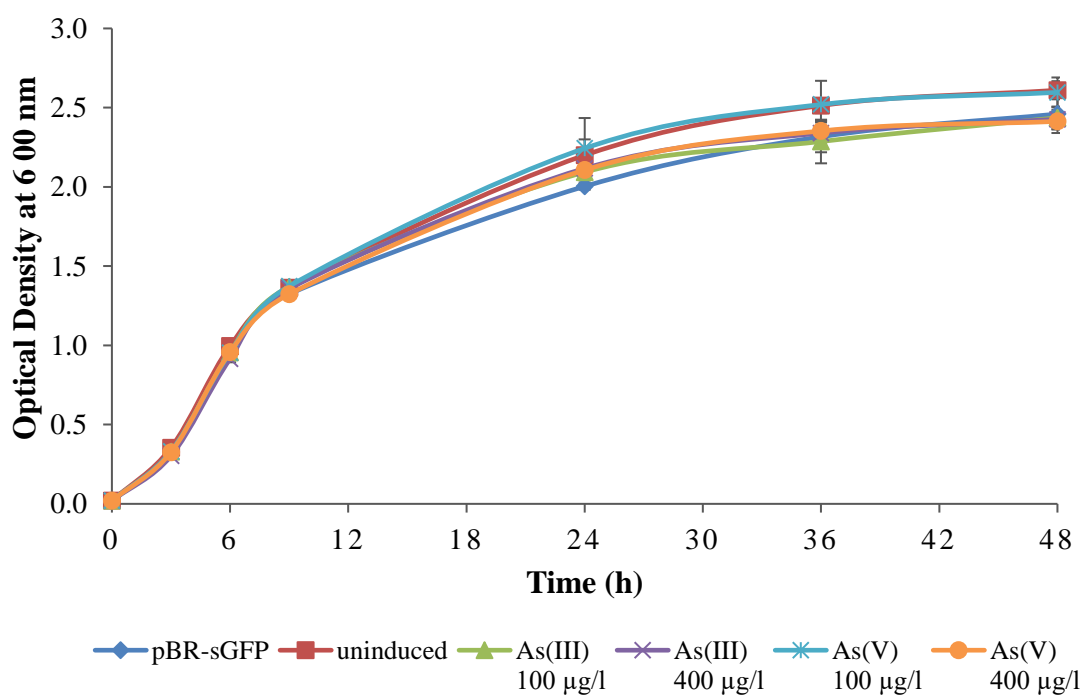
PzntA DNA Sequence (upstream region of zntA gene)

Ecogene3.0 GenePage for the zntA gene of *Escherichia coli* K-12

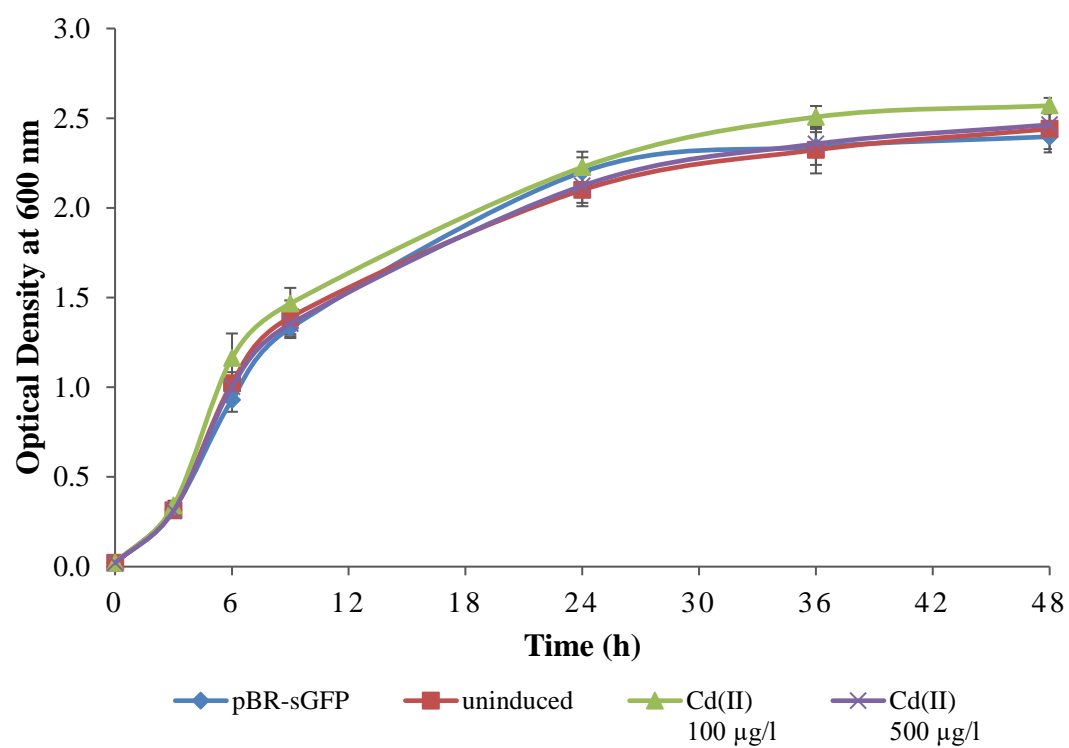
FASTA		Coordinates		TFBS		SITES	
<input checked="" type="checkbox"/>	ZntR	Overlap	Positions				
	TAATCGGTTT	TTCCCGCTTG	TTGCTCACCA	CCACCAGCTT	TTGCTGGAGC		
3605451	GGAGCCATAT	CATTATCAGC	TTTTTCCCGT	CGCTGTTGCA	TAAAACGAAA	[-1000	-9]
3605501	CGATGCGGCG	ACGACAATTA	AGCCAATGAT	AACAATAAAG	AAAAGAGGTG	[-950	-90]
3605551	GT TTGCTCAT	CTTTATCCCT	CATCGGAAAA	TGCGGAAATA	AGCATACCCT	[-900	-85]
3605601	GCCAGTTATG	GTGTTGTCAT	CCGTCCACCC	TCGCCACTAA	ACTGGAAGCA	[-850	-80]
3605651	AGACCGTAGG	CATTCCGCTT	ACGAAAAAAT	AACGAATTCA	AGGAACTAAG	[-800	-75]
3605701	ATGCTTTGGT	CGTTTATCGC	TGTCTGTCTT	TCCGCATGGC	TATCTGTGGA	[-750	-70]
3605751	TGCATCGTAT	CGTGGGCCAA	CCTGGCAACG	CTGGGTGTTT	AAACCGTTAA	[-700	-65]
3605801	CCCTTCTTCT	CCTGCTGTTA	CTGGCCTGGC	AAGCGCCGAT	GTTTCGACGC	[-650	-60]
3605851	ATTAGCTATC	TGGTGCTGGC	AGGGCTGTGC	GCCTCACTGC	TGGGCGATGC	[-600	-55]
3605901	GCTAACCCTG	TTGCCACGTC	AACGTCTGAT	GTACGCCATC	GGCGCGTTTT	[-550	-50]
3605951	TCCTCTCGCA	CCTGCTGTAC	ACCATCTATT	TCGCCAGTCA	GATGACGCTC	[-500	-45]
3606001	TCTTTCTTCT	GGCCTCTACC	ACTGGTGCTG	CTGGTTCTGG	GTGCGCTGTT	[-450	-40]
3606051	ACTGGCGATT	ATCTGGACGC	GCCTGGAAGA	GTACCGTTGG	CCTATCTGCA	[-400	-35]
3606101	CGTTTATCGG	CATGACGCTG	GTGATGGTGT	GGCTGGCAGG	TGAACTGTGG	[-350	-30]
3606151	TTCTTCCGTC	CGACCGCTCC	GGCGCTCTCT	GCGTTTGTTG	GCGCTTCGTT	[-300	-25]
3606201	GCTGTTTATC	AGTAACTTTG	TCTGGCTGGG	GAGCCACTAT	CGCCGACGCT	[-250	-20]
3606251	TCCGTGCGGA	TAACGCGATT	GCTGCGGCCT	GCTACTTTGC	CGGTCACTTC	[-200	-15]
3606301	CTGATCGTCC	GCTCGCTGTA	TCTCTGATAA	AACTTGACTC	TGGAGTCGAC	[-150	-10]
3606351	TCCAGAGTGT	ATCCTTCGGT	TAATGAGAAA	AACTTAACC	GGAGGATGCC	[-100	-51]
3606401						[-50	-1]
	ATGTCGACTC	CTGACAATCA	CGGCAAGAAA	GCCCCTCAAT	TTGCTGCGTT		
3606451	CAAACCGCTA	ACCACGGTAC	AGAACGCCAA	CGACTGTTGC	TGCGACGGCG	[1	50]
3606501	CATGTTCCAG	CACGCCAACT	CTCTCTGAAA	ACGTCTCCGG	CACCCGCTAT	[51	100]
3606551	AGCTGGAAAG	TCAGCGGCAT	GGACTGCGCC	GCCTGTGCGC	GCAAGGTAGA	[101	150]

D. GROWTH CURVES

The growth curves of pBR-sGFP, and uninduced and arsenic induced pBR-arsR773 cultures (n = 3)



The growth curves of pBR-sGFP, and uninduced and cadmium induced pBR-PzntA cultures (n = 3)



E. ONE-WAY ANOVA RESULTS

A) As(III) Detection by Arsenic Bioreporter in M9 Supplemented Medium (incubation = 2 hours)

Descriptives

RFU2h

	N	Mean	Std. Deviation	Std. Error	95% Confidence Interval for Mean		Minimum	Maximum
					Lower Bound	Upper Bound		
uninduced	3	39412.6667	26628.44874	15373.94205	-26736.0671	105561.4004	9101.00	59038.00
10 µg/l	3	259620.0000	14071.03440	8123.91550	224665.6128	294574.3872	243388.00	268357.00
25 µg/l	3	659191.0000	81424.12061	47010.23795	456922.2713	861459.7287	604104.00	752719.00
50 µg/l	3	1364563.333	14260.22673	8233.14574	1329138.966	1399987.700	1.35E+6	1.38E+6
75 µg/l	3	1947869.667	83242.60588	48060.14092	1741083.570	2154655.763	1.90E+6	2.04E+6
150 µg/l	3	3072605.000	159048.6307	91826.76974	2677506.299	3467703.701	2.97E+6	3.26E+6
Total	18	1223876.944	1082482.026	255143.4605	685571.2969	1762182.592	9101.00	3.26E+6

ANOVA

RFU2h

	Sum of Squares	df	Mean Square	F	Sig.
Between Groups	1.984E+13	5	3.968E+12	595.708	.000
Within Groups	7.993E+10	12	6661018022		
Total	1.992E+13	17			

Post Hoc Tests

Multiple Comparisons

Dependent Variable: RFU2h

	(I) samples2h	(J) samples2h	Mean Difference (I-J)	Std. Error	Sig.	95% Confidence Interval	
						Lower Bound	Upper Bound
Tukey HSD	uninduced	10 µg/l	-220207.333	66638.41746	.055	-444040.5044	3625.8377
		25 µg/l	-619778.333 [*]	66638.41746	.000	-843611.5044	-395945.1623
		50 µg/l	-1325150.67 [*]	66638.41746	.000	-1548983.84	-1101317.50
		75 µg/l	-1908457.00 [*]	66638.41746	.000	-2132290.17	-1684623.83
		150 µg/l	-3033192.33 [*]	66638.41746	.000	-3257025.50	-2809359.16

**B) As(III) Detection by Arsenic Bioreporter in MOPS Supplemented Medium
(incubation = 3.5 hours)**

Descriptives

RFU3.5h								
	N	Mean	Std. Deviation	Std. Error	95% Confidence Interval for Mean		Minimum	Maximum
Uninduced	3	111971.3333	47203.86224	27253.16257	-5289.5610	229232.2277	79401.00	166106.00
10 µg/l	3	472738.3333	55169.31370	31852.01812	335690.1606	609786.5060	439144.00	536410.00
25 µg/l	3	1398737.667	116024.7275	66986.90768	1110516.265	1686959.068	1.27E+6	1.49E+6
50 µg/l	3	2415740.333	35783.62073	20659.68306	2326848.892	2504631.775	2.38E+6	2.45E+6
75 µg/l	3	3694416.333	38519.80603	22239.42038	3598727.831	3790104.836	3.65E+6	3.72E+6
150 µg/l	3	5244928.667	289691.7337	167253.6004	4525294.506	5964562.827	5.06E+6	5.58E+6
Total	18	2223088.778	1859972.174	438399.6457	1298146.376	3148031.180	79401.00	5.58E+6

ANOVA

RFU3.5h					
	Sum of Squares	df	Mean Square	F	Sig.
Between Groups	5.860E+13	5	1.172E+13	667.058	.000
Within Groups	2.108E+11	12	1.757E+10		
Total	5.881E+13	17			

Post Hoc Tests

Multiple Comparisons

Dependent Variable: RFU3.5h

		(I) samples3.5h	(J) samples3.5h	Mean Difference (I-J)	Std. Error	Sig.	95% Confidence Interval	
Tukey HSD	Uninduced	10 µg/l		-360767.000	108227.7120	.052	-724295.3203	2761.3203
		25 µg/l		-1286766.33*	108227.7120	.000	-1650294.65	-923238.0131
		50 µg/l		-2303769.00*	108227.7120	.000	-2667297.32	-1940240.68
		75 µg/l		-3582445.00*	108227.7120	.000	-3945973.32	-3218916.68
		150 µg/l		-5132957.33*	108227.7120	.000	-5496485.65	-4769429.01

C) As(V) Detection by Arsenic Bioreporter in MOPS Supplemented Medium

(incubation = 2 hours)

Descriptives

RFU2h

	N	Mean	Std. Deviation	Std. Error	95% Confidence Interval for Mean		Minimum	Maximum
					Lower Bound	Upper Bound		
Uninduced	3	78130.3333	34671.75244	20017.74561	-7999.0744	164259.7411	50785.00	117127.00
10 µg/l	3	491543.3333	39962.63867	23072.44019	392270.6356	590816.0311	445560.00	517876.00
25 µg/l	3	973484.3333	9468.05642	5466.38492	949964.3773	997004.2893	967884.00	984416.00
50 µg/l	3	1572822.667	152464.0605	88025.16635	1194080.944	1951564.389	1.42E+6	1.73E+6
75 µg/l	3	2030218.667	71844.18670	41479.26053	1851747.813	2208689.520	1.95E+6	2.08E+6
150 µg/l	3	3242177.333	123305.1811	71190.27950	2935870.283	3548484.384	3.10E+6	3.31E+6
Total	18	1398062.778	1079721.082	254492.6996	861130.1157	1934995.440	50785.00	3.31E+6

ANOVA

RFU2h

	Sum of Squares	df	Mean Square	F	Sig.
Between Groups	1.973E+13	5	3.945E+12	509.049	.000
Within Groups	9.300E+10	12	7749971930		
Total	1.982E+13	17			

Post Hoc Tests

Multiple Comparisons

Dependent Variable: RFU2h

	(I) samples2h	(J) samples2h	Mean Difference (I-J)	Std. Error	Sig.	95% Confidence Interval	
						Lower Bound	Upper Bound
Tukey HSD	Uninduced	10 µg/l	-413413.000 [*]	71879.39867	.001	-654850.2122	-171975.7878
		25 µg/l	-895354.000 [*]	71879.39867	.000	-1136791.21	-653916.7878
		50 µg/l	-1494692.33 [*]	71879.39867	.000	-1736129.55	-1253255.12
		75 µg/l	-1952088.33 [*]	71879.39867	.000	-2193525.55	-1710651.12
		150 µg/l	-3164047.00 [*]	71879.39867	.000	-3405484.21	-2922609.79

**D) Cd(II) Detection by Cadmium Bioreporter in M9 Supplemented Medium
(incubation = 3.5 hours)**

Descriptives

RFU3.5h

	N	Mean	Std. Deviation	Std. Error	95% Confidence Interval for Mean		Minimum	Maximum
					Lower Bound	Upper Bound		
Uninduced	3	1.2407	.81789	.47221	-.7911	3.2724	.30	1.75
2 µg/l	3	2.0127	.84062	.48533	-.0756	4.1009	1.04	2.50
5 µg/l	3	3.5510	.76572	.44209	1.6488	5.4532	2.67	4.03
10 µg/l	3	4.6277	.84121	.48567	2.5380	6.7174	3.66	5.16
25 µg/l	3	6.7210	.68110	.39323	5.0291	8.4129	5.95	7.23
50 µg/l	3	8.1977	.79853	.46103	6.2140	10.1813	7.29	8.78
100 µg/l	3	9.3610	.75970	.43861	7.4738	11.2482	8.49	9.87
Total	21	5.1017	3.00816	.65643	3.7324	6.4710	.30	9.87

ANOVA

RFU3.5h

	Sum of Squares	df	Mean Square	F	Sig.
Between Groups	172.284	6	28.714	46.225	.000
Within Groups	8.696	14	.621		
Total	180.980	20			

Post Hoc Tests

Multiple Comparisons

Dependent Variable: RFU3.5h

	(I) sample3.5h	(J) sample3.5h	Mean Difference (I-J)	Std. Error	Sig.	95% Confidence Interval	
						Lower Bound	Upper Bound
Tukey HSD	Uninduced	2 µg/l	-.77200	.64352	.883	-2.9694	1.4254
		5 µg/l	-2.31033*	.64352	.037	-4.5077	-.1130
		10 µg/l	-3.38700*	.64352	.002	-5.5844	-1.1896
		25 µg/l	-5.48033*	.64352	.000	-7.6777	-3.2830
		50 µg/l	-6.95700*	.64352	.000	-9.1544	-4.7596
		100 µg/l	-8.12033*	.64352	.000	-10.3177	-5.9230

E) Cd(II) Detection by Cadmium Bioreporter in MOPS Supplemented Medium (incubation = 1.5 hours)

Descriptives

RFU1.5h

	N	Mean	Std. Deviation	Std. Error	95% Confidence Interval for Mean		Minimum	Maximum
					Lower Bound	Upper Bound		
Uninduced	3	.1207	.06658	.03844	-.0447	.2861	.06	.19
2 µg/l	3	1.0640	.18400	.10623	.6069	1.5211	.88	1.25
5 µg/l	3	1.2340	.13623	.07865	.8956	1.5724	1.08	1.32
10 µg/l	3	2.1707	.07511	.04336	1.9841	2.3572	2.10	2.25
25 µg/l	3	2.4997	.11201	.06467	2.2214	2.7779	2.38	2.60
50 µg/l	3	2.7953	.14965	.08640	2.4236	3.1671	2.70	2.97
100 µg/l	3	2.3783	.19814	.11440	1.8861	2.8705	2.16	2.55
Total	21	1.7518	.92541	.20194	1.3306	2.1730	.06	2.97

ANOVA

RFU1.5h

	Sum of Squares	df	Mean Square	F	Sig.
Between Groups	16.854	6	2.809	143.850	.000
Within Groups	.273	14	.020		
Total	17.128	20			

Post Hoc Tests

Multiple Comparisons

Dependent Variable: RFU1.5h

	(I) sample1.5h	(J) sample1.5h	Mean Difference (I-J)	Std. Error	Sig.	95% Confidence Interval	
						Lower Bound	Upper Bound
Tukey HSD	Uninduced	2 µg/l	-.94333 [*]	.11410	.000	-1.3329	-.5537
		5 µg/l	-1.11333 [*]	.11410	.000	-1.5029	-.7237
		10 µg/l	-2.05000 [*]	.11410	.000	-2.4396	-1.6604
		25 µg/l	-2.37900 [*]	.11410	.000	-2.7686	-1.9894
		50 µg/l	-2.67467 [*]	.11410	.000	-3.0643	-2.2851
		100 µg/l	-2.25767 [*]	.11410	.000	-2.6473	-1.8681

F) As(III) Detection by Agar Immobilized Arsenic Bioreporter in M9 Supplemented Medium
(incubation = 3 hours)

Descriptives

RFU3h								
	N	Mean	Std. Deviation	Std. Error	95% Confidence Interval for Mean		Minimum	Maximum
Uninduced	3	.3250	.19152	.11057	Lower Bound	Upper Bound	.13	.52
10 µg/l	3	1.5953	.13870	.08008	1.2508	1.9399	1.48	1.75
25 µg/l	3	2.8210	.21800	.12586	2.2795	3.3625	2.60	3.04
50 µg/l	3	2.7013	.23537	.13589	2.1166	3.2860	2.47	2.94
75 µg/l	3	3.7563	.07524	.04344	3.5694	3.9432	3.70	3.84
100 µg/l	3	4.4920	.11447	.06609	4.2076	4.7764	4.36	4.56
150 µg/l	3	5.9120	.36831	.21264	4.9971	6.8269	5.50	6.20
Total	21	3.0861	1.76145	.38438	2.2843	3.8879	.13	6.20

ANOVA

RFU3h					
	Sum of Squares	df	Mean Square	F	Sig.
Between Groups	61.428	6	10.238	228.777	.000
Within Groups	.627	14	.045		
Total	62.054	20			

Post Hoc Tests

Multiple Comparisons

Dependent Variable: RFU3h

		(I) sample3h	(J) sample3h	Mean Difference (I-J)	Std. Error	Sig.	95% Confidence Interval	
							Lower Bound	Upper Bound
Tukey HSD	Uninduced	10 µg/l		-1.27033*	.17272	.000	-1.8601	-.6806
		25 µg/l		-2.49600*	.17272	.000	-3.0858	-1.9062
		50 µg/l		-2.37633*	.17272	.000	-2.9661	-1.7866
		75 µg/l		-3.43133*	.17272	.000	-4.0211	-2.8416
		100 µg/l		-4.16700*	.17272	.000	-4.7568	-3.5772
		150 µg/l		-5.58700*	.17272	.000	-6.1768	-4.9972

G) As(III) Detection by Agar Immobilized Arsenic Bioreporter in MOPS Supplemented Medium
(incubation = 6 hours)

Descriptives

RFU6h

	N	Mean	Std. Deviation	Std. Error	95% Confidence Interval for Mean		Minimum	Maximum
					Lower Bound	Upper Bound		
Uninduced	3	.7353	.04350	.02512	.6273	.8434	.70	.79
10 µg/l	3	1.5603	.12947	.07475	1.2387	1.8819	1.41	1.64
25 µg/l	3	3.7593	.11593	.06693	3.4713	4.0473	3.66	3.89
50 µg/l	3	5.2950	.20010	.11553	4.7979	5.7921	5.14	5.52
75 µg/l	3	6.8950	.37054	.21393	5.9745	7.8155	6.50	7.23
100 µg/l	3	8.7117	.29576	.17076	7.9770	9.4464	8.49	9.05
150 µg/l	3	11.9650	2.37556	1.37153	6.0638	17.8662	9.32	13.92
Total	21	5.5602	3.85915	.84213	3.8036	7.3169	.70	13.92

ANOVA

RFU6h

	Sum of Squares	df	Mean Square	F	Sig.
Between Groups	285.980	6	47.663	56.167	.000
Within Groups	11.880	14	.849		
Total	297.860	20			

Post Hoc Tests

Multiple Comparisons

Dependent Variable: RFU6h

	(I) sample6h	(J) sample6h	Mean Difference (I-J)	Std. Error	Sig.	95% Confidence Interval	
						Lower Bound	Upper Bound
Tukey HSD	Uninduced	10 µg/l	-.82500	.75215	.919	-3.3933	1.7433
		25 µg/l	-3.02400*	.75215	.017	-5.5923	-.4557
		50 µg/l	-4.55967*	.75215	.000	-7.1280	-1.9914
		75 µg/l	-6.15967*	.75215	.000	-8.7280	-3.5914
		100 µg/l	-7.97633*	.75215	.000	-10.5446	-5.4080
		150 µg/l	-11.22967*	.75215	.000	-13.7980	-8.6614

H) As(V) Detection by Agar Immobilized Arsenic Bioreporter in MOPS Supplemented Medium
(incubation = 5 hours)

Descriptives

RFU5h

	N	Mean	Std. Deviation	Std. Error	95% Confidence Interval for Mean		Minimum	Maximum
					Lower Bound	Upper Bound		
Uninduced	3	.6003	.09152	.05284	.3730	.8277	.51	.69
10 µg/l	3	2.0877	.21316	.12307	1.5582	2.6172	1.85	2.27
25 µg/l	3	3.5277	.36258	.20933	2.6270	4.4284	3.11	3.79
50 µg/l	3	6.0040	.38775	.22387	5.0408	6.9672	5.73	6.45
75 µg/l	3	8.8240	.25348	.14635	8.1943	9.4537	8.56	9.07
100 µg/l	3	10.9740	.26902	.15532	10.3057	11.6423	10.67	11.19
150 µg/l	3	12.5807	.58747	.33918	11.1213	14.0400	11.94	13.10
Total	21	6.3712	4.35046	.94935	4.3909	8.3515	.51	13.10

ANOVA

RFU5h

	Sum of Squares	df	Mean Square	F	Sig.
Between Groups	376.895	6	62.816	537.954	.000
Within Groups	1.635	14	.117		
Total	378.529	20			

Post Hoc Tests

Multiple Comparisons

Dependent Variable: RFU5h

	(I) sample5h	(J) sample5h	Mean Difference (I-J)	Std. Error	Sig.	95% Confidence Interval	
						Lower Bound	Upper Bound
Tukey HSD	Uninduced	10 µg/l	-1.48733 [*]	.27901	.002	-2.4400	-.5346
		25 µg/l	-2.92733 [*]	.27901	.000	-3.8800	-1.9746
		50 µg/l	-5.40367 [*]	.27901	.000	-6.3564	-4.4510
		75 µg/l	-8.22367 [*]	.27901	.000	-9.1764	-7.2710
		100 µg/l	-10.37367 [*]	.27901	.000	-11.3264	-9.4210
		150 µg/l	-11.98033 [*]	.27901	.000	-12.9330	-11.0276

I) As(III) Detection by Alginate Immobilized Arsenic Bioreporter in M9 Supplemented Medium
(incubation = 5 hours)

Descriptives

RFU5h

	N	Mean	Std. Deviation	Std. Error	95% Confidence Interval for Mean		Minimum	Maximum
					Lower Bound	Upper Bound		
Uninduced	3	1.4567	.34894	.20146	.5899	2.3235	1.21	1.86
10 µg/l	3	3.8550	.09702	.05601	3.6140	4.0960	3.76	3.95
25 µg/l	3	7.6903	1.50797	.87063	3.9443	11.4363	6.16	9.18
50 µg/l	3	10.2223	1.55952	.90039	6.3483	14.0964	9.19	12.02
75 µg/l	3	13.6290	2.66400	1.53806	7.0113	20.2467	11.69	16.67
100 µg/l	3	15.0190	2.80077	1.61702	8.0615	21.9765	12.60	18.09
150 µg/l	3	23.7423	2.46273	1.42186	17.6246	29.8601	21.70	26.48
Total	21	10.8021	7.30826	1.59479	7.4754	14.1288	1.21	26.48

ANOVA

RFU5h

	Sum of Squares	df	Mean Square	F	Sig.
Between Groups	1016.525	6	169.421	45.890	.000
Within Groups	51.687	14	3.692		
Total	1068.212	20			

Post Hoc Tests

Multiple Comparisons

Dependent Variable: RFU5h

	(I) sample5h	(J) sample5h	Mean Difference (I-J)	Std. Error	Sig.	95% Confidence Interval	
						Lower Bound	Upper Bound
Tukey HSD	Uninduced	10 µg/l	-2.39833	1.56885	.725	-7.7553	2.9586
		25 µg/l	-6.23367 [*]	1.56885	.018	-11.5906	-.8767
		50 µg/l	-8.76567 [*]	1.56885	.001	-14.1226	-3.4087
		75 µg/l	-12.17233 [*]	1.56885	.000	-17.5293	-6.8154
		100 µg/l	-13.56233 [*]	1.56885	.000	-18.9193	-8.2054
		150 µg/l	-22.28567 [*]	1.56885	.000	-27.6426	-16.9287

J) As(III) Detection by Alginate Immobilized Arsenic Bioreporter in MOPS Supplemented Medium
(incubation = 5 hours)

Descriptives

RFU5h

	N	Mean	Std. Deviation	Std. Error	95% Confidence Interval for Mean		Minimum	Maximum
					Lower Bound	Upper Bound		
Uninduced	3	.5097	.10980	.06339	.2369	.7824	.43	.63
10 µg/l	3	2.9647	.18726	.10811	2.4995	3.4298	2.77	3.15
25 µg/l	3	5.6250	.27666	.15973	4.9377	6.3123	5.32	5.86
50 µg/l	3	12.5457	2.10748	1.21676	7.3104	17.7809	10.39	14.61
75 µg/l	3	19.8523	.97946	.56549	17.4192	22.2854	18.86	20.81
100 µg/l	3	26.5690	2.34014	1.35108	20.7558	32.3822	24.62	29.17
150 µg/l	3	27.9423	2.87313	1.65880	20.8051	35.0796	25.59	31.15
Total	21	13.7155	10.78132	2.35268	8.8079	18.6231	.43	31.15

ANOVA

RFU5h

	Sum of Squares	df	Mean Square	F	Sig.
Between Groups	2286.225	6	381.038	138.519	.000
Within Groups	38.511	14	2.751		
Total	2324.737	20			

Post Hoc Tests

Multiple Comparisons

Dependent Variable: RFU5h

	(I) sample5h	(J) sample5h	Mean Difference (I-J)	Std. Error	Sig.	95% Confidence Interval	
						Lower Bound	Upper Bound
Tukey HSD	Uninduced	10 µg/l	-2.45500	1.35420	.561	-7.0790	2.1690
		25 µg/l	-5.11533*	1.35420	.026	-9.7394	-.4913
		50 µg/l	-12.03600*	1.35420	.000	-16.6600	-7.4120
		75 µg/l	-19.34267*	1.35420	.000	-23.9667	-14.7186
		100 µg/l	-26.05933*	1.35420	.000	-30.6834	-21.4353
		150 µg/l	-27.43267*	1.35420	.000	-32.0567	-22.8086

K) As(V) Detection by Alginate Immobilized Arsenic Bioreporter in MOPS Supplemented Medium

(incubation = 5 hours)

Descriptives

RFU5h

	N	Mean	Std. Deviation	Std. Error	95% Confidence Interval for Mean		Minimum	Maximum
					Lower Bound	Upper Bound		
Uninduced	3	.5097	.10980	.06339	.2369	.7824	.43	.63
10 µg/l	3	4.5870	1.18868	.68628	1.6342	7.5398	3.47	5.84
25 µg/l	3	10.6410	2.15621	1.24489	5.2847	15.9973	8.44	12.75
50 µg/l	3	20.4610	2.14059	1.23587	15.1435	25.7785	18.06	22.18
75 µg/l	3	30.1657	1.96294	1.13330	25.2895	35.0419	27.90	31.43
100 µg/l	3	32.9657	2.80401	1.61890	26.0001	39.9312	30.63	36.08
150 µg/l	3	37.9690	2.85561	1.64869	30.8753	45.0627	35.35	41.02
Total	21	19.6141	14.06528	3.06930	13.2117	26.0166	.43	41.02

ANOVA

RFU5h

	Sum of Squares	df	Mean Square	F	Sig.
Between Groups	3895.587	6	649.265	148.882	.000
Within Groups	61.053	14	4.361		
Total	3956.640	20			

Post Hoc Tests

Multiple Comparisons

Dependent Variable: RFU5h

	(I) sample5h	(J) sample5h	Mean Difference (I-J)	Std. Error	Sig.	95% Confidence Interval	
						Lower Bound	Upper Bound
Tukey HSD	Uninduced	10 µg/l	-4.07733	1.70508	.271	-9.8995	1.7448
		25 µg/l	-10.13133 [*]	1.70508	.001	-15.9535	-4.3092
		50 µg/l	-19.95133 [*]	1.70508	.000	-25.7735	-14.1292
		75 µg/l	-29.65600 [*]	1.70508	.000	-35.4781	-23.8339
		100 µg/l	-32.45600 [*]	1.70508	.000	-38.2781	-26.6339
		150 µg/l	-37.45933 [*]	1.70508	.000	-43.2815	-31.6372

CURRICULUM VITAE

PERSONAL INFORMATION

Surname, Name : Elçin, Evrim
Nationality : Turkish (TC)
Date and Place of Birth : 20 June 1987, Aydın
Phone : +90 506 776 20 19
E-mail : evrim.elcin@metu.edu.tr

EDUCATION

Degree	Institution	Year of Graduation
MS	METU Biotechnology	2013
BS	METU Molecular Biology and Genetics	2010
High School	Süleyman Demirel Anatolian High School, Aydın	2005

WORK EXPERIENCE

Year	Place	Enrollment
2013-Present	METU Biological Sciences	Research Assistant
2019-Present	Universal Wiser Publisher	Editor
2009	Jacobs University Bremen	Intern

FOREIGN LANGUAGES

Advanced English, German

PUBLICATIONS

1. Sonmez, C., Elcin, E., Akin, D., Oktem, H. A., & Yucel, M. (2016). Evaluation of novel thermo-resistant *Micractinium* and *Scenedesmus* sp. for efficient biomass and lipid production under different temperature and nutrient regimes. *Bioresource Technology*, 211, 422–428.
2. Elcin, E., & Öktem, H. A. (2019). Whole-cell fluorescent bacterial bioreporter for arsenic detection in water. *International Journal of Environmental Science and Technology*, 16(10), 5489–5500.

3. Elcin, E., & Öktem, H. A. Immobilization of fluorescent bacterial bioreporter for arsenic detection. Manuscript submitted to Journal of Environmental Health Science and Engineering, and revised.

4. Elcin, E., & Öktem, H. A. Whole-cell fluorescent bacterial bioreporter for environmental cadmium detection. Manuscript under preparation.

ORAL PRESENTATION

Elçin, E., Öktem, H.A. (2017). Tam Hücre Bakteriyel Biyosensörleri Kullanılarak Sudaki Ağır Metallerin Tespit Edilmesi. S-ÇB-6. Oral presentation in Uluslararası Katılımlı 19. Ulusal Biyoteknoloji Kongresi.

PROJECTS and SCHOLARSHIPS

TÜBİTAK - NRDIO (Hungary) Joint Research Project: Toxic Industrial Chemical Monitoring via Drone Integrated Whole Cell Biosensor Arrays, Project No: 217E115, 2018-2021.

The Scientific and Technological Research Council of Turkey, TÜBİTAK-2205 Yurt İçi Lisans Burs Programı, Undergraduate Scholarship (September 2005- June 2010)

The Scientific and Technological Research Council of Turkey), TÜBİTAK- 2210 Doğrudan Yurt İçi Yüksek Lisans Burs Programı, Graduate Scholarship (September 2010- June 2013)

The Scientific and Technological Research Council of Turkey), TÜBİTAK- 2211-E Doğrudan Yurt İçi Doktora Burs Programı, Graduate Scholarship (September 2013- June 2019)

COMPUTER SKILLS

MS Office applications

Minitab (Biostatistics Software, Minitab Release 13.2 statistic software)

IBM SPSS Statistics 25.0 software